

10-23-2019

Thioenamide Synthesis Inspired by Peptide Macrocycles

Joshua Allen Lutz

Louisiana State University and Agricultural and Mechanical College

Follow this and additional works at: https://digitalcommons.lsu.edu/gradschool_dissertations

 Part of the [Organic Chemistry Commons](#)

Recommended Citation

Lutz, Joshua Allen, "Thioenamide Synthesis Inspired by Peptide Macrocycles" (2019). *LSU Doctoral Dissertations*. 5066.

https://digitalcommons.lsu.edu/gradschool_dissertations/5066

This Dissertation is brought to you for free and open access by the Graduate School at LSU Digital Commons. It has been accepted for inclusion in LSU Doctoral Dissertations by an authorized graduate school editor of LSU Digital Commons. For more information, please contact gradetd@lsu.edu.

THIOENAMIDE SYNTHESIS INSPIRED BY PEPTIDE MACROCYCLES

A Dissertation

Submitted to the Graduate Faculty of the
Louisiana State University and
Agricultural and Mechanical College
in partial fulfillment of the
requirements for the degree of
Doctor of Philosophy

in

The Department of Chemistry

by

Joshua Allen Lutz
B.A., Louisiana State University, 2010
B.S., Louisiana State University in Shreveport, 2014
December 2019

To My Family...

To my siblings, Christian, Audrey, Amanda, Krissy, and Brandon, who remind me who I am and
where I came from, and always provide guidance back when I need it

To my lifelong friends, Aaron and Sutter, for unwavering companionship through time and
distance

To my father, Jeffrey Lutz, for teaching me the honor in responsibility and a hard day's work

To my mother, Kerry Young, for providing an example of how to selflessly care for people my
whole life

...This Dissertation Is For You

Acknowledgments

The first and by far most important thank you goes to Professor Carol M. Taylor. Her guidance, support, understanding, and mentorship has gone above and beyond anything that I could have asked for. She has consistently provided a beacon of hard-work and indomitable integrity that will forever influence my view of what a true scholar should be. Even as chair of the department, she always made time to meet with me and review my progress. Our weekly meetings regularly gave me exactly what I needed somehow, be it a great idea for an experiment or simply words of encouragement to usher me through the hardships of research. I am indebted to her and ever thankful for my decision to join her research group.

Thank you to my committee members from the Chemistry Department: Dr. Justin Ragains and Dr. Graca Vicente. They have always been available and responsive with any and all assistance that I asked of them. I would also like to extend thanks to Dr. Edward Benoit for taking on the responsibility of being the Dean's representative on my committee.

My laboratory time at LSU has been copious, but enjoyable. This is in large part due to my lab mates. I would like to thank Dr. Joyeeta Roy and Dr. Samuel Kutty for their friendship during the difficult middle years of my PhD. Dr. Jyoti Mukherjee joined the Taylor lab later in my studies, but had an enormous impact. His levity and fun demeanor has added so much joy, and his scientific guidance has helped me tremendously; for these I extend my thanks. I would also like to thank Elora Doskey for suffering me with such persistence and grace. She was a joy to train as an undergraduate.

Lastly, I must thank Dr. Thomas Weldeghiorghis and Dr. Rafael Cueto for their often timely assistance with NMR and HPLC respectively.

Table of Contents

Acknowledgments	iii
List of Abbreviations and Symbols	vi
Abstract	ix
Chapter 1. Introduction to Peptide Antibiotics and the Aminovinylcysteine Motif	1
1.1. A Brief History of Antibiotics	1
1.2. Activity of Antibiotics and Bacterial Resistance	2
1.3. Lantibiotics	7
1.4. Cypemycin	11
1.5. Biosynthesis of AviCys and AviMeCys	12
1.6. Previous Chemical Approaches to AviCys	13
1.7. Notes	16
Chapter 2. Acid-Promoted (Thio)Enamide Formation	20
2.1. Acid-Mediated (Thio)Enamide Formation	20
2.2. Early Design of a Tripeptide Substrate for Thioenamide Formation	21
2.3. Synthesis of the Acetal-Functionalized Cysteine Residue	22
2.4. Model Tripeptide Synthesis	24
2.5. Mechanistic Investigations	26
2.6. Condensations with Acetamide	29
2.7. Experimental Procedures	35
2.8. NMR Spectra	46
2.9. Crystallographic data for lantionine 36	69
2.10. Notes	76
Chapter 3. Cysteine Epimerization and an Improved Synthesis of the Building Block in Enantioenriched Form	78
3.1. A Strange Problem	78
3.2. Imidazolidinone: Evidence for Epimerization	79
3.3. The Canary in the Coal Mine	80
3.4. The Usual Suspects	82
3.5. A New Electrophile	84
3.6. Epimerization during Thioenamide Formation	85
3.7. The Epimerization Strikes Back	88
3.8. Return of the Phthalimido	90
3.9. Experimental Procedures	93
3.10. NMR Spectra	100

3.11. HPLC Chromatograms for Selected Compounds	114
3.12. Notes	120
Chapter 4. Peptidyl Thioenamide Synthesis and Macrocyclization.....	121
4.1. Imidazolidinone: a Thioenamide Interrupted.....	121
4.2. Double Amine Protection-Benzyl Groups	123
4.3. Tetrachlorophthalimide (Tcp).....	126
4.4. Acid and Amine Deprotection	134
4.5. Free Amino Acid Peptide.....	137
4.6. Macrocycle.....	139
4.7. Future Work	141
4.8. Experimental Procedures	143
4.9. NMR Spectra	149
4.10. HPLC Chromatograms of Selected Compounds	161
4.11. Notes	164
List of References.....	166
Vita	173

List of Abbreviations and Symbols

AIBN	azobisisobutyronitrile
Ac	acetyl
All	allyl
amu	atomic mass unit
Ar	aryl
AviCys	<i>S</i> -[(<i>Z</i>)-2-aminovinyl]- <i>D</i> -cysteine
AviMeCys	<i>S</i> -[(<i>Z</i>)-2-aminovinyl]-(3 <i>S</i>)-3-methyl- <i>D</i> -cysteine
Bn	benzyl
Boc	<i>tert</i> -butyl carbonate
BOP	(benzotriazol-1-yloxy) <i>tris</i> (dimethylamino)phosphonium hexafluorophosphate
n-Bu	<i>n</i> -butyl
t-Bu	<i>tert</i> -butyl
<i>C. diff</i>	<i>Clostridium difficile</i>
CAMPs	cationic antimicrobial peptides
Cbz	carbobenzyloxy
COSY	correlation spectroscopy
dba	dibenzylideneacetone
DBU	1,8-diazabicyclo(5.4.0)undec-7-ene
DCC	<i>N,N'</i> -dicyclohexylcarbodiimide
DCM	dichloromethane
Dha	dehydroalanine
Dhb	dehydrobutyrine
DMF	dimethylformamide
DMSO	dimethylsulfoxide

DNA	deoxyribonucleic acid
DPPB	1,4-bis(diphenylphosphino)butane
Et	ethyl
EDC	1-ethyl-3-(3-dimethylaminopropyl)-carbodiimide
Fmoc	fluorenylmethyloxycarbonyl
HATU	1-[<i>bis</i> (dimethylamino)methylene]-1H-1,2,3-triazolo[4,5-b]pyridinium 3-oxid hexafluorophosphate
HFCD	homo-oligomeric flavin-containing cysteine decarboxylases
HMBC	heteronuclear multiple bond correlation
HOBt	hydroxybenzotriazole
HPLC	high performance liquid chromatography
HRMS	high resolution mass spectrometry
HSQC	heteronuclear single quantum coherence
IR-20	ion exchange resin-20
LanB	lanthionine synthetase B
LanC	lanthionine synthetase C
LanM	lanthionine synthetase M
LC-MS	liquid chromatography mass spectrometry
Me	methyl
MRSA	methicillin resistant <i>Staphylococcus aureus</i>
MSB	methyl 2-[(succinimidooxy)carbonyl]benzoate
NBO	natural bond order
NHS	<i>N</i> -hydroxy succinimide
NMR	nuclear magnetic resonance
PG	peptidoglycan

Pht	phthalimido
PMB	<i>para</i> -methoxybenzyl
PNB	<i>para</i> -nitrobenzyl
<i>p</i> TSOH	<i>para</i> -toluene sulfonic acid
RP-HPLC	reverse phase high performance liquid chromatography
rRNA	ribosomal ribonucleic acid
SPPS	solid phase peptide synthesis
TBAFe	[Bu ₄ N][Fe(CO) ₃ (NO)]
TBAHS	tetrabutylammonium hydrogen sulfate
TBDPS	<i>tert</i> -butyldiphenylsilyl
Tcp	tetrachlorophthalimido
TES	triethylsilane
TFA	trifluoroacetic acid
THF	tetrahydrofuran
TIPS	triisopropylsilyl
TLC	thin layer chromatography
TMEDA	tetramethylethylenediamine
TMS	tetramethylsilane
TOMAC	tetraoctylmethylammonium chloride
Trt	triphenylmethyl
Ts	<i>para</i> -toluenesulfonyl
VISA	vancomycin intermediate resistant <i>Staphylococcus aureus</i>

Standard 3 letter codes are utilized throuout the document for amino acids

Abstract

Despite advances in medicine, antibiotic resistance threatens to return once preventable diseases to the human population. The microbisporicins are 24-amino acid antibiotic peptides belonging to the lantibiotic class, which pathogens have been slow to develop resistance. The uncommon post-translational modification *S*-[(*Z*)-2-aminovinyl]-*D*-cysteine (AviCys) is likely crucial to their activity, and appears in a small number of other peptides with compelling biological activities. Total synthesis of an AviCys-containing peptide has eluded the chemical community.

The primary challenge of AviCys synthesis is the construction of a thioenamide functional group. We demonstrate that acid-promoted reactions between an amide and acetal produce the desired *Z*-thioenamide. We use mechanistic calculations to highlight the stereoelectronic control of this transformation, while careful examination of reaction byproducts helped us to optimize the yield and selectivity. To this end, we developed a stereoselective method for *Z*-thioenamide generation in a model system.

While progressing to peptidyl thioenamide formation, we encountered an issue with the stereochemistry of our cysteine building block. Examination of the diastereomeric products of reactions with our cysteine building block led us to conclude that it was racemic. We used chiral HPLC and Mosher's derivatization to determine the steps responsible for racemization. We redesigned the synthesis of the cysteine building block to produce enantiomerically enriched material.

Early attempts at thioenamide formation between amino acid derived coupling partners showed us that double protection of the α -amino amide amine was required. The optimal amine

protection was as a tetrachlorophthalimide (Tcp). We protected valinamide with Tcp and formed a thioenamide *en route* to the C-terminal ring of cypemycin, an AviCys-containing peptide with antileukemia activity. Deprotection of the Tcp amine was achieved, under carefully controlled conditions, followed by coupling with Boc-leucine to form a tripeptide. Liberation of the terminal acid and amine was achieved, though classic conditions for deprotection had to be tweaked for compatibility of the thioenamide functional group. Macrocyclization was accomplished to form a Pht-capped cypemycin C-terminal ring.

Chapter 1. Introduction to Peptide Antibiotics and the Aminovinylcysteine Motif

1.1. A Brief History of Antibiotics

The earliest antibiotic to be discovered from nature, mycophenolic acid (**1**), dates back to 1893. Bartolomeo Gosio, an Italian microbiologist, isolated this antibiotic from *Penicillium glaucum* as a crystalline solid.^{1,2} In addition to being an antibiotic, mycophenolic acid also shows antifungal, antiviral, antitumor, and anti-psoriasis properties.³ A derivative of the compound is currently available to physicians, though as an immunosuppressant for transplant patients rather than an antibiotic.⁴

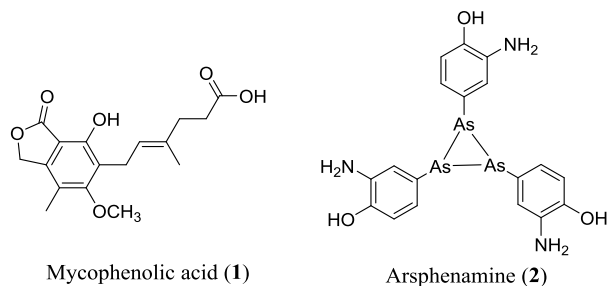


Figure 1.1. Early Antibiotic Discoveries

The world saw its first man-made antibiotic, arsphenamine (**2**), in the early twentieth century. German scientist Paul Ehrlich synthesized the compound, based on cell-staining dyes (i.e., arsanilic acid). His hope was to target cell walls, just as the dyes selectively stained them. He first proposed the concepts of *chemotherapia specifica* (chemotherapy) and *zauberkugel* (magic bullet), referencing sought-after specificity of therapeutics.⁵ In 1910, arsphenamine was approved as the premier treatment for syphilis, and would remain so for 40 years.⁶

No history of antibiotics would be complete without the discovery of penicillin in 1928, arguably the greatest breakthrough in medical history.⁷ In a now famously serendipitous turn-of-events, scientist Alexander Fleming noticed a fungal contamination (later determined to be

Penicillium notatum, now *P. chrysogenum*) growing in one of his *S. aureus* cultures. The fungus appeared to be killing the bacteria, so Fleming postulated that it must be secreting a bactericidal compound. The compound was later isolated by Ernst Boris Chain and Norman Heatley and eventually used clinically in 1941.⁸ The immense potential of the compound was so apparent that the Anglo-American penicillin project was launched during World War II in an effort to isolate the compound in large enough quantities to aid the allied troops dying from infection overseas.^{9,10} By 1945, penicillin was available to the public. Fleming's keen observation and curiosity generated a drug that has saved countless lives. From the launchpad of the three exemplary discoveries described above, the library of antibiotics has expanded to more than 150 compounds.¹¹ Increased use of bactericidal (kills bacteria) and bacteriostatic (prevents bacterial growth) compounds has generated a number of highly resistant strains that threaten to make the impressive library irrelevant in the fight against infectious pathogens.

1.2. Activity of Antibiotics and Bacterial Resistance

There have been four principal targets for antibacterial activity: 1) enzymes involved in cell wall biosynthesis, 2) nucleic acid metabolism, 3) protein synthesis, and 4) membrane disruption. Dozens of compounds, manipulating one or more of these mechanisms, have been approved for clinical use. Resistance in bacteria is also achieved through four fundamental methods: 1) drug alteration, 2) binding site alteration, 3) metabolic pathway alteration, and 4) increased efflux to the extra cellular space through increased activity of membrane pumps. One or more of these strategies are active in resistant bacteria and must be circumvented in order to treat an infection. The following section will describe some prototypical compounds, illustrating each mechanism of bactericidal activity, as well as how the four mechanisms of resistance have produced problematic bacterial strains.

1.2.1. Inhibitors of Cell Wall Biosynthesis: β -Lactams - Drug Alteration

Beta-lactam antibiotics, such as penicillin, inhibit the synthesis of peptidoglycan (PG), thereby targeting the biosynthetic pathway that produces cell wall.¹² Bacterial cells constantly destroy and replace their cell wall, so inhibition of its synthesis leads to bactericidal activity.¹³ In beta-lactams this activity is achieved through mimicking the C-terminus of the natural peptide ligand of the D-Ala-D-Ala carboxypepsidase enzyme (Fig. 1.2).¹⁴ This enzyme is responsible for cross-linking of the peptidoglycan in the cell wall. The beta-lactam antibiotic binds irreversibly to the enzyme and prevents continuation of this process.

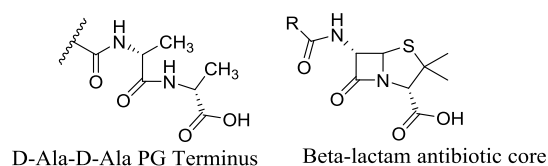
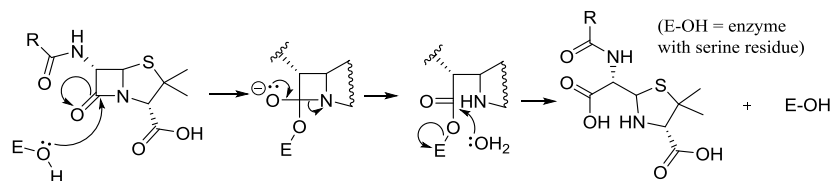


Figure 1.2. Comparison of PG natural ligand and beta-lactam

Resistance to penicillin was first mentioned in a report by Abraham and Chain, that described an enzyme capable of destroying the beta-lactam antibiotic.¹⁵ These enzymes were soon named penicillinases, reflecting their high affinity and irreversible, covalent binding of this class of compounds.¹⁶ The nucleophilic alcohol side chain of an active-site serine residue opens the beta-lactam ring and covalently binds penicillin to the enzyme (Scheme 1.1). Hydrolysis of this acyl-enzyme intermediate regenerates the enzyme and releases the inactive free di-acid derivative of penicillin. This mechanism of resistance is representative of drug alteration/degradation and is also adopted by pathogens resistant to aminoglycosides, streptogramins, and lincosamide antibiotics.¹⁷



Scheme 1.1. Mechanism of action of penicillinase

1.2.2. Disruption of DNA Metabolism: Quinolones - Binding Site Alteration

Quinolone antibiotics, named for their aromatic core structure, achieve their bactericidal activity through inhibition of DNA duplication (nucleic acid metabolism).¹⁸ The quinolones act on gyrase and topoisomerase IV, two highly homologous enzymes responsible for aiding the unwinding, replication, and reunification of DNA during transcription.¹⁹ Crystal structures have shown that quinolones bind irreversibly to the enzymes.

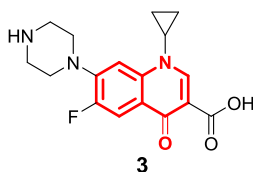


Figure 1.3. Ciprofloxacin (3), a quinolone antibiotic (quinolone core in red)

Resistance to quinolone antibiotics has arisen through multiple of the four main mechanisms, with the most widely-studied being alteration of the gyrase and/or topoisomerase IV active site. Mutations in genes lead to small changes in the DNA that encodes for the enzyme's binding sites. Several mutations have been observed but two are predominant in resistant bacteria: changes to a N-terminal tyrosine that is in the active site for DNA-binding and a change from serine to tryptophan in the site where quinolone binds.^{20,21} These mutated enzymes are still functional in terms of DNA transcription, but bind quinolone antibiotics relatively poorly.

1.2.3. Inhibitors of Protein Synthesis: Tetracyclines - Increased Efflux

The tetracyclines are a group of antibiotics that inhibit protein synthesis within bacterial cells. These compounds are capable of binding to both rRNA and a subunit of the ribosome to inhibit translation.²² This dual action leads to their activity against a range of bacterial infections, viruses, and even protozoa. The dominant mechanism of resistance towards tetracycline is an increased efflux of the drug out of the cell.²³ A gene mutation codes for a transmembrane protein capable of pumping tetracycline out of the cell using a pH gradient. This pump leads to minimal drug reaching the ribosome, or rRNA, and subsequently no activity.

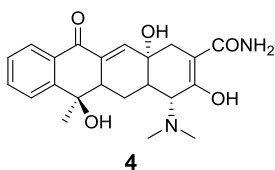


Figure 1.4. Tetracycline parent compound

1.2.4. Membrane Disruption: Polymixins - Alteration of Transmembrane Lipids

The polymixins are substantially higher molecular weight molecules relative to the previous examples given. They are nonribosomal peptide antibiotics generated as part of the defense mechanism of rival bacteria. Polymixins achieve bactericidal activity through binding to gram-negative cell membranes and creating pores through hydrophobic interactions.²⁴ These peptide antibiotics are currently used as last resort drugs against multi-drug resistant infections caused by gram-negative bacteria.

Polymixins can also be classified as cationic antimicrobial peptides (CAMPs), bearing a net positive charge. Some bacteria have adapted to use electrostatic repulsion of their cell wall to achieve resistance. Enzymes, in species of both *Salmonella* and *Escherichia*, have been identified that add positively charged 4-amino-4-deoxy-L-arabinose to their transmembrane

lipids.²⁵ The modification prevents polymyxins from binding to the membrane and forming the lethal pores.

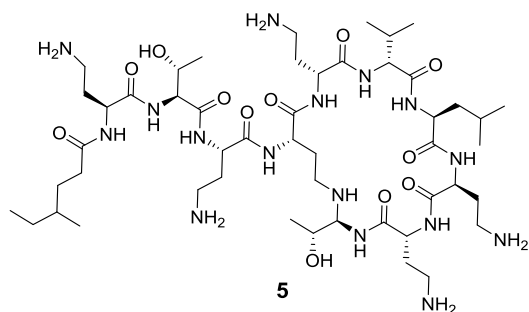


Figure 1.5. Colistin: a polymyxin antibiotic

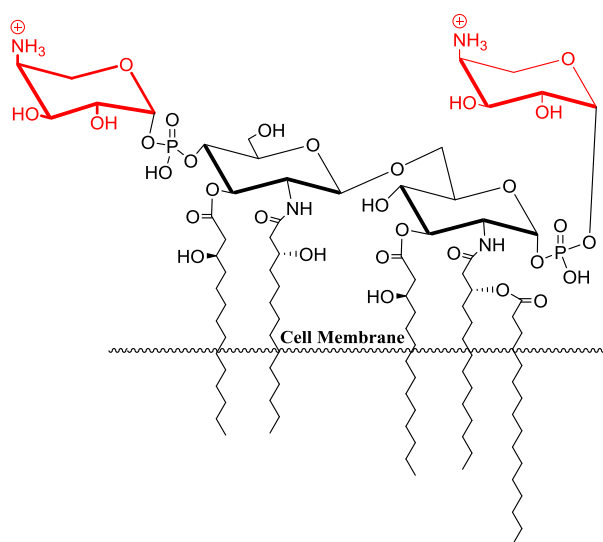


Figure 1.6. Lipid II_B with 4-amino-4-deoxy-L-arabinose (red) attached

The above discussion is an attempt to illustrate some of the diversity of antimicrobial activity and the equally diverse methods that pathogens have developed to resist treatment. There are two million reports of resistant infections and 23,000 deaths per year as a result of untreatable infections.²⁶ Antibiotic resistance will undoubtedly remain one of the most dire challenges for years to come and new treatments must be sought to combat the issue.

1.3. Lantibiotics

Lantibiotics derive their name from their antibiotic activity and the inclusion of the posttranslationally generated thioether *bis*-amino acids, lanthionine (**6**) and methyllanthionine (**7**). Bacteria have been slow to develop resistance to lantibiotics, and some lantibiotics are effective against the most dangerous drug-resistant pathogens.

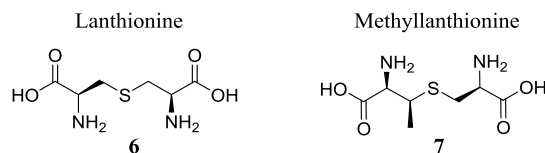


Figure 1.7. *Bis*-amino acids of the lantibiotics

1.3.1. Nisin

The most widely studied lantibiotic is nisin (**8**), a 34-amino acid peptide with five lanthionine-bridged rings, that has been used in food preservation for more than 40 years.²⁷ Nisin has a broad range of antibiotic activity against gram-positive pathogens, achieving its bactericidal activity through two methods: pore formation in the cell membrane and inhibition of peptidoglycan formation.²⁸ Though nisin resistance has been observed, the slow development and continued effectiveness of the lantibiotic highlights the difficulty that bacteria have circumventing the activity.²⁹

1.3.2. Microbisporicins

More recently, the microbisporicins were isolated and characterized by Lazzarini *et al.* The group used a screening method designed to locate cell wall synthesis inhibitors that did not fall into the category of glycopeptides or β -lactams, classes of antibacterial molecules that have been met with significant microbial resistance. The mixture contained two major congeners of a 24-amino acid peptide. A combination of peptides produced by the actinomycete *Microbispora* sp was patented in 2005, as the antibiotic 107891.³⁰

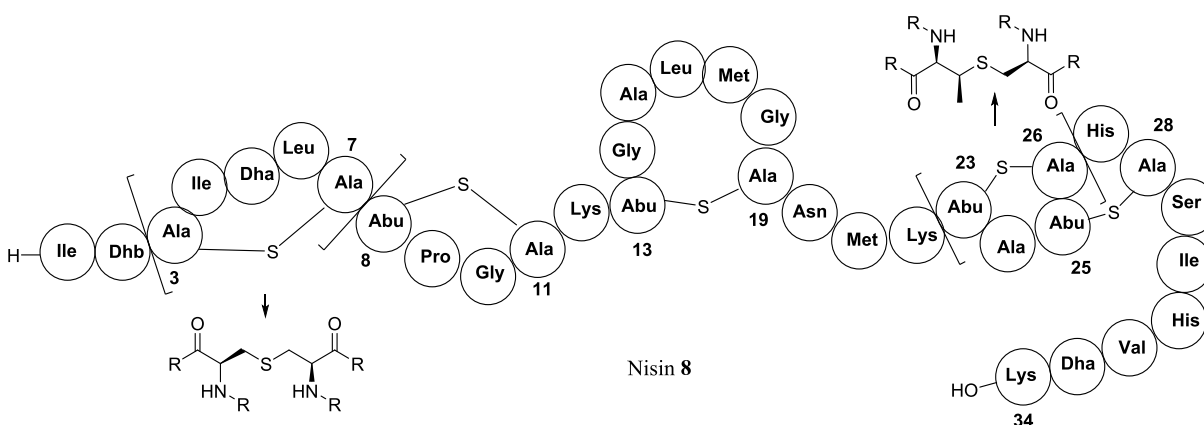


Figure 1.8. Nisin (**8**) and definition of (methyl)lanthionine structure

The mechanism of action of the microbisporicins was found to involve binding to lipid II and inhibition of cell wall biosynthesis in a fashion similar to conventional glycopeptide antibiotics such as vancomycin, an antibiotic commonly used in dire cases of resistant strains such as *Clostridium difficile*.³¹ However, microbisporicin does not bind to the D-Ala-D-Ala moiety of the lipid intermediate that vancomycin binds to; thus microbisporicin is non-competitive with vancomycin. Additionally, the microbisporicins show good to excellent activity against the most difficult infections to treat. Against methicillin resistant *S. aureus* (MRSA), vancomycin intermediate resistant *S. aureus* (VISA), and *Clostridium difficile* (*C. diff*) the effectiveness is 0.13, 2.0, and <0.125 $\mu\text{g/mL}$ minimum inhibitory concentration (MIC) respectively.³² The ability to administer the lantibiotic concomitantly with vancomycin and the powerful therapeutic potential against problematic pathogens has generated much attention for the group of peptides as therapeutic agents.

The two congeners characterized by Castiglione and Lazzarini (A_1 and A_2) differed in the level of hydroxylation at Pro-14 (Fig. 1.9).^{30,32} In 2014, Maffioli *et al.* reported that the lantibiotic can exist as a more complex mixture and characterized the additional congeners B_0 , B_1 , B_2 , F_0 , F_1 , and F_2 .³³ These congeners varied in the level of hydroxylation at Pro-14, the

chlorination of Trp-4, the presence of a sulfoxide in the lanthionine A ring, and inclusion of an additional tripeptide, Gly-Pro-Ala, at the *N*-terminus. They compared the activities of the various congeners and found that antibiotic potency increased with the level of hydroxylation at Pro-14 and the chlorination of Trp-4, and decreased upon oxidation of the thioether in the A-ring to a sulfoxide and addition of the three N-terminal amino acids (Fig. 1.9). An additional variation, resulting from use of KBr in the growth medium, was characterized by Cruz *et al.* as a brominated tryptophan residue, rather than a chlorinated one.³⁴ This family of related compounds, named NAI-108, shows a small increase in antibacterial activity relative to its chlorinated counterpart. Cruz also identified congeners within NAI-108 that varied at the level of hydroxylation at Pro-14, labelling them A₀, A₁, and A₂ corresponding to 0, 1, and 2 hydroxyl groups respectively.

The microbisporicins contain an *S*-[(*Z*)-2-aminovinyl]-*D*-cysteine (AviCys) residue (Fig. 1.9 and 1.10) at the C-terminus, i.e., a decarboxylated lanthionine derivative incorporated into the E-ring. This structural motif is also found in other natural products, including the lantibiotics gallidermin³⁵ and mersacidin,³⁶ as well as some non-lantibiotics cypemycin³⁷ and thioviridamide.³⁸

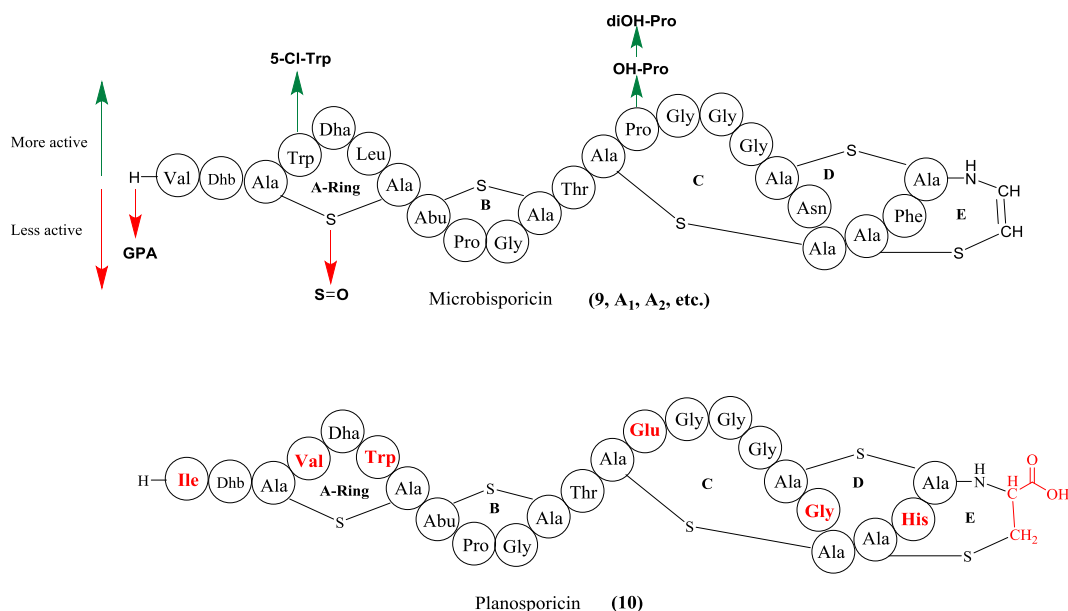


Figure 1.9. Activity of microbisporicin congeners and comparison of sequence with planosporicin

The AviCys-containing peptides isolated to-date have all displayed potent biological activities, including anticancer,³⁷ prophylactic,³⁹ and antibacterial.³⁰ The importance of the AviCys residue is highlighted by a comparison of the lantibiotics, planosporicin and the microbisporicins (Fig. 1.9 and 1.10). The peptides have highly homologous sequences, but planosporicin has a C-terminal acid and a regular lanthionine residue instead of AviCys in the E-ring. Against most bacterial strains, planosporicin is two orders of magnitude less effective vis-à-vis bactericidal activity, when compared with the major A₁ and A₂ variants of the microbisporicins.³² *The aim of my graduate research has been the synthesis of AviCys-containing macrocycles and their incorporation into natural products. The two natural products that inspire this research are the lantibiotic microbisporicins and the linaridin, cypemycin.*

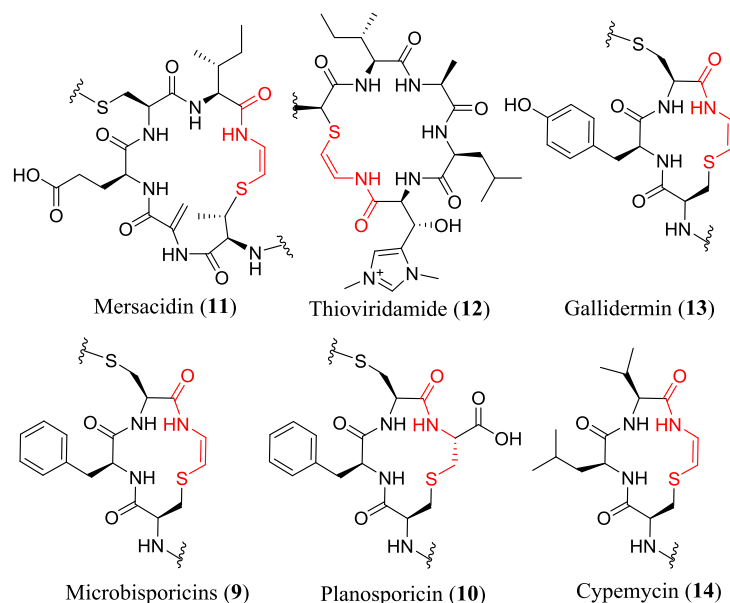


Figure 1.10. C-terminal AviCys containing peptide macrocycles

1.4. Cypemycin

Cypemycin (Fig. 1.11) was isolated from *Streptomyces sp.* OH-4156 by Omura and coworkers in 1993.³⁷ The compound showed both promising cytotoxic activity against leukemia cells (IC_{50} 1.3 $\mu\text{g/mL}$) and antibiotic activity against *Micrococcus luteus* (MIC 0.2 $\mu\text{g/mL}$). The peptide structure was determined the following year by the same group. Cypemycin is a 21-amino acid peptide with an N,N-dimethylalanine residue at the N-terminus, several dehydrobutyrines, and an AviCys (Fig. 1.11).⁴⁰

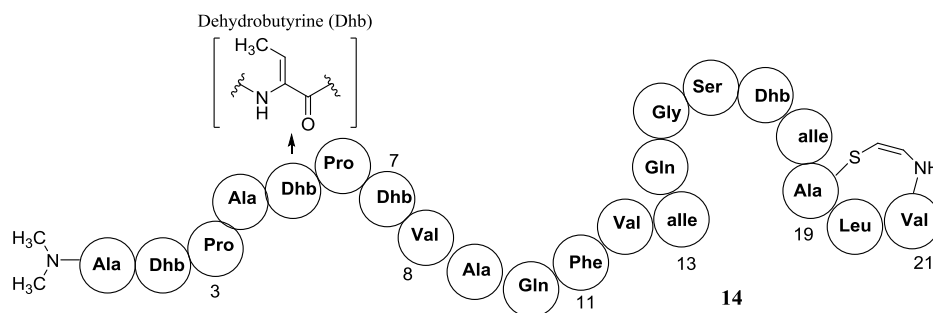


Figure 1.11. Cypemycin (14)

The AviCys-containing macrocycles of the microbisporicins and cypemycin are the same size ring (13 atoms), but the cypemycin ring presents less of a challenge in terms of the chemical synthesis. The C-terminal macrocycle of the microbisporicins is interlocked with an additional thioether ring, greatly increasing the difficulty of synthesis (Figure 1.12). Early attempts, discussed in Chapter 2, on the synthesis of a microbisporicin AviCys analog were unsuccessful. The cypemycin ring serves as a valuable synthetic target and a simplified system to explore the synthesis of the AviCys post-translational modification.

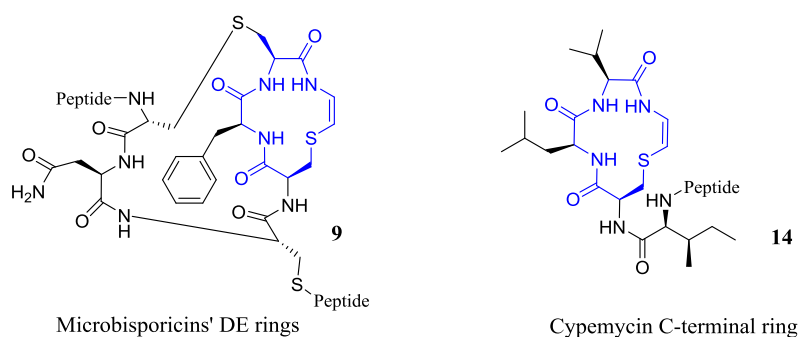
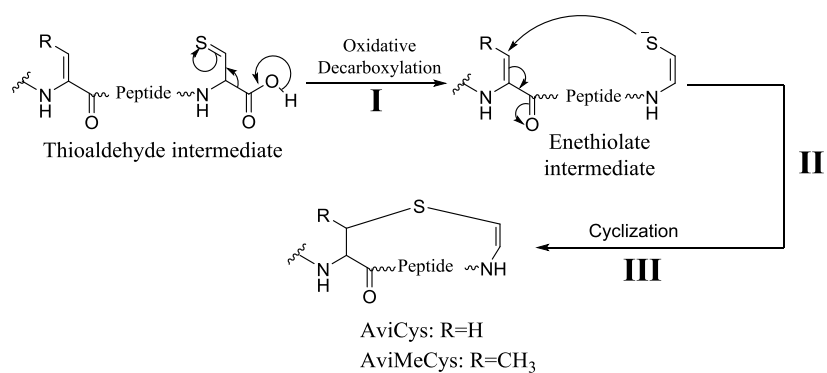


Figure 1.12. Comparison of microbisporicin DE ring system and cypemycin C-terminal ring

1.5. Biosynthesis of AviCys and AviMeCys

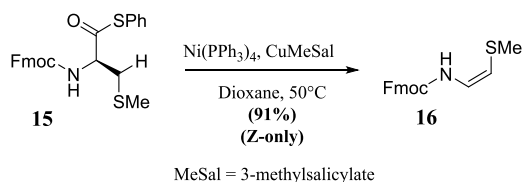
Biosynthesis of AviCys and AviMeCys occurs necessarily at the C-terminus of the peptide and is catalyzed by a family of enzymes called homo-oligomeric flavin-containing cysteine decarboxylases (HFCD).⁴¹⁻⁴⁵ These enzymes generate a thioaldehyde ($RCH=S$) in the side chain of the C-terminal cysteine. A flavin cofactor is involved in an oxidative decarboxylation (Step I), producing a reactive enethiolate anion (Scheme 1.2). This anion attacks, in a Michael addition, at a dehydroalanine (Dha) or a dehydrobutyrine (Dhb) upstream in the peptide (Step II) and forms the AviCys or AviMeCys residue respectively (Step III). Once post-translational modifications of the prepeptide are complete, an N-terminal leader peptide is cleaved and the mature peptide is transported out of the cell.



Scheme 1.2. Conceptualizing AviCys and AviMeCys biosynthesis

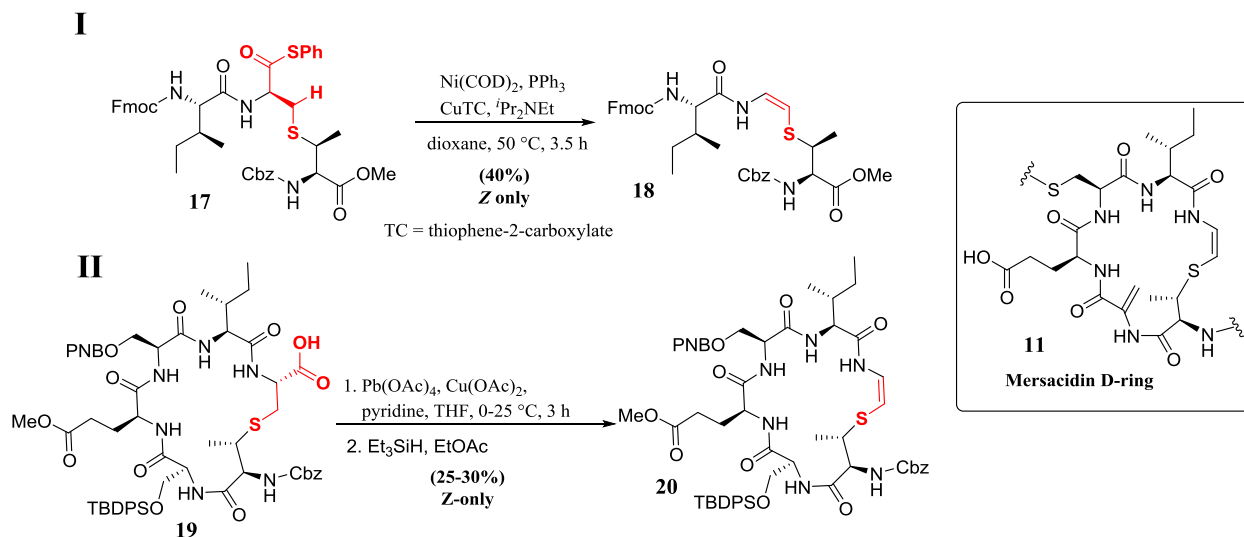
1.6. Previous Chemical Approaches to AviCys

VanNieuwenhze and coworkers described a pseudo-biomimetic approach involving decarbonylation of a thioester to give the necessary unsaturation.^{46,47} The method relies on the installation of a thioester that is eliminated under metal catalysis. They were able to achieve high yields in simple systems (Scheme 1.3).



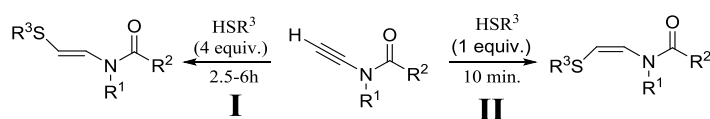
Scheme 1.3. VanNieuwenhze's thioenamide synthesis

However, when a model peptide **17**, mimicking the D-ring AviMeCys functionality of mersacidin, was subjected to the optimized conditions, the yield dropped drastically, albeit the reaction proceeded with favorable stereoselectivity (Scheme 1.4, equation I). When modified conditions were applied to the decarbonylation of the cyclic peptide **19** (Scheme 1.4, equation II), VanNieuwenhze and coworkers were able to achieve only a modest 30% yield. These conditions are promising, but low yields and the requirement for preformed lanthionines with suitable leaving groups makes incorporation into total synthesis a challenge.



Scheme 1.4. VanNieuwenhze synthesis of mersacidin D-ring analog

Castle and co-workers reported a method for thioenamide formation in 2010 by way of a thiyl radical reacting with a terminal ynamide.⁴⁸ They found that *E/Z*-selectivity could be controlled by reaction conditions (Scheme 1.5). Their examples showed that the product distribution was determined thermodynamically (path I) if the reaction was allowed to run long (2.5-6 h) and with excess thiol. These conditions led to the *E* isomer ($J = 13.6$ Hz) in as high a ratio as 33:1 with thiophenol (Scheme 1.5, $R^3 = \text{Ph}$).



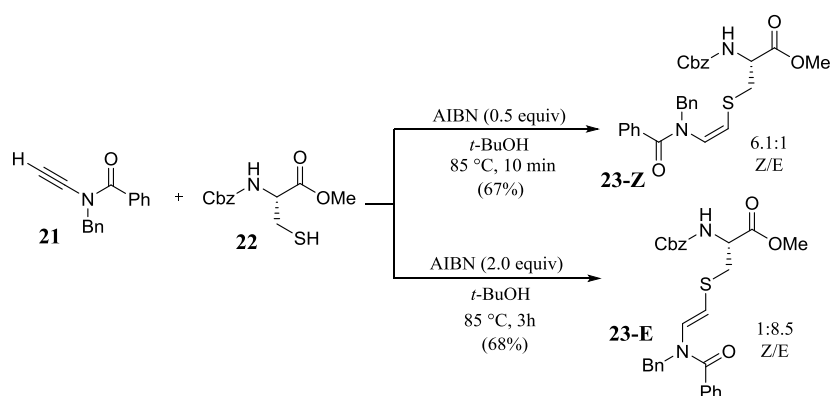
Scheme 1.5. Castle's method employing radical addition

However, kinetic control (path II) could be achieved with brief reaction times and a single equivalent of thiol. These conditions led to reliable production of the *Z*-thioenamide ($J = 7.9$ Hz for olefinic protons) in good yield with *Z:E* ratios as high as 11:1 in the case of *n*-butanethiol (Scheme 1.5, $R^3 = n\text{Bu}$). Castle makes note of a single example of an exceptionally bulky thiol,

^tBuSH, in which both sets of reaction conditions led to the *Z* product exclusively in reduced yield (41%).

In an attempt to place this method within the broader scope of peptide chemistry, Castle's group demonstrated that the control of *E/Z* selectivity translates well to cysteine-derived thiols (Scheme 1.6). While the ability to control which isomer is generated makes this an appealing method, the radical mechanism makes it troublesome in the context of complex peptides. Only tertiary ynamides were used in the study, presumably due to unwanted side reactions resulting from homolytic cleavage of the nitrogen-hydrogen bonds in non-tertiary amides. Additionally, there were no amino acid derived amides used in this study. Further functionalization of the amide nitrogen, aimed at producing peptidyl products, presents a significant challenge. No further reports have appeared from the Castle Group in this area.

The approaches of Castle and VanNieuwenhze described above are the only two published efforts at thioenamide synthesis with the aim of natural product peptides. While both methods have their benefits, a range of complementary approaches is often required to achieve total synthesis. The paucity of methods to generate AviCys hints at the considerable challenges in the formation of this unique and biomedically important functional group.



Scheme 1.6. Castle's thioenamide synthesis

1.7. Notes

1. Bentley, R., "Mycophenolic Acid: A One Hundred Year Odyssey from Antibiotic to Immunosuppressant," *Chem. Rev.*, **2000**, 100, 3801-3825.
2. Regueira, T.B.; Kildegaard, K.R.; Hansen, B.G.; Mortensen, U.H.; Hertweck, C.; Nielsen, J., "Molecular Basis for Mycophenolic Acid Biosynthesis in *Penicillium brevicompactum*," *App. Env. Microbiol.*, **2011**, 77, 3035-3043.
3. Kitchin, J. E.; Pomeranz, M. K.; Pak, G.; Washenik, K.; Shupack, J. L., "Rediscovering Mycophenolic Acid: A Review of its Mechanism, Side Effects, and Potential Uses," *J. Am. Acad. Dermatol.*, **1997**, 37, 445-449.
4. Wu, J. C. "Mycophenolate Mofetil: Molecular Mechanisms of Action," *Perspect. Drug Discov. Des.*, **1994**, 2, 185-204.
5. Williams, K.J., "The Introduction of 'Chemotherapy' Using Arsphenamine—The First Magic Bullet," *J. Royal Soc. Med.*, **2009**, 102, 343-348.
6. Rasmussen, D.H., "The Treatment of Syphilis," *Surv. Ophthalmol.*, **1969**, 14, 184-197.
7. Fleming, A. "The Antibacterial Action of Cultures of a *Penicillium*, with Special Reference to their Use in the Isolation of *B. influenzae*," *Brit. J. Exp. Pathol.*, **1929**, 10, 226-236.
8. Chain, E.; Florey, H.W.; Gardner, A.D.; Heatley, N.G.; Jennings, M.A.; Orr-Ewing, J.; Sanders, A.G., "Penicillin as a Chemotherapeutic Agent," *Lancet*, **1940**, II, 226-228.
9. Science History Institute. Alexander Fleming. <https://www.sciencehistory.org/historical-profile/alexander-fleming> (accessed January 10th, 2019).
10. Nicolaou, K.C.; Rigol, S., "A Brief History of Antibiotics and Select Advances in Their Synthesis," *J. Antibiot.*, **2018**, 71, 153-184.
11. eMed Expert. Interesting Facts about Antibiotics. <https://www.emedexpert.com/tips/antibiotics-facts.shtml> (accessed January 14th, 2019).
12. Ghuysen, J.M., "Molecular Structures of Penicillin-Binding Proteins and beta-Lactamases," *Trends Microbiol.*, **1994**, 10, 372-380.
13. Park, J.T.; Uehara, T., "How Bacteria Consume Their Own Exoskeletons (Turnover and Recycling of Cell Wall Peptidoglycan)," *Microbiol. Mol. Biol. Rev.*, **2008**, 72, 211-227.
14. Nguyen-Distèche, M.; Leyh-Bouille, M.; Ghuysen J.M., "Isolation of the Membrane-Bound 26,000-Mr Penicillin-Binding Protein of *Streptomyces* Strain K15 in the Form of a Penicillin-Sensitive D-alanyl-D-alanine-Cleaving Transpeptidase," *Biochem. J.*, **1982**, 207, 109-115.

15. Abraham, E.P.; Chain, E., "An Enzyme from Bacteria Able to Destroy Penicillin," *Nature*, **1940**, 146, 837.
16. Knott-Hunziker, V.; Waley, S.G.; Orlek, B.S.; Sammes P.G., "Penicillinase Active Sites: Labeling of Serine-44 in beta-Lactamase I by 6-beta-Bromopenicillanic Acid," *FEBS Lett.*, **1979**, 99, 59-61.
17. Munita, J. M.; Arias, C.A., "Mechanisms of Antibiotic Resistance," *Microbiol. Spectr.*, **2016**, 4, 1-24.
18. Hooper, D. C., "Emerging Mechanisms of Fluoroquinolone Resistance," *Emerg. Infect. Dis.*, **2001**, 7, 337-341.
19. Hiasa, H.; Yousef, D.O.; Mariani, K.J., "DNA Strand Cleavage is Required for Replication Fork Arrest by a Frozen Topoisomerase-Quinolone-DNA Ternary Complex," *J. Biol. Chem.*, **1996**, 271, 26424-26429.
20. Willmott, C.J.; Maxwell, A., "A Single Point Mutation in the DNA Gyrase A Protein Greatly Reduces Binding of Fluoroquinolones to the Gyrase-DNA Complex," *Antimicrob. Agents Chemother.*, **1993**, 37, 126-127.
21. Berger, J.M.; Gamblin, S.J.; Harrison, S.C.; Wang, J.C., "Structure and Mechanism of DNA Topoisomerase II," *Nature*, **1996**, 379, 225-232.
22. Chukwudi, C.U., "rRNA Binding Sites and the Molecular Mechanism of Action of the Tetracyclines," *Antimicrob. Agents Chemother.*, **2016**, 60, 4433-4441.
23. Levy, S.B., "Active Efflux Mechanism for Antimicrobial Resistance," *Antimicrob. Agents Chemother.*, **1992**, 36, 695-703.
24. Velkov, T.; Roberts, K.D.; Nation, R.L.; Philip, E.; Li, J., "Pharmacology of Polymixins: New Insights into an 'Old' Class of Antibiotics," *Future Microbiol.*, **2013**, 8, 711-724.
25. Trent, M.S.; Ribeiro, A. A.; Lin, S.; Cotter, R.J.; Raetz, C.R.H., "An Inner Membrane Enzyme in *Salmonella* and *Escherichia coli* that Transfers 4-Amino-4-deoxy-L-arabinose to Lipid A. Induction in Polymixin-Resistant Mutants and Role of a Novel Lipid-Linked Donor," *J. Biol. Chem.*, **2001**, 276, 43122-43131.
26. Health Research Funding. 11 Scary Statistics on Antibiotic Resistance. <https://healthresearchfunding.org/11-scary-statistics-on-antibiotic-resistance/> (accessed January 26th, 2019).
27. Delves-Broughton, J.; Blackburn, P.; Evans, R. J.; Hugenholtz, J., "Applications of the Bacteriocin, Nisin," *Antonie van Leeuwenhoek*, **1996**, 69, 193-202.
28. Brötz, H.; Josten, M.; Wiedemann, I.; Schneider, U.; Götz, F.; Bierbaum, G.; Sahl, H.G., "Role of Lipid-Bound Peptidoglycan Precursors in the Formation of Pores by Nisin, Epidermin and Other Lantibiotics," *Mol. Microbiol.*, **1998**, 30, 317-327.

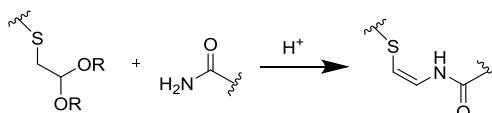
29. Zhou, H.; Fang, J.; Tian, Y.; Lu, X.Y., "Mechanisms of Nisin Resistance in Gram-Positive Bacteria," *Ann. of Microbiol.*, **2014**, 64, 413-420.
30. Lazzarini, A.; Gastaldo, L.; Candiani, G.; Ciciliato, I.; Losi, D.; Marinelli, F.; Selva, E.; Parenti, F. "Antibiotic 107891, its Factors A1 and A2, Pharmaceutically Acceptable Salts and Compositions, and Use Thereof," International Publication Number WO 20050233952 A1 20051020, International Publication Date 17 February **2005**.
31. Drugs.com website for vancomycin hydrochloride:
<https://web.archive.org/web/20150906002445/http://www.drugs.com/monograph/vancocin.html> (accessed July 2nd, 2019).
32. Castiglione, F.; Lazzarini, A.; Carrano, L.; Corti, E.; Ciciliato, I.; Gastaldo, L.; Candiani, P.; Losi, D.; Marinelli, F.; Selva, E.; Parenti, F. "Determining the Structure and Mode of Action of Microbisporicin, a Potent Lantibiotic Active Against Multiresistant Pathogens," *Chem. Biol.*, **2008**, 15, 22-31.
33. Maffioli, S.I.; Iorio, M.; Sosio, M.; Monciardini, P.; Gaspari, E.; Donadio, S. "Characterization of the Congeners in the Lantibiotic NAI-107 Complex," *J. Nat. Prod.*, **2014**, 77, 79-84.
34. Cruz, J.C.S.; Iorio, M.; Monciardini, P.; Simone, M.; Brunati, C.; Gaspari, E.; Maffioli, S.I.; Wellington, E.; Sosio, M.; Donadio, S. "Brominated Variant of the Lantibiotic NAI-107 with Enhanced Antibacterial Potency," *J. Nat. Prod.*, **2015**, 78, 2642-2647.
35. Kellner, R.; Jung, G.; Horner, T.; Zaehner, H.; Schnell, N.; Entian, K. D.; Goetz, F. "Gallidermin: a New Lanthionine-Containing Polypeptide Antibiotic," *Eur. J. Biochem.*, **1988**, 177, 53-59.
36. Chatterjee, S.; Chatterjee, S.; Lad, S.J.; Shashikant, J.; Phansalker, M. S.; Rupp, R. H.; Ganguli, B. N.; Fehlhaber, H. W.; Kogler, H., "Mersacidin, a New Antibiotic from *Bacillus*: Fermentation, Isolation, Purification, and Chemical Characterization," *J. Antibiot.*, **1992**, 45, 832-838.
37. Komiyama, K.; Otoguro, K.; Segawa, T.; Shiomi, K.; Yang, H.; Takahashi, Y.; Hayashi, M.; Otani, T.; Omura, S. "A New Antibiotic, Cypemycin - Taxonomy, Fermentation, Isolation and Biological Characteristics," *J. Antibiot.*, **1993**, 46, 1666-1671.
38. Hayakawa, Y.; Sasaki, K.; Nagai, K.; Shin-ya, K.; Furihata, K. "Structure of Thioviridamide, a Novel Apoptosis Inducer From *Streptomyces olivoviridis*," *J. Antibiot.*, **2006**, 59, 6-10.
39. Cotter, P. D.; Hill, C.; Ross, R. P. "Bacterial Lantibiotics: Strategies to Improve Therapeutic Potential," *Curr. Protein Pept. Sci.*, **2005**, 6, 61-75.
40. Minami, Y.; Yoshida, K.; Azuma, R.; Urakawa, A.; Kawauchi, T.; Otani, T., "Structure of Cypemycin, a New Peptide Antibiotic," *Tetrahedron Lett.*, **1994**, 35, 80001-80004.

41. Repka, L.M.; Chekan, J.R.; Nair, S. K.; van der Donk, W. A., "Mechanistic Understanding of Lanthipeptide Biosynthetic Enzymes," *Chem. Rev.*, **2017**, 117, 5457-5520.
42. Sit, C.S.; Yoganathan, S.; Vederas, J.C., "Biosynthesis of Aminovinyl-Cysteine-Containing Peptides and Its Application in the Production of Potential Drug Candidates," *Acc. Chem. Res.* **2011**, 44, 261-268.
43. Liu, L.; Chan, S.; Mo, T.; Ding, W.; Yu, S.; Zhang, Q.; Yuan, S., "Movements of the Substrate-Binding Clamp of Cypemycin Decarboxylase CypD," *J. Chem. Inf. Model*, **2019**, 59, 2924-2929.
44. Ding, W.; Yuan, N.; Mandalapu, D.; Mo, T.; Dong, S.; Zhang, Q., "Cypemycin Decarboxylase CypD is not Responsible for Aminovinyl-cysteine (AviCys) Ring Formation," *Org. Lett.*, **2018**, 20, 7670-7673.
45. Mo, T.; Liu, W.; Ji, W.; Zhao, J.; Chen, T.; Ding, W.; Yu, S.; Zhang, Q., "Biosynthetic Insights into Linaridin Natural Products from Genome Mining and Precursor Peptide Mutagenesis," *ACS Chem. Biol.*, **2017**, 12, 1484-1488.
46. Garcia-Reynaga, P.; Carrillo, A.; VanNieuwenhze, M. "Decarbonylative Approach to the Synthesis of Enamides from Amino Acids: Stereoselective Synthesis of the (Z)-Amino-D-Cysteine Unit of Mersacidin," *Org. Lett.*, **2012**, 14, 1030-1033.
47. Carrilo, A. K.; VanNieuwenhze, M.S. "Synthesis of the AviMeCys-containing D-ring of Mersacidin," *Org. Lett.*, **2012**, 14, 1034-1037.
48. Banerjee, B.; Litvinov, D.; Kang, J.; Bettale, J.; Castle, S. "Stereoselective Additions of Thiyl Radicals to Terminal Ynamides" *Org. Lett.*, **2010**, 12, 2650-2652.

Chapter 2. Acid-Promoted (Thio)Enamide Formation

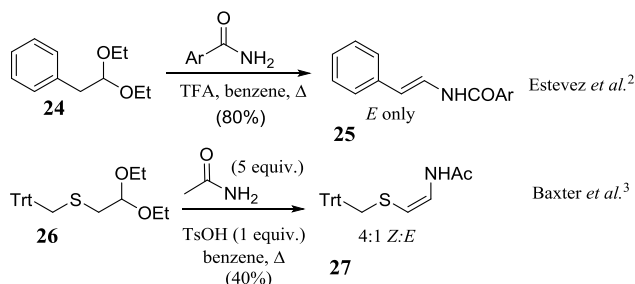
2.1. Acid-Mediated (Thio)Enamide Formation

We envisioned an alternative approach to thioenamide formation consisting of condensation of an amide with an acetal followed by elimination (Scheme 2.1). Despite the first report of such a reaction as early as 1953,¹ there are very few examples in the literature since and the influence of the substrate structure on the stereochemical outcome was unstudied.



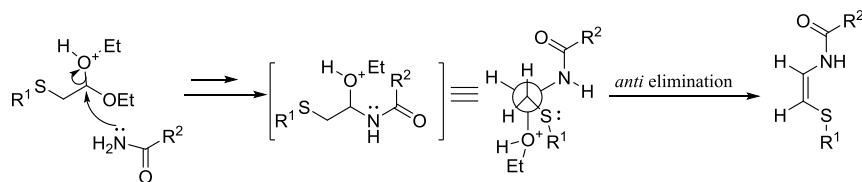
Scheme 2.1. Generic acid-mediated thioenamide formation

Two examples encouraged us to believe that we could achieve the desired *cis* stereochemistry through electronic effects (Scheme 2.2).^{2,3} The noteworthy difference in the work of Baxter, relative to that of Estevez, is a β -sulfur substituent, which reverses the stereoselectivity of the reaction.



Scheme 2.2. Precedent for influence of β -substituent on stereochemical outcome

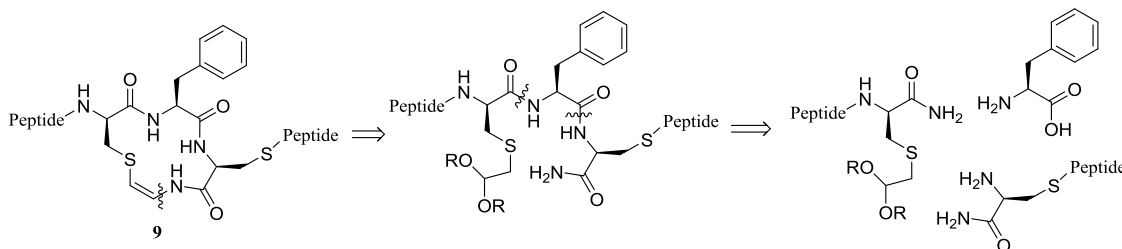
We hypothesized that the sulfur atom influences the transformation to be *Z*-selective through a preferred conformation with inherent gauche interactions between the electronegative atoms during the elimination step.⁴ *Anti* elimination from this conformation would yield selectively the *cis* product (Scheme 2.3).



Scheme 2.3. Originally proposed mechanism for Z-enamide formation

2.2. Early Design of a Tripeptide Substrate for Thioenamide Formation

At the outset it was ambitiously envisioned that the key reaction would take place via an intramolecular reaction in a preformed tripeptide (Scheme 2.4). This strategy would allow us to perform the more pedestrian reactions such as amine and carboxylic acid deprotection as well as peptide bond formation before generation of our thioenamide. Additionally, the ring strain of potential transition states during thioenamide generation/cyclization would reinforce our desired *cis* stereochemistry about the olefinic bond.



Scheme 2.4. Retrosynthetic analysis of the E-ring of microbisporicin

To study the macrocyclization reaction, a tripeptide was designed that would mimic the amino acid sequence found in the microbisporicin E-ring (Scheme 2.4 and Figure 2.1) but would not introduce the complexities of the larger peptide. This required:

- (a) a cysteine bearing an acetal-functionalized side chain;
- (b) *N*-terminal protection that reduces the nucleophilicity of the *N*-terminal amine and thus prevents competing reaction with acetal;
- (c) an amide at the *C*-terminus; and

(d) alaninamide (H-L-Ala-NH₂) to be used as a substitute for H-L-Cys-NH₂ to reduce complexity relative to the native sequence

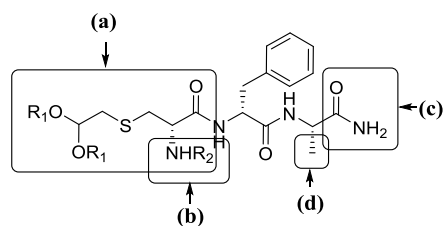


Figure 2.1. Model tripeptide for initial studies

2.3. Synthesis of the Acetal-Functionalized Cysteine Residue

Cysteine building block **28** (Figure 2.2) was designed to fulfil our criteria. An allyl group was chosen for protection of the carboxylic acid due to the non-acidic conditions used in cleavage.

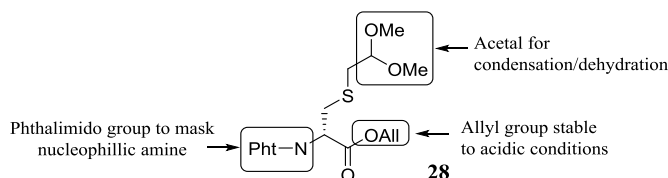
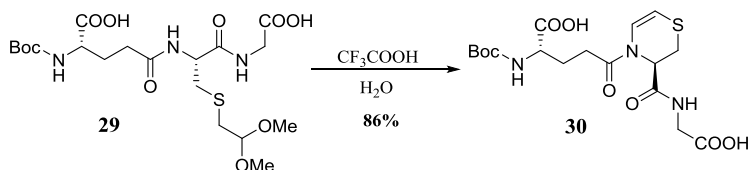


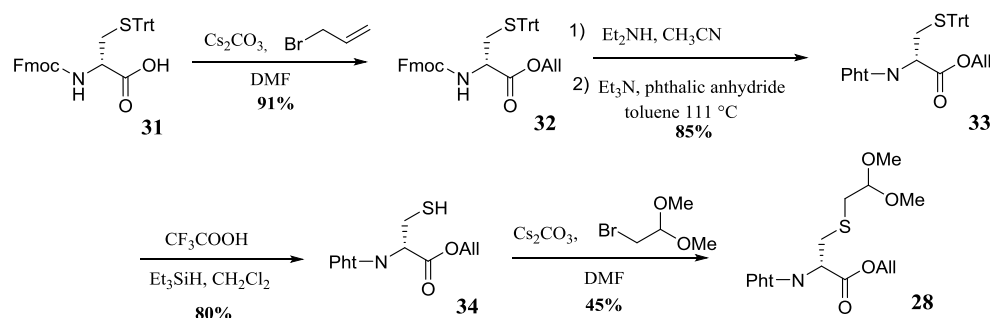
Figure 2.2. Acetal-modified cysteine

A dimethoxy acetal was chosen due to commercial availability of starting materials and based on the work of Carter and Mash in which a thioenamide was formed intramolecularly (Scheme 2.5).⁵ This example shows that even a secondary amide can react in high yields in the context of a 6-membered ring. Based on this precedent, a phthalimido group was chosen for divalent amine protection.



Scheme 2.5. Thioenamide formation by Carter and Mash

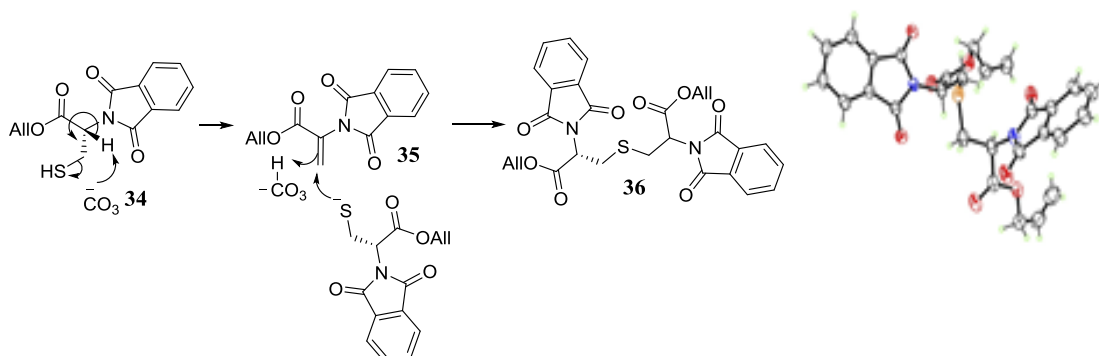
The first task involved replicating and optimizing the work of a previous group member, Katie Moreaux. Synthesis of the requisite cysteine derivative began with commercially available Fmoc-D-Cys(Trt)-OH (**31**). Treatment with cesium carbonate and allyl bromide afforded allyl ester **32** in good yield (Scheme 2.6). This was followed by deprotection of the amine using diethylamine and reprotection with phthalic anhydride, assisted by triethylamine. Originally, Fmoc removal was performed using piperidine and the free amine purified before reprotection. However, it was found that amine deprotection using the more volatile diethylamine eliminated the need for purification before reprotection and resulted in better overall yields of cysteine derivative **33**. Detritylation of the side chain thiol using trifluoroacetic acid and triethylsilane as a trityl cation scavenger gave free thiol **34**. Monitoring the deprotection was difficult due to the trityl ether **33** and the free thiol **34** being indistinguishable via TLC. The reaction progress needed to be monitored via ^1H NMR, observing the generation of the thiol proton as a doublet of doublets at 1.54 ppm. Alkylation of the thiol was accomplished in mediocre yield using cesium carbonate and 2-bromo-1,1-dimethoxyethane to render target building block **28**.



Scheme 2.6. Synthesis of suitably protected cysteine

The low yield of the alkylation can be partly attributed to the formation of the dimeric side product **36** whose structure was confirmed by X-ray crystallography (Scheme 2.7). This side product is likely the result of dehydroalanine formation followed by 1,4-addition of a

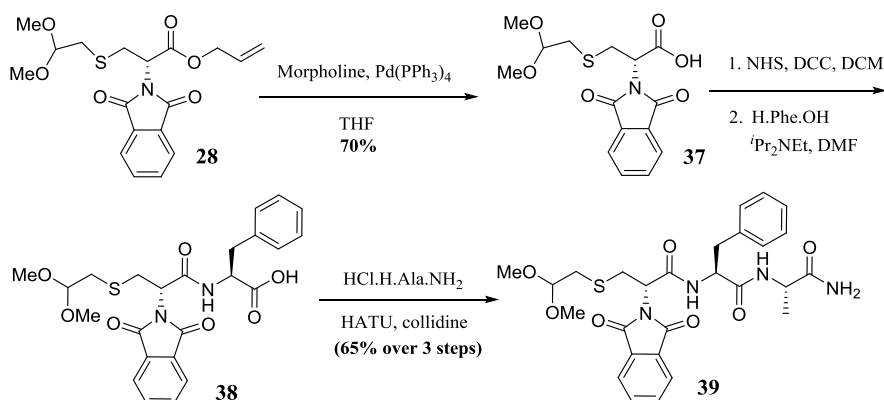
thiolate anion. Unfortunately, extensive attempts to optimize the alkylation reaction further were unsuccessful.



Scheme 2.7. Mechanism for formation of dimerization side product 36 in S-alkylation reaction

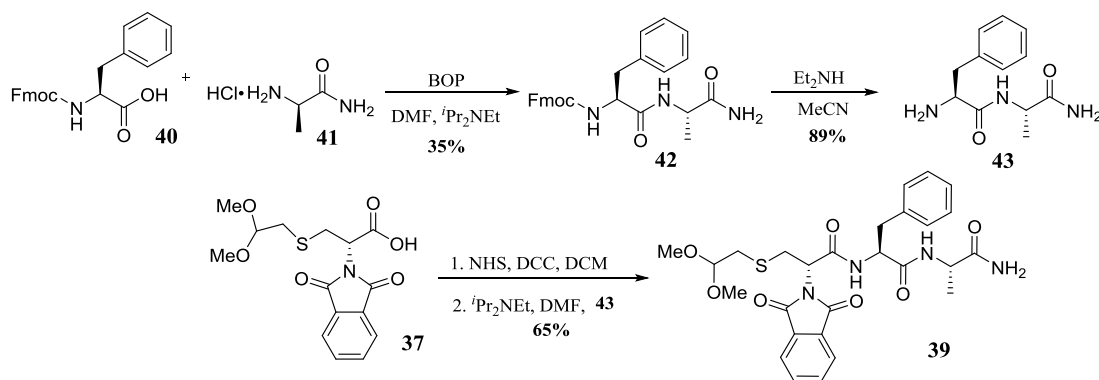
2.4. Model Tripeptide Synthesis

Acetal-bearing cysteine **28** was incorporated into the model tripeptide system required for the intramolecular formation of AviCys (Scheme 2.8). Selective deprotection of the allyl ester was accomplished using catalytic palladium (0). Free acid **37** was activated as its *N*-hydroxysuccinimide (NHS) ester, followed by coupling with *L*-phenylalanine. The dipeptide acid was then coupled with alaninamide to give the desired tripeptide **39**. The transformation from free acid **37** to tripeptide **39** was accomplished in 65% yield over two steps, but analysis by HPLC revealed the presence of at least three distinct compounds, inseparable by flash chromatography. These compounds were each found to have the same mass by LC-MS. We explored a different approach to tripeptide **39** in the hope that this would give a single product.



Scheme 2.8. Synthesis of model tripeptide

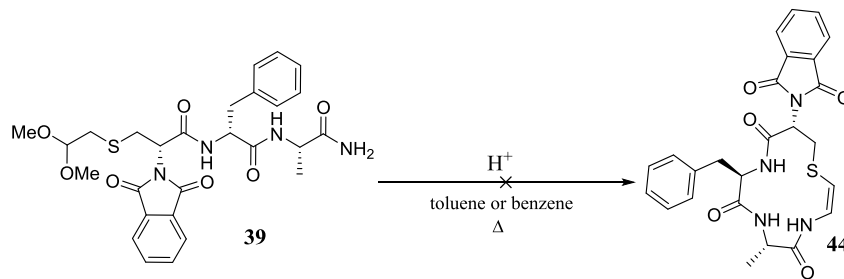
A second approach to tripeptide formation proved more effective (Scheme 2.9). Coupling of Fmoc-Phe-OH (**40**) and alaninamide (**41**) afforded an Fmoc-protected dipeptide (**42**), albeit in low yield. Deprotection of the amine to give dipeptide **43** and coupling with cysteine building block **37**, led to the desired tripeptide (**39**) in good yield, although the HPLC trace of this material still revealed two major compounds (with the same M^+), which were again not separable by flash chromatography. While we were not able to achieve homogenous tripeptide, it proved to be the preferred method for tripeptide formation.



Scheme 2.9. Second Generation synthesis of tripeptide

We next attempted the intramolecular dehydrative condensation/cyclization of model tripeptide **39** (Scheme 2.10). Most often, mixtures of the two isomeric species of **39** were used for cyclization studies. Following literature examples, a protic acid (TFA or *p*TsOH) in an

aromatic solvent (benzene or toluene) was used to promote the desired reaction.^{2,3} Unfortunately, significant degradation occurred and neither starting material **39** nor desired product **44** was ever isolated from the reaction mixture. It was clear that our proposed mechanistic pathway for thioenamide generation needed to be better understood in order to achieve a useful transformation in practice.

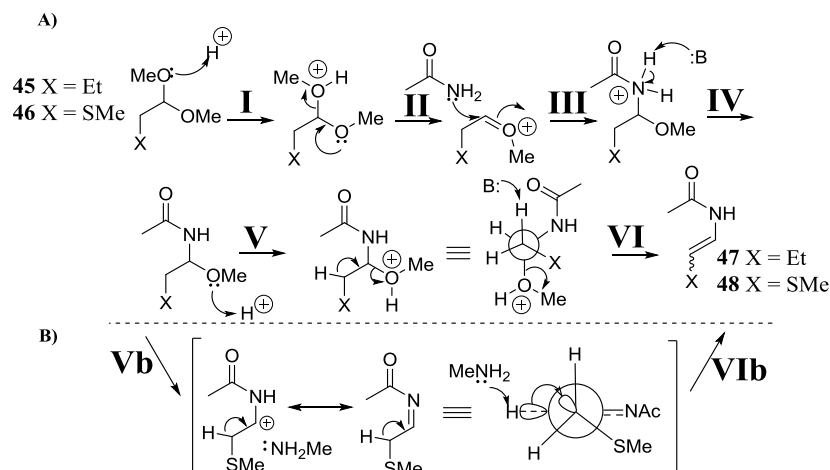


Scheme 2.10. Intramolecular AviCys formation

2.5. Mechanistic Investigations

Inspired by the examples in Scheme 2.2, we studied the mechanistic basis for the stereochemical phenomenon in regard to acid-mediated, stereoselective *Z*-thioenamide formation. Computational studies were performed, in collaboration with Visal Don Subasinghe and Dr. Revati Kumar, for the two simplified substrates shown in Scheme 2.11 on the pathway of the reaction mechanism.

The thioether, in the β -position relative to the acetal, is instrumental in determining the stereochemical outcome. The two electronegative groups at C_α will favor a gauche relationship with the C_β -S substituent, promoting *anti*-elimination from the conformer drawn in step VI (Scheme 6, A).⁴ In the absence of an electronegative β -substituent the energy difference between the relevant conformations is reduced allowing sterics to play a much larger role and likely favoring the *E*-product.



Scheme 2.11. A. Proposed mechanism for thioenamide formation; B. Variations revealed by calculations

Relative energies of reactants, transition states and products were determined for Steps I-VI. Steps I and II were found to be concerted. Step III displayed no unexpected behavior. Steps IV and V were also found to be concerted and, indeed, to proceed further to a delocalized cationic species (Step Vb). Stabilization is observed by donation of the lone pair of the nitrogen into the empty p-orbital, as shown in Scheme 2.11B.

The two series showed minimal variations in energetics and no difference in orientations until Step VI. The intermediacy of a carbocation in both cases is suggestive of an E1-like mechanism. At this key juncture in the calculations, methylamine was used as a base to assist proton abstraction: the intermediate cation derived from acetal **45** loses a proton, with no transition state, leading rapidly to the *E*-isomer. In contrast, for this step in the reaction of **46**, there is a discernable transition state in which there has been rotation about the C-C bond, leading to a conformation in which the transition state is stabilized, by an additional 4.04 kcal mol⁻¹, by hyperconjugative donation from the σ -orbital of the C-H bond into the σ^* -orbital of the adjacent C-S bond. This is consistent with our original hypothesis that there is a rotational barrier to elimination, leading to a hyperconjugative stabilization of electronegative substituents.

Interestingly, Natural Bond Orbital (NBO) analyses⁶ revealed a partial positive charge on the sulfur atom of the final product **48**. This charge generates an electrostatic attraction with both the oxygen and the nitrogen of the newly formed enamide, stabilizing the *Z*-isomer by 1.8 kcal mol⁻¹ relative to the *E*-isomer. More details on these calculations can be found in our published work.⁷

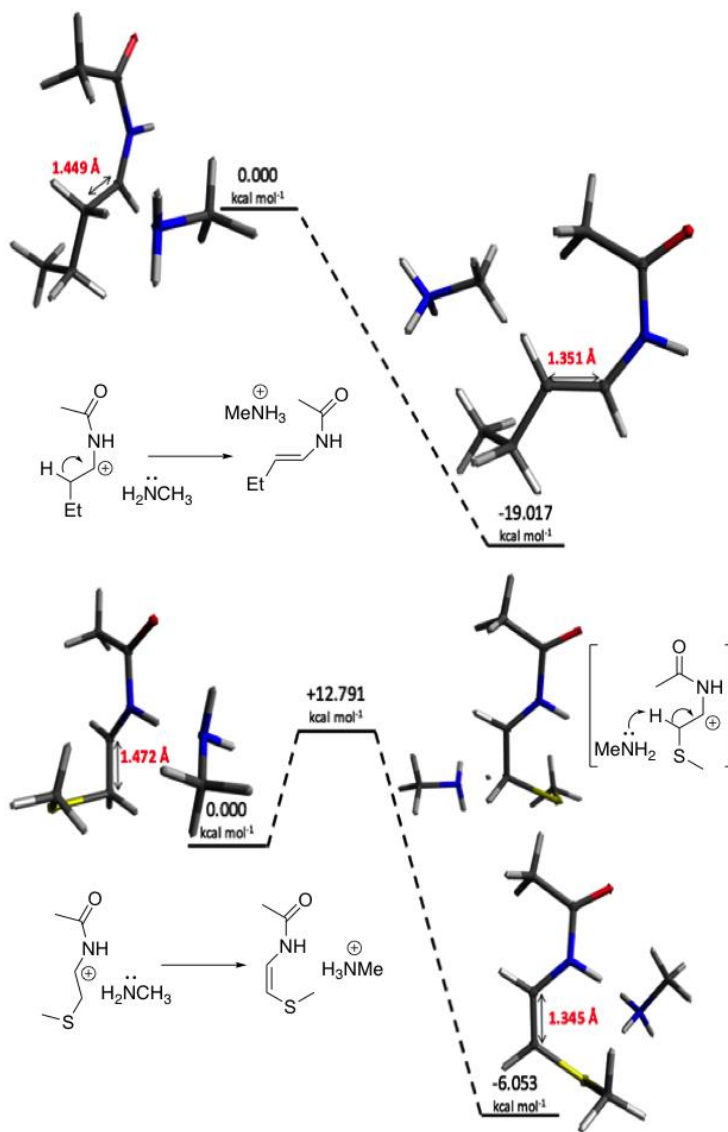
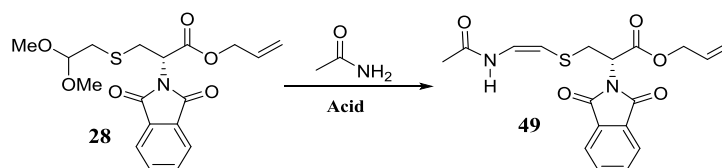


Figure 2.3. Energy profile diagram for step VIa

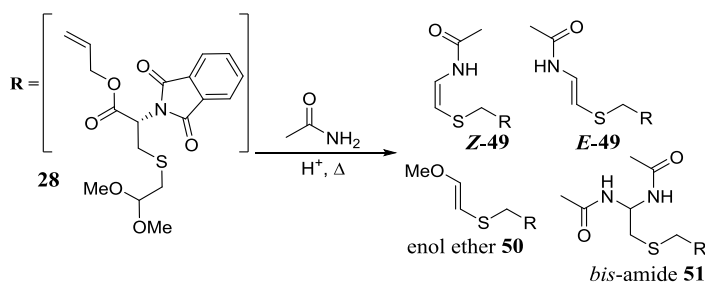
2.6. Condensations with Acetamide

With insight from our computational studies we began condensations using previously prepared cysteine **28** and acetamide (Scheme 2.12), by analogy to both Baxter's work and with insight from our modeled reactions.



Scheme 2.12. General acetamide condensation

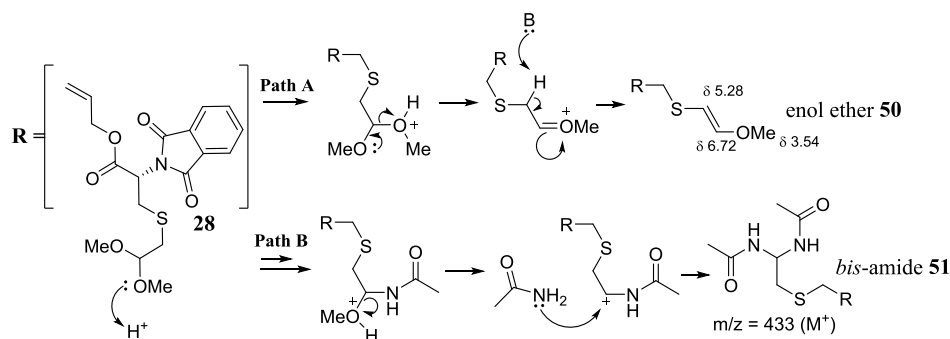
Experiments began with equimolar amounts of cysteine building block **28** and *p*TsOH.H₂O. Baxter employed an acetal concentration of 1 mg/mL in benzene, and this also worked well for our study. Attempts to raise the overall reaction concentration resulted in lower yields. The anticipated products, *Z*- and *E*-**49**, were isolated in a 4:1 ratio; *Z*-**49** could be isolated pure in 40% yield (Scheme 2.13). This assignment of stereochemistry is based on the coupling constants for the olefinic protons: 7.4 Hz (*Z*) and 13.6 Hz (*E*).^{8,9,10}



Scheme 2.13. Condensation of **28** with acetamide

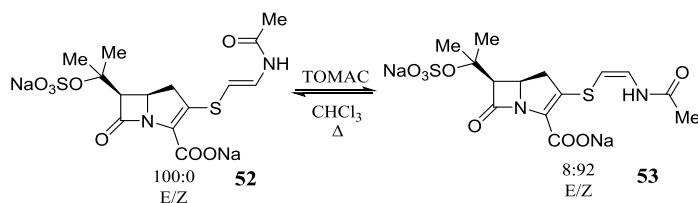
A minor product of the reaction mixture was vinyl methyl ether **50** (16%), resulting from premature elimination of methanol from the oxocarbenium intermediate (Scheme 2.14, path A). The assignment of this structure was made based both on the ¹H NMR peak at 3.54 ppm (methyl ether) as well as the *trans*-olefinic protons at 5.28 and 6.72 ppm split only once each, with a

coupling constant of 10.0 Hz. Additionally, *bis*-amide **51** arising from two sequential additions of acetamide (Scheme 2.14, path B), could be observed in trace amounts, as evidenced by mass spectrometry.



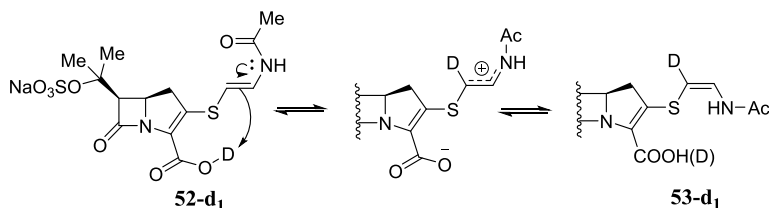
Scheme 2.14. Formation of enol ether and bis-amide side products and pertinent spectroscopic data

Interestingly, the *E*-isomer was difficult to obtain pure and equilibrated to a mixture of *E*- and *Z*-isomers, upon standing, even at low temperature. Harada *et al.* previously reported conversion of carbapenem antibiotics containing *E*-thioenamide side chains, to the corresponding *Z*-isomers (Scheme 2.15).¹¹ Starting with **52**, an *E*-thioenamide-containing carbapenem isolated from nature, they were able to shift the position of the *E/Z* equilibrium significantly using quaternary ammonium halide salts at reflux in chloroform. The optimal ammonium salt for this conversion was tetraoctyl methyl ammonium chloride (TOMAC), converting the material to the *cis* isomer in 92% yield.



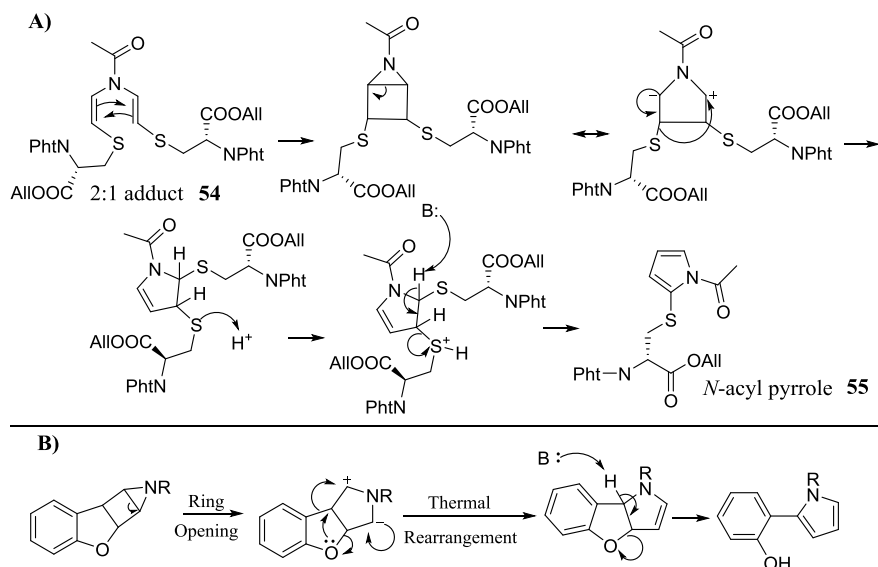
Scheme 2.15. Harada's conversion to *cis*-thioenamide

Deuteration of the carboxylic acid before isomerization (Scheme 2.16) led to 84% deuterium incorporation at the olefinic position adjacent to the sulfur, leading Harada *et al.* to conclude that proton exchange takes place intramolecularly. Using this information, they proposed the mechanism in Scheme 2.16 whereby the nitrogen lone pair stabilizes a positive charge in the pi system as the pi electrons abstract the acidic proton of the carboxylic acid.



Scheme 2.16. Harada's proposed mechanism of isomerization

With a view to employing more synthetically valuable amides in the future, we scaled back to a stoichiometric amount of acetamide. This led to the formation of 2:1 adduct **54** (Scheme 2.17A), in 81% yield, testifying to the increased nucleophilicity of the enamide **49** over acetamide. The ¹H NMR spectrum indicated two distinct coupling constants for the two sets of olefinic protons, 14.6 and 11.4 Hz. The second elimination appears to be under steric control, affording the *E*-enamide. If the reaction was allowed to run overnight, under these conditions, *N*-acyl pyrrole **55** could be isolated in 38% yield. The identification of the pyrrole structure was consistent with aromatic signals in the ¹H NMR spectrum at 6.25, 7.14, and 7.25 ppm, and with splitting patterns characteristic of pyrroles substituted at the 2-position. We propose that the 2:1 adduct undergoes pericyclic ring closure followed by a thermal rearrangement, analogous to a transformation reported by Kurita *et al.* (Scheme 2.17B).¹²

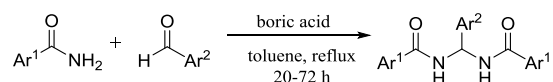


Scheme 2.17. A. Mechanism for formation of pyrrole **51** from 2:1 adduct **54** B. Analogous mechanism proposed by Kurita

We investigated a range of acids vis-à-vis our desired transformation. A key advance was the discovery that a Lewis acid, boron trifluoride diethyl etherate, was effective. Catalytic and equimolar amounts of $\text{BF}_3 \cdot \text{OEt}_2$ were insufficient to produce the desired product in useful amounts. When the number of equivalents of Lewis acid was increased to five, consumption of starting material occurred rapidly and the yield increased beyond that achieved with protic acids (*e.g.*, pTsOH and TFA). Elimination of the second equivalent of methanol occurs more quickly and the vinyl ether does not form at all under these conditions. Product formation occurs in 40-45% with a 5:1 *Z:E* ratio in only 40 minutes but further reaction/degradation of the product is observed if the reaction is continued longer. While the reaction time and yield of desired product were improved with $\text{BF}_3 \cdot \text{Et}_2\text{O}$, only trace amounts of known side products were observed via crude ^1H NMR and no starting material was recovered.

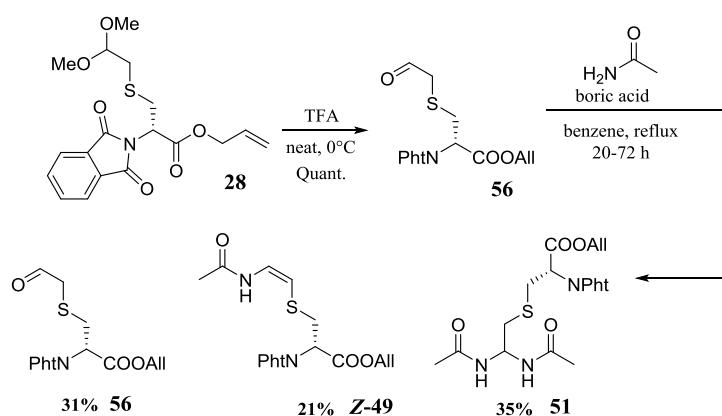
In an attempt to modulate the ratio of desired reactivity versus degradation, a milder Lewis acid was studied. Boric acid is a remarkably inexpensive reagent (~11¢/g) that has been used by Harichandran *et al.* to catalyze the generation of *bis*-amides (Scheme 2.18).¹³ They

showed that *bis*-amides could be formed from a range of aldehydes and amides with only 15 mole percent boric acid in toluene.



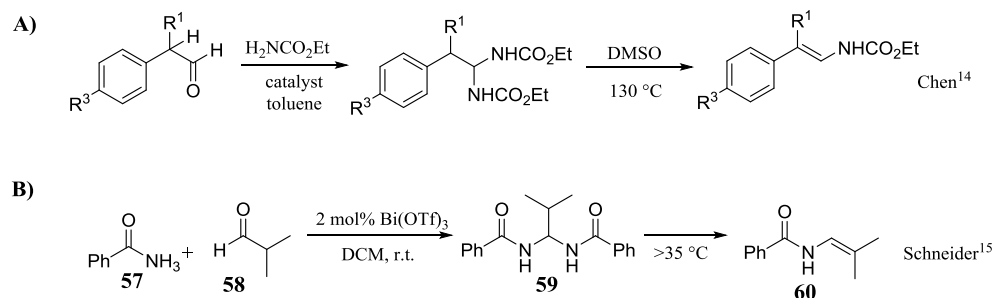
Scheme 2.18. Harichandran's aromatic bis-amide formation

As expected, boric acid was not acidic enough to activate acetal **28**, in our case, and only trace amounts of product were formed. Revealing aldehyde **56** prior to condensation/dehydration (Scheme 2.19) serves two purposes: elimination of the potential methyl vinyl ether side product and lowering the required acidity to promote the desired reaction. When aldehyde **56** was reacted with acetamide and boric acid in benzene, the desired *Z*-product was isolated in 21% yield along with recovered aldehyde starting material **56** (31%) and *bis*-amide **51** (35%).



Scheme 2.19. Reaction of aldehyde **56** with acetamide and boric acid in benzene

Chen *et al.* heated *bis*-amides in DMSO to convert them to their corresponding enamides (Scheme 2.20A).¹⁴ Schneider *et al.* investigated a simple two component system (Scheme 2.20B) on their way towards three component amido substitution using amides and aldehydes.¹⁵



Scheme 2.20. Enamide formation

They found that *bis*-amide formation occurs rapidly at room temperature, but elimination occurs rapidly to generate the enamide at temperatures above 35 °C. We leveraged these facts and changed our solvent to toluene to simultaneously decrease the formation of *bis*-amide and increase reactivity to consume all the aldehyde. It was found that commencing the reaction with a single equivalent of acetamide, and adding additional equivalents over time also reduced the formation of *bis*-amide. With these modifications to the method, the yield of desired product was increased to 57% with an isolated *Z*:*E* ratio of 8:1 (Table 2.1). These optimized conditions are summarized with some of the other conditions investigate in Table 2.1.

Table 2.1. Thioenamide formation

	Reaction Conditions	Z-49	E-49	56	50	51
1	Protic acid (TFA or pTsOH), benzene, 80 °C, 4 h	40%	10%	0%	16%	trace
2	Boron trifluoride, benzene, 80 °C, 45 min	45%	8%	0%	0%	0%
3	Boric acid, benzene, 80 °C, 5 d	21%	not isolated	31%	N/A	35%
4	Boric acid, toluene, 111 °C, 2 d	57%	6%	0%	N/A	0%

We speculate that the increase in desired reactivity with Lewis acids is the result of their ability to coordinate to both the amide nucleophile and the aldehyde electrophile. Protic acids lack this ability to generate a six-membered ring transition state template for the transformation (Figure 2.4).

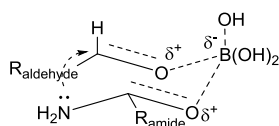


Figure 2.4. Coordinated transition state with Lewis acid

In summary, we described a new chemical approach to the synthesis of *Z*-thioenamides that involves condensation of an aldehyde and amide under mild, Lewis acidic conditions at elevated temperatures. Based on stereoelectronic predictions, and supported by computational insights into the mechanism of the addition-elimination reaction, the approach capitalizes on sulfur's electronic properties to steer the reaction via a mechanism whereby it further supports a preferred conformation that leads to stereoselective formation of the *Z*-product. Careful manipulation of reagents and reaction conditions subsequently led to an increase in yield and stereoselectivity of the desired reaction.

2.7. Experimental Procedures

2.7.1. General Methods

All reactions were performed under a dry nitrogen atmosphere unless otherwise noted. Reagents were obtained from commercial sources and used directly; exceptions are noted. Diethylamine and triethylamine were dried, distilled from CaH₂, and stored over KOH pellets. Flash chromatography was performed using flash silica gel (40-63 μ) from Aldrich Inc. Reactions were followed by TLC on pre-coated silica plates (200 μ, F-254, from Merck Inc.). The compounds were visualized by UV fluorescence or by staining with KMnO₄, iodine, or

ninhydrin. HPLC was performed on a Waters 600 system, interfaced with EmpowerTM software, and equipped with a Waters 2487 UV detector, monitoring absorption at 218 and 254 nm. All columns were 250 mm long. Analytical work was conducted on 4.6 mm diameter columns with a flow rate of 1 mL min⁻¹: Daicel® Chiralcel OD-H (chiral), Econosil® silica 10 μ (normal phase), or Altima® C18 10 μ (RP). Semi-preparative RP work was conducted on a 10 mm diameter Altima® C18 10 μ column with a flow rate of 3 or 4 mL min⁻¹. Eluents for HPLC work are detailed in each procedure. Nuclear Magnetic Resonance spectra were recorded on a Bruker AV-400 Nanobay or a Bruker AV-500 Prodigy liquid spectrometer. Proton NMR data is reported in ppm downfield from TMS as an internal standard or calibrated on solvent peaks. High resolution mass spectra were recorded using an Agilent 6210 time-of-flight mass spectrometer with electrospray ionization.

2.7.2. Synthesis of cysteine building block **28** (Scheme 2.6)

Fmoc-D-Cys(Trt)-OAll (32). Allyl bromide (130 μL, 182 mg, 1.50 mmol, 1.0 equiv.) and Cs₂CO₃ (244 mg, 0.749 mmol, 0.5 equiv.) were added to a solution of Fmoc-D-Cys(Trt)-OH (**31**) (869 mg, 1.484 mmol, 1.0 equiv.) in DMF (7 mL). The mixture was stirred overnight at rt under N₂. The mixture was diluted with EtOAc (100 mL) and washed with water (50 mL). The aqueous layer was extracted a second time with EtOAc (50 mL) and the organic layers combined, washed with brine (50 mL), filtered through MgSO₄, and concentrated. The residue was subjected to flash chromatography, eluting with 5:1 hexanes-EtOAc to isolate **32** as a colorless solid (856 mg, 92%). *R_f* 0.25 (4:1 hexanes-EtOAc). ¹H NMR (400 MHz, CDCl₃) δ 2.52-2.75 (m, 2H), 4.22 (t, *J* = 6.6 Hz 1H), 4.29-4.42 (m, 3H), 4.54-4.67 (m, 2H), 5.19-5.34 (m, 1H), 5.24 (d, *J* = 10.8 Hz, 1H), 5.29 (d, *J* = 16.8 Hz, 1H), 5.80-5.93 (m, 1H), 7.15-7.32 (m, 11H), 7.36-7.43 (m, 8H), 7.60 (d, *J* = 5.4 Hz, 2H), 7.75 (d, *J* = 6.4, 2H); ¹³C NMR (100 MHz, CDCl₃) δ

34.2, 47.2, 53.1, 66.4, 67.2, 67.3, 118.9, 120.1, 125.2, 127.0, 127.2, 127.8, 128.2, 129.6, 131.5, 141.4, 143.9, 144.0, 144.4, 155.7, 170.3. HRMS (ESI) calcd for $C_{40}H_{35}NNaO_4S$ ($M+Na$)⁺: calcd 648.2179; obsd 648.2178.

Pht-D-Cys(Trt)-OAll (33). Diethylamine (10 mL) was added to a solution of Fmoc-D-Cys(Trt)-OAll (**32**) (1.476 g, 2.36 mmol, 1.0 equiv.) in acetonitrile (10 mL). The mixture was stirred under N_2 for 2 h at rt. The solution was concentrated and the residue dissolved in toluene (15 mL). To this mixture was added phthalic anhydride (350 mg, 2.36 mmol, 1.0 equiv.) and triethylamine (658 μ L, 480 mg, 4.72 mmol, 2.0 equiv.). The mixture was heated at reflux under Dean-Stark conditions for 16 h. The mixture was concentrated and the residue purified by flash chromatography eluting with 3:1 hexanes-ethyl acetate to isolate **33** as a colorless solid (1.079 g, 86%). R_f 0.45 (2:1 hexanes-EtOAc). 1H NMR (400 MHz, $CDCl_3$) δ 3.02 (dd, J = 13.6, 4.5 Hz, 1H), 3.39 (dd, J = 13.6 Hz, 11.2 Hz, 1H), 4.42 (dd, J = 11.2, 4.5 Hz, 1H), 4.45-4.55 (m, 1H), 5.10-5.16 (m, 2H), 5.67-5.78 (m, 1H), 7.19 (t, J = 7.2 Hz, 3H), 7.22-7.28 (m, 6H), 7.38 (d, J = 7.4 Hz, 6H), 7.70 (dd, J = 5.4, 3.0 Hz, 2H), 7.82 (dd, J = 5.4, 3.0 Hz, 2H); ^{13}C NMR (100 MHz, $CDCl_3$) δ 30.9, 51.9, 60.5, 66.4, 67.6, 118.5, 123.7, 126.9, 128.1, 129.7, 131.3, 131.8, 134.3, 144.4, 167.3, 167.7. HRMS (ESI) calcd for $C_{33}H_{27}NNaO_4S$ ($M+Na$)⁺: calcd 556.1553; obsd 556.1566.

Pht-D-Cys(H)-OAll (34). Trifluoroacetic acid (75 μ L, 0.985 mmol, 5.0 equiv.) and triethylsilane (152 μ L, 0.985 mmol, 5.0 equiv.) were added to a solution of Pht-D-Cys(Trt)-OAll (**33**) (105 mg, 0.197 mmol, 1.0 equiv.) in CH_2Cl_2 (7 mL) at 0 °C. After 10 min, the mixture was allowed to warm to rt was stirred under N_2 for 2 h at rt. The mixture was concentrated and the residue purified by flash chromatography eluting with 5:1 hexanes-ethyl acetate to isolate **34** as a colorless oil (51 mg, 0.175 mmol, 89%). R_f 0.25 (4:1 hexanes-EtOAc). 1H NMR (400 MHz,

CDCl₃) δ 1.54 (dd, J = 9.6, 8.1 Hz, 1H), 3.29-3.50 (m, 2H), 4.67 (d, J = 5.7 Hz, 2H), 4.97 (dd, J = 10.4, 5.2 Hz, 1H), 5.24 (dd, J = 10.5, 1.1 Hz, 1H), 5.29 (dd, J = 17.2, 1.3 Hz, 1H), 5.82-5.92 (m, 1H), 7.78 (dd, J = 5.4, 3.0 Hz, 2H), 7.90 (dd, J = 5.4, 3.0 Hz, 2H); ¹³C NMR (100 MHz, CDCl₃) δ 23.9, 55.0, 66.7, 119.1, 123.8, 131.3, 131.8, 134.4, 134.5, 167.5, 167.6. HRMS (ESI) calcd for C₁₄H₁₃NO₄S (M+H)⁺: calcd 292.0565; obsd 292.0631.

Pht-D-Cys[SCH₂CH(OMe)₂]-OAll (28). Cesium carbonate (252 mg, 0.772 mmol, 1.0 equiv.) was slowly added to a solution of 2-bromo-1,1-dimethoxyethane (**35**) (91.2 μ L, 0.772 mmol, 1.0 equiv.) and Pht-D-Cys-OAll (**34**) (225 mg, 0.772 mmol, 1.0 equiv.) in DMF (6 mL) at 40 °C. This solution was stirred for 16 h at 40 °C under N₂. The mixture was diluted with EtOAc (100 mL) and washed with water (100 mL). The aqueous layer was extracted a second time with EtOAc (100 mL) and the organic layers were combined, washed with brine (50 mL), filtered through MgSO₄, concentrated, and the residue purified by flash chromatography eluting with 5:1→3:1 hexanes-EtOAc to isolate **28** as a yellow oil (131 mg, 45%). R_f 0.50 (1:1 hexanes-EtOAc). ¹H NMR (400 MHz, CDCl₃) δ 2.64 (dd, J = 14.0, 5.0 Hz, 1H), 2.76 (dd, J = 14.0, 5.7 Hz, 1H), 3.36 (s, 6H), 3.39 (dd, J = 14.3, 11.4 Hz, 1H), 3.54 (dd, J = 14.3, 4.4 Hz, 1H), 4.49 (t, J = 5.4 Hz, 1H), 4.67 (d, J = 5.5 Hz, 2H), 5.10 (dd, J = 11.4, 4.4 Hz, 1H), 5.23 (d, J = 10.4 Hz, 1H), 5.29 (d, J = 17.0 Hz, 1H), 5.80-5.92 (m, 1H), 7.75 (dd, J = 5.4, 3.1 Hz, 2H), 7.88 (dd, J = 5.4, 3.1 Hz, 2H); ¹³C NMR (100 MHz, CDCl₃) δ 31.3, 33.5, 51.3, 53.2, 53.8, 66.4, 104.8, 118.7, 123.5, 131.3, 131.7, 134.2, 167.4, 167.8. HRMS (ESI) calcd for C₁₈H₂₁NNaO₆S (M+Na)⁺: calcd 402.0982; obsd 402.0987.

2.7.3. First generation synthesis of tripeptide **39** (Scheme 2.8)

Pht-Cys[SCH₂CH(OMe)₂]-Phe-Ala-NH₂ (39). Morpholine (93.4 μ L, 94.1 mg, 1.08 mmol, 3 equiv.) was added to a solution of Pht-D-Cys(CH₂CH(OMe)₂)-OAll (**28**) (137 mg, 0.361 mmol,

1.0 equiv.) and Pd(PPh₃)₄ (42 mg, 0.036 mmol, 0.1 equiv.) in THF (15 mL). This solution was stirred for 20 min under N₂. The mixture was diluted with EtOAc (50 mL) and washed with 5 % aq. citric acid (25 mL). The aqueous layer was extracted a second time with EtOAc (25 mL) and the organic layers were combined, washed with brine (25 mL), filtered through MgSO₄, concentrated, and the residue purified by flash chromatography eluting with 2:1→1:4 hexanes-EtOAc to isolate free acid **37** as a colorless oil (89 mg, 72%).

N-Hydroxysuccinimide (35.2 mg, 0.306 mmol, 1.0 equiv.) and *N,N'*-dicyclohexylcarbodiimide (63.1 mg, 0.306 mmol, 1.0 equiv.) were added sequentially to a solution of Pht-Cys[CH₂CH(OMe)₂]-OH (**37**) (104 mg, 0.306 mmol, 1.0 equiv.) in CH₂Cl₂ (10 mL) at 0 °C. The solution was stirred for 20 min and then allowed to warm to rt and stirring was continued for 3 h under N₂. The mixture was filtered through a plug of cotton in a Pasteur pipette to remove the urea precipitate and the filtrate volume was reduced to 5 mL and placed in the freezer for 2 h. The mixture was filtered again and the solution concentrated. The residue was dissolved in DMF (5 mL) and *L*-phenylalanine (50.5 mg, 0.306 mmol, 1.0 equiv.) was added. The solution was cooled to 0 °C and ⁱPr₂NEt (64.1 μL, 47.6 mg, 0.368 mmol, 1.2 equiv.) was added dropwise and the mixture left to stir for 18 h under N₂. The mixture was diluted with ethyl acetate (50 mL) and washed with water (50 mL), 10% aq. citric acid (50 mL) and brine (50 mL). The organic layer was dried over MgSO₄, filtered and concentrated under reduced pressure. The residue, crude acid **38** (149 mg), was used immediately in the next reaction.

Alaninamide hydrochloride (38 mg, 0.306 mmol, 1.0 equiv.) was added to a solution of dipeptide acid **38** (149 mg, 0.306 mmol, 1.0 equiv.) in CH₂Cl₂ (7 mL). The mixture was cooled to 0 °C and collidine (81.5 μL, 74 mg, 0.612 mmol, 2.0 equiv.) was added dropwise, followed by HATU (116.4 mg, 0.306 mmol, 1.0 equiv.). The solution was allowed to warm to rt and stirred

under N₂ for 16 h. The mixture was concentrated and the residue purified by flash chromatography eluting with 4% CH₃OH in CH₂Cl₂ to isolate a mixture which was further purified by HPLC eluting with a linear gradient of 25-65 % MeCN in H₂O over 24 min, retention time 17.5-20.0 min. This colorless solid **39** (115 mg, 68%) was composed of four compounds, all with the same molecular ion according to electrospray HRMS. A portion was further purified, using the same HPLC conditions, collecting the major compound **39**, R_T 18 min. *R_f* 0.44 (10% MeOH in CH₂Cl₂). ¹H NMR (400 MHz, CDCl₃) δ 1.37 (d, *J* = 7.2 Hz, 3H), 2.60 (dd, *J* = 14.0, 5.0 Hz, 1H), 2.68 (dd, *J* = 14.0, 5.6 Hz, 1H), 3.02 (dd, *J* = 14.0, 6.2 Hz, 1H), 3.11 (dd, *J* = 14.3, 10.4 Hz, 1H), 3.22 (dd, *J* = 14.0, 5.6 Hz, 1H), 3.32 (s, 3H), 3.33 (s, 3H), 3.48 (dd, *J* = 14.3, 5.5 Hz, 1H), 4.44 (t, *J* = 5.3 Hz, 1H), 4.50 (t, *J* = 7.5 Hz, 1H), 4.56 (app. q, *J* = 6.0 Hz, 1H), 4.99 (dd, *J* = 10.4, 5.5 Hz, 1H), 5.30 (br s, 1H), 6.41 (br s, 1H), 6.53 (d, *J* = 6.0 Hz, 1H), 6.59 (d, *J* = 7.8 Hz, 1H), 6.97-7.05 (m, 5H), 7.79-7.90 (m, 4H). ¹³C NMR (125 MHz, CDCl₃) δ 17.4, 29.9, 31.6, 34.0, 37.4, 49.0, 52.4, 53.9, 54.3, 55.9, 104.8, 124.0, 127.5, 129.1, 129.4, 131.7, 134.7, 136.1, 167.9, 169.1, 170.2, 174.4. HRMS (ESI) calcd for C₂₇H₃₂N₄NaO₇S (M+Na)⁺: calcd 579.1884; obsd 579.1891.

2.7.4. Second generation synthesis of tripeptide **39** (Scheme 2.9)

Fmoc-Phe-Ala-NH₂ (**42**). A solution of Fmoc-Phe-OH (**40**) (539 mg, 1.389 mmol, 1.0 equiv.) and HCl·H-Ala-NH₂ (**41**) (173 mg, 1.389 mmol, 1.0 equiv.) in DMF (8 mL) was cooled to 0 °C. To this solution was added BOP reagent (614 mg, 1.389 mmol, 1.0 equiv.) followed by dropwise addition of ^tPr₂EtN (960 μL, 713 mg, 5.560 mmol, 4.0 equiv.) and the solution was stirred under N₂ for 16 h. The reaction mixture was poured onto crushed ice (75 g) in a beaker and left to stand. After 2 h, the precipitate was collected by vacuum filtration. The dried solid was triturated with cold diethyl ether (25 mL x 2) and filtered to give **42** as a colorless solid (225 mg,

35%). R_f 0.16 (5% MeOH in CH_2Cl_2). ^1H NMR (400 MHz, DMSO-d_6) δ 1.22 (d, $J = 7.0$ Hz, 3H), 2.76 (dd, $J = 13.7, 10.9$ Hz, 1H), 3.04 (dd, $J = 13.7, 3.8$ Hz, 1H), 4.10-4.17 (m, 3H), 4.19-4.30 (m, 2H), 7.02 (br s, 1H), 7.17 (t, $J = 7.1$ Hz, 1H), 7.21-7.34 (m, 6H), 7.40 (td, $J = 7.4, 1.8$ Hz, 2H), 7.60-7.65 (m, 3H), 7.87 (d, $J = 7.5$ Hz, 2H), 8.05 (d, $J = 7.4$ Hz, 1H). ^{13}C NMR (125 MHz, DMSO-d_6) δ 18.4, 30.7, 35.7, 37.3, 46.5, 48.0, 56.1, 65.6, 120.0, 125.2, 125.3, 126.1, 127.0, 127.5, 128.0, 129.2, 138.1, 140.6, 143.7 (2C), 155.7, 162.2, 170.9, 174.0. HRMS (ESI) calcd for $\text{C}_{27}\text{H}_{27}\text{N}_3\text{NaO}_4$ ($\text{M}+\text{Na}$) $^+$: calcd 480.1894; obsd 480.1902.

Pht-Cys[$\text{SCH}_2\text{CH}(\text{OMe})_2$]-Phe-Ala-NH $_2$ (39**).** Diethylamine (6 mL, 50% v/v of total reaction mixture) was added to a suspension of Fmoc-Phe-Ala-NH $_2$ (**42**) (148 mg, 0.323 mmol, 1.0 equiv.) in MeCN (6 mL). The mixture was stirred for 2 h under N_2 , concentrated, and purified by flash chromatography eluting with 1% \rightarrow 8% CH_3OH in CH_2Cl_2 to isolate amine **43** as a colorless oil (68 mg, 89%). ^1H NMR (400 MHz, CDCl_3) δ 1.34 (d, $J = 7.0$ Hz, 3H), 2.71 (dd, $J = 13.6, 9.1$ Hz, 1H), 3.17 (dd, $J = 13.6, 3.9$ Hz, 1H), 3.64 (dd, $J = 8.7, 3.9$ Hz, 1H), 4.47 (app p, $J = 7.0$ Hz, 1H), 6.26 (br s, 1H), 6.86 (br s, 1H), 7.17-7.31 (m, 5H), 7.86 (d, $J = 7.4$ Hz, 1H).

N-Hydroxysuccinimide (37 mg, 0.323 mmol, 1.0 equiv.) and by *N,N'*-dicyclohexylcarbodiimide (67 mg, 0.323 mmol, 1.0 equiv.) were added sequentially to a solution of Pht-Cys($\text{CH}_2\text{CH}(\text{OMe})_2$)-OH (**37**) (110 mg, 0.323 mmol, 1.0 equiv.) in CH_2Cl_2 (10 mL) at 0 °C. The solution was stirred for 20 min and then allowed to warm to room to rt and stirring continued for 3 h under N_2 . The mixture was filtered through a plug of cotton in a Pasteur pipette to remove the urea precipitate and the filtrate volume was reduced to 5 mL and placed in the freezer for 2 h. The mixture was filtered again and the solution concentrated. The residue was dissolved in DMF (5 mL) and to this solution was added dipeptide amine **43** (76 mg, 0.323 mmol, 1.0 equiv.). The solution was cooled to 0 °C and $i\text{Pr}_2\text{NEt}$ (85 μL , 63 mg, 0.485 mmol, 1.5

equiv.) was added dropwise and left to stir for 18 h under N₂. The mixture was diluted with ethyl acetate (50 mL) and washed with water (50 mL), and brine (50 mL). The organic layer was dried over MgSO₄, concentrated, and the residue purified by flash chromatography eluting with 4 % CH₃OH in CH₂Cl₂ to isolate a mixture of compounds of identical molecular weight as colorless solid **39** (115 mg, 65%). The same HPLC method to that used in the first generation tripeptide synthesis (section 3.10) was used to isolate and purify the most abundant compound for characterization. ¹H, ¹³C NMR, and mass spectrometry data were identical to 1st generation tripeptide.

2.7.5. Synthesis of thioenamide **49** and side products **50**, **54**, **55** (Scheme 2.13)

Thioenamide (49) and Side Products. *para*-Toluenesulfonic acid (17 mg, 0.089 mmol, 1.0 equiv.) was added to a solution of protected cysteine **28** (33 mg, 0.087 mmol, 1.0 equiv.) in benzene (33 mL), followed by addition of acetamide (26 mg, 0.435 mmol, 5.0 equiv.). The solution was heated to reflux under N₂. After 4 h, the solution was concentrated under vacuum and the residue was purified by flash chromatography eluting with 4:1→3:1→1:1 hexanes-EtOAc to isolate three products:

Methyl Vinyl Ether (**50**) as a colorless oil (5 mg, 16%). *R_f* 0.52 (1:1 hexanes: EtOAc). ¹H NMR (500 MHz, CDCl₃) δ 3.29 (dd, *J* = 14.4, 4.2 Hz, 1H), 3.37 (dd, *J* = 14.4, 11.3 Hz, 1H), 3.54 (s, 3H), 4.65 (d, *J* = 5.6 Hz, 2H), 5.05 (dd, *J* = 11.3, 4.2 Hz, 1H), 5.21 (d, *J* = 12.2 Hz, 1H), 5.22 (d, *J* = 10.4 Hz, 1H), 5.28 (d, *J* = 17.3 Hz, 1H), 5.81-5.91 (m, 1H), 6.72 (d, *J* = 12.2 Hz, 1H), 7.76 (dd, *J* = 5.4, 3.1 Hz, 2H), 7.89 (dd, *J* = 5.4, 3.1, 2H); ¹³C NMR (125 MHz, CDCl₃) δ 34.7, 51.4, 56.8, 66.7, 92.1, 119.1, 123.8, 131.4, 132.0, 134.4, 157.5, 167.7, 168.3. HRMS (ESI) calcd for C₁₇H₁₈NO₅S (M+H)⁺: calcd 348.0900; obsd 348.0931.

cis-Thioenamide (**Z-49**) as a pale yellow oil (13 mg, 40%). R_f 0.25 (1:1 hexanes-EtOAc). ^1H NMR (400 MHz, CDCl_3) δ 2.10 (s, 3H), 3.41 (dd, $J = 14.6, 4.3$ Hz, 1H), 3.48 (dd, $J = 14.6, 10.9$ Hz, 1H), 4.66 (d, $J = 5.7$ Hz, 2H), 4.99 (dd, $J = 10.9, 4.3$ Hz, 1H), 5.21 (d, $J = 7.5$ Hz, 1H), 5.24 (d, $J = 11.2$ Hz, 1H), 5.27 (d, $J = 17.2$ Hz, 1H), 5.80-5.92 (m, 1H), 7.06 (dd, $J = 11.1, 7.5$ Hz, 1H), 7.76-7.81 (m, 1H), 7.77 (dd, $J = 5.3, 3.1$ Hz, 2H), 7.79-7.85 (m, 1H), 7.88 (dd, $J = 5.3, 3.1$ Hz, 2H); ^{13}C NMR (125 MHz, CDCl_3) δ 23.3, 34.1, 52.9, 66.9, 99.4, 119.3, 123.8, 130.2, 131.3, 131.7, 134.7, 167.5, 167.7, 167.9. HRMS (ESI) calcd for $\text{C}_{18}\text{H}_{19}\text{N}_2\text{NO}_5\text{S}$ ($\text{M}+\text{H}$) $^+$: calcd 375.1009; obsd 375.0997.

trans-Thioenamide (**E-49**) as a pale yellow oil (4 mg, 12%). R_f 0.12 (1:1 hexanes-EtOAc). ^1H NMR (400 MHz, CDCl_3) δ 1.98 (s, 3H), 3.40 (app. s, 1H), 3.42 (d, $J = 2.5$ Hz, 1H), 4.66 (d, $J = 5.7$ Hz, 2H), 5.04 (dd, $J = 9.1, 6.7$ Hz, 1H), 5.23 (dd, $J = 10.4, 1.3$ Hz, 1H), 5.28 (dd, $J = 17.2, 1.3$ Hz, 1H), 5.63 (d, $J = 13.2$ Hz, 1H), 5.80-5.92 (m, 1H), 7.04 (dd, $J = 13.2, 10.8$ Hz, 1H), 7.06-7.13 (m, 1H), 7.75 (dd, $J = 5.4, 3.0$ Hz, 2H), 7.88 (dd, $J = 5.4, 3.0$ Hz, 2H); ^{13}C NMR (125 MHz, CDCl_3) δ 23.3, 29.8, 33.8, 51.7, 66.8, 102.5, 119.1, 123.9, 130.4, 131.4, 131.9, 134.4, 166.5, 167.6, 168.0. HRMS (ESI) calcd for $\text{C}_{18}\text{H}_{19}\text{N}_2\text{O}_5\text{S}$ ($\text{M}+\text{H}$) $^+$: calcd 375.1009; obsd. 375.1010

2:1 Adduct 54. *para*-Toluenesulfonic acid (18 mg, 0.092 mmol, 1.0 equiv.) was added to a solution of protected cysteine **28** (35 mg, 0.092 mmol, 1.0 equiv.) in benzene (26 mL), followed by addition of acetamide (5 mg, 0.092 mmol, 1.0 equiv.). This solution was heated to reflux under N_2 . After 4 h, the solution was concentrated under vacuum and the crude product was purified by flash chromatography eluting with 2:1 \rightarrow 1:1 hexanes-EtOAc to isolate **54** as a pale yellow oil (26 mg, 81%). R_f 0.24 (1:1 hexanes-EtOAc). ^1H NMR (400 MHz, CDCl_3) δ 2.17 (s, 1.5H), 2.18 (s, 1.5H), 3.34 (dd, $J = 14.3, 4.0$ Hz, 0.5H), 3.35 (dd, $J = 14.3, 4.0$ Hz, 0.5H), 3.48 (dd, $J = 10.9, 7.2$ Hz, 1H), 3.51-3.61 (m, 2H), 4.62-4.64 (m, 2H), 4.65-4.70 (m, 2H), 4.86 (dd, J

= 10.9, 4.0 Hz, 0.5H), 4.92 (dd, J = 10.8, 4.1 Hz, 0.5H), 5.10 (dd, J = 10.0, 5.3 Hz, 1H), 5.18-5.33 (m, 4H), 5.78-5.94 (m, 2H), 6.09 (d, J = 14.7 Hz, 0.5H), 6.10 (d, J = 14.7 Hz, 0.5H), 6.33 (d, J = 14.7 Hz, 0.5H), 6.36 (d, J = 14.7 Hz, 0.5H), 7.09 (d, J = 11.3 Hz, 1H), 7.67-7.91 (m, 8H), 8.26 (d, J = 11.3 Hz, 0.5H), 8.31 (d, J = 11.3 Hz, 0.5H); ^{13}C NMR (100 MHz, CDCl_3) δ 14.3, 21.2, 23.3, 23.4, 32.4, 32.5, 32.7, 33.0, 51.8, 52.0, 53.5, 53.6, 60.5, 66.8, 66.9, 111.2, 111.4, 119.1, 119.2, 119.3, 122.3, 122.5, 123.8 (2C), 124.0 (2C), 129.4, 129.5, 130.8, 131.0, 131.2, 131.4, 131.6, 131.7, 131.9, 134.2, 134.3, 134.7, 167.2, 167.3, 167.4, 167.5, 167.7, 167.8, 167.9 (2C). HRMS (ESI) calcd for $\text{C}_{34}\text{H}_{31}\text{N}_3\text{O}_9\text{S}_2$ ($\text{M}+\text{H}$) $^+$: calcd 690.1574; obsd 690.1584.

Pyrrole 55. *para*-Toluenesulfonic acid (17 mg, 0.087 mmol, 1.0 equiv.) was added to a solution of protected cysteine **28** (33 mg, 0.087 mmol, 1.0 equiv.) in benzene (20 mL), followed by addition of acetamide (5 mg, 0.087 mmol, 1.0 equiv.). The solution was heated to reflux under N_2 . After 22 h, the solution was concentrated under vacuum and the crude product was purified by flash chromatography eluting with 2:1 \rightarrow 1:1 hexanes-EtOAc to isolate **55** as a yellow oil (13 mg, 38%). R_f 0.51 (1:1 hexanes-EtOAc). ^1H NMR (400 MHz, CD_3OD) δ 2.35 (s, 3H), 3.48 (dd, J = 14.8, 3.8 Hz, 1H), 3.67 (dd, J = 14.8, 11.3 Hz, 1H), 4.65 (dt, J = 5.7, 1.4 Hz, 2H), 5.10 (dd, J = 11.3, 3.8 Hz, 1H), 5.20 (ddd, J = 10.5, 2.6, 1.5 Hz, 1H), 5.27 (ddd, J = 17.2, 3.1, 1.5 Hz, 1H), 5.89 (ddt, 17.2, 10.5, 5.6 Hz, 1H), 6.25 (dd, J = 3.4, 1.7 Hz, 1H), 7.14 (dd, J = 3.4, 2.4 Hz, 1H), 7.21 (dd, J = 2.2, 1.8 Hz, 1H), 7.82-7.84 (m, 4H); ^{13}C NMR (100 MHz, CDCl_3) δ 21.9, 34.2, 54.0, 67.5, 117.3, 118.6, 118.9, 121.6, 123.4, 124.4, 132.7, 132.8, 135.7, 168.7, 168.8, 169.3. HRMS (ESI) calcd for $\text{C}_{20}\text{H}_{19}\text{N}_2\text{O}_5\text{S}$ ($\text{M}+\text{H}$) $^+$: calcd 399.1009; obsd 399.1017.

Thioenamide 49 using $\text{BF}_3\cdot\text{OEt}_2$. Acetamide (15 mg, 0.132 mmol, 5.0 equiv.) and boron trifluoride diethyl etherate (31 μL , 36 mg, 0.250 mmol, 5.0 equiv.) were added sequentially to a solution of cysteine **28** (19 mg, 0.050 mmol, 1.0 equiv.) in benzene (11 mL). The solution was

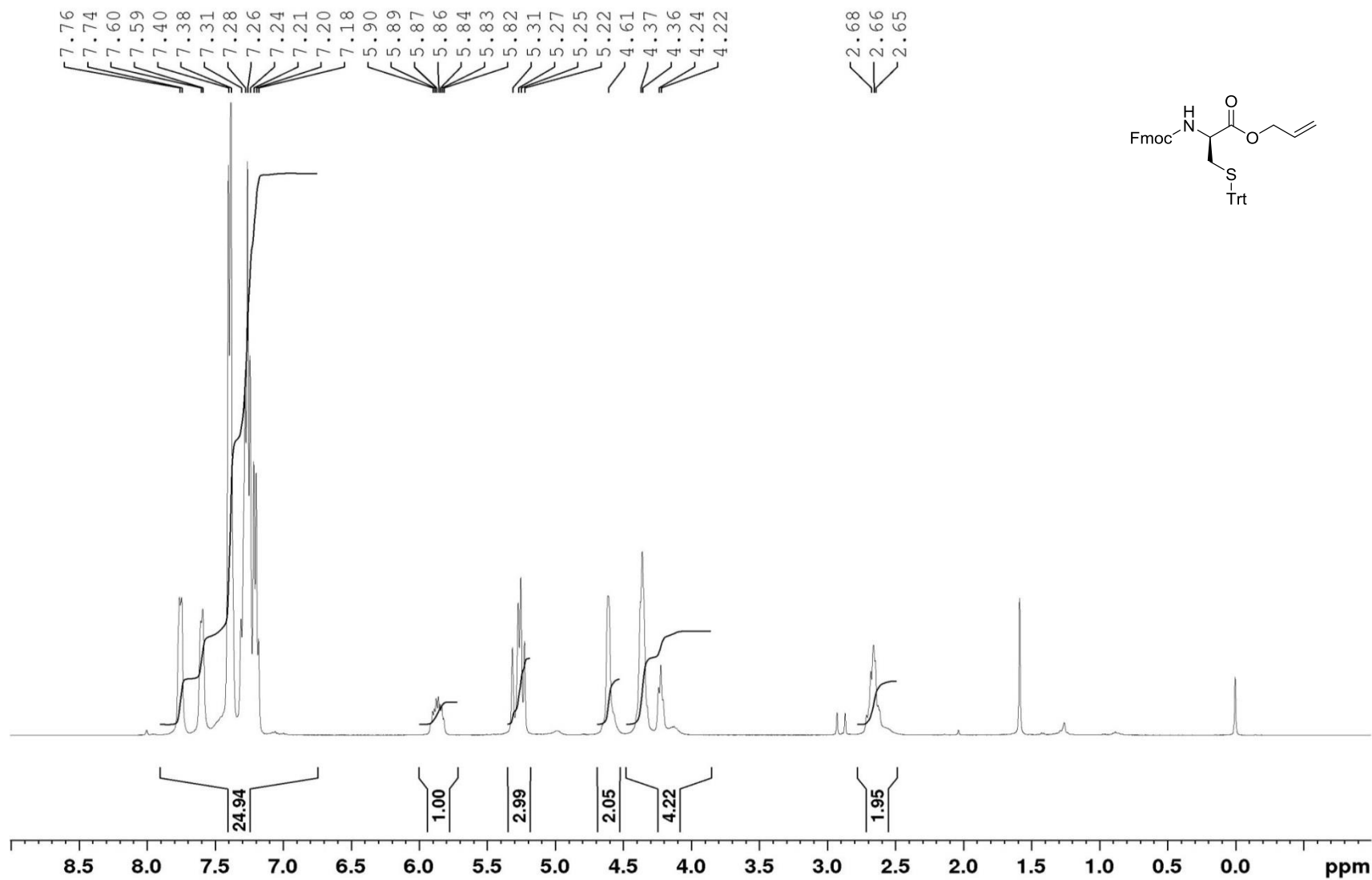
heated to reflux under N₂. After 40 min, the solution was concentrated under vacuum and the residue subjected to flash chromatography eluting with 3:1→1:1 hexanes-EtOAc to isolate *cis*-thioenamide **Z-49** (9 mg, 47%) and *trans*-thioenamide **E-49** (2 mg, 10%) as two pale yellow oils. See characterization above.

Aldehyde 56. Trifluoroacetic acid (1 mL) at 0 °C was added slowly to a round bottomed flask charged with protected cysteine **28** (24 mg, 0.063 mmol, 1.0 equiv.) at 0 °C. The solution was stirred under N₂ in an ice bath. After 1 h, the solution was concentrated and subjected to flash chromatography, eluting with 3:1 hexanes-EtOAc to isolate **56** (20 mg, 95%). *R_f* 0.50 (1:1 hexanes-EtOAc). ¹H NMR (400 MHz, CDCl₃) δ 3.20 (dd, *J* = 14.5, 2.4 Hz, 1H), 3.29-3.35 (m, 3H), 4.66 (dd, *J* = 5.8, 0.9 Hz, 2H), 5.01 (dd, *J* = 9.6, 6.3 Hz, 1H), 5.23 (dd, *J* = 10.4, 1.0 Hz, 1H), 5.29 (dd, *J* = 17.2, 1.3 Hz, 1H), 5.81-5.92 (m, 1H), 7.77, (dd, *J* = 5.4, 3.1, 2H), 7.89 (dd, *J* = 5.4, 3.0, 2H), 9.49 (dd, *J* = 4.1, 2.4 Hz, 1H); ¹³C NMR (100 MHz, CDCl₃) δ 30.6, 40.6, 50.8, 66.9, 119.2, 123.9, 131.2, 131.8, 134.5, 167.5, 167.5, 193.5.

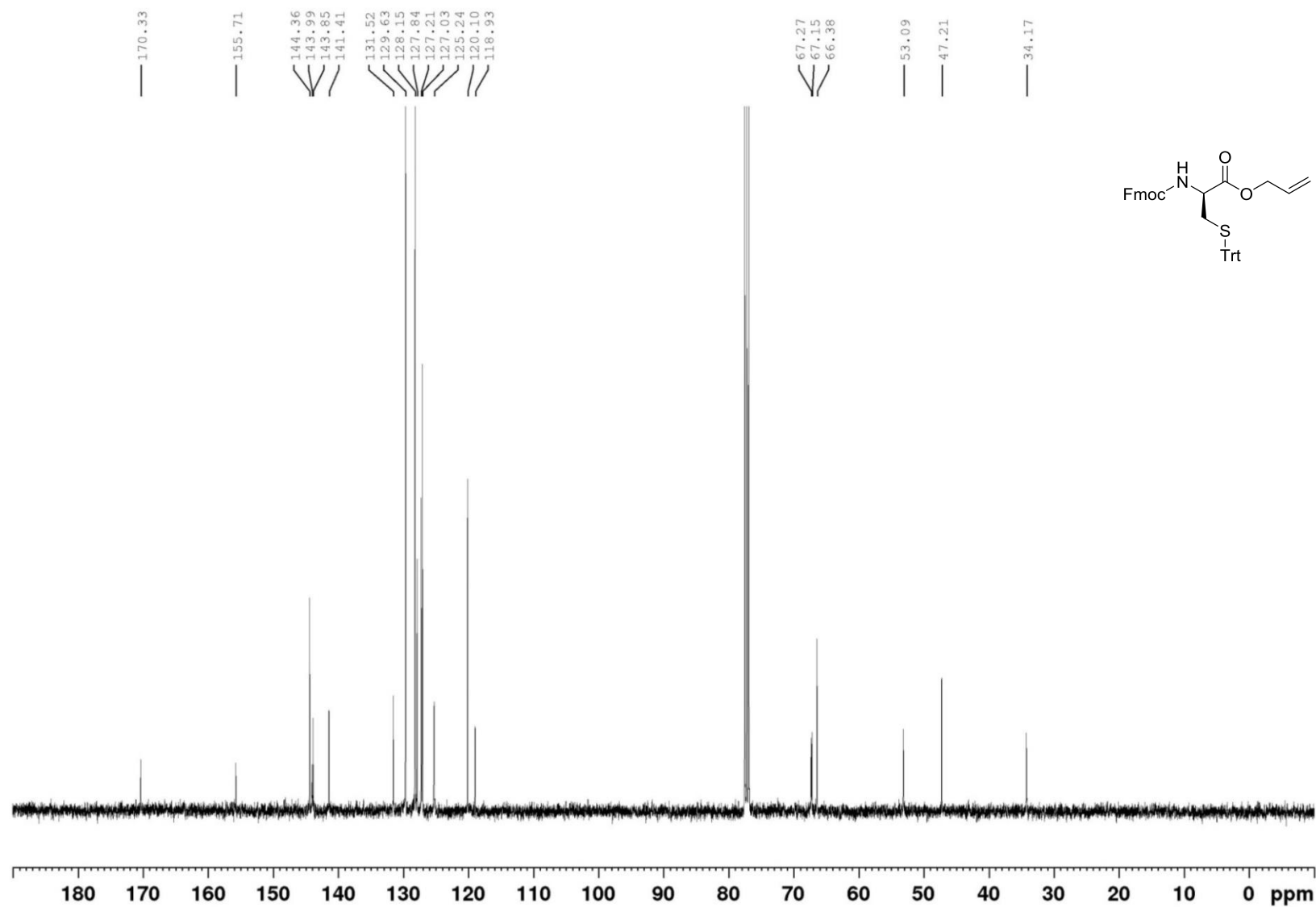
Thioenamide 49 using B(OH)₃. Acetamide (4 mg, 0.075 mmol, 1.0 equiv.) and boric acid (23 mg, 0.375 mmol, 1.0 equiv.) were added sequentially to a solution of cysteine aldehyde **56** (25 mg, 0.075 mmol, 1.0 equiv.) in toluene (25 mL) under N₂. The solution was stirred and heated at reflux, with 1 equivalent of acetamide added daily until ¹H NMR of the crude mixture showed consumption of aldehyde **56**. After 3 days, the total amount of acetamide added was 22 mg (0.375 mmol, 5.0 equiv.). The solution was concentrated and the residue subjected to flash chromatography eluting with 3:1→1:1 hexanes-EtOAc to isolate *cis*-thioenamide **Z-49** (16 mg, 57%) and *trans*-thioenamide **E-49** (2 mg, 7%), each as a pale yellow oil. See characterization above.

2.8. NMR Spectra

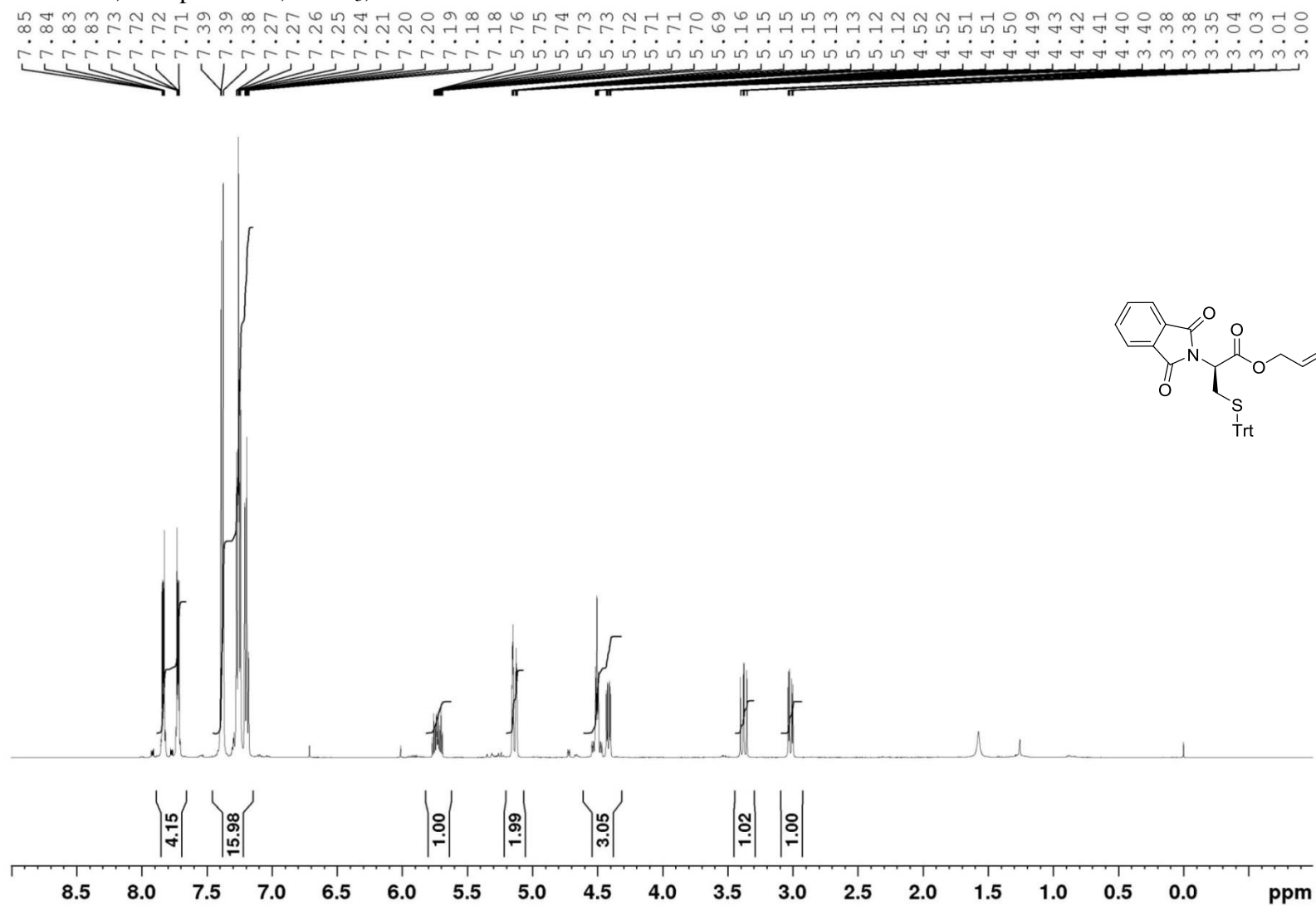
^1H NMR, Compound **32**, CDCl_3 , 400 MHz



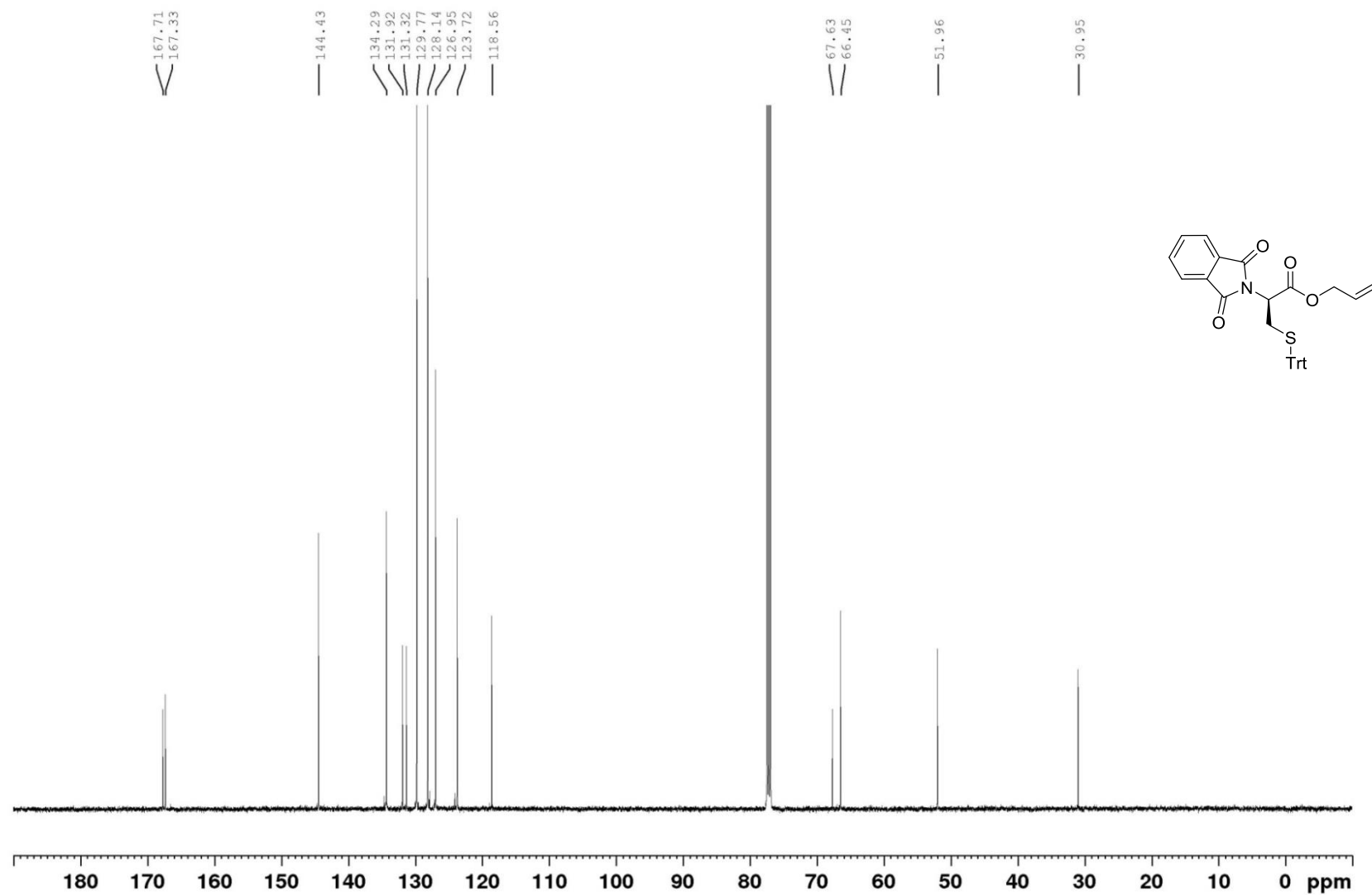
^{13}C NMR, Compound **32**, CDCl_3 , 100 MHz



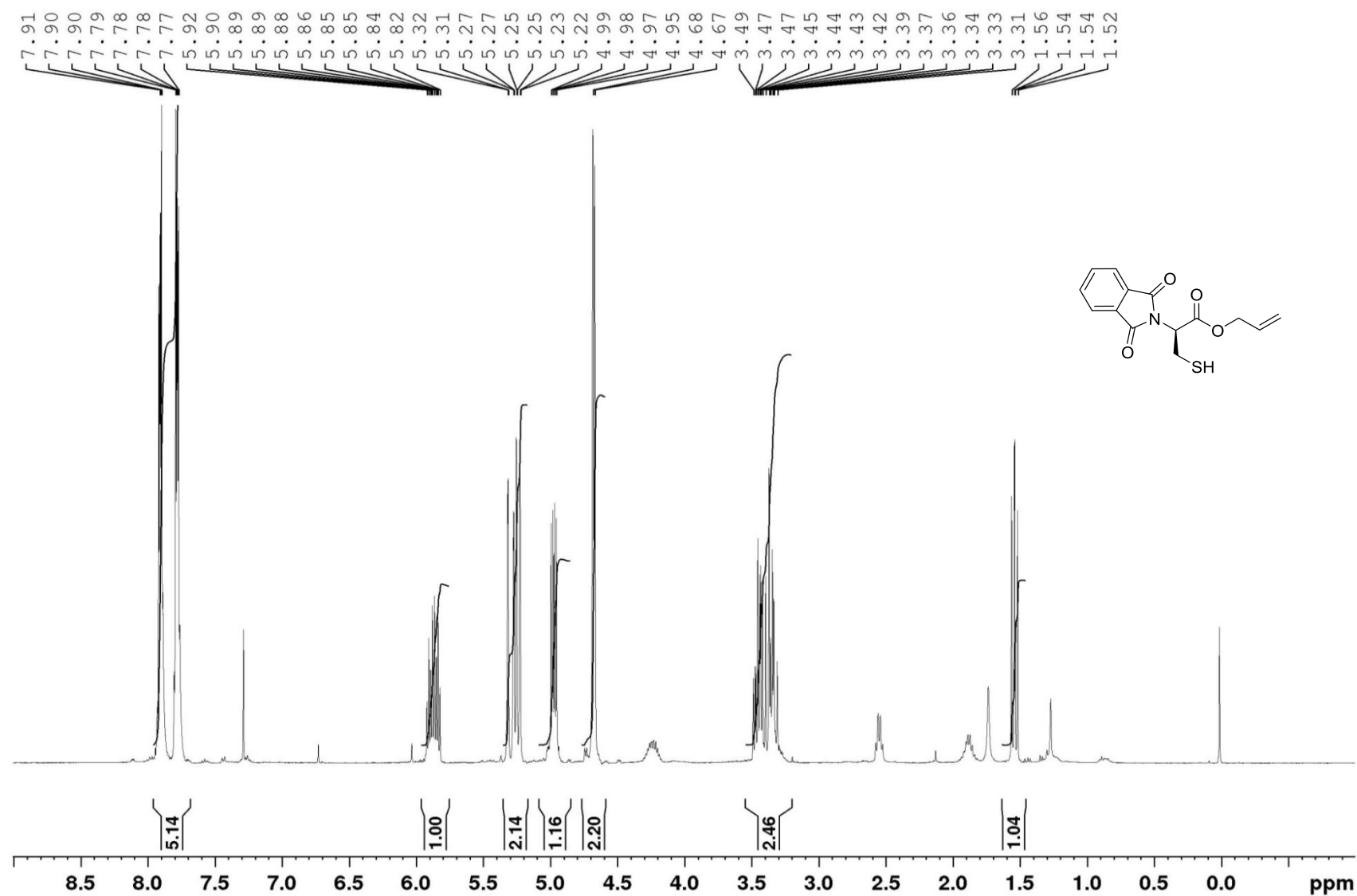
^1H NMR, Compound **33**, CDCl_3 , 400 MHz



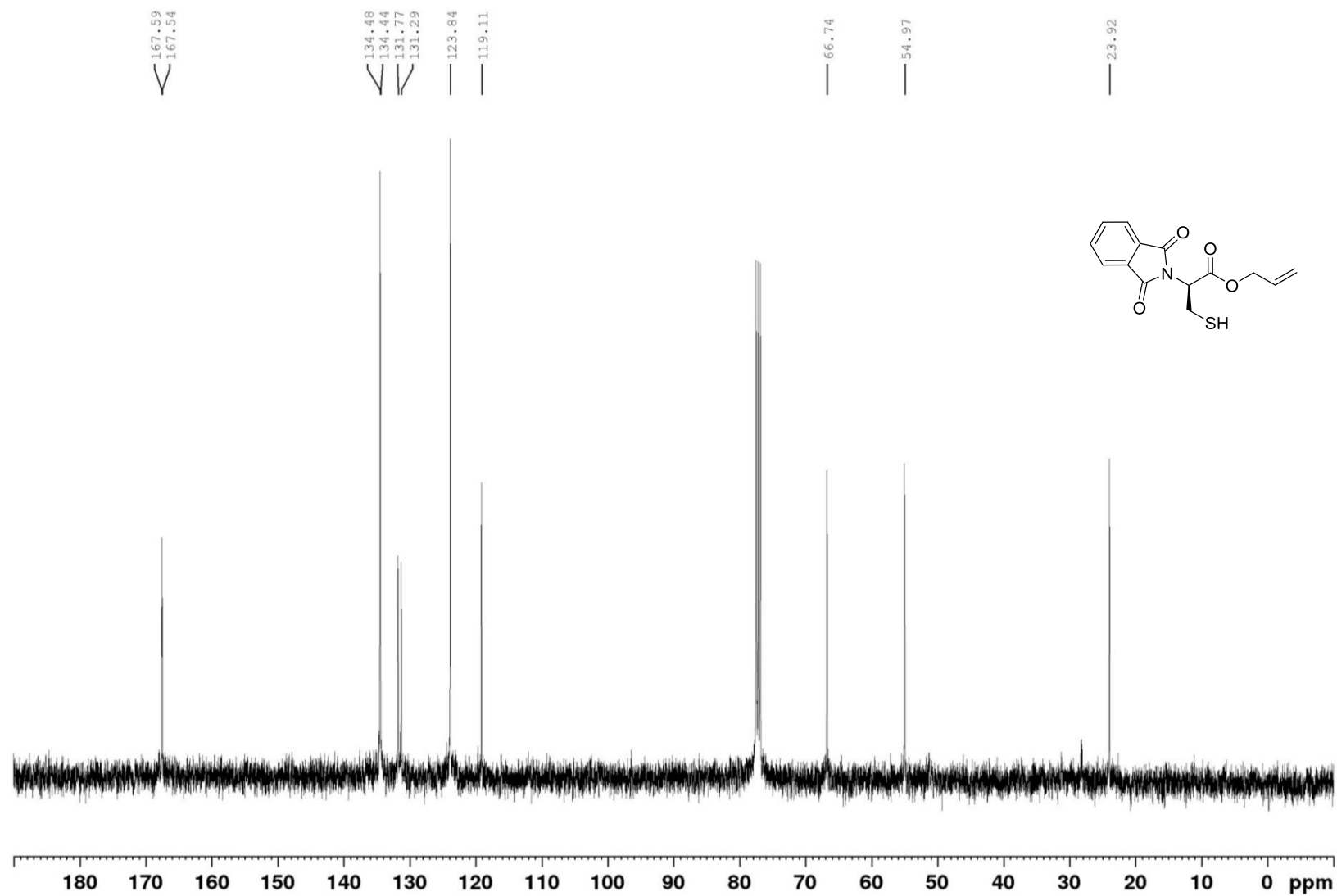
^{13}C NMR, Compound **33**, CDCl_3 , 100 MHz



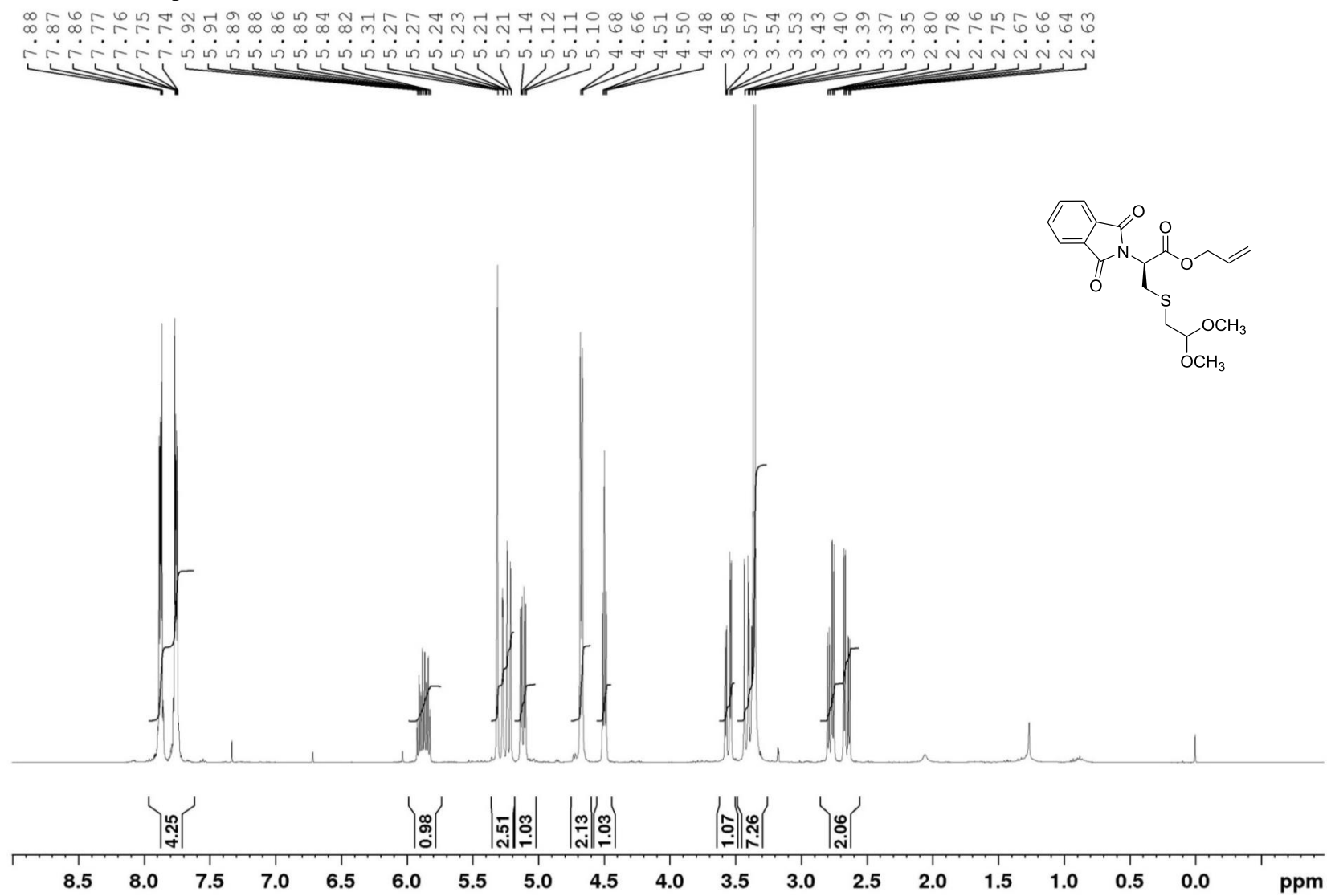
^1H NMR, Compound **34**, CDCl_3 , 400 MHz



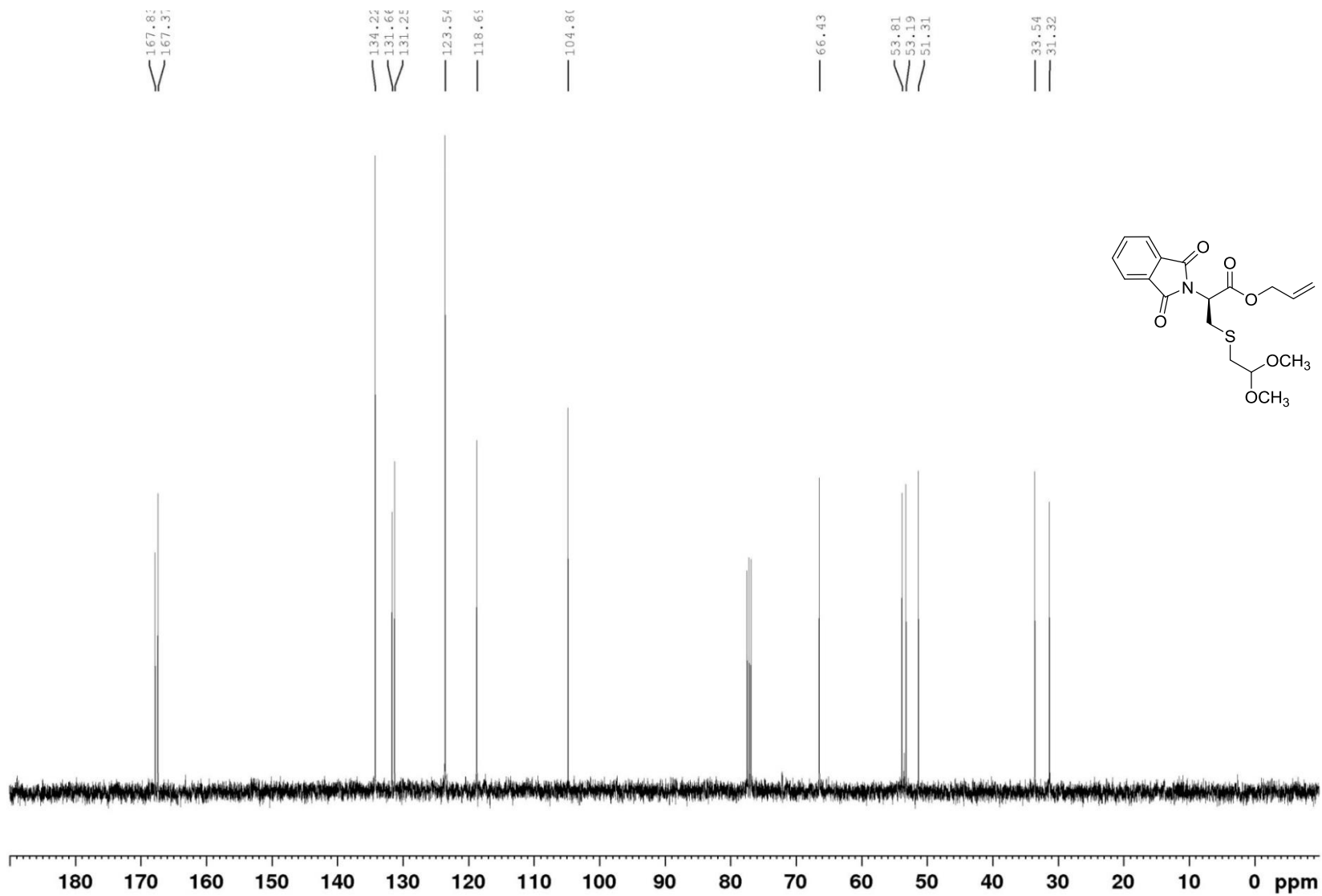
^{13}C NMR, Compound **34**, CDCl_3 , 100 MHz



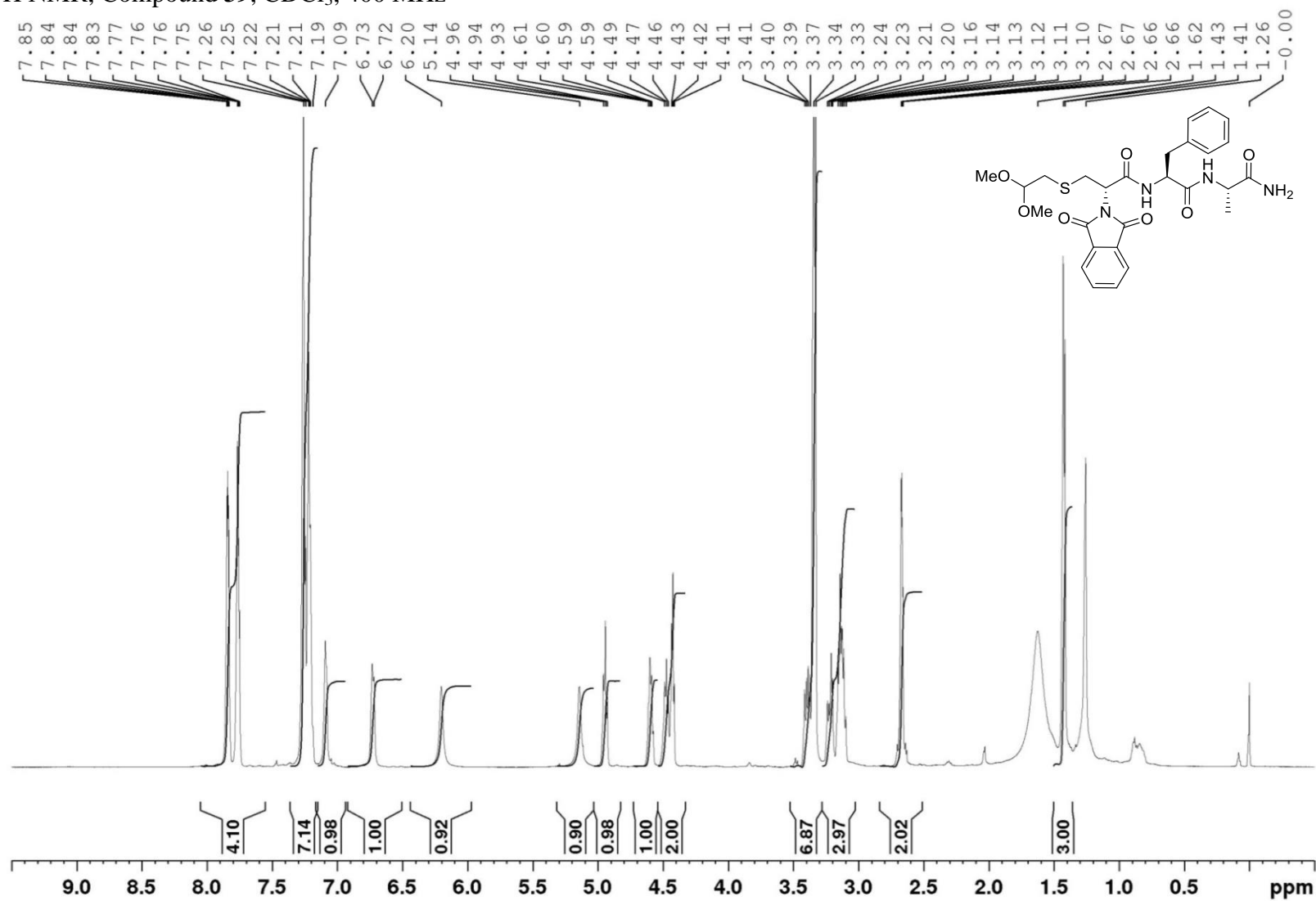
^1H NMR, Compound **28**, CDCl_3 , 400 MHz



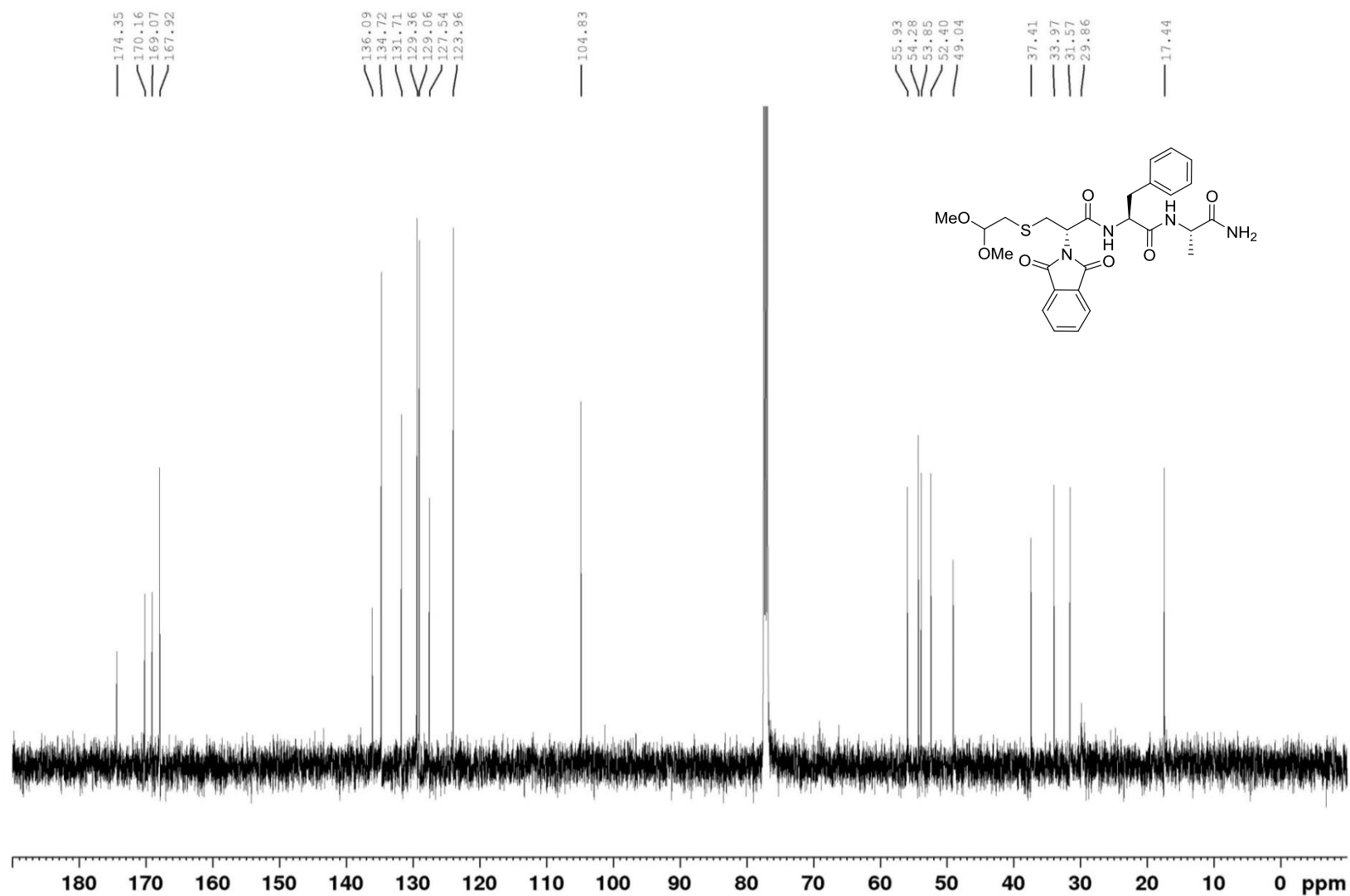
^{13}C NMR, Compound **28**, CDCl_3 , 100 MHz



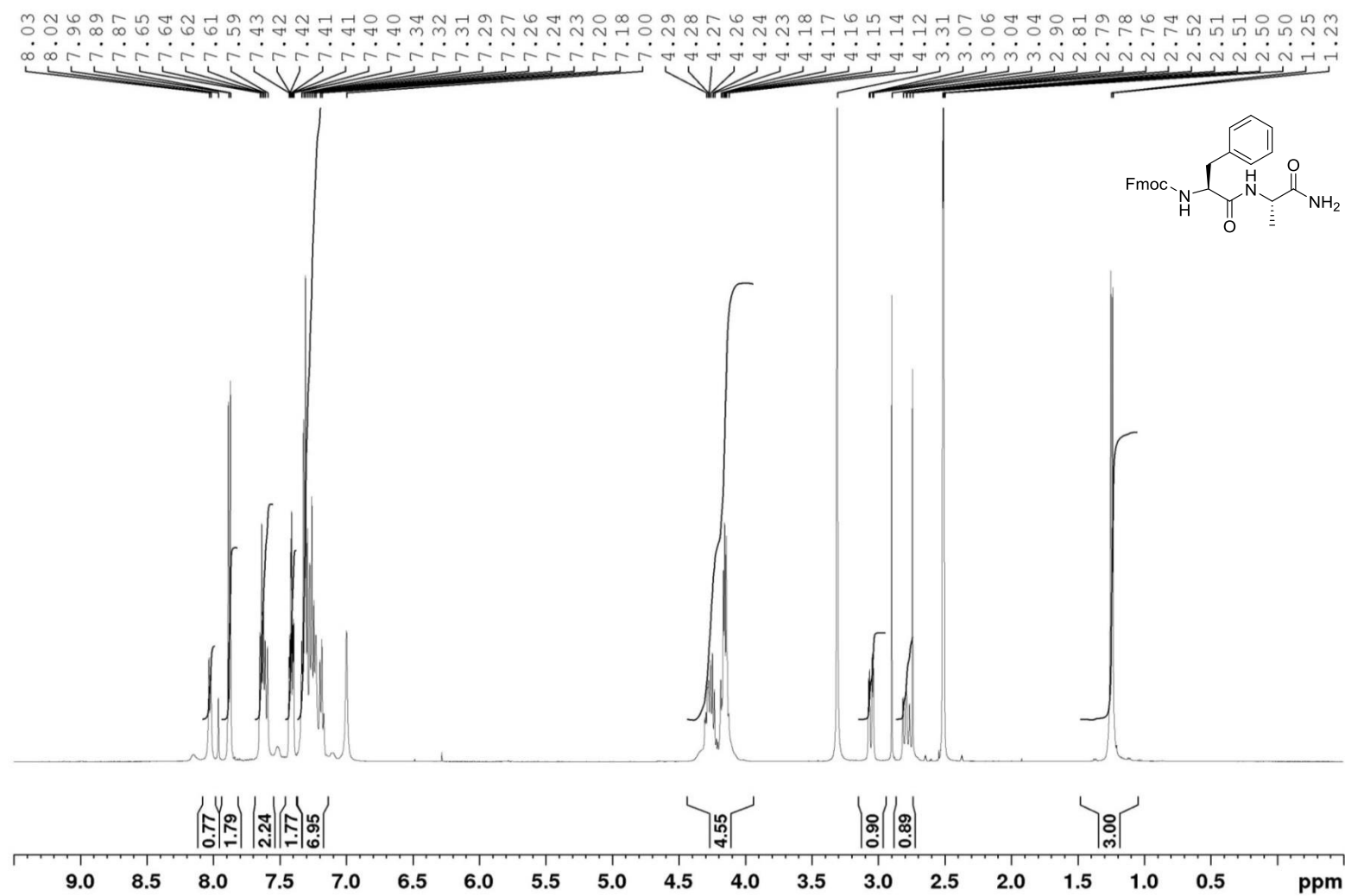
^1H NMR, Compound **39**, CDCl_3 , 400 MHz



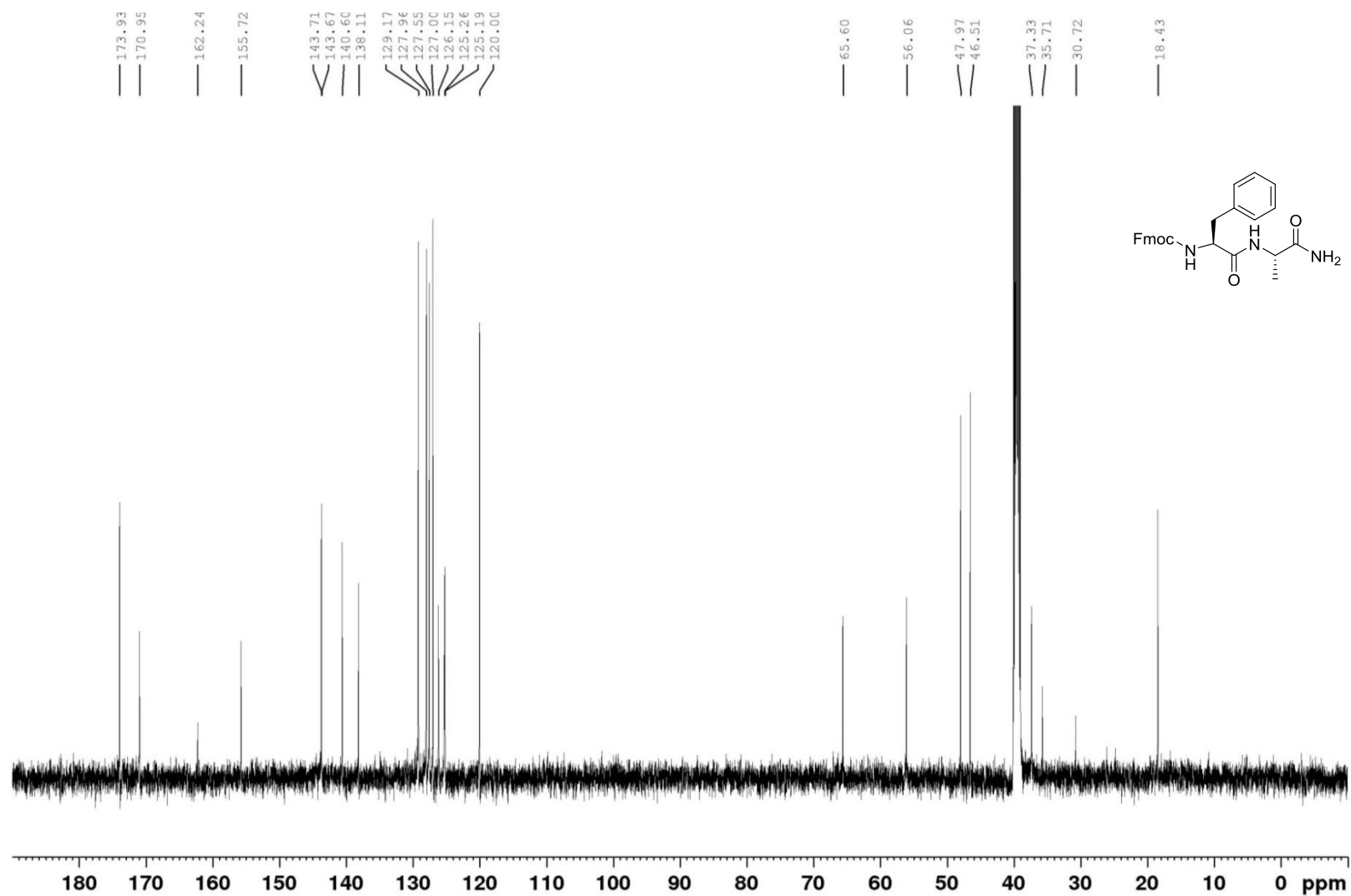
^{13}C NMR, Compound **39**, CDCl_3 , 125 MHz



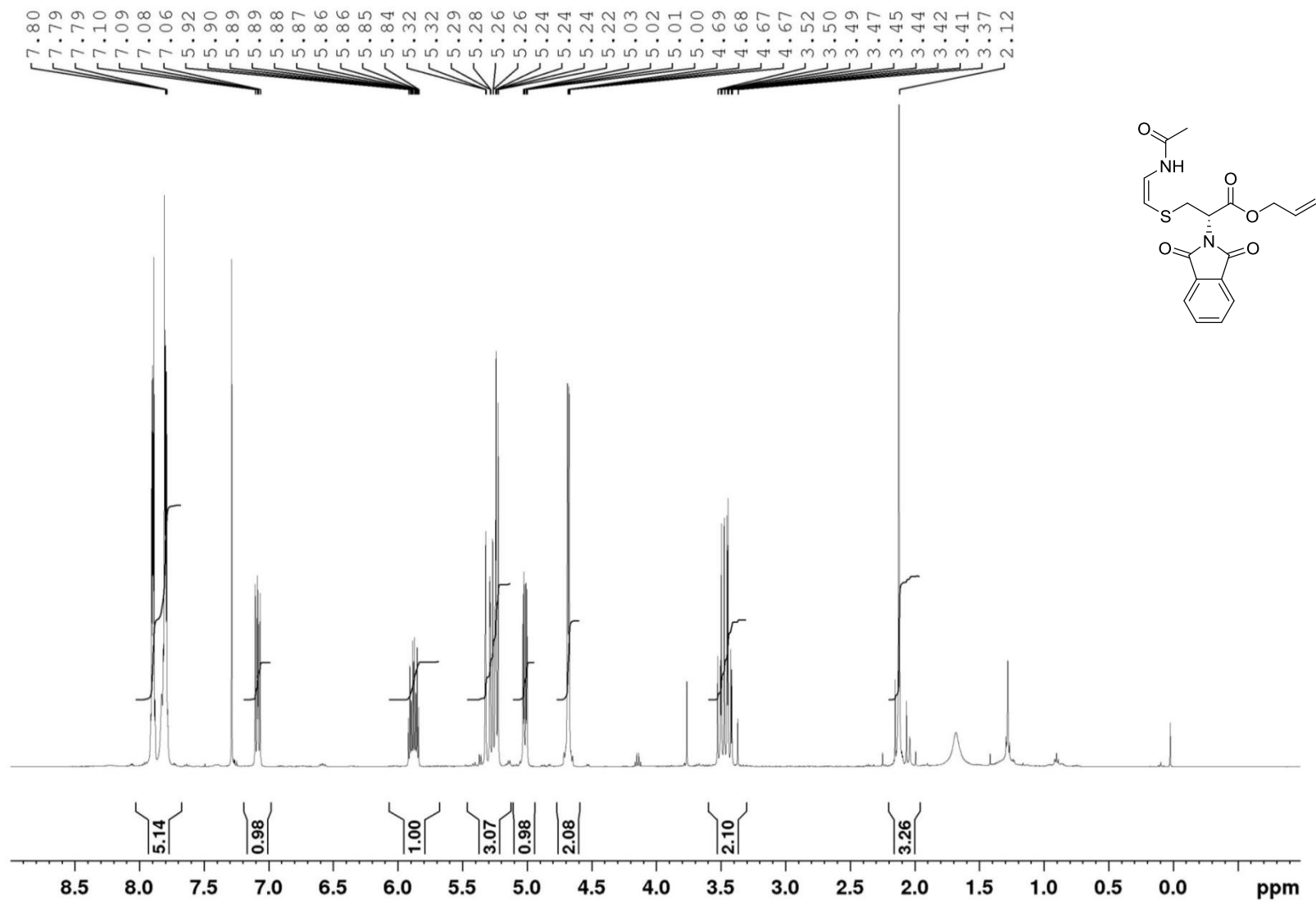
^1H NMR, Compound **42**, DMSO- d_6 , 400 MHz



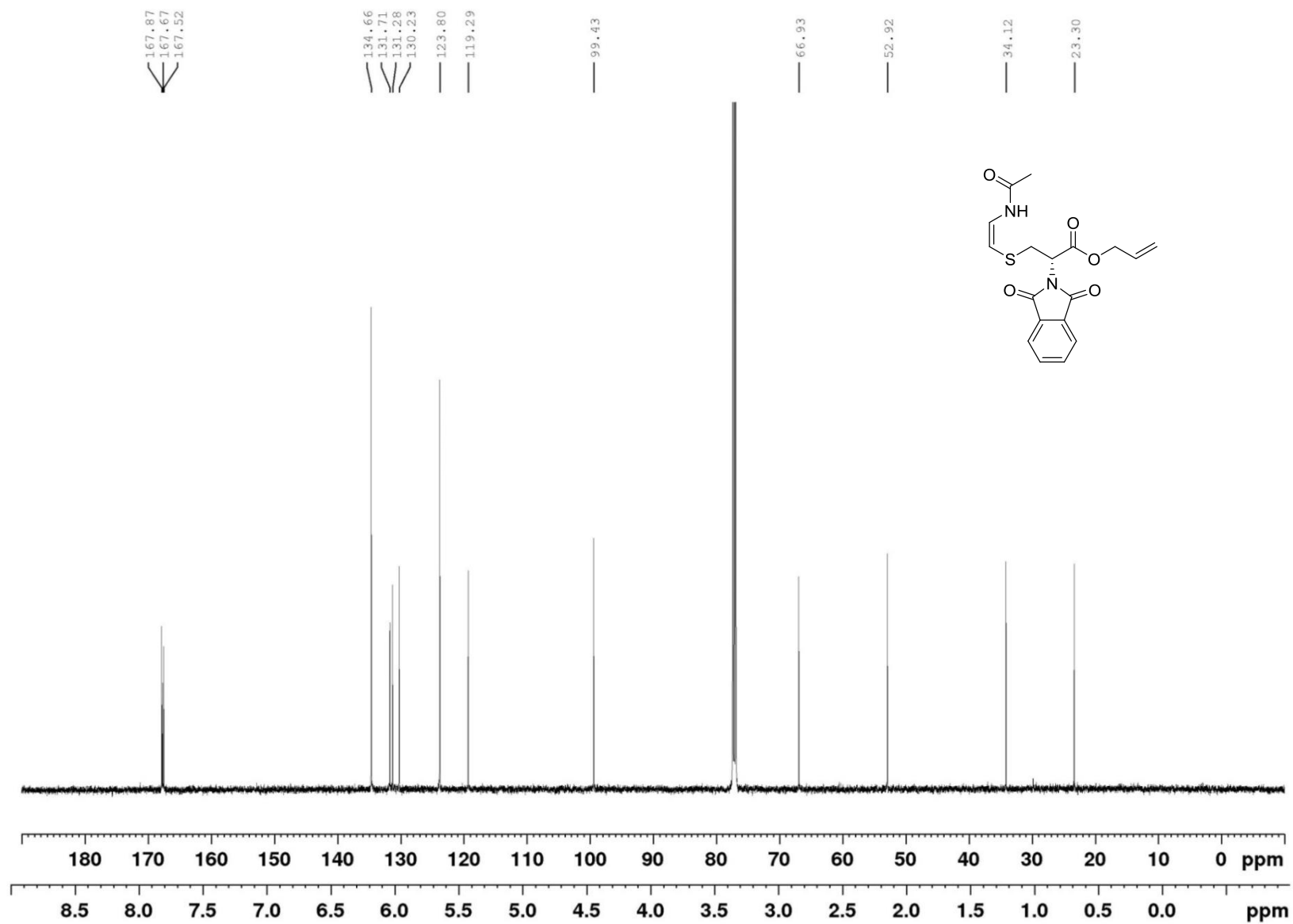
^{13}C NMR, Compound **42**, DMSO- d_6 , 125 MHz



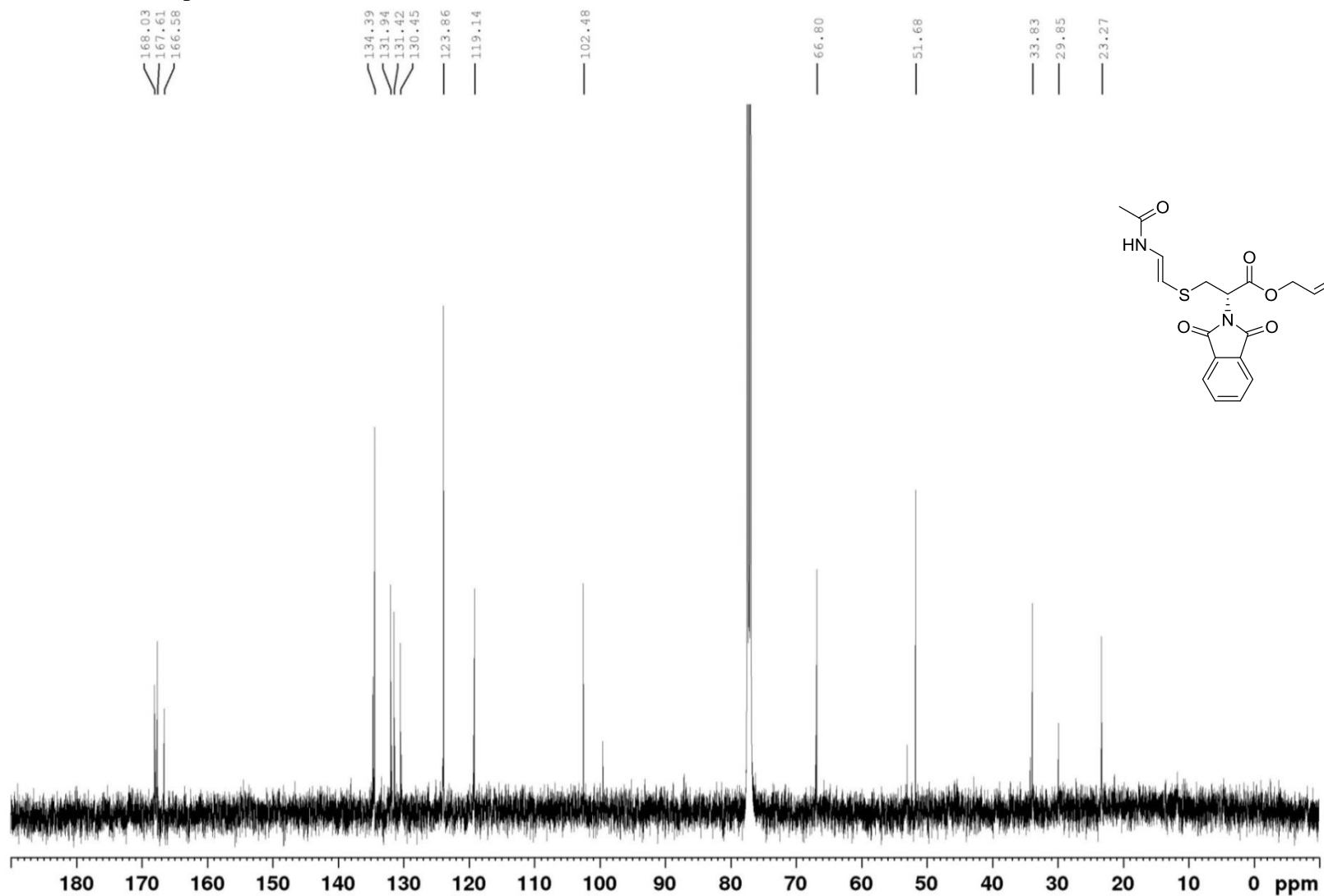
^1H NMR, Compound **Z-49**, CDCl_3 , 500 MHz



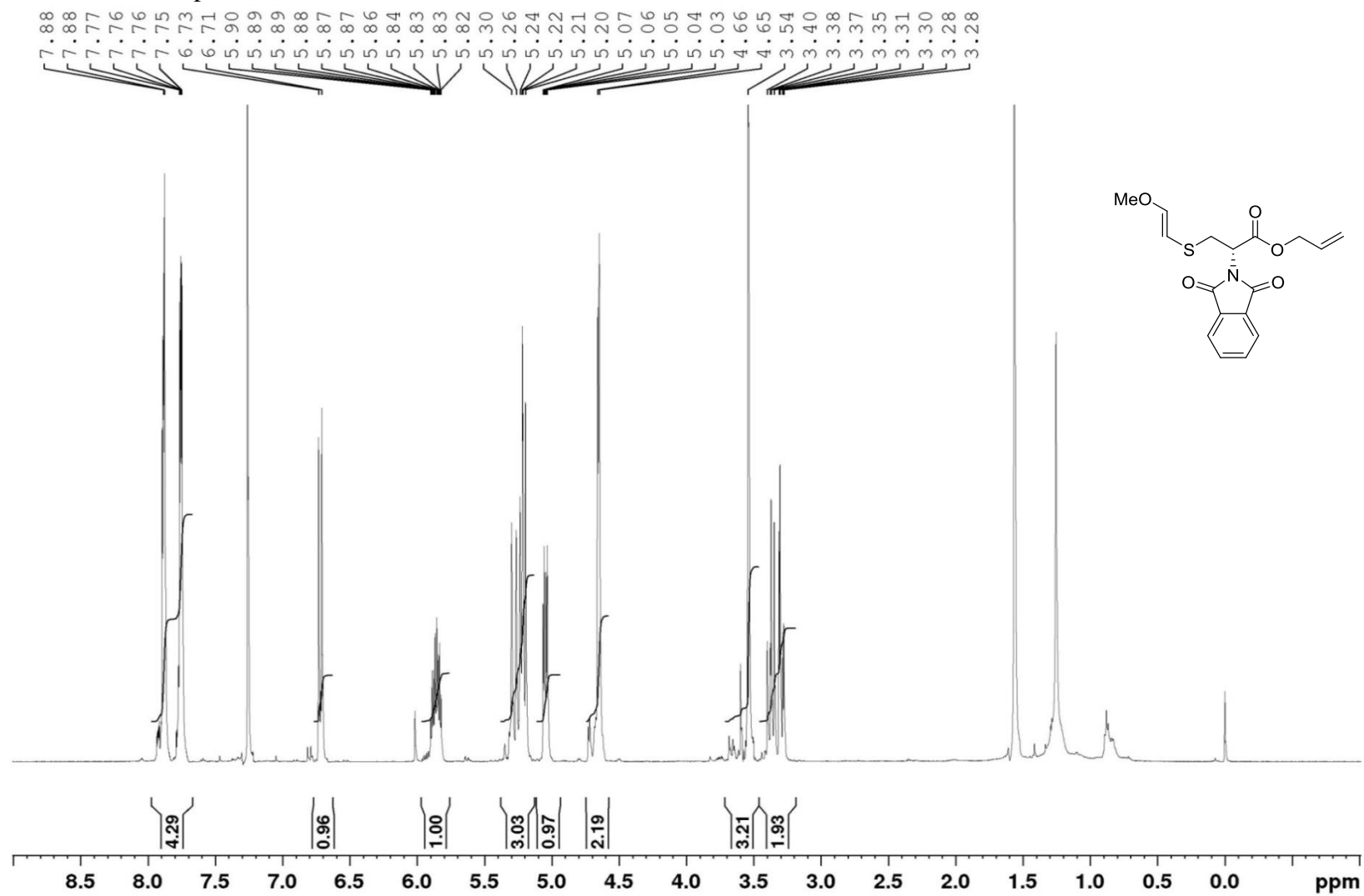
^{13}C NMR, Compound **Z-49**, CDCl_3 , 125 MHz



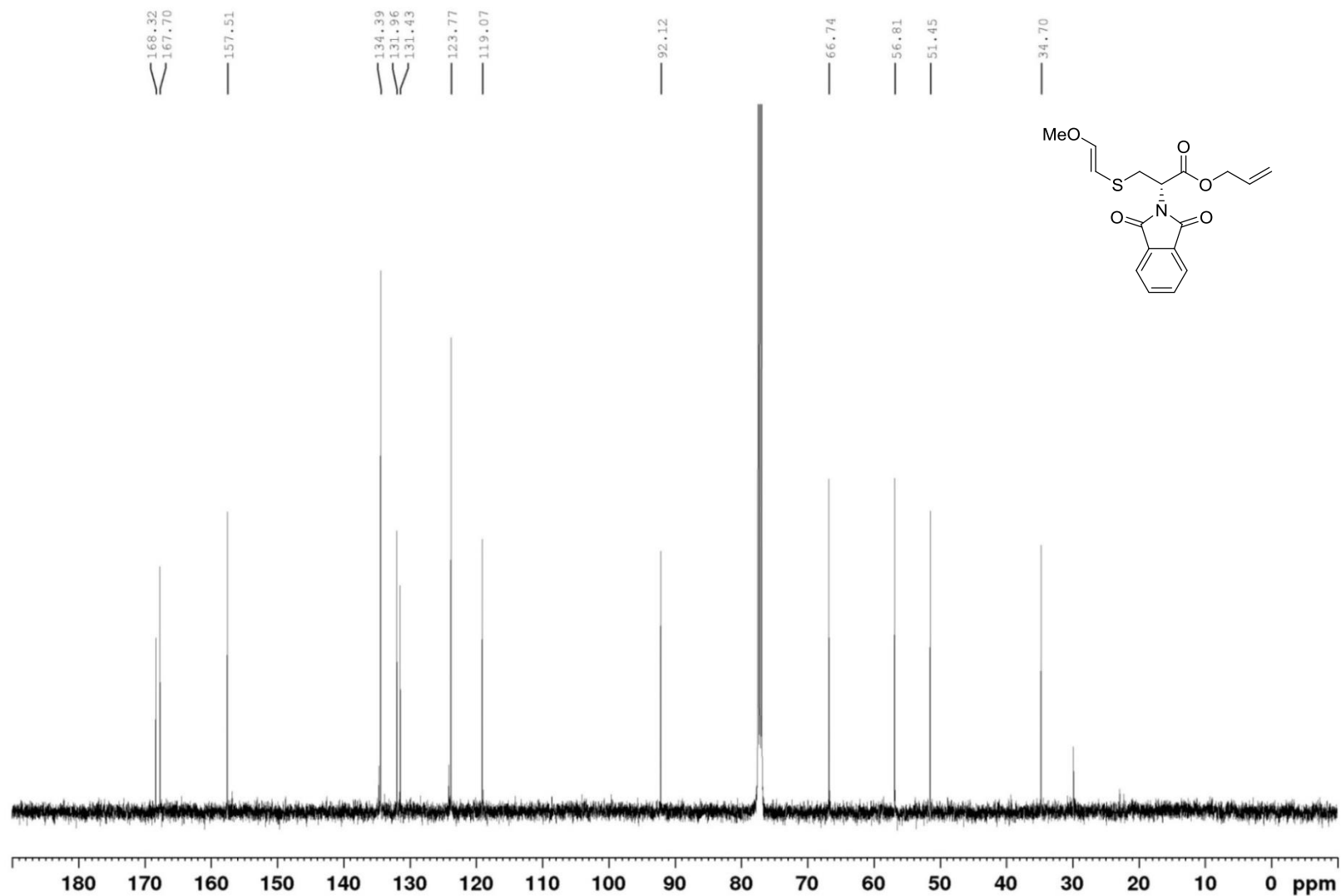
^{13}C NMR Compound ***E-49***, CDCl_3 , 125 MHz



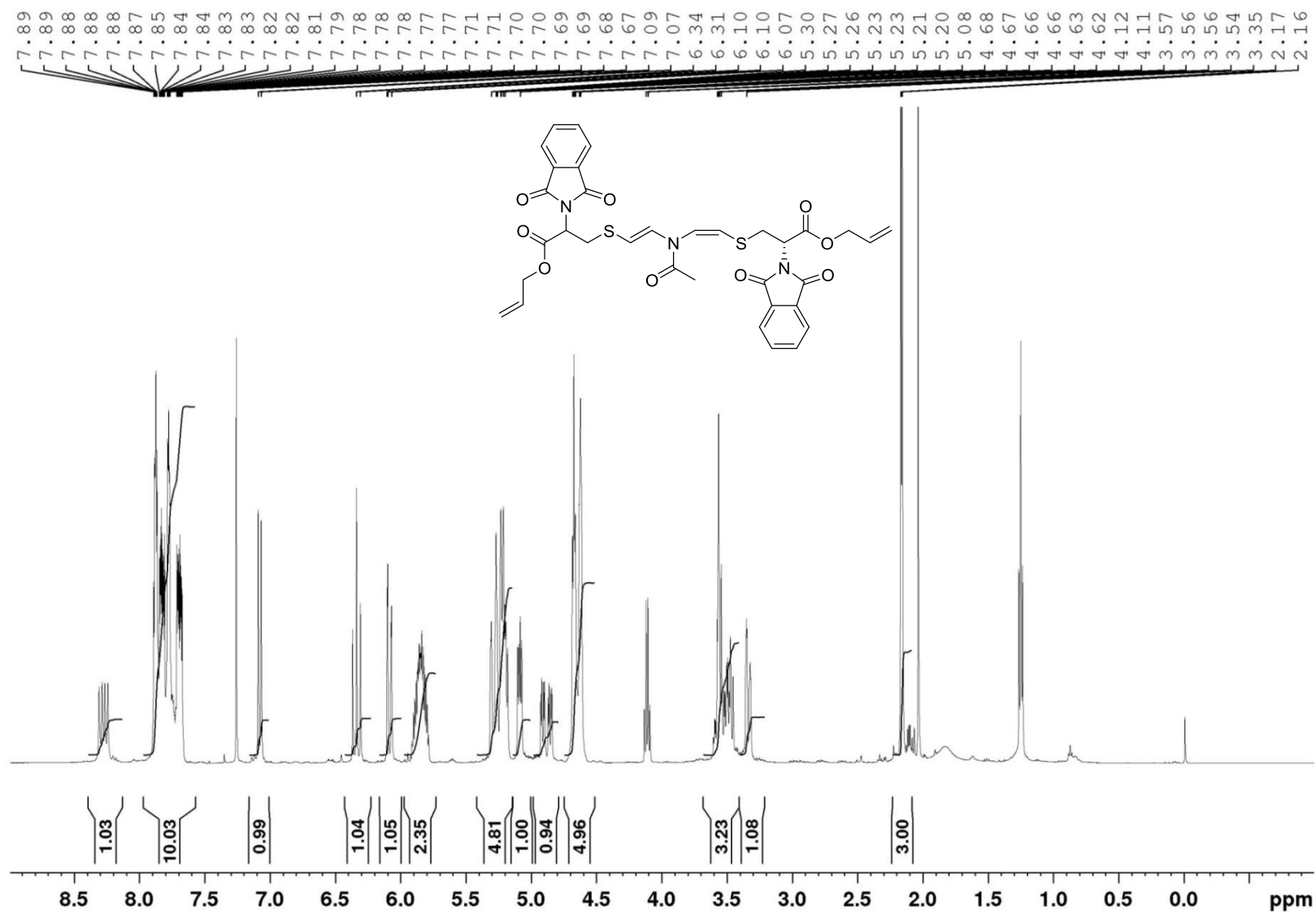
¹H NMR, Compound **50**, CDCl₃, 500 MHz



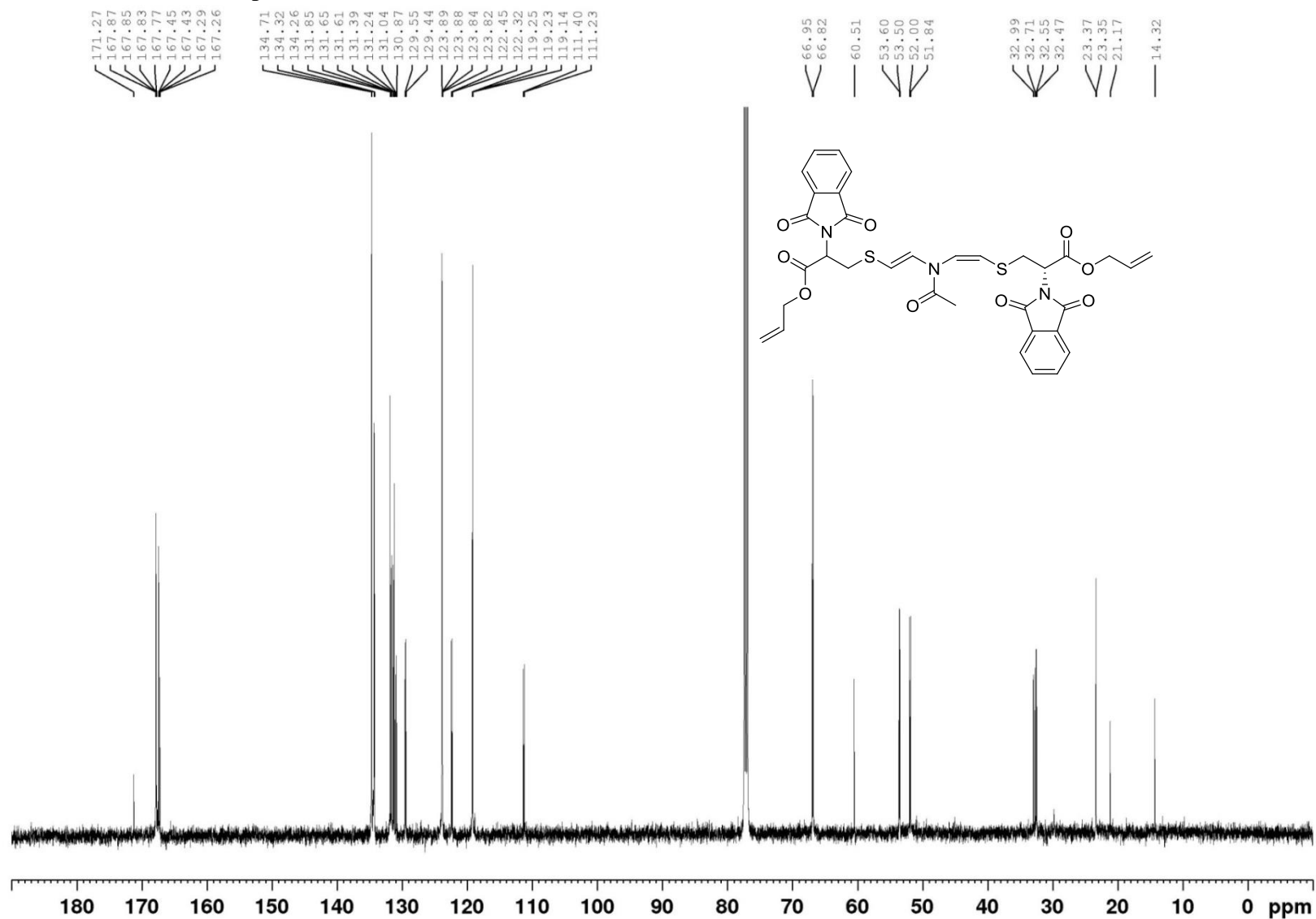
^{13}C NMR, Compound **50**, CDCl_3 , 125 MHz



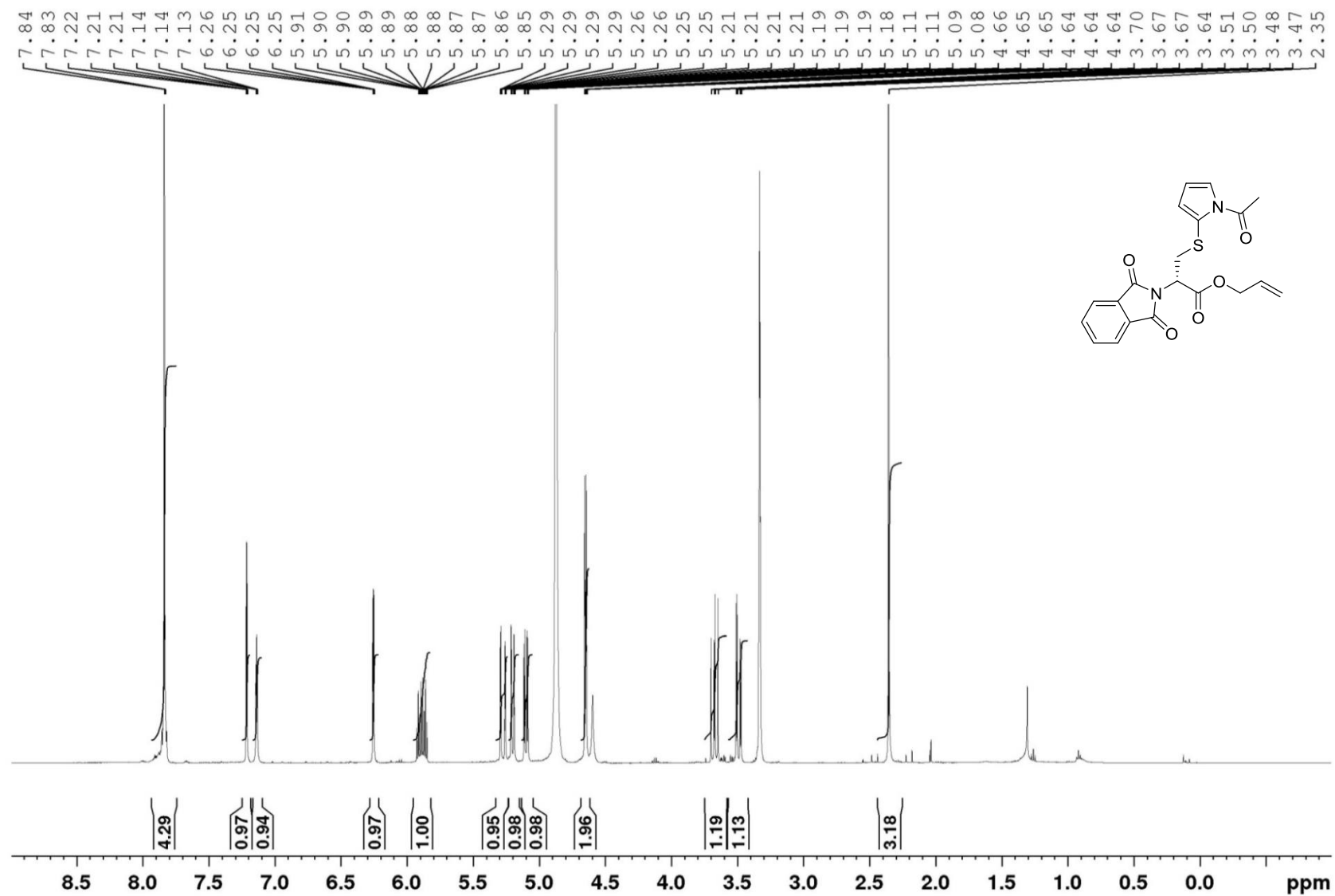
^1H NMR, Compound **54**, CDCl_3 , 400 MHz



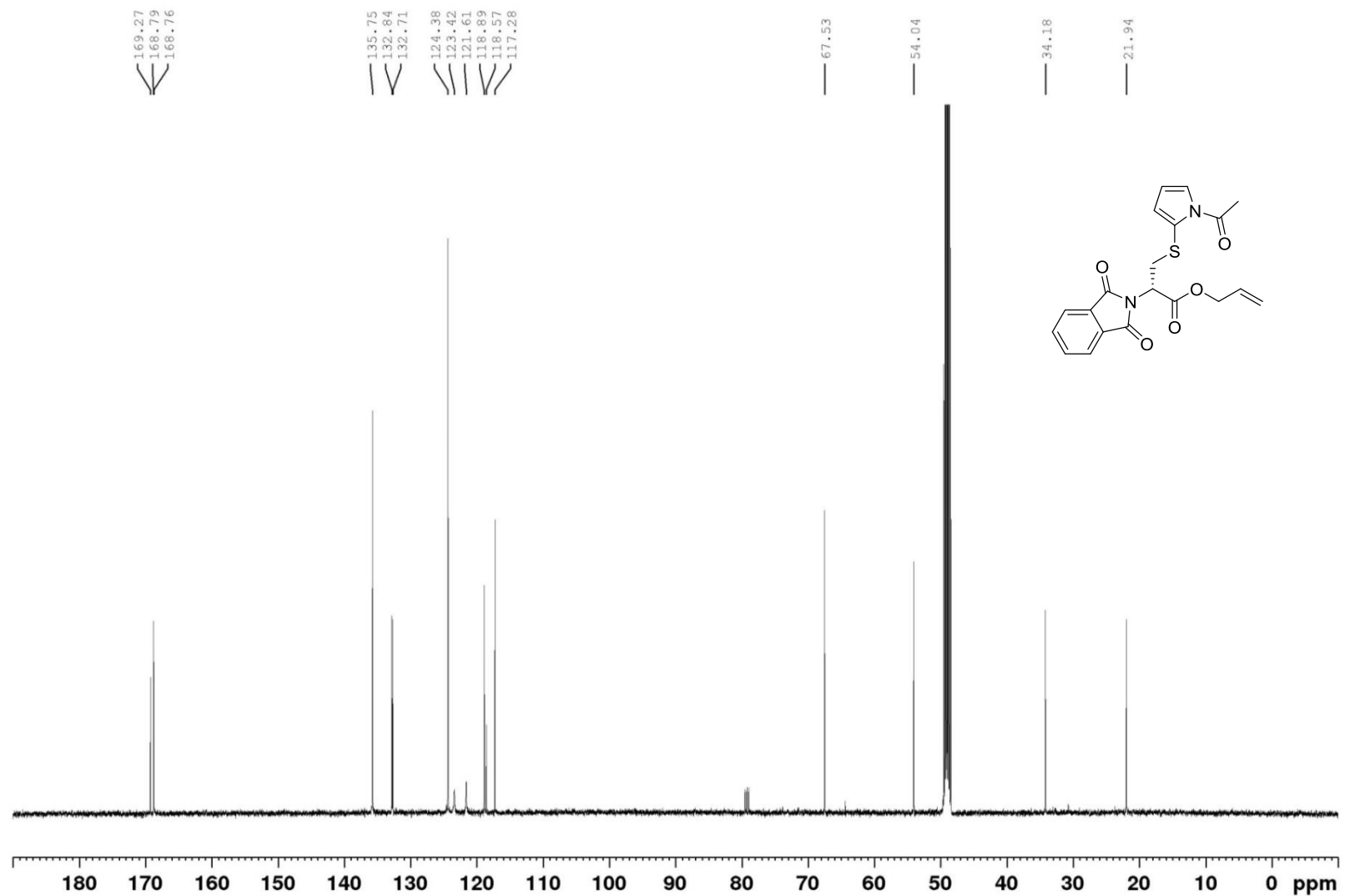
^{13}C NMR, Compound **54**, CDCl_3 , 100 MHz



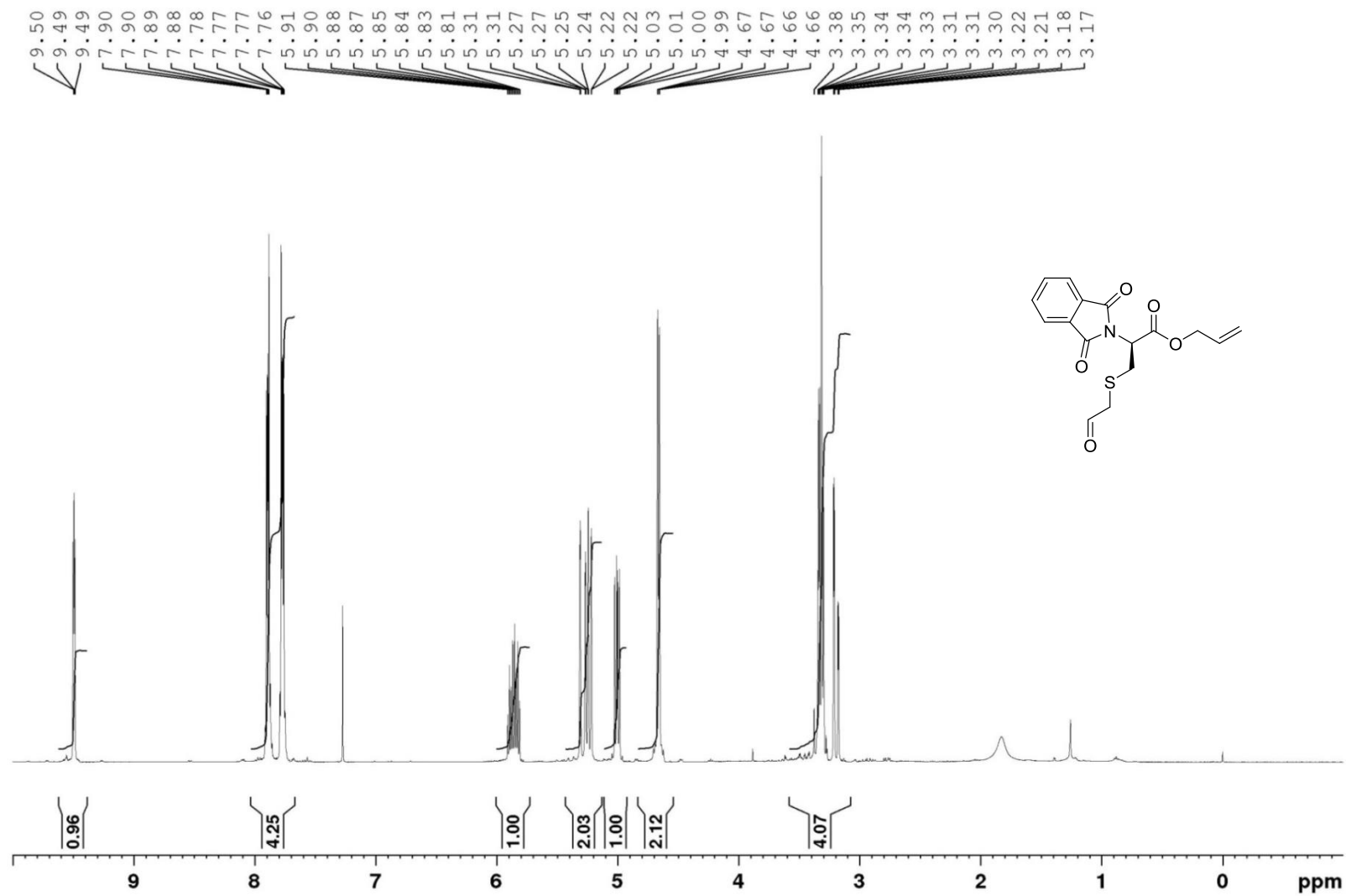
^1H NMR, Compound **55**, CD_3OD , 400 MHz



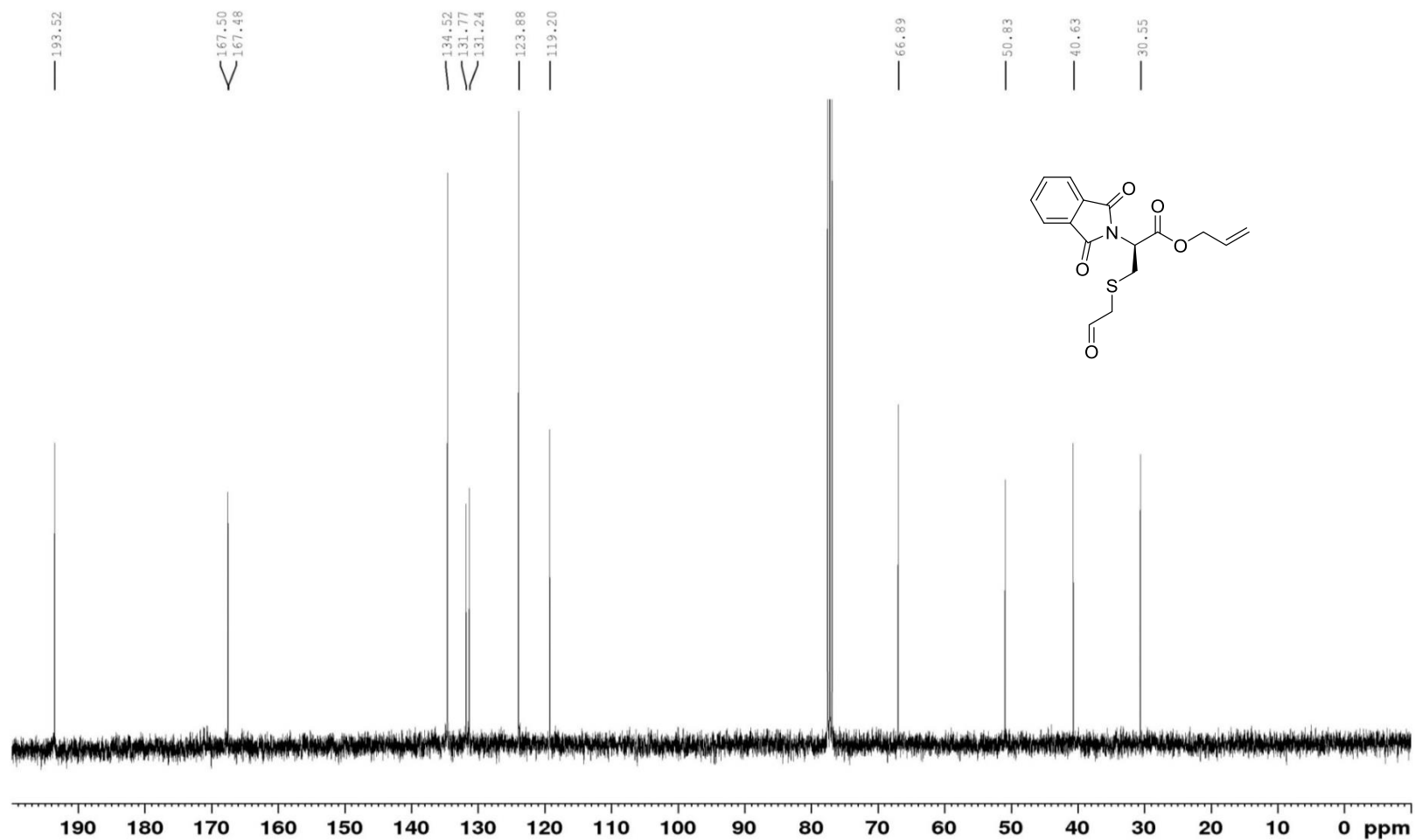
^{13}C NMR Compound **55**, CDCl_3 , 100 MHz



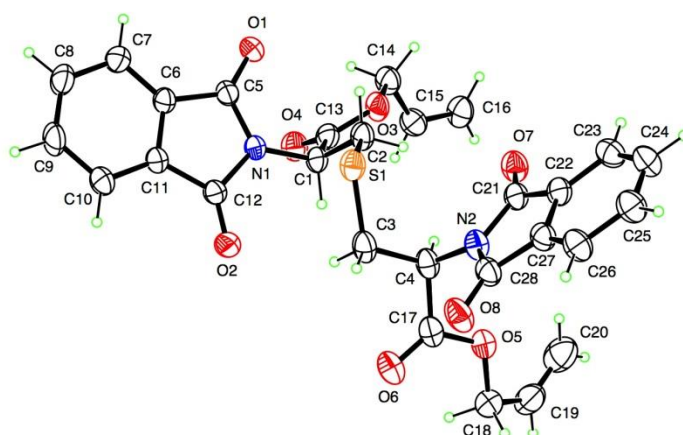
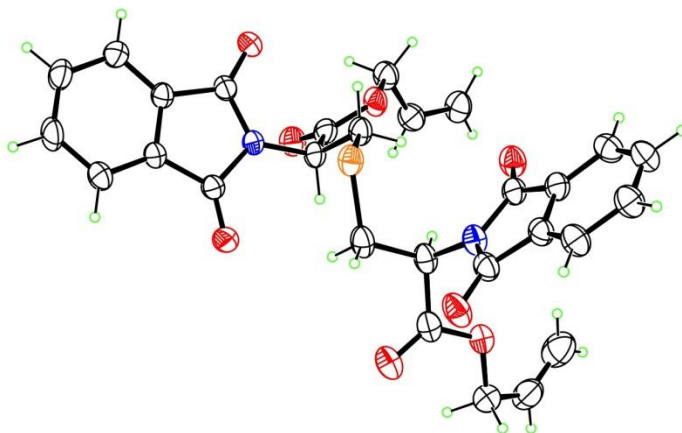
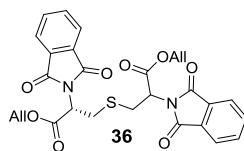
^1H NMR, Compound **56**, CDCl_3 , 400 MHz



^{13}C NMR, Compound **56**, CDCl_3 , 100 MHz



2.9. Crystallographic data for lanthionine 36



Lanthionine 36

Computing details

Data collection: Bruker *APEX3*; cell refinement: Bruker *SAINT*; data reduction: Bruker *SAINT*; program(s) used to solve structure: *SHELXS97* (Sheldrick, 2008); program(s) used to refine structure: *SHELXL2014/7* (Sheldrick, 2014).

(Lutz2)

Crystal data

$C_{28}H_{24}N_2O_8S$	$F(000) = 1144$
$M_r = 548.55$	$D_x = 1.399 \text{ Mg m}^{-3}$
Monoclinic, $P2_1/n$	Cu $K\alpha$ radiation, $\lambda = 1.54184 \text{ \AA}$
$a = 10.9013 (5) \text{ \AA}$	Cell parameters from 6843 reflections
$b = 9.5023 (4) \text{ \AA}$	$\theta = 3.5\text{--}68.2^\circ$
$c = 25.5829 (11) \text{ \AA}$	$\mu = 1.58 \text{ mm}^{-1}$
$\beta = 100.623 (3)^\circ$	$T = 90 \text{ K}$
$V = 2604.6 (2) \text{ \AA}^3$	Lath, colourless
$Z = 4$	$0.23 \times 0.13 \times 0.07 \text{ mm}$

Data collection

Bruker Kappa APEX-II DUO	21861 measured reflections
diffractometer	4739 independent reflections
Radiation source: $I\mu S$ microfocus	3924 reflections with $I > 2\sigma(I)$
QUAZAR multilayer optics monochromator	$R_{\text{int}} = 0.048$
φ and ω scans	$\theta_{\text{max}} = 68.3^\circ$, $\theta_{\text{min}} = 3.5^\circ$
Absorption correction: multi-scan	$h = -12 \rightarrow 13$
<i>SADABS</i> (Sheldrick, 2004)	$k = -10 \rightarrow 11$
$T_{\text{min}} = 0.719$, $T_{\text{max}} = 0.898$	$l = -30 \rightarrow 30$

Refinement

Refinement on F^2	Hydrogen site location: inferred from neighbouring sites
Least-squares matrix: full	H-atom parameters constrained
$R[F^2 > 2\sigma(F^2)] = 0.051$	$w = 1/[\sigma^2(F_o^2) + (0.073P)^2 + 1.9851P]$
$wR(F^2) = 0.143$	where $P = (F_o^2 + 2F_c^2)/3$
$S = 1.05$	$(\Delta/\sigma)_{\text{max}} < 0.001$
4739 reflections	$\Delta\rho_{\text{max}} = 0.74 \text{ e \AA}^{-3}$
352 parameters	$\Delta\rho_{\text{min}} = -0.25 \text{ e \AA}^{-3}$
0 restraints	

Special details

Geometry

All e.s.d.'s (except the e.s.d. in the dihedral angle between two l.s. planes) are estimated using the full covariance matrix. The cell e.s.d.'s are taken into account individually in the estimation of e.s.d.'s in distances, angles and torsion angles; correlations between e.s.d.'s in cell parameters are only used when they are defined by crystal symmetry. An approximate (isotropic) treatment of cell e.s.d.'s is used for estimating e.s.d.'s involving l.s. planes.

Fractional atomic coordinates and isotropic or equivalent isotropic displacement parameters (\AA^2)

	<i>x</i>	<i>y</i>	<i>z</i>	$U_{\text{iso}}^*/U_{\text{eq}}$
S1	0.57769 (5)	0.44064 (7)	0.83971 (2)	0.03767 (19)

O1	0.70114 (15)	0.57856 (18)	0.68793 (7)	0.0350 (4)
O2	0.45051 (16)	0.21918 (19)	0.72270 (7)	0.0383 (4)
O3	0.91565 (14)	0.3787 (2)	0.76607 (7)	0.0379 (4)
O4	0.81424 (16)	0.2731 (2)	0.69187 (7)	0.0411 (4)
O5	0.71956 (17)	−0.0253 (2)	0.93358 (7)	0.0437 (5)
O6	0.53034 (16)	−0.0238 (2)	0.88131 (7)	0.0450 (5)
O7	0.86366 (16)	0.3646 (2)	0.94012 (7)	0.0415 (4)
O8	0.49213 (16)	0.2066 (2)	0.97623 (7)	0.0471 (5)
N1	0.59637 (17)	0.3933 (2)	0.71714 (8)	0.0305 (4)
N2	0.67334 (18)	0.2661 (2)	0.94695 (8)	0.0353 (5)
C1	0.6963 (2)	0.3406 (3)	0.75818 (9)	0.0316 (5)
H1	0.6722	0.2434	0.7674	0.038*
C2	0.7150 (2)	0.4268 (3)	0.80940 (10)	0.0347 (5)
H2A	0.7420	0.5228	0.8016	0.042*
H2B	0.7832	0.3837	0.8354	0.042*
C3	0.5474 (2)	0.2604 (3)	0.85575 (10)	0.0397 (6)
H3A	0.4688	0.2571	0.8699	0.048*
H3B	0.5348	0.2041	0.8226	0.048*
C4	0.6500 (2)	0.1931 (3)	0.89582 (10)	0.0351 (6)
H4	0.7285	0.1989	0.8809	0.042*
C5	0.6068 (2)	0.5080 (3)	0.68495 (9)	0.0303 (5)
C6	0.4844 (2)	0.5238 (3)	0.64895 (9)	0.0313 (5)
C7	0.4443 (2)	0.6232 (3)	0.61035 (10)	0.0378 (6)
H7	0.4978	0.6959	0.6024	0.045*
C8	0.3213 (2)	0.6116 (3)	0.58356 (11)	0.0439 (6)
H8	0.2901	0.6783	0.5567	0.053*
C9	0.2434 (2)	0.5057 (3)	0.59500 (11)	0.0448 (7)
H9	0.1600	0.5012	0.5759	0.054*
C10	0.2851 (2)	0.4049 (3)	0.63416 (11)	0.0398 (6)
H10	0.2317	0.3322	0.6423	0.048*
C11	0.4072 (2)	0.4157 (3)	0.66045 (9)	0.0316 (5)
C12	0.4791 (2)	0.3268 (3)	0.70310 (9)	0.0307 (5)
C13	0.8147 (2)	0.3269 (3)	0.73418 (10)	0.0337 (5)
C14	1.0318 (2)	0.3790 (3)	0.74485 (11)	0.0404 (6)
H14A	1.0879	0.4532	0.7629	0.048*
H14B	1.0128	0.4014	0.7064	0.048*
C15	1.0959 (2)	0.2417 (3)	0.75261 (11)	0.0416 (6)
H15	1.0503	0.1592	0.7403	0.050*
C16	1.2135 (2)	0.2286 (4)	0.77585 (11)	0.0462 (7)
H16A	1.2609	0.3096	0.7885	0.055*
H16B	1.2511	0.1380	0.7800	0.055*
C17	0.6228 (2)	0.0367 (3)	0.90286 (10)	0.0376 (6)
C18	0.7161 (3)	−0.1785 (3)	0.93608 (12)	0.0452 (7)
H18A	0.6699	−0.2167	0.9021	0.054*
H18B	0.6728	−0.2086	0.9650	0.054*
C19	0.8459 (3)	−0.2326 (4)	0.94621 (12)	0.0536 (8)
H19	0.8554	−0.3318	0.9448	0.064*
C20	0.9467 (3)	−0.1603 (4)	0.95659 (14)	0.0650 (9)
H20A	0.9427	−0.0606	0.9585	0.078*
H20B	1.0253	−0.2064	0.9624	0.078*
C21	0.7788 (2)	0.3478 (3)	0.96435 (10)	0.0342 (5)
C22	0.7642 (2)	0.4038 (3)	1.01701 (10)	0.0342 (5)

C23	0.8459 (2)	0.4838 (3)	1.05307 (11)	0.0410 (6)
H23	0.9228	0.5166	1.0452	0.049*
C24	0.8105 (3)	0.5140 (3)	1.10124 (11)	0.0441 (6)
H24	0.8650	0.5674	1.1271	0.053*
C25	0.6974 (3)	0.4681 (3)	1.11253 (11)	0.0436 (6)
H25	0.6760	0.4905	1.1459	0.052*
C26	0.6144 (2)	0.3894 (3)	1.07563 (11)	0.0412 (6)
H26	0.5361	0.3594	1.0829	0.049*
C27	0.6511 (2)	0.3572 (3)	1.02831 (10)	0.0345 (5)
C28	0.5905 (2)	0.2682 (3)	0.98285 (10)	0.0365 (6)

Atomic displacement parameters (\AA^2)

	U^{11}	U^{22}	U^{33}	U^{12}	U^{13}	U^{23}
S1	0.0271 (3)	0.0477 (4)	0.0374 (3)	0.0064 (3)	0.0036 (2)	0.0015 (3)
O1	0.0283 (8)	0.0362 (10)	0.0384 (9)	−0.0063 (7)	0.0007 (7)	0.0010 (7)
O2	0.0310 (8)	0.0372 (10)	0.0448 (10)	−0.0038 (7)	0.0023 (7)	0.0058 (8)
O3	0.0215 (8)	0.0509 (11)	0.0395 (9)	0.0010 (7)	0.0011 (7)	0.0044 (8)
O4	0.0348 (9)	0.0469 (11)	0.0413 (10)	0.0025 (8)	0.0064 (7)	−0.0009 (8)
O5	0.0386 (10)	0.0469 (12)	0.0409 (10)	−0.0048 (8)	−0.0048 (8)	0.0030 (8)
O6	0.0325 (9)	0.0546 (12)	0.0455 (10)	−0.0024 (9)	0.0012 (8)	−0.0097 (9)
O7	0.0301 (9)	0.0545 (12)	0.0394 (10)	−0.0017 (8)	0.0053 (7)	−0.0003 (8)
O8	0.0315 (9)	0.0667 (14)	0.0430 (10)	−0.0122 (9)	0.0065 (8)	−0.0089 (9)
N1	0.0223 (9)	0.0327 (11)	0.0340 (10)	−0.0009 (8)	−0.0015 (8)	0.0036 (8)
N2	0.0286 (10)	0.0438 (13)	0.0323 (10)	0.0014 (9)	0.0022 (8)	−0.0036 (9)
C1	0.0228 (11)	0.0350 (13)	0.0345 (12)	0.0023 (10)	−0.0010 (9)	0.0044 (10)
C2	0.0251 (11)	0.0423 (15)	0.0352 (13)	0.0029 (10)	0.0017 (9)	0.0021 (11)
C3	0.0259 (12)	0.0553 (17)	0.0359 (13)	−0.0001 (11)	0.0006 (10)	−0.0006 (12)
C4	0.0245 (11)	0.0479 (16)	0.0320 (12)	0.0003 (10)	0.0025 (9)	−0.0037 (11)
C5	0.0276 (11)	0.0310 (13)	0.0308 (12)	0.0001 (10)	0.0017 (9)	−0.0024 (10)
C6	0.0257 (11)	0.0327 (13)	0.0338 (12)	0.0024 (9)	0.0007 (9)	0.0013 (10)
C7	0.0340 (13)	0.0373 (14)	0.0406 (14)	0.0003 (11)	0.0028 (10)	0.0060 (11)
C8	0.0359 (13)	0.0497 (17)	0.0422 (15)	0.0063 (12)	−0.0028 (11)	0.0099 (12)
C9	0.0258 (12)	0.0586 (18)	0.0451 (15)	0.0039 (12)	−0.0064 (10)	0.0039 (13)
C10	0.0256 (12)	0.0470 (16)	0.0443 (14)	−0.0034 (11)	0.0000 (10)	0.0034 (12)
C11	0.0256 (11)	0.0344 (13)	0.0328 (12)	0.0001 (10)	0.0004 (9)	0.0007 (10)
C12	0.0253 (11)	0.0314 (13)	0.0343 (12)	−0.0006 (9)	0.0029 (9)	0.0014 (10)
C13	0.0285 (12)	0.0360 (14)	0.0355 (13)	0.0038 (10)	0.0026 (10)	0.0048 (11)
C14	0.0283 (12)	0.0499 (16)	0.0422 (14)	−0.0012 (11)	0.0046 (10)	0.0029 (12)
C15	0.0336 (13)	0.0457 (16)	0.0455 (15)	−0.0023 (11)	0.0079 (11)	−0.0016 (12)
C16	0.0317 (13)	0.0576 (18)	0.0488 (16)	0.0075 (12)	0.0065 (11)	0.0041 (14)
C17	0.0312 (13)	0.0496 (16)	0.0313 (12)	−0.0015 (11)	0.0043 (10)	−0.0044 (11)
C18	0.0459 (15)	0.0463 (17)	0.0418 (15)	−0.0063 (13)	0.0036 (12)	0.0053 (12)
C19	0.0533 (18)	0.0547 (19)	0.0526 (17)	0.0041 (15)	0.0094 (14)	0.0162 (15)
C20	0.057 (2)	0.068 (2)	0.070 (2)	0.0123 (18)	0.0100 (16)	0.0181 (18)
C21	0.0255 (11)	0.0381 (14)	0.0369 (13)	0.0008 (10)	0.0003 (10)	0.0032 (11)
C22	0.0270 (11)	0.0377 (14)	0.0363 (13)	0.0030 (10)	0.0017 (9)	0.0019 (11)
C23	0.0312 (12)	0.0429 (15)	0.0480 (15)	−0.0050 (11)	0.0050 (11)	−0.0028 (12)
C24	0.0431 (15)	0.0452 (16)	0.0416 (14)	−0.0083 (12)	0.0015 (11)	−0.0100 (12)
C25	0.0426 (14)	0.0470 (16)	0.0414 (14)	−0.0018 (12)	0.0081 (11)	−0.0091 (12)
C26	0.0311 (12)	0.0473 (16)	0.0449 (14)	−0.0006 (11)	0.0064 (11)	−0.0071 (12)
C27	0.0284 (12)	0.0351 (14)	0.0381 (13)	0.0020 (10)	0.0009 (10)	−0.0006 (11)

C28	0.0274 (12)	0.0405 (14)	0.0396 (13)	−0.0011 (11)	0.0005 (10)	−0.0016 (11)
-----	-------------	-------------	-------------	--------------	-------------	--------------

Geometric parameters (Å, °)

S1—C3	1.806 (3)	C8—C9	1.383 (4)
S1—C2	1.813 (2)	C8—H8	0.9500
O1—C5	1.218 (3)	C9—C10	1.400 (4)
O2—C12	1.205 (3)	C9—H9	0.9500
O3—C13	1.337 (3)	C10—C11	1.381 (3)
O3—C14	1.467 (3)	C10—H10	0.9500
O4—C13	1.197 (3)	C11—C12	1.484 (3)
O5—C17	1.331 (3)	C14—C15	1.477 (4)
O5—C18	1.458 (4)	C14—H14A	0.9900
O6—C17	1.203 (3)	C14—H14B	0.9900
O7—C21	1.215 (3)	C15—C16	1.316 (4)
O8—C28	1.205 (3)	C15—H15	0.9500
N1—C5	1.384 (3)	C16—H16A	0.9500
N1—C12	1.412 (3)	C16—H16B	0.9500
N1—C1	1.456 (3)	C18—C19	1.483 (4)
N2—C21	1.391 (3)	C18—H18A	0.9900
N2—C28	1.402 (3)	C18—H18B	0.9900
N2—C4	1.461 (3)	C19—C20	1.281 (5)
C1—C2	1.527 (4)	C19—H19	0.9500
C1—C13	1.534 (3)	C20—H20A	0.9500
C1—H1	1.0000	C20—H20B	0.9500
C2—H2A	0.9900	C21—C22	1.484 (4)
C2—H2B	0.9900	C22—C23	1.385 (4)
C3—C4	1.513 (3)	C22—C27	1.390 (3)
C3—H3A	0.9900	C23—C24	1.388 (4)
C3—H3B	0.9900	C23—H23	0.9500
C4—C17	1.532 (4)	C24—C25	1.388 (4)
C4—H4	1.0000	C24—H24	0.9500
C5—C6	1.483 (3)	C25—C26	1.398 (4)
C6—C7	1.378 (3)	C25—H25	0.9500
C6—C11	1.393 (3)	C26—C27	1.377 (4)
C7—C8	1.393 (4)	C26—H26	0.9500
C7—H7	0.9500	C27—C28	1.491 (4)
C3—S1—C2	103.20 (12)	N1—C12—C11	105.3 (2)
C13—O3—C14	116.4 (2)	O4—C13—O3	125.1 (2)
C17—O5—C18	116.4 (2)	O4—C13—C1	122.3 (2)
C5—N1—C12	111.80 (19)	O3—C13—C1	112.5 (2)
C5—N1—C1	124.58 (19)	O3—C14—C15	111.6 (2)
C12—N1—C1	123.5 (2)	O3—C14—H14A	109.3
C21—N2—C28	112.1 (2)	C15—C14—H14A	109.3
C21—N2—C4	123.3 (2)	O3—C14—H14B	109.3
C28—N2—C4	124.5 (2)	C15—C14—H14B	109.3
N1—C1—C2	113.4 (2)	H14A—C14—H14B	108.0
N1—C1—C13	108.28 (19)	C16—C15—C14	122.8 (3)
C2—C1—C13	113.58 (19)	C16—C15—H15	118.6
N1—C1—H1	107.0	C14—C15—H15	118.6
C2—C1—H1	107.0	C15—C16—H16A	120.0

C13—C1—H1	107.0	C15—C16—H16B	120.0
C1—C2—S1	114.59 (17)	H16A—C16—H16B	120.0
C1—C2—H2A	108.6	O6—C17—O5	124.4 (3)
S1—C2—H2A	108.6	O6—C17—C4	125.0 (2)
C1—C2—H2B	108.6	O5—C17—C4	110.5 (2)
S1—C2—H2B	108.6	O5—C18—C19	108.8 (2)
H2A—C2—H2B	107.6	O5—C18—H18A	109.9
C4—C3—S1	114.31 (18)	C19—C18—H18A	109.9
C4—C3—H3A	108.7	O5—C18—H18B	109.9
S1—C3—H3A	108.7	C19—C18—H18B	109.9
C4—C3—H3B	108.7	H18A—C18—H18B	108.3
S1—C3—H3B	108.7	C20—C19—C18	127.2 (3)
H3A—C3—H3B	107.6	C20—C19—H19	116.4
N2—C4—C3	113.0 (2)	C18—C19—H19	116.4
N2—C4—C17	111.1 (2)	C19—C20—H20A	120.0
C3—C4—C17	110.8 (2)	C19—C20—H20B	120.0
N2—C4—H4	107.2	H20A—C20—H20B	120.0
C3—C4—H4	107.2	O7—C21—N2	124.9 (2)
C17—C4—H4	107.2	O7—C21—C22	129.4 (2)
O1—C5—N1	123.9 (2)	N2—C21—C22	105.7 (2)
O1—C5—C6	129.5 (2)	C23—C22—C27	121.5 (2)
N1—C5—C6	106.60 (19)	C23—C22—C21	129.7 (2)
C7—C6—C11	122.2 (2)	C27—C22—C21	108.8 (2)
C7—C6—C5	130.1 (2)	C22—C23—C24	117.1 (2)
C11—C6—C5	107.7 (2)	C22—C23—H23	121.5
C6—C7—C8	116.6 (2)	C24—C23—H23	121.5
C6—C7—H7	121.7	C23—C24—C25	121.5 (3)
C8—C7—H7	121.7	C23—C24—H24	119.2
C9—C8—C7	121.7 (2)	C25—C24—H24	119.2
C9—C8—H8	119.1	C24—C25—C26	121.1 (3)
C7—C8—H8	119.1	C24—C25—H25	119.4
C8—C9—C10	121.2 (2)	C26—C25—H25	119.4
C8—C9—H9	119.4	C27—C26—C25	117.1 (2)
C10—C9—H9	119.4	C27—C26—H26	121.5
C11—C10—C9	117.0 (2)	C25—C26—H26	121.5
C11—C10—H10	121.5	C26—C27—C22	121.7 (2)
C9—C10—H10	121.5	C26—C27—C28	130.7 (2)
C10—C11—C6	121.2 (2)	C22—C27—C28	107.6 (2)
C10—C11—C12	130.3 (2)	O8—C28—N2	124.4 (2)
C6—C11—C12	108.5 (2)	O8—C28—C27	129.8 (2)
O2—C12—N1	124.4 (2)	N2—C28—C27	105.8 (2)
O2—C12—C11	130.3 (2)		
C5—N1—C1—C2	78.5 (3)	C14—O3—C13—C1	−175.9 (2)
C12—N1—C1—C2	−105.9 (3)	N1—C1—C13—O4	−46.6 (3)
C5—N1—C1—C13	−48.6 (3)	C2—C1—C13—O4	−173.6 (2)
C12—N1—C1—C13	127.0 (2)	N1—C1—C13—O3	134.6 (2)
N1—C1—C2—S1	57.4 (3)	C2—C1—C13—O3	7.6 (3)
C13—C1—C2—S1	−178.36 (17)	C13—O3—C14—C15	−83.7 (3)
C3—S1—C2—C1	62.4 (2)	O3—C14—C15—C16	−126.9 (3)
C2—S1—C3—C4	63.2 (2)	C18—O5—C17—O6	6.6 (4)
C21—N2—C4—C3	−107.4 (3)	C18—O5—C17—C4	−169.5 (2)

C28—N2—C4—C3	69.2 (3)	N2—C4—C17—O6	123.7 (3)
C21—N2—C4—C17	127.3 (2)	C3—C4—C17—O6	−2.9 (3)
C28—N2—C4—C17	−56.1 (3)	N2—C4—C17—O5	−60.3 (3)
S1—C3—C4—N2	60.2 (3)	C3—C4—C17—O5	173.2 (2)
S1—C3—C4—C17	−174.32 (17)	C17—O5—C18—C19	150.8 (2)
C12—N1—C5—O1	−176.8 (2)	O5—C18—C19—C20	6.6 (5)
C1—N1—C5—O1	−0.8 (4)	C28—N2—C21—O7	−179.1 (2)
C12—N1—C5—C6	3.5 (3)	C4—N2—C21—O7	−2.0 (4)
C1—N1—C5—C6	179.6 (2)	C28—N2—C21—C22	1.9 (3)
O1—C5—C6—C7	−1.5 (4)	C4—N2—C21—C22	179.0 (2)
N1—C5—C6—C7	178.1 (3)	O7—C21—C22—C23	−3.4 (5)
O1—C5—C6—C11	179.1 (3)	N2—C21—C22—C23	175.5 (3)
N1—C5—C6—C11	−1.3 (3)	O7—C21—C22—C27	179.6 (3)
C11—C6—C7—C8	0.8 (4)	N2—C21—C22—C27	−1.5 (3)
C5—C6—C7—C8	−178.6 (3)	C27—C22—C23—C24	0.7 (4)
C6—C7—C8—C9	−0.1 (4)	C21—C22—C23—C24	−175.9 (3)
C7—C8—C9—C10	−0.1 (5)	C22—C23—C24—C25	−1.0 (4)
C8—C9—C10—C11	−0.4 (4)	C23—C24—C25—C26	−0.1 (5)
C9—C10—C11—C6	1.0 (4)	C24—C25—C26—C27	1.4 (4)
C9—C10—C11—C12	−179.7 (3)	C25—C26—C27—C22	−1.6 (4)
C7—C6—C11—C10	−1.3 (4)	C25—C26—C27—C28	175.1 (3)
C5—C6—C11—C10	178.2 (2)	C23—C22—C27—C26	0.6 (4)
C7—C6—C11—C12	179.3 (2)	C21—C22—C27—C26	177.9 (2)
C5—C6—C11—C12	−1.2 (3)	C23—C22—C27—C28	−176.8 (2)
C5—N1—C12—O2	174.6 (2)	C21—C22—C27—C28	0.5 (3)
C1—N1—C12—O2	−1.5 (4)	C21—N2—C28—O8	179.2 (3)
C5—N1—C12—C11	−4.2 (3)	C4—N2—C28—O8	2.3 (4)
C1—N1—C12—C11	179.7 (2)	C21—N2—C28—C27	−1.6 (3)
C10—C11—C12—O2	5.2 (5)	C4—N2—C28—C27	−178.6 (2)
C6—C11—C12—O2	−175.5 (3)	C26—C27—C28—O8	2.6 (5)
C10—C11—C12—N1	−176.1 (3)	C22—C27—C28—O8	179.7 (3)
C6—C11—C12—N1	3.2 (3)	C26—C27—C28—N2	−176.4 (3)
C14—O3—C13—O4	5.3 (4)	C22—C27—C28—N2	0.6 (3)

2.10. Notes

1. Franke, W.; Kraft, R. "Cyclization with Acetoacetaldehyde Bisacetal," *Ber.*, **1953**, 86, 797-800.
2. Estevez, J.C.; Villaverde, M.C.; Estevez, R.J.; Castedo, L. "A New Synthesis of Styrylamides," *Synth. Commun.*, **1993**, 23, 1081-1085.
3. Baxter, A.J.G.; Ponsford, R.J.; Southgate, R. "Synthesis of Olivanic Acid Analogs. Preparation of 7-Oxo-1-azabicyclo-[3.2.0]hept-2-ene-2-carboxylates Containing the 3-(2-Acetamido-ethenylthio) Side Chain," *J.C.S., Chem. Commun.*, **1980**, 429-431.
4. Wolfe, S.; Tel, L.M.; Liang, J.H.; Csizmadia, I.G. "Stereochemical Consequences of Adjacent Electron Pairs. Theoretical Study of Rotation-Inversion in Ethylene Dicarbanion," *J. Am. Chem. Soc.*, **1972**, 4, 1361-1364.
5. Li, Y.; Carter, D.E.; Mash, E.A. "Synthesis and Structure of the Glutathione Conjugate of Chloroacetaldehyde," *Synth. Commun.*, **2002**, 32, 1579-1583.
6. Reed, A.E.; Weinstock, R. B.; Weinhold, F. "Natural Population Analysis," *J. Chem. Phys.* **1985**, 83, 735-746
7. Lutz, J.A.; Subasinghe Don, V.; Kumar, R.; Taylor, C.M. "Influence of Sulfur on Acid-Mediated Enamide Formation," *Org. Lett.*, **2017**, 19, 5146-5149.
8. Nakamura, Y.; Ishii, K.; Ono, E.; Ishihara, M.; Kohda, T.; Yokogawa, Y.; Shibai, H. "A Novel Naturally Occurring Carbapenem Antibiotic, AB-110-D, Produced by *Kitasatosporia papulosa* novo Sp." *J. Antibiot.*, **1988**, 41, 707-711.
9. Garcia-Reynaga, P.; Carrillo, A.K.; VanNieuwenhze, M.S. "Decarbonylative Approach to the Synthesis of Enamides from Amino Acids: Stereoselective Synthesis of the (Z)-Aminovinyl-D-Cysteine Unit of Mersacidin," *Org. Lett.*, **2012**, 14, 1030-1033.
10. Banerjee, B.; Litvinov, D.N.; Kang, J.; Bettale, J.D.; Castle, S.L. "Stereoselective Additions of Thiyl Radicals to Terminal Ynamides" *Org. Lett.*, **2010**, 12, 2650-2652.
11. Harada, S.; Tsubotani, S.; Asai, M.; Okonogi, K.; Kondo, M. "Synthesis and Biological Activities of the (Z) Isomers of Carbapenem Antibiotics," *J. Med. Chem.* **1983**, 26, 271-275.
12. Kurita, J.; Sakai, H.; Yamada, S.; Tsuchiya T. "Novel Thermal Rearrangements of Tetrahydroazirinocyclobutabenzofuran Derivatives," *J. C. S., Chem. Commun.*, **1987**, 285-286.
13. Harichandran, G., Amalraj, S.D., Shanmugam, P. "Boric Acid Catalyzed Efficient Synthesis of Symmetrical *N, N'*-(Alkylidene) Bis[amide] Derivatives," *J. Iran Chem. Soc.*, **2011**, 298-305.

14. Chen, C-C., Chen, L-Y., Lin, R-Y., Chu, C-Y., Dai, S.A. "A Non-acyl Azide Route to Isoquinolin-1(2*H*)-one Derivatives Via β -Styryl Carbamates," *Heterocycles*, **2009**, 78, 2979-2992.
15. Schneider, A.E., Manolikakes, G. "Bi(OTf)₃-Catalyzed Multicomponent α -Amidoalkylation Reactions," *J. Org. Chem.*, **2015**, 80, 6193-6212.

Chapter 3. Cysteine Epimerization and an Improved Synthesis of the Building Block in Enantioenriched Form

3.1. A Strange Problem

As we moved from couplings of aldehyde **56** with acetamide to reactions involving amino amide coupling partners, we noticed a recurring theme in the thioenamide products. The NMR spectra always displayed multiple species of the desired product. Though epimerization issues are always under consideration in peptide chemistry, we were aware that restricted conformations, especially with an unprecedented functional group with hydrogen bonding capacity, could also explain the presence of multiple species on the timescale of ^1H NMR experiments. Given the scarcity of thioenamide-containing compounds in the literature, we proceeded with our optimization of amino amide thioenamide formation, always carefully bearing in mind this strange problem.

Thioenamide **62** (see Chapter 4 for more detail of this reaction) was the first compound to yield two sets of sharp, distinguishable thioenamide ^1H NMR signals that definitively revealed a 1:1 ratio of the two species (Figure 3.1). The thioenamide olefin protons adjacent to the amide nitrogen clearly showed a *cis* relationship ($J = 7.4$ Hz) about the double bond in *both* species. The minor *trans* thioenamide isomer ($J = 13.8$ Hz) was removed via column chromatography prior to this analysis. The curious 1:1 mixture gave us pause, as both conformational bias and epimerization would be expected to produce a *degree* of isomerization, rather than a perfect equimolar mixture. This pivotal result encouraged us to review previous reactions involving our cysteine building block and strongly consider the possibility of racemization.

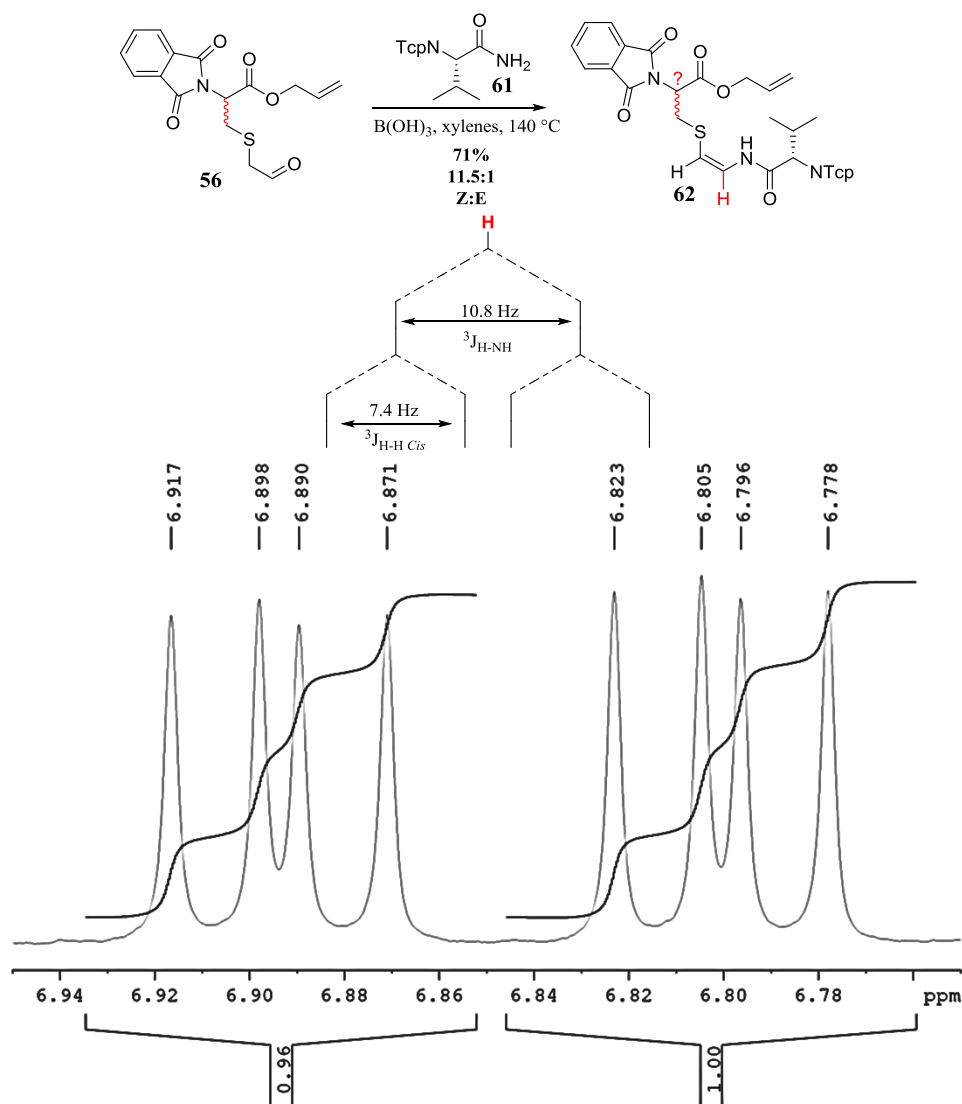
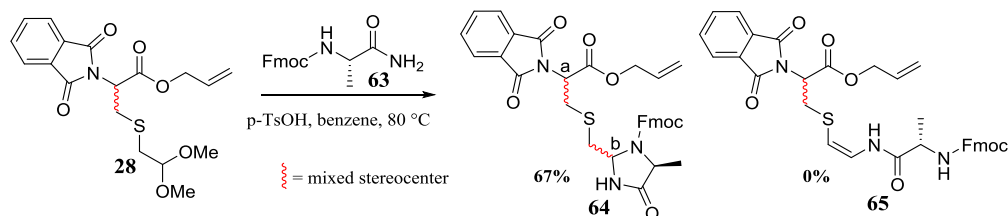


Figure 3.1. Formation of thioenamide **62** and ^1H NMR (CDCl₃, 400 MHz, 6.75–7.00 ppm region) evidence for two sets of *cis* thioenamide protons (H shown in red on **62**)

3.2. Imidazolidinone: Evidence for Epimerization

When cysteine-derived acetal **28** was reacted with alaninamide **63**, instead of thioenamide **65**, we obtained imidazolidinone **64** (Scheme 3.1). For further details of this reaction, see Chapter 4. With the generation of a new stereocenter, imidazolidinone **64** is predicted to be a mixture of diastereomers about the newly formed stereocenter (Scheme 3.1, compound **64**, center b). Two species could be separated via flash chromatography. However,

characterization using NMR revealed that each specimen was, itself, a mixture of two compounds. This observation was consistent with a scrambled stereocenter at C α in cysteine **28** resulting in a more complicated mixture of compound **64** than anticipated, i.e. epimers at both a and b (Scheme 3.1). This result demonstrated that it was not specifically the thioenamide functional group that was responsible for the mixture of apparently isomeric compounds.



Scheme 3.1. Formation of imidazolidinone **64**

3.3. The Canary in the Coal Mine

An even earlier indication that there was something awry in the synthesis of our cysteine building block was the observation that tripeptide **39** (see Chapter 2, Scheme 2.8) was obtained as a mixture of at least three compounds, inseparable by flash chromatography. In this context, the mixture could arise from a racemic cysteine **28**, in combination with epimerization taking place at the phenylalanine α -carbon during peptide coupling (Figure 3.2, A). Indeed, when the order of events for tripeptide formation was changed, so that epimerization of phenylalanine was less likely (see Chapter 2, Scheme 2.9), the product mixture was simplified to two compounds with the same molecular mass (Figure 3.2, B). This early result showed, in retrospect, that the issue of isomeric species could be traced back to our original cysteine building block.

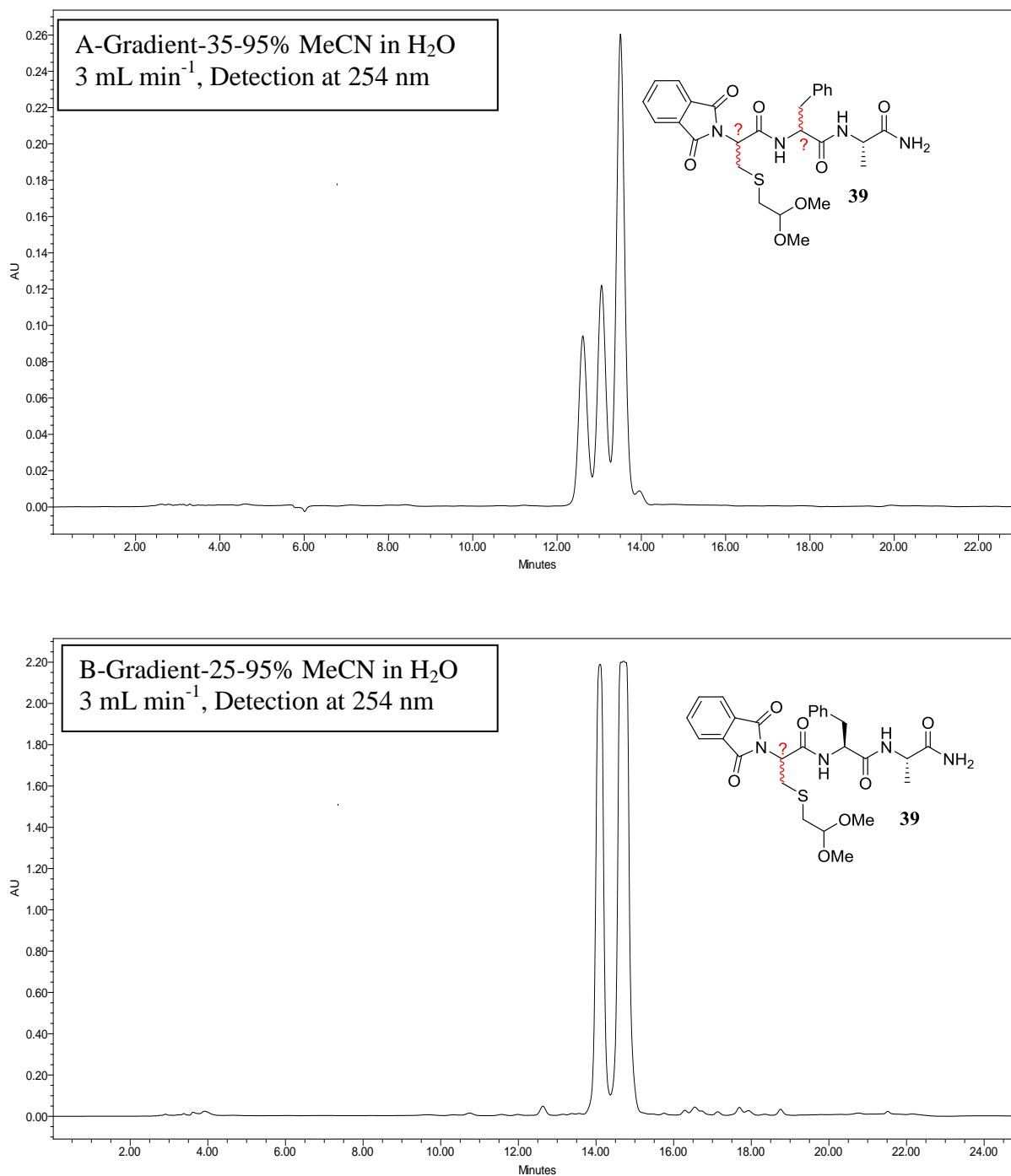
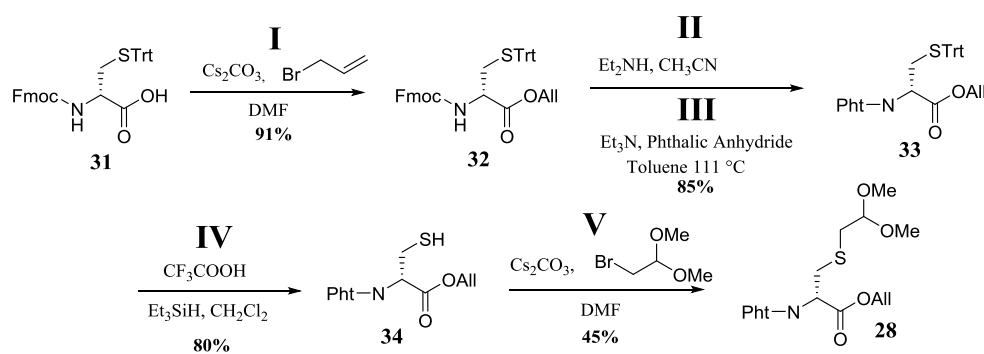


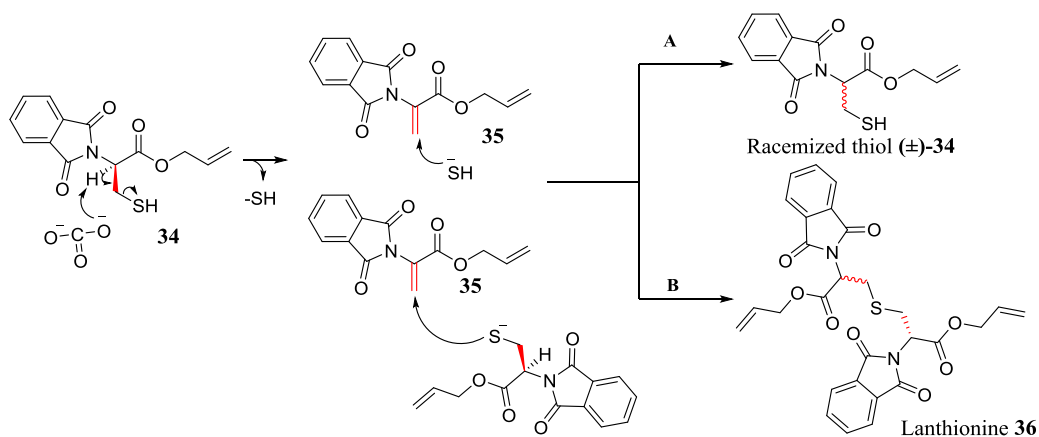
Figure 3.2. HPLC Chromatograms of tripeptide **39**. (A) Synthesized according to Scheme 2.8 (first generation) and (B) Synthesized according to Scheme 2.9 (second generation) Column-Altima 10 μ m, C18 (250 mm \times 10 mm)

3.4. The Usual Suspects

The most obvious culprit, in terms of a reaction with the potential to be accompanied by racemization, was the thiol alkylation (Scheme 3.2, step **V**). Alkaline conditions, coupled with the strong electron-withdrawing nature of the phthalimido group, prime this step for elimination of the thiolate anion. Racemization could arise after protonation of a dehydroalanine (Scheme 3.3). Additionally, the previous isolation of dimeric thioether **36** illuminated the high potential for elimination and conjugate addition.



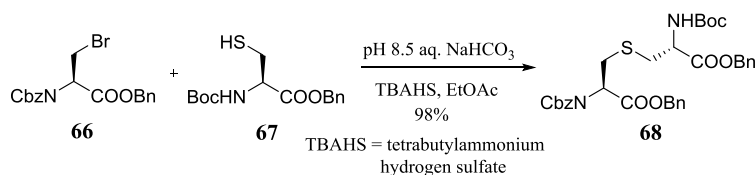
Scheme 3.2. 1st Generation route to cysteine **28** (reprinted scheme 2.6)



Scheme 3.3. Proposed mechanism for racemization and dimer formation during 1st generation alkylation

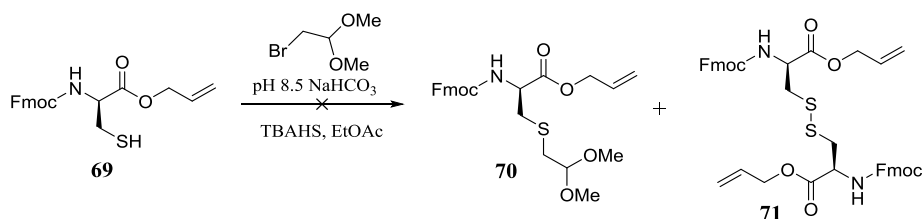
Epimerization of cysteine is a well-documented issue.¹⁻⁵ A proven approach to minimizing elimination during alkylation of cysteine thiols is to use mild, buffered, phase-

transfer conditions.⁶ Thus, Zha and Schmidt reported the formation of lanthionine **68** via alkylation of cysteine **67** (Scheme 3.4).



Scheme 3.4. Schmidt's racemization-free lanthionine formation

To compensate for the strong electron-withdrawing nature of the phthalimido protecting group, we took a step backwards and attempted alkylation of Fmoc-protected cysteine **69** (Scheme 3.5). Disappointingly, the desired thioether **70** was not observed.

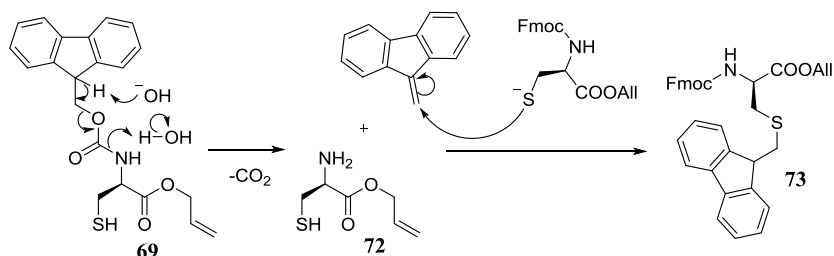


Scheme 3.5. Phase transfer conditions applied to Fmoc-D-Cys(H)-OAll (**69**)

A host of alterations to the reaction conditions including changes in temperature, equivalents of electrophile, solvent, pH, and concentration all failed to produce any of the desired compound. These reactions regularly yielded a mixture of starting material thiol and the corresponding disulfide **71**.

When the pH was raised to >10, using NaOH, *S*-fluorenylmethyl adduct **73** was isolated in 18% yield (Scheme 3.6). This arises from β -elimination of dibenzofulvene and subsequent addition of unreacted thiol **69** across the double bond. The fact that these reactions failed to produce desired product **70** (Scheme 3.5), even in the presence of excess 2-bromo-1,1-dimethoxy acetal, but could generate fluorenylmethyl thioether **73**, albeit in low yield, was a crucial result. This indicated that 2-bromo-1,1-dimethoxyethane was not a capable electrophile for our

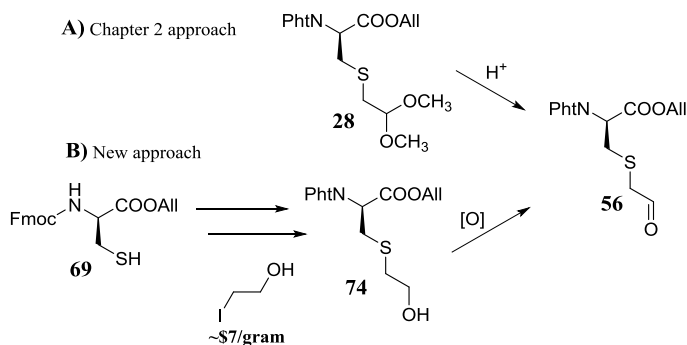
transformation and urged us to find an alternative approach. The more reactive 2-iodo-1,1-dimethoxyethane was not commercially available, and attempts to generate it from 2-bromo-1,1-dimethoxyethane were unsuccessful.



Scheme 3.6. Mechanism of formation of S-fluorenylmethyl adduct **73**

3.5. A New Electrophile

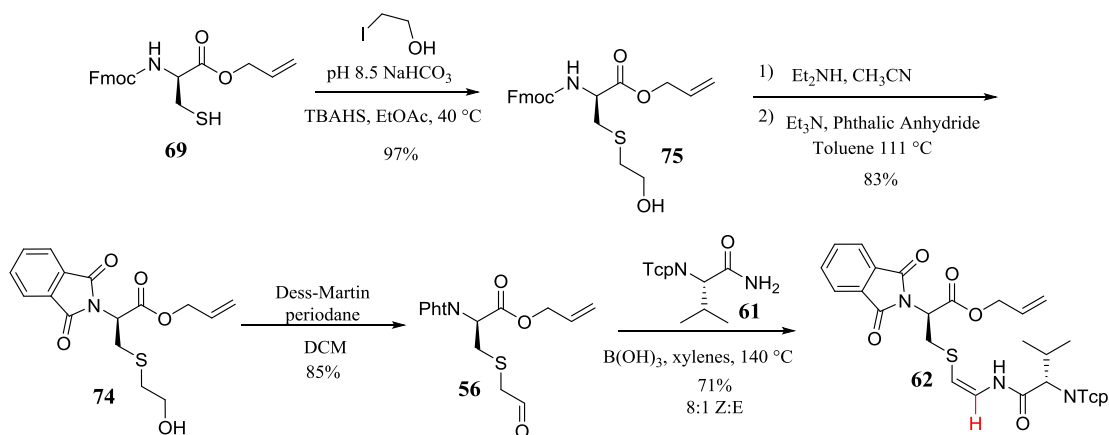
The original synthesis of aldehyde **56** required hydrolysis of the acetal functionality in compound **28**. We envisioned an alternative approach towards aldehyde **56** involving oxidation from alcohol **74** (Scheme 3.7).



Scheme 3.7. Generation of aldehyde **56**

Using 2-iodoethanol, we were able to increase the yield of our alkylation to 97% with gentle heating (Scheme 3.8). Alkylation was followed by typical conditions for Fmoc removal and reprotection of the α -amine as the phthalimide. Oxidation of the primary alcohol using Dess-Martin periodane proceeded smoothly to yield aldehyde **56**, setting the stage for thioenamide formation. Notwithstanding these new, mild reaction conditions for alkylation, the thioenamide

product **62**, generated via our new alkylation conditions, still yielded a mixture of two compounds; though now in a 1.0:0.7 ratio (Figure 3.3).



Scheme 3.8. Improved alkylation and oxidation to aldehyde **56**

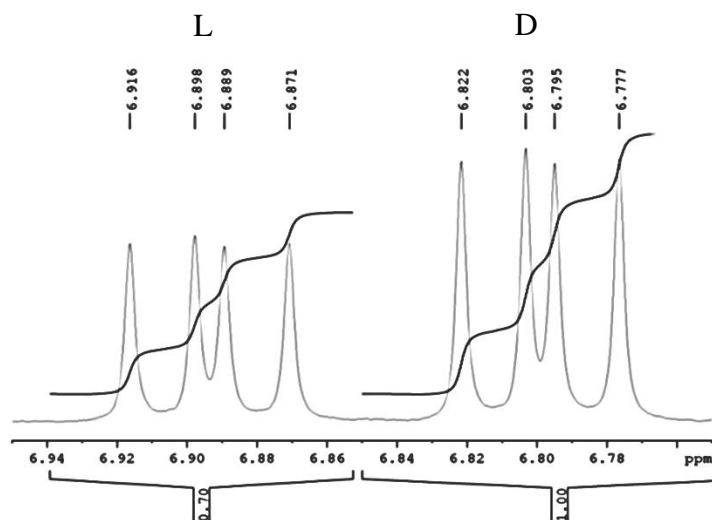


Figure 3.3. ¹H NMR of thioenamide **62** synthesized via Scheme 3.8 invoking the phase transfer alkylation (¹H NMR, CDCl₃, 400 MHz)

3.6. Epimerization during Thioenamide Formation

The small change in the ratio of signals in the proton NMR suggested that our hypothesis of racemization was correct, but involved more than one step in the sequence contributing to the erosion of stereochemistry at C α . The most disconcerting prospect was that one of those reactions was thioenamide formation, the step that we spent a great deal of time optimizing, and

for which there is no literature precedent. To determine this possibility, we investigated the stereochemistry of our starting material, alcohol **74**, and then reacted under our Lewis acid promoted thioenamide formation.

Investigation began with examination of cysteine alcohol **74** (Scheme 3.8) via chiral HPLC (Figure 3.4). This analysis revealed that isomerization had already taken place. Separation of the two enantiomers by chiral HPLC afforded us the opportunity to measure their optical rotations. The values, $[\alpha]_{\text{D}}^{25} = +59.8$ (*c* 0.5, CHCl₃) and -62.9 (*c* 0.5, CHCl₃), served as further confirmation that their relationship was enantiomeric. While the near 54% to 46% ratio of isomers pointed strongly to previous reactions being problematic, we also needed to determine the level of epimerization during our thioenamide-forming reaction.

Oxidation of the (+)-enantiomer was followed by thioenamide formation, again using Tcp-Val-NH₂ (**61**), to form thioenamide **62**. The ¹H NMR spectrum of the crude product showed a single diastereomer (Figure 3.5)! This happy result reassured us that thioenamide generation can be achieved without damage to the diastereomeric ratio.

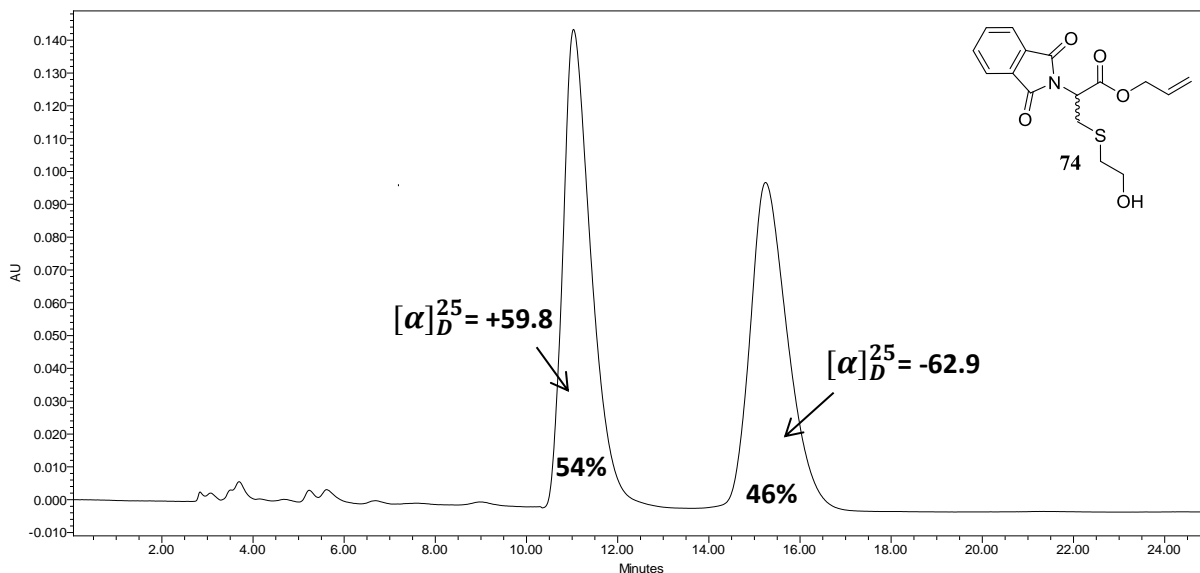


Figure 3.4. Chiral HPLC separation of enantiomers of phthalimido-protected cysteine **74**; (Chiralcel OD-H [cellulose tris(3,5-dimethylphenylcarbamate)] column from Daicel; 4.6 x 25 mm Method-Isocratic 20% isopropanol 80% n-hexane, 1 mL min⁻¹, detection at 254 nm), optical rotations measured in chloroform at 25 °C

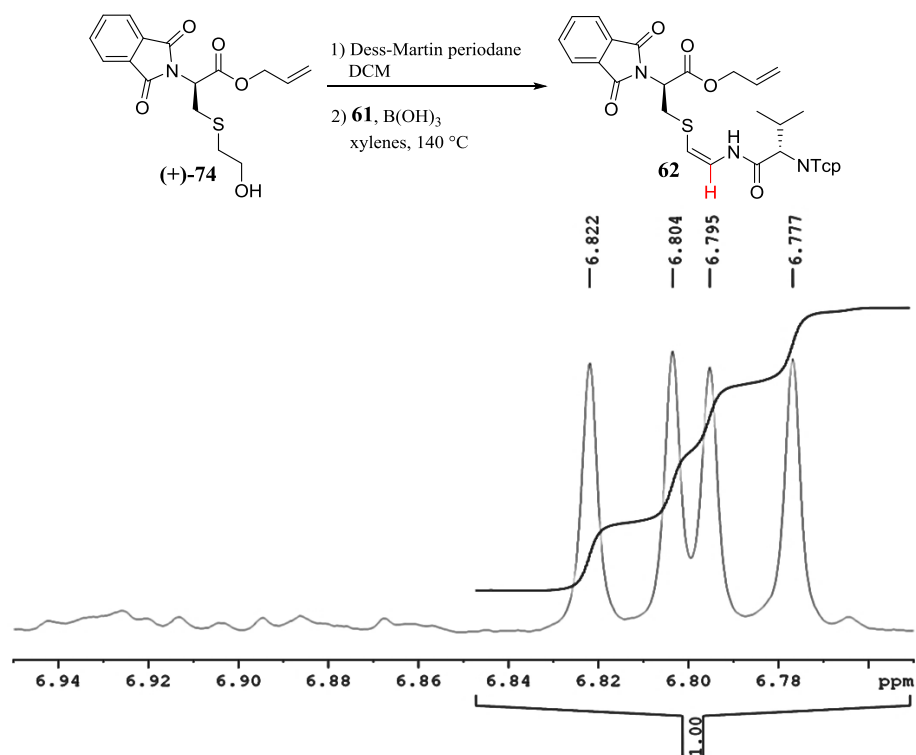


Figure 3.5. Thioenamide generated from pure (+) enantiomer (¹H NMR, CDCl₃, 400 MHz)

3.7. The Epimerization Strikes Back

Clearly, the alkylation reaction conditions were only partially to blame for racemization. Epimerization was occurring elsewhere in the synthesis of our building block, perhaps in multiple steps. We took a step backwards in our synthetic route to phthalimide **74** and investigated the stereochemical integrity of Fmoc-protected cysteine **75**. First, using chiral HPLC we investigated Fmoc-protected cysteine **75** (Figure 3.6). While the peak was broad, there appeared to be only a single isomer.

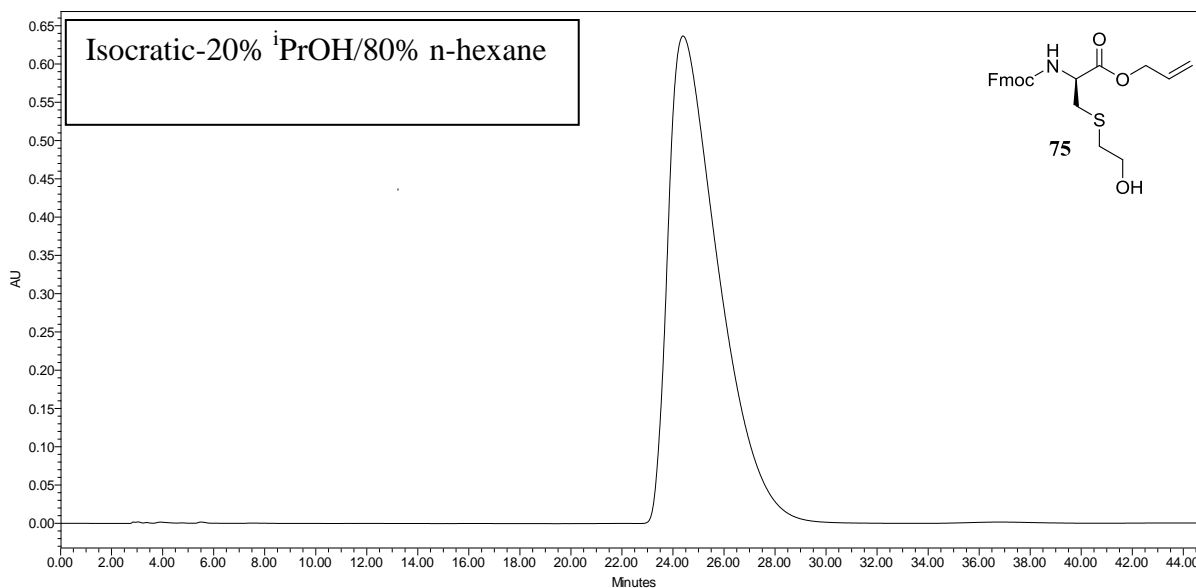
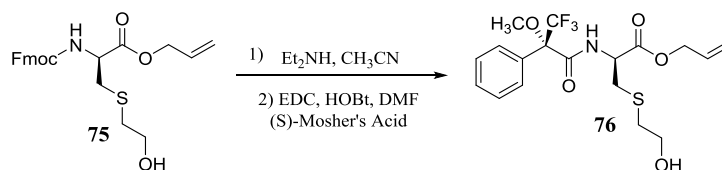


Figure 3.6. Chiral HPLC trace of Fmoc-D-Cys(ethanol)-OAll (**75**)

Mosher derivatives can be used to determine the enantiomeric purity of a compound by measuring the ratio of the diastereomeric adducts.^{7,8} Accordingly, we generated Mosher amide **76** after Fmoc removal from **75** (Scheme 3.9).



Scheme 3.9. Mosher's amide synthesis

This analysis allowed us to determine the degree of epimerization resulting from our amine deprotection and confirm that of all reactions preceding it. Derivative **76** contains a trifluoromethyl group and can therefore be analyzed by ^{19}F NMR. The fluorine atoms of different diastereomers should have distinct chemical shifts enabling us to measure the ratio of original isomers. With this approach, we observed 4-5% of the minor diastereomer of Mosher derivative **76** (Figure 3.7).

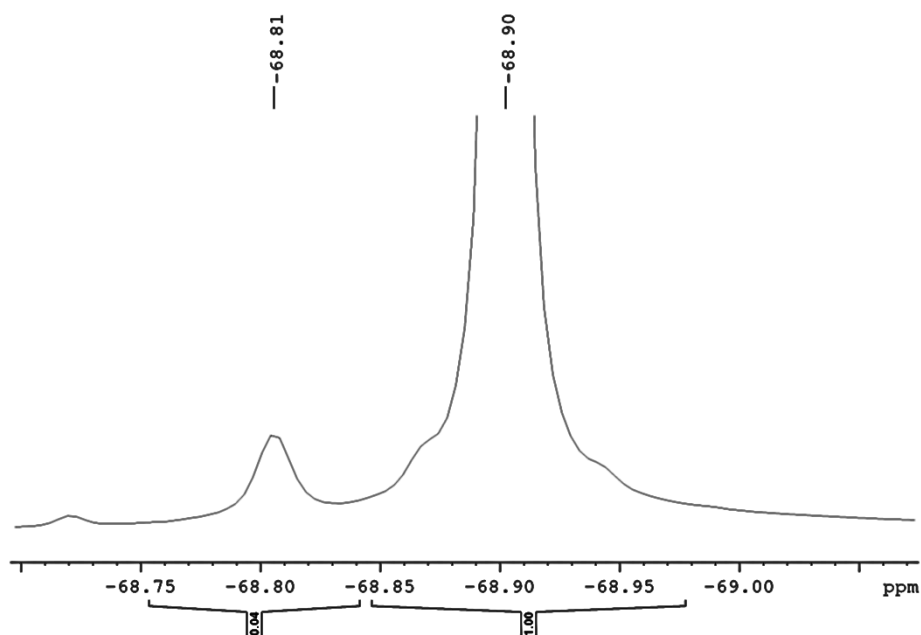


Figure 3.7. ^{19}F NMR (CDCl_3 , 376 MHz) of Mosher's amide **76**

To corroborate this result we also performed chiral HPLC of Mosher's amide **76** (Figure 3.8). This showed that the product was no more than 5% epimerized at this stage in the synthesis. The degree of epimerization, determined by two different methods, was in good agreement.

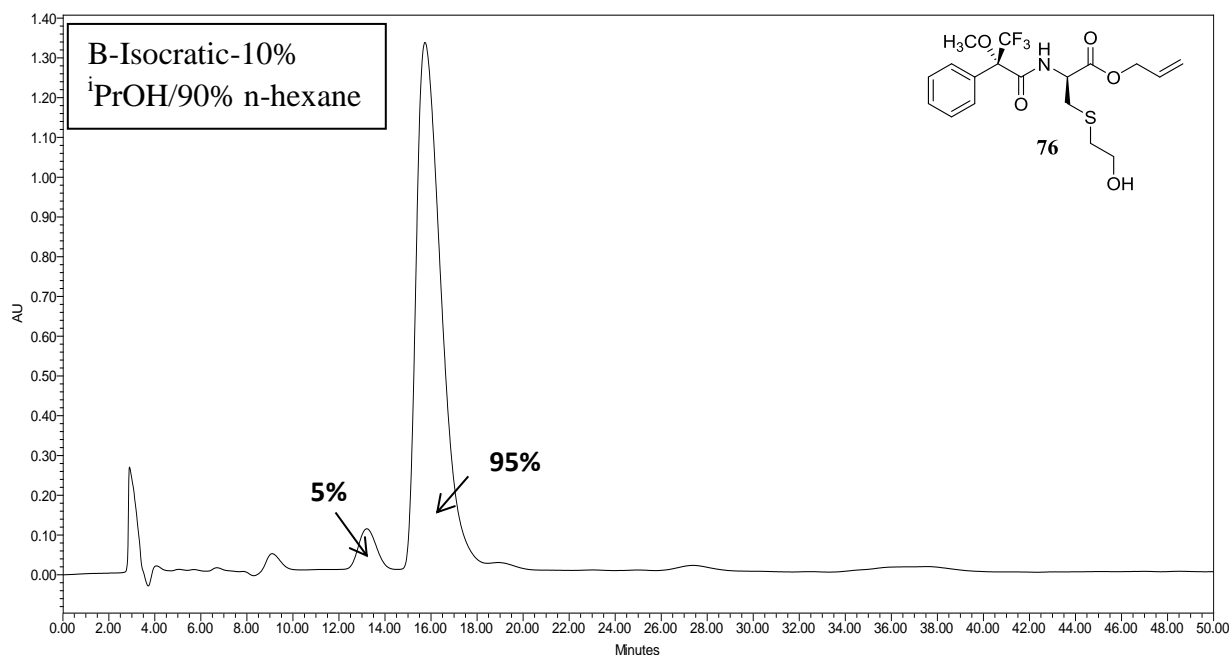
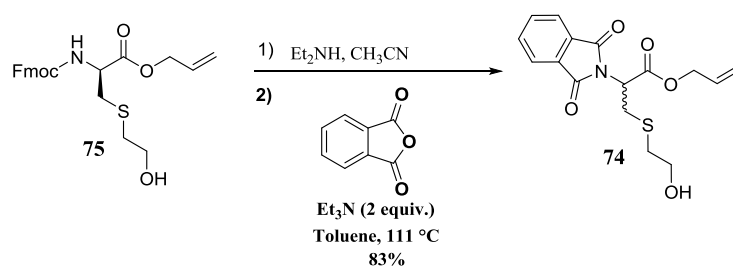


Figure 3.8. Chiral HPLC chromatogram of Mosher's Amide **76**

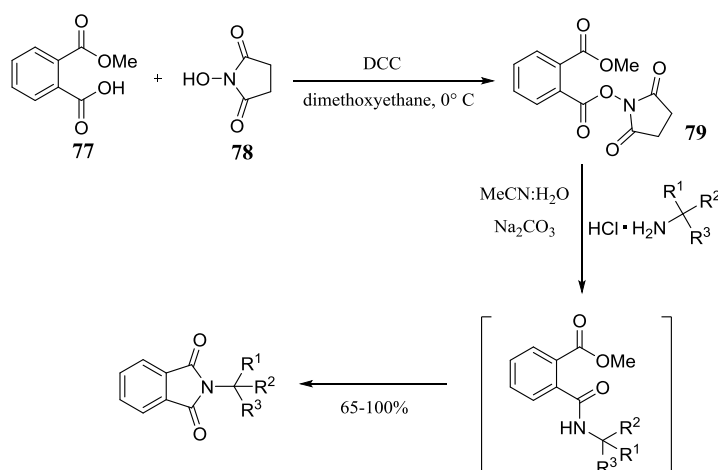
3.8. Return of the Phthalimido

At this juncture, all evidence pointed to conditions employed for the formation of the phthalimide being responsible for substantial epimerization of our cysteine α -carbon. This transformation had always been performed with two equivalents of triethylamine at high temperature (Scheme 3.10). Reducing the equivalents of base, and using a less basic reagent (pyridine) were ineffective at reducing the degree of epimerization. Catalytic base (triethylamine or diisopropylethylamine) led to very little desired product. Even weak bases, such as pyridine, still scrambled the stereocenter to the same degree. Lowering the temperature of the reaction was also an ineffective strategy.



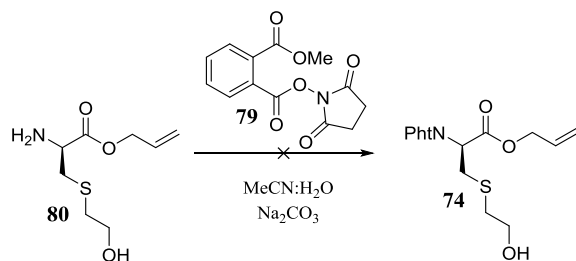
Scheme 3.10. Fmoc removal and phthalimido protection

Experimentation with phthalimide sources other than phthalic anhydride eventually led us to a report by Casimir *et al.* using methyl 2-[(succinimidooxy)carbonyl]benzoate (MSB, **79**) to install the amine protecting group (Scheme 3.11).⁹ Casimir reported racemization-free synthesis of a small range of amino acids and peptides, but not cysteine itself.



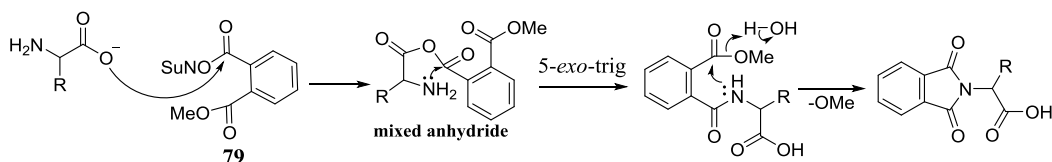
Scheme 3.11. Casimir's phthalimido protection method

Initial attempts to exchange the Fmoc protection for the phthalimido group using the conditions of Casimir with MSB were disappointing, resulting in degradation of material and no desired product (Scheme 3.12).



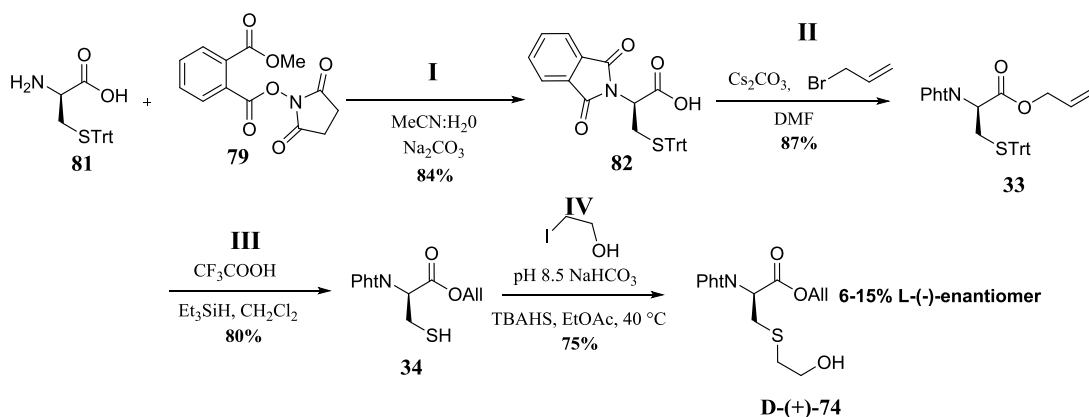
Scheme 3.12. Failed attempt at phthalimido protection

Many of the examples reported by Casimir were performed on free amino acids, rather than esters. We hypothesized that the acid functionality facilitates the coupling of the amine by first forming the mixed anhydride (Scheme 3.13). The anhydride is then set up to undergo intramolecular amide formation and subsequent 5-*exo*-trig cyclization to generate the imide.



Scheme 3.13. Proposed mixed anhydride mechanism for phthalimido formation

To test our mixed anhydride hypothesis, we subjected *S*-trityl-cysteine **81** to Casimir's conditions (Scheme 3.14). The transformation proceeded smoothly with a yield of 84%. While this was good news, it necessitated alteration of the order of events to generate enantioenriched alcohol **74**. The yield of the allyl ester formation remained high, but the alkylation step dropped to 75%. Chiral HPLC was used to determine the purity of alcohol **74** produced via this route. The product contained only 6-15% of the undesired enantiomer via this improved route (Figure 3.9, c.f. Figure 3.1 for racemic mixture). Reactions I-III have been performed on multiple gram scale, while the alkylation (step IV) has been done with 800 mg with little-to-no drop in yield for any step. This scale and level of epimerization was considered within acceptable range to continue on with our material towards synthesis of the C-terminal ring cypemycin.



Scheme 3.14. Improved route to alcohol **74**

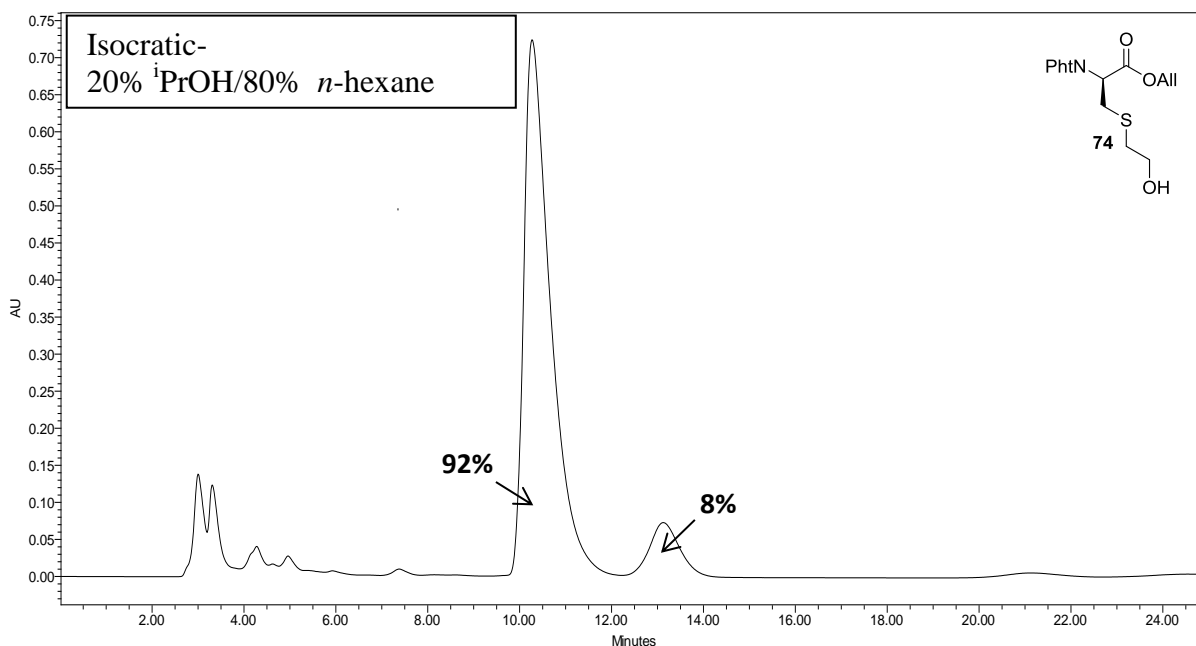


Figure 3.9. Chiral HPLC of alcohol (+)-74 (Chiracel OD-H) Column-Chiracel OD-H, 1 mL min⁻¹, detection at 254 nm (4.6 mm x 250 mm)

3.9. Experimental Procedures

3.9.1. General Methods As is 2.7.1

3.9.2. Synthesis of tetrachlorophthalimide-protected valinamide **61** and thioenamide **62** (Scheme 3.1)

Tcp-L-Val-NH₂ (61). Tetrachlorophthalic anhydride (2.257 g, 7.89 mmol, 1.0 equiv.) and triethylamine (2.5 mL, 1.82 g, 17.94 mmol, 2.3 equiv.) were added to a solution of valinamide

hydrochloride (1.205 g, 7.89 mmol, 1.0 equiv.) in toluene (85 mL). The mixture was heated at reflux under Dean-Stark conditions for 16 h. The mixture was diluted with EtOAc (200 mL) and washed with a 5% aqueous citric acid solution (200 mL). The aqueous layer was extracted a second time with EtOAc (50 mL) and the organic layers combined, washed with brine (50 mL), filtered through MgSO₄, and concentrated. The residue was subjected to flash chromatography, eluting with 3:1 hexanes-EtOAc to isolate **61** as a colorless solid (2.294 g, 76%). *R_f* 0.23 (2:1 hexanes-EtOAc). ¹H NMR (500 MHz, CDCl₃) δ 0.88 (d, *J* = 6.7 Hz, 3H), 1.14 (d, *J* = 6.6 Hz, 3H), 2.77-2.88 (m, 1H), 4.39 (d, *J* = 11.2 Hz, 1H), 5.82 (br s, 1H), 6.60 (br s, 1H); ¹³C NMR (125 MHz, CDCl₃) δ 19.6, 20.0, 27.4, 63.3, 127.0, 130.3, 140.9, 163.8, 170.1. HRMS (ESI) calcd for C₁₃H₁₀Cl₄N₂O₃ (M+H)⁺: calcd 382.9518; obsd 382.9524.

Mixture of diastereomers of thioenamide dipeptide 62. Boric acid (29 mg, 0.465 mmol, 5.0 equiv.) and Tcp-Val-NH₂ (**61**) (36 mg, 0.093 mmol, 1.0 equiv.) were added to a solution of **56** (31 mg, 0.093 mmol, 1.0 equiv.) in xylenes (31 mL). This mixture was brought to reflux and stirred for 24 h under N₂. Additional Tcp-Val-NH₂ **61** (13 mg, 0.4 equiv.) was added and reflux continued for an additional 16 h. The mixture was concentrated and the crude residue was subjected to flash chromatography, eluting with 5:1->4:1 hexanes-EtOAc to isolate **Z-62** [46 mg, 71%; *R_f* 0.41 (2:1 hexanes-EtOAc)] and **E-62** [(4 mg, 6% *R_f* 0.37 (2:1 hexanes-EtOAc)], each as a yellow solid. Data for **Z-62** as a 1:1 mixture of diastereomers about the C-α of cysteine. ¹H NMR (400 MHz, CDCl₃) δ 0.88 (d, *J* = 6.6 Hz, 1.5H), 0.89* (d, *J* = 6.7 Hz, 1.5H), 1.08 (d, *J* = 6.6 Hz, 1.5H), 1.13* (d, *J* = 6.6 Hz, 1.5H) 2.83 (dq, *J* = 11.1, 6.6 Hz, 0.5H), 2.94* (dq, *J* = 10.7, 6.7 Hz, 0.5H), 3.40 (dd, *J* = 14.8, 3.7 Hz, 0.5H), 3.42* (dd, *J* = 14.6, 4.2 Hz, 0.5H), 3.50* (dd, *J* = 14.6, 10.8 Hz, 0.5H), 3.56 (dd, *J* = 14.8, 11.4 Hz, 0.5H), 4.48* (d, *J* = 10.7 Hz, 0.5H), 4.49 (d, *J* = 11.1 Hz, 0.5H) 4.60-4.77 (m, 2H), 4.91 (dd, *J* = 11.4, 3.7 Hz, 0.5H), 4.98* (dd, *J* = 10.7, 4.0

Hz, 0.5H), 5.19-5.36 (m, 3H), 5.77-5.97 (m, 1H), 6.78 (dd, $J = 10.7, 7.4$ Hz, 0.5H), 6.87* (dd, $J = 10.8, 7.4$ Hz, 0.5H), 7.72-7.76 (m, 3H), 7.72-7.94 (m, 4H); ^{13}C NMR (125 MHz, CDCl_3) δ 19.5*, 19.8, 19.9, 20.4*, 27.0*, 27.5, 29.9*, 32.9, 33.2*, 53.1*, 53.5, 62.*, 63.5, 66.9, 66.9*, 102.5*, 102.8, 119.2, 119.3*, 123.8, 124.0*, 127.3*, 127.5, 128.0*, 128.5, 130.21, 131.3*, 131.5, 131.7, 134.6, 140.7, 163.7*, 164.2, 164.9, 165.4, 167.5, 167.5, 167.7*, 167.9. HRMS (ESI) calcd for $\text{C}_{29}\text{H}_{23}\text{Cl}_4\text{N}_3\text{O}_7\text{S}$ ($\text{M}+\text{H}$) $^+$: calcd 698.0084; obsd 698.0079

*NMR signals from undesired diastereomer resulting from L-cysteine

3.9.3. Synthesis of imidazolidinone **64** (Scheme 3.1)

Imidazolidinone 64. *para*-Toluenesulfonic acid (42 mg, 0.219 mmol, 1.0 equiv.) and Fmoc-L-Ala-NH₂ (68 mg, 0.219 mmol, 1.0 equiv.) were added to a solution of **28** (83 mg, 0.219, 1.0 equiv.) in benzene (50 mL). This solution was brought to reflux and stirred under N₂ for 16 h. The mixture was concentrated and the residue subjected to flash chromatography, eluting with 2:1->1:1 hexanes-EtOAc to isolate **64** as a yellow solid (52 mg, 67%). R_f 0.40 (1:2 hexanes-EtOAc). ^1H NMR (500 MHz, CDCl_3) δ 1.13 (app t, $J = 8.2$ Hz, 2H), 1.33 (br s, 1H), 2.03-2.14 (m, 0.5H), 2.40-2.58(m, 1H), 2.69 (dd, $J = 13.5, 7.1$ Hz, 0.5H), 2.84-3.56 (m, 4H), 3.81 (br s, 0.7H), 4.06 (br s, 0.3H), 4.24 (app t, 5.1 Hz, 1H), 4.50-5.24 (m, 5H), 5.21 (d, $J = 10.4$ Hz, 1H), 5.27 (dd, $J = 17.2, 1.3$ Hz, 1H), 5.84 (ddt, $J = 17.2, 10.4, 5.8$ Hz, 1H), 6.78-7.08 (m, 1H), 7.32 (t, $J = 7.2$ Hz, 2H) 7.30-7.44 (m, 2H), 7.52-7.57 (m, 2H), 7.73-7.77 (m, 4H), 7.84-7.90 (m, 2H); ^{13}C NMR* (125 MHz, CDCl_3) δ 17.5, 17.7, 18.0, 18.1, 31.3, 32.6, 37.2, 38.2, 47.3, 51.2, 52.1, 54.8, 66.9, 68.5, 69.1, 119.3, 120.2, 123.9 (2C), 124.6, 124.8, 127.3, 128.0, 131.3, 131.7, 134.6, 141.5, 143.7, 154.1, 167.6, 167.7, 173.4. HRMS (ESI) calcd for $\text{C}_{34}\text{H}_{32}\text{N}_3\text{O}_7\text{S}$ ($\text{M}+\text{H}$) $^+$: calcd 626.1955; obsd 626.1961

*Contains diastereomers, often indistinguishable from one another

3.9.4. First phase transfer alkylation of cysteine (Scheme 3.8)

Fmoc-D-Cys[S(CH₂CH₂OH)]-OAll (75). Trifluoroacetic acid (0.675 mL, 1.005 g, 8.813 mmol, 5.0 equiv.) and triethylsilane (1.408 mL, 1.025 g, 8.813 mmol, 5.0 equiv.) were added to a solution of **32** (1.103 g, 1.763 mmol, 1.0 equiv.) in DCM (10 mL) at 0 °C. After 5 min, the solution was allowed to warm to rt over 1 h. The mixture was concentrated and subjected to flash chromatography, eluting in 5:1 hexanes-EtOAc to isolate free thiol **69** (525 mg, 78%). *R_f* 0.34 (3:1 hexanes-EtOAc).

2-Iodoethanol (214 µL, 471 mg, 2.74 mmol, 2.0 equiv.) followed by aqueous 0.5 M NaHCO₃ (34 mL) was added to a solution of thiol **69** in EtOAc (34 mL). To this biphasic mixture was added tetrabutylammonium hydrogen sulfate (2.3 g, 6.85 mmol, 5.0 equiv.) and the mixture was vigorously stirred for 16 h at rt. The mixture was diluted with EtOAc (100 mL) and washed with saturated NaHCO₃ (75 mL). The aqueous layer was extracted a second time with EtOAc (50 mL) and the organic layers were combined, washed with brine (50 mL), filtered through MgSO₄, concentrated, and the residue purified by flash chromatography eluting with 3:1→1:1 hexanes-EtOAc to isolate alcohol **75** as a colorless solid (568 mg, 97%). *R_f* 0.34 (1:1 hexanes-EtOAc). ¹H NMR (500 MHz, CDCl₃) δ 2.37 (br s, 1H), 2.72 (dd, *J* = 14.2, 6.0 Hz, 1H), 2.77 (dd, *J* = 14.2, 5.7 Hz, 1H), 3.01 (dd, *J* = 14.5, 5.6 Hz, 1H), 3.04 (dd, *J* = 14.5, 5.2 Hz, 1H), 3.68-3.77 (m, 2H), 4.24 (t, *J* = 7.0 Hz, 1H), 4.37-4.46 (m, 2H), 4.60-4.72 (m, 3H), 5.28 (d, *J* = 10.4 Hz, 1H), 5.36 (d, *J* = 17.2 Hz, 1H), 5.81 (d, *J* = 8.0 Hz, 1H), 5.88-5.95 (m, 1H), 7.32 (t, *J* = 7.5 Hz, 2H), 7.40 (t, *J* = 7.5 Hz, 2H), 7.61 (d, *J* = 5.0 Hz, 2H), 7.77 (d, *J* = 7.5 Hz, 2H); ¹³C NMR (125 MHz, CDCl₃) δ 35.0, 36.4, 47.2, 54.2, 61.0, 64.6, 66.6, 67.3, 119.5, 120.1, 125.2, 127.2, 127.9, 131.4, 141.4, 143.8, 143.9, 155.5, 156.0, 170.5. HRMS (ESI) calcd for C₂₃H₂₆NO₅S (M+H)⁺: calcd 428.1526; obsd. 428.1543

3.9.5. Synthesis of Mosher's amide **76** (Scheme 3.9)

(S)-Methoxy(trifluoromethyl)phenylacetyl-D-Cys[S(CH₂CH₂OH)]-OAll **76.** Diethylamine (2 mL, 50% v/v) was added to a solution of Fmoc-D-Cys(ethanol)-OAll **75** (39 mg, 0.0912 mmol, 1.0 equiv.) in MeCN (2 mL) and the mixture was stirred under N₂ for 1.5 h. The mixture was concentrated and the crude residue was taken directly into the next step.

(S)-3,3,3-Trifluoro-2-methoxy-2-phenylpropanoic acid (21 mg, 0.0912 mmol, 1.0 equiv.) was dissolved in DMF (0.5 mL) and to this solution was added EDC (14 mg, 0.091 mmol, 1.0 equiv.) and HOBt (14 mg, 0.091 mmol, 1.0 equiv.) sequentially. This mixture was allowed to stir under N₂ for 25 min at rt.

The crude, free amine mixture was dissolved in DMF (0.5 mL) and this solution was added dropwise to the solution of activated Mosher's acid. The mixture was stirred under N₂ for 16 h. The mixture was diluted with EtOAc (75 mL) and washed with H₂O (75 mL). The aqueous layer was extracted a second time with EtOAc (50 mL). The organic layers were combined, washed with brine (50 mL), filtered through MgSO₄, concentrated, and the residue purified by flash chromatography eluting with 4:1 hexanes-EtOAc to isolate Mosher's amide **76** as a colorless oil (12 mg, 32%). *R_f* 0.32 (1:1 hexanes-EtOAc). ¹H NMR (500 MHz, CDCl₃) δ 2.28 (br s, 1H), 2.72-2.82 (m, 2H), 3.06 (dd, *J* = 14.1, 6.1 Hz, 1H), 3.11 (dd, *J* = 14.1, 4.9 Hz, 1H), 3.42 (d, ⁵*J*_{HF} = 1.3 Hz, 3H), 3.73 (dd, *J* = 11.5, 6.3 Hz, 1H), 3.78 (dd, *J* = 11.5, 6.0 Hz, 1H), 4.64 (ddt, *J* = 13.0, 5.9, 1.3 Hz, 1H), 4.69 (ddt, *J* = 13.0, 5.9, 1.3 Hz, 1H), 4.90 (ddd, *J* = 8.1, 6.0, 5.0 Hz, 1H), 5.29 (dd, *J* = 10.5, 1.3 Hz, 1H), 5.35 (dd, *J* = 17.2, 1.3 Hz, 1H), 5.86-5.95 (m, 1H), 7.40-7.42 (m, 3H), 7.54-7.57 (m, 2H), 7.76 (d, *J* = 8.0 Hz, 1H); ¹³C NMR (125 MHz, CDCl₃) δ 34.3, 36.2, 52.5, 55.2, 61.0, 66.7, 119.6, 127.7, 128.7, 128.8, 129.8, 131.3, 132.0, 166.7, 169.9. ¹⁹F NMR (376 MHz, CDCl₃, unreferenced) δ -68.81 (0.06H), -68.90 (0.94H)

3.9.6. Enantioenriched synthesis of cysteine alcohol **74** and oxidation to **56** (Scheme 3.14)

Pht-D-Cys(Trt)-OH (82). To a stirred suspension of H-D-Cys(Trt)-OH (**81**) (632 mg, 1.739 mmol, 1.0 equiv.) and Na₂CO₃ (737 mg, 6.956 mmol, 4.0 equiv.) in H₂O (10 mL) was added MeCN (16 mL) and methyl 2-((Succinimidooxy)carbonyl)benzoate (MSB)⁹ (482 mg, 1.739 mmol, 1.0 equiv.). The mixture was allowed to stir for 16 h. The mixture was diluted with EtOAc (150 mL) and washed with 1M aq. HCl (150 mL). The aqueous layer was extracted a second time with EtOAc (50 mL). The organic layers were combined, washed with brine (50 mL), filtered through MgSO₄, concentrated, and the residue purified by flash chromatography eluting with 2% methanol in DCM to isolate acid **82** as a colorless solid (746 mg, 86%). *R_f* 0.30 (streaky) (9:1 CH₂Cl₂:MeOH). ¹H NMR (500 MHz, CDCl₃) δ 2.96 (dd, *J* = 13.8, 4.5 Hz, 1H), 3.41 (dd, *J* = 13.8, 11.2 Hz, 1H), 4.34 (dd, *J* = 11.2, 4.5 Hz, 1H), 7.17-7.31 (m, 10H), 7.35-7.38 (m, 5H), 7.70 (dd, *J* = 5.5, 3.0 Hz, 2H), 7.81 (dd, *J* = 5.5, 3.0 Hz, 2H); ¹³C NMR (125 MHz, CDCl₃) δ 30.7, 51.6, 67.7, 123.8, 127.0, 128.2, 129.8, 131.9, 134.3, 144.4, 167.3, 173.2. HRMS (ESI -ve ion) calcd for C₃₀H₂₃NO₄S (M-H): calcd 492.1275; obsd 492.1277

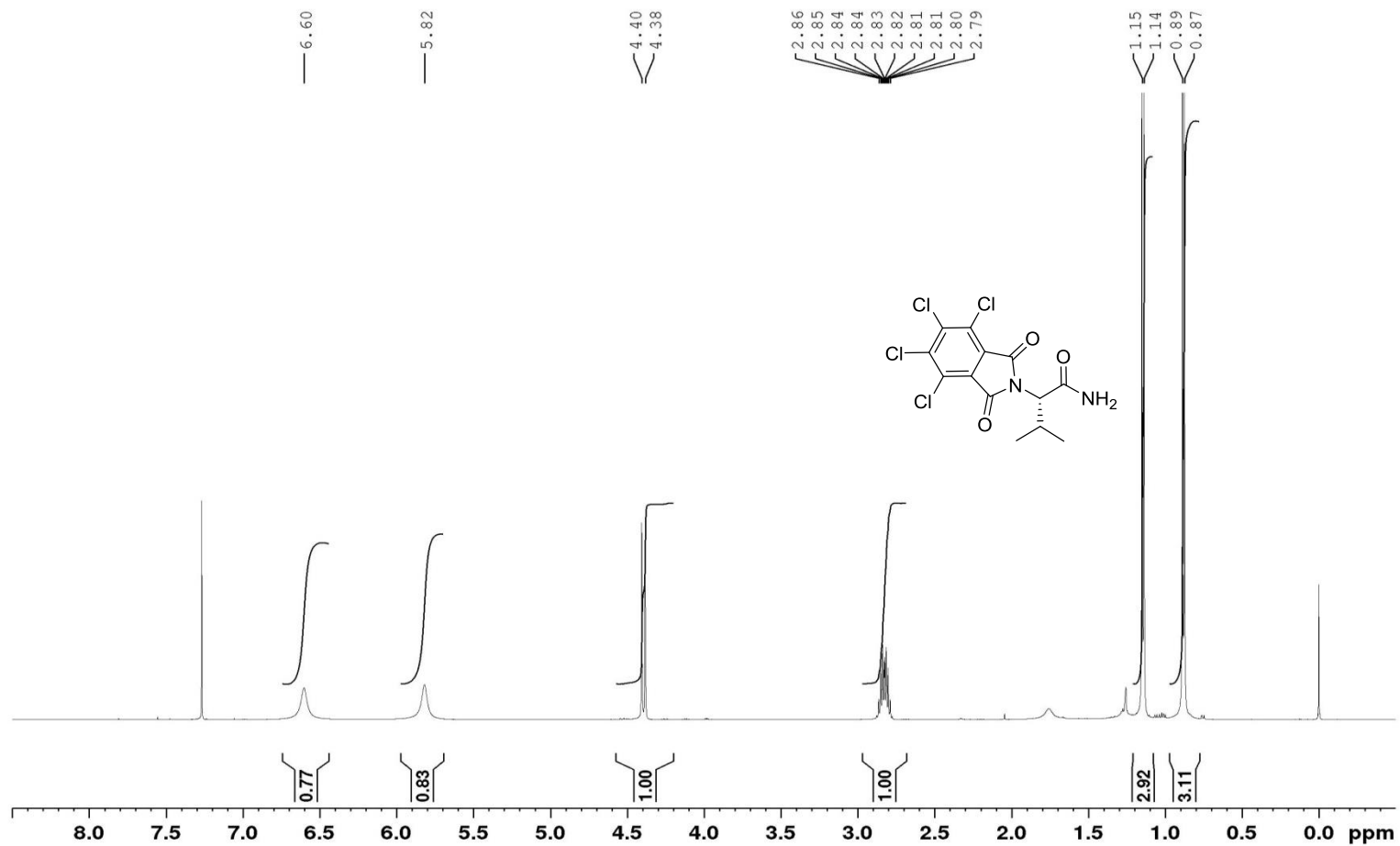
Pht-D-Cys(Trt)-OAll (33). Allyl bromide (73 μL, 102 mg, 0.847 mmol, 1.1 equiv.) and Cs₂CO₃ (125 mg, 0.385 mmol, 0.5 equiv.) were added to a solution of Pht-D-Cys(Trt)-OH (**82**) (380 mg, 0.770 mmol, 1.0 equiv.) in DMF (3 mL). The mixture was stirred overnight at rt under N₂. The mixture was diluted with EtOAc (150 mL) and washed with water (75 mL). The aqueous layer was extracted a second time with EtOAc (75 mL). The organic layers were combined, washed with brine (50 mL), filtered through MgSO₄, and concentrated. The residue was subjected to flash chromatography, eluting with 5:1 hexanes-EtOAc to isolate **33** as a colorless solid (358 mg, 87%). *Characterization identical for racemic (±)-33.*

Pht-D-Cys[S(CH₂CH₂OH)]-OAll [(+)-74]. 2-Iodoethanol (163 μ L, 360 mg, 2.094 mmol, 2.0 equiv.) and aqueous 0.5 M NaHCO₃ (26 mL) were added to a solution of thiol **34** (305 mg, 1.047 mmol, 1.0 equiv.) in EtOAc (26 mL). To this biphasic mixture was added tetrabutylammonium hydrogen sulfate (1.78 g, 5.235 mmol, 5.0 equiv.) and the mixture was vigorously stirred for 16 h at rt under N₂. The mixture was diluted with EtOAc (100 mL) and washed with saturated NaHCO₃ (75 mL). The aqueous layer was extracted a second time with EtOAc (50 mL) and the organic layers were combined, washed with brine (50 mL), filtered through MgSO₄, concentrated, and the residue purified by flash chromatography eluting with 4:1 \rightarrow 1:1 hexanes-EtOAc to isolate alcohol (+)-**74** as a colorless solid (262 mg, 75%). *R_f* 0.46 (2:1 EtOAc-hexanes) ¹H NMR (400 MHz, CDCl₃) δ 2.46 (br s, 1H), 2.68 (ddd, *J* = 13.8, 6.5, 5.6 Hz, 1H), 2.81 (dt, *J* = 13.8, 5.6 Hz, 1H), 3.38 (dd, *J* = 14.4, 11.1 Hz, 1H), 3.44 (dd, *J* = 14.4, 5.0 Hz, 1H), 3.71-3.80 (m, 2H), 4.66 (d, *J* = 1.3 Hz, 1H), 4.67 (d, *J* = 1.3 Hz, 1H) 5.07 (dd, *J* = 11.1, 5.0 Hz, 1H), 5.23 (dd, *J* = 10.5, 1.2 Hz, 1H), 5.29 (dd, *J* = 17.2, 1.4 Hz, 1H), 5.82-5.91 (m, 1H), 7.78 (dd, *J* = 5.5, 3.1 Hz, 2H), 7.89 (dd, *J* = 5.5, 3.1 Hz, 2H); ¹³C NMR (125 MHz, CDCl₃) δ 31.2, 35.3, 51.7, 60.9, 66.7, 119.0, 123.7, 131.2, 131.6, 164.5, 155.6, 167.6, 167.8. HRMS (ESI) calcd for C₁₆H₁₈NO₅S (M+H)⁺: calcd 336.0900; obsd 336.0909.

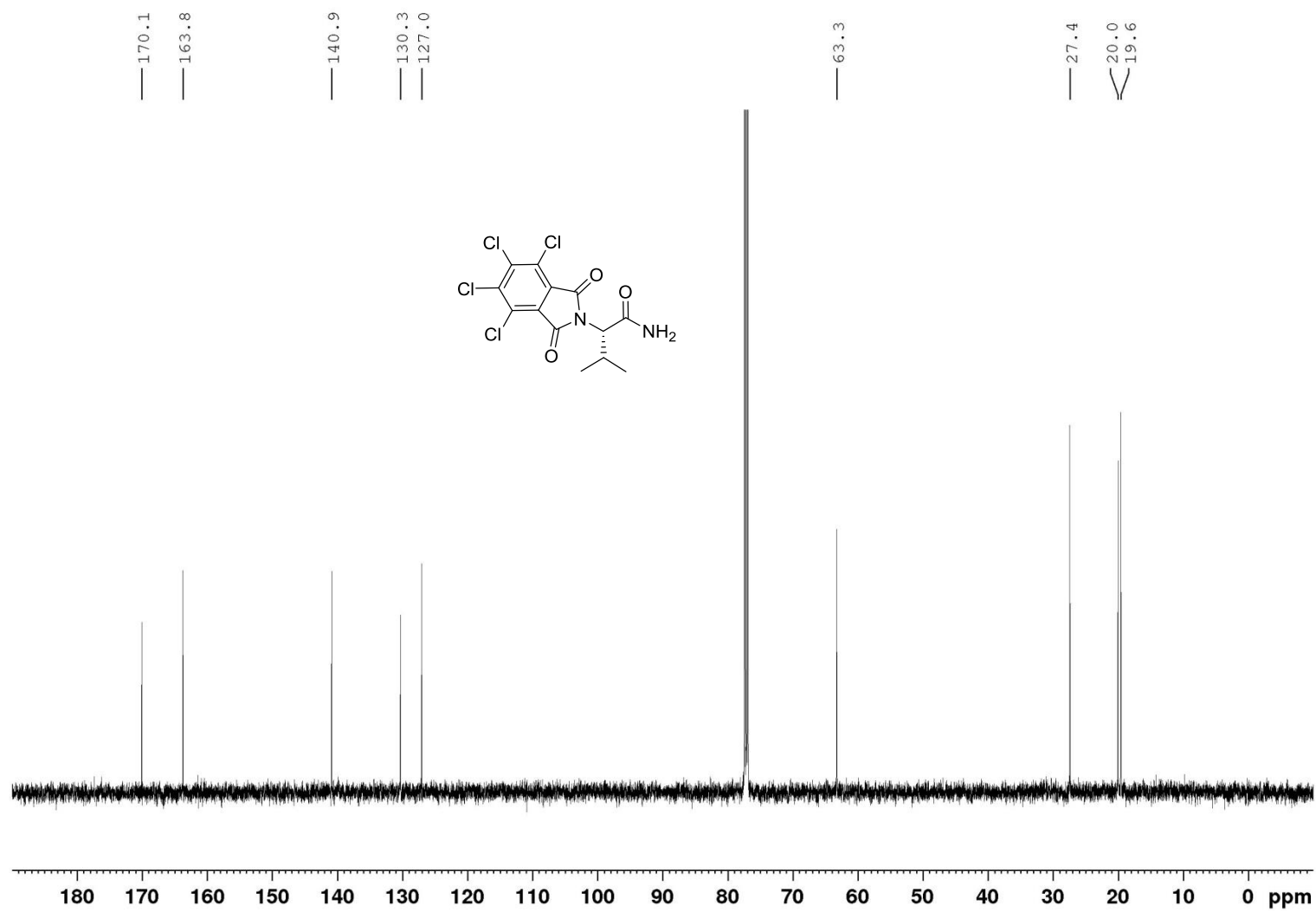
Aldehyde (56). Dess-Martin periodane (61 mg, 0.144 mmol, 2.0 equiv.) was added to a solution of alcohol **74** (24 mg, 0.072 mmol, 1.0 equiv.) in DCM (1 mL). This mixture was allowed to stir under N₂ for 4 h. The mixture was concentrated and subjected to flash chromatography, eluting with 4:1 hexanes-EtOAc to isolate **56** as a colorless oil (20 mg, 84%). *Characterization identical for racemic 56.*

3.10. NMR Spectra

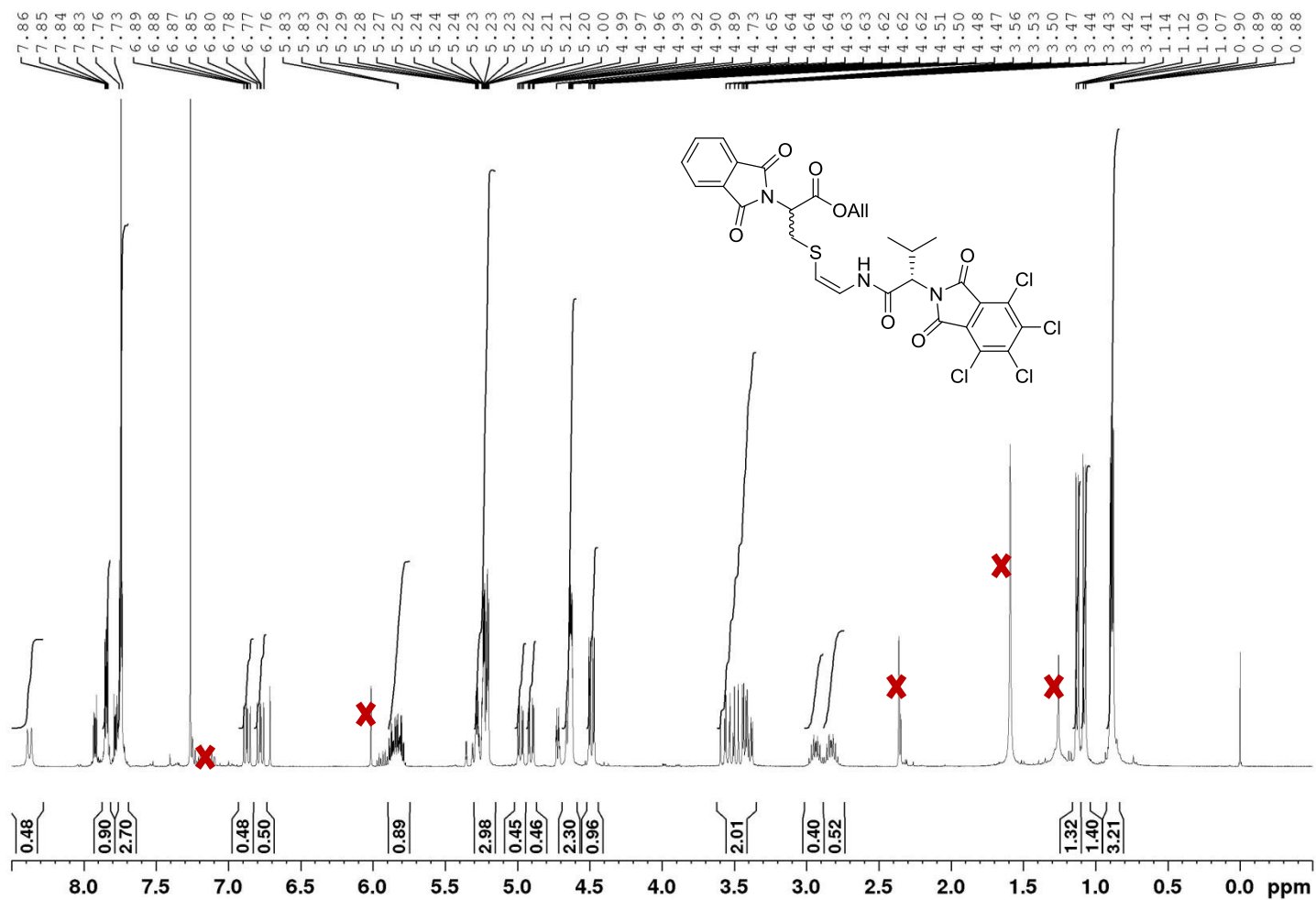
^1H NMR, Compound **61**, CDCl_3 , 500 MHz



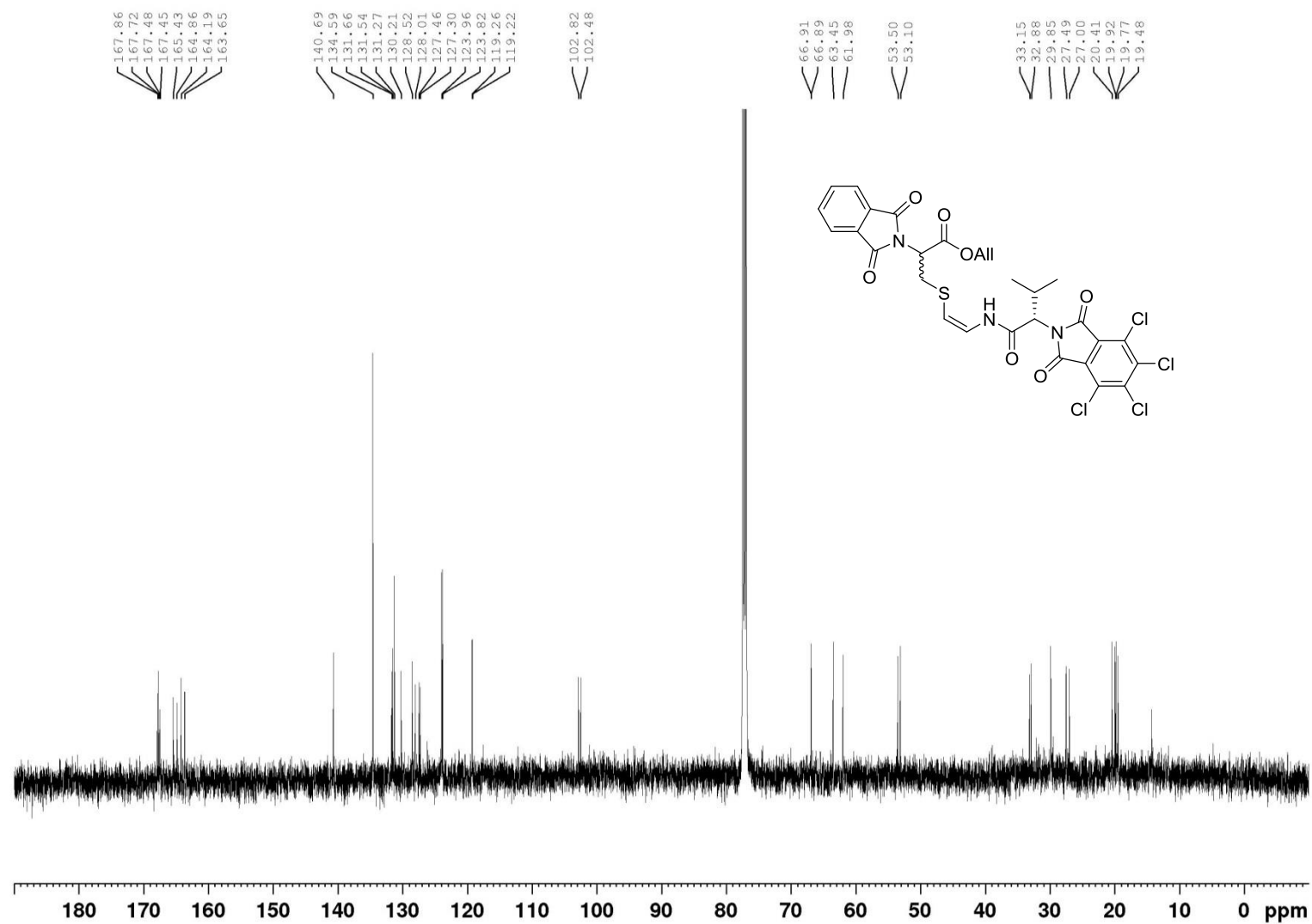
^{13}C NMR, Compound **61**, CDCl_3 , 125 MHz

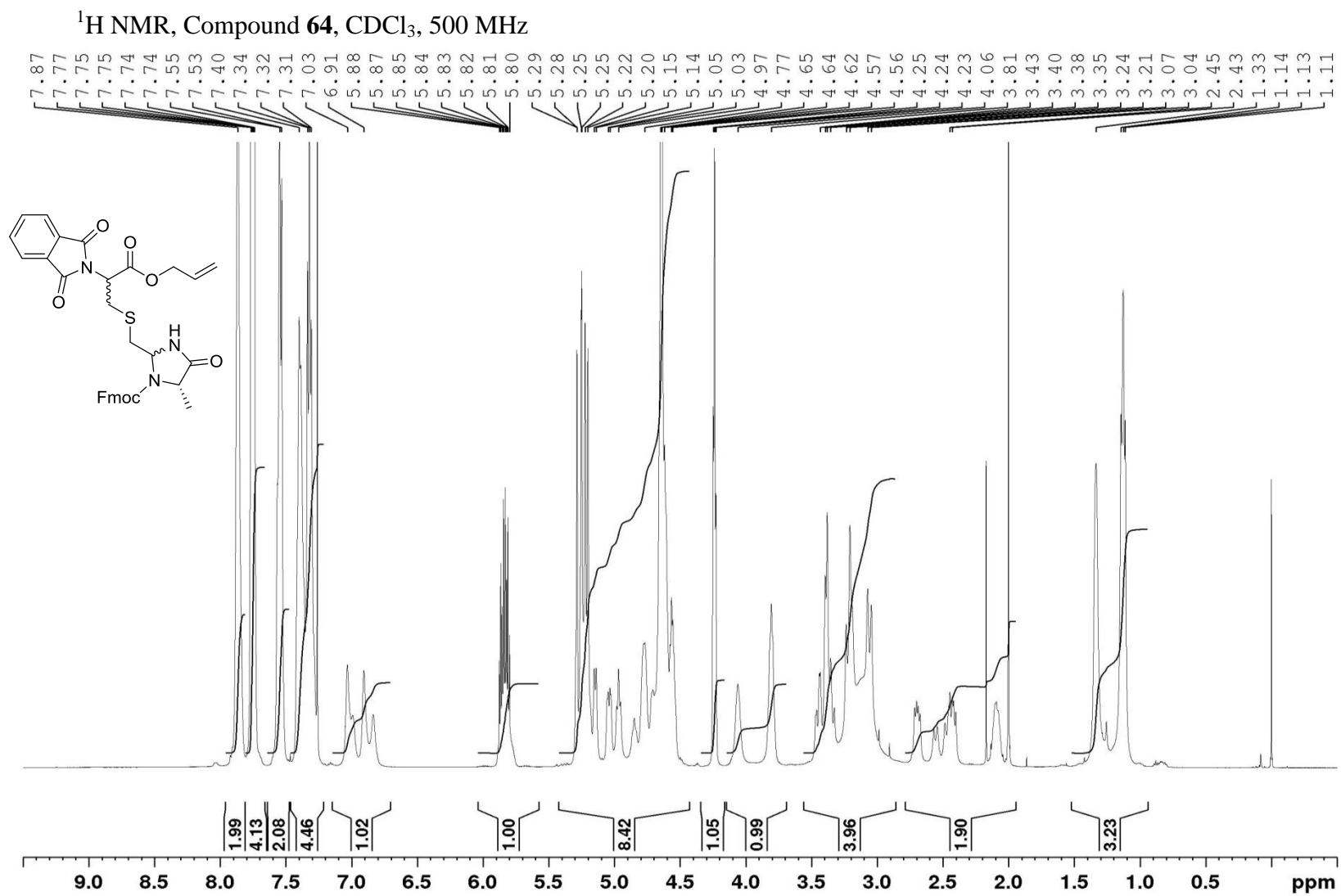


^1H NMR, Compound Z-62 as a mixture of diastereomers, CDCl_3 , 500 MHz

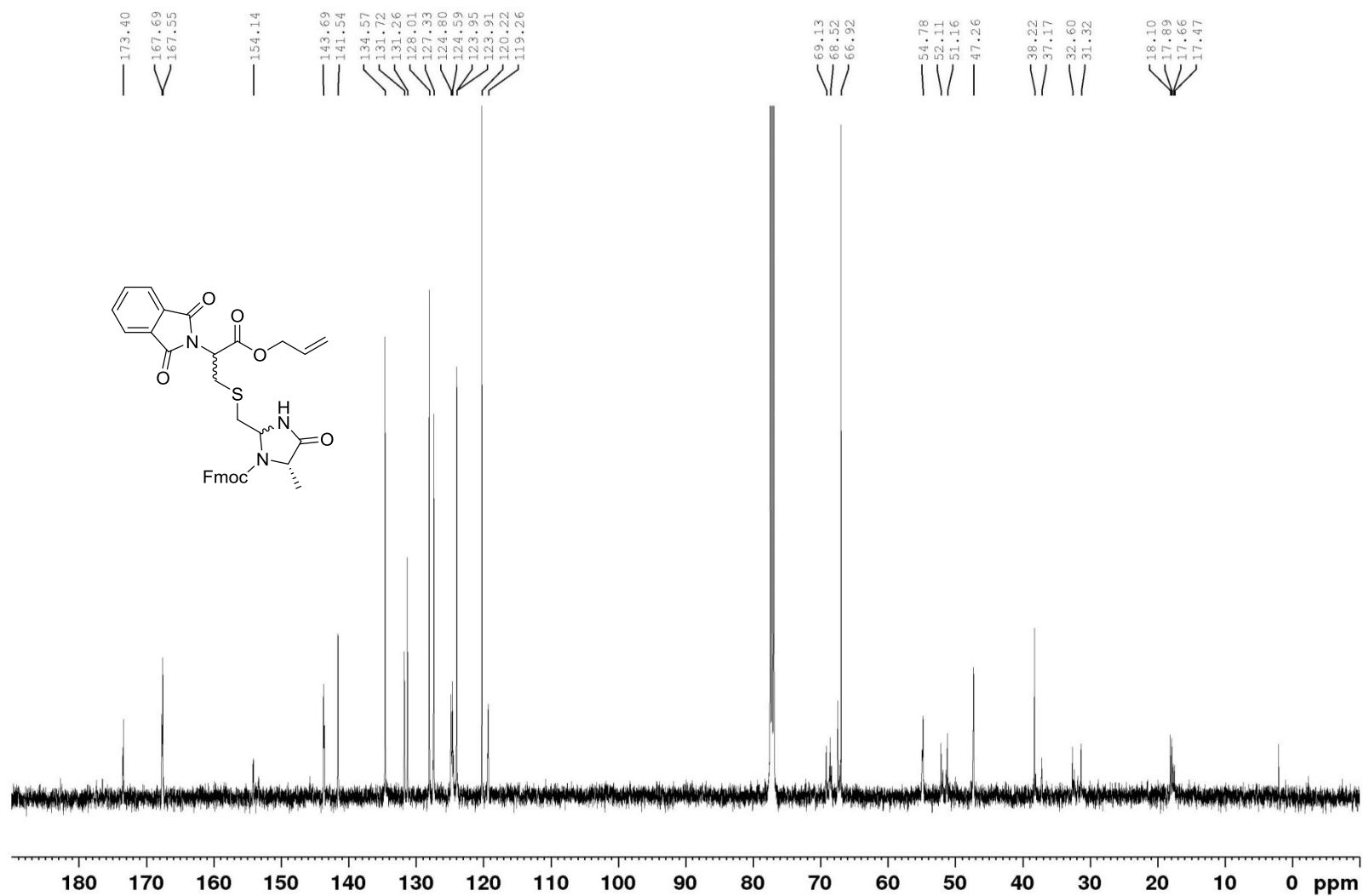


^{13}C NMR, Compound **Z-62** as a mixture of diastereomers, CDCl_3 , 125 MHz

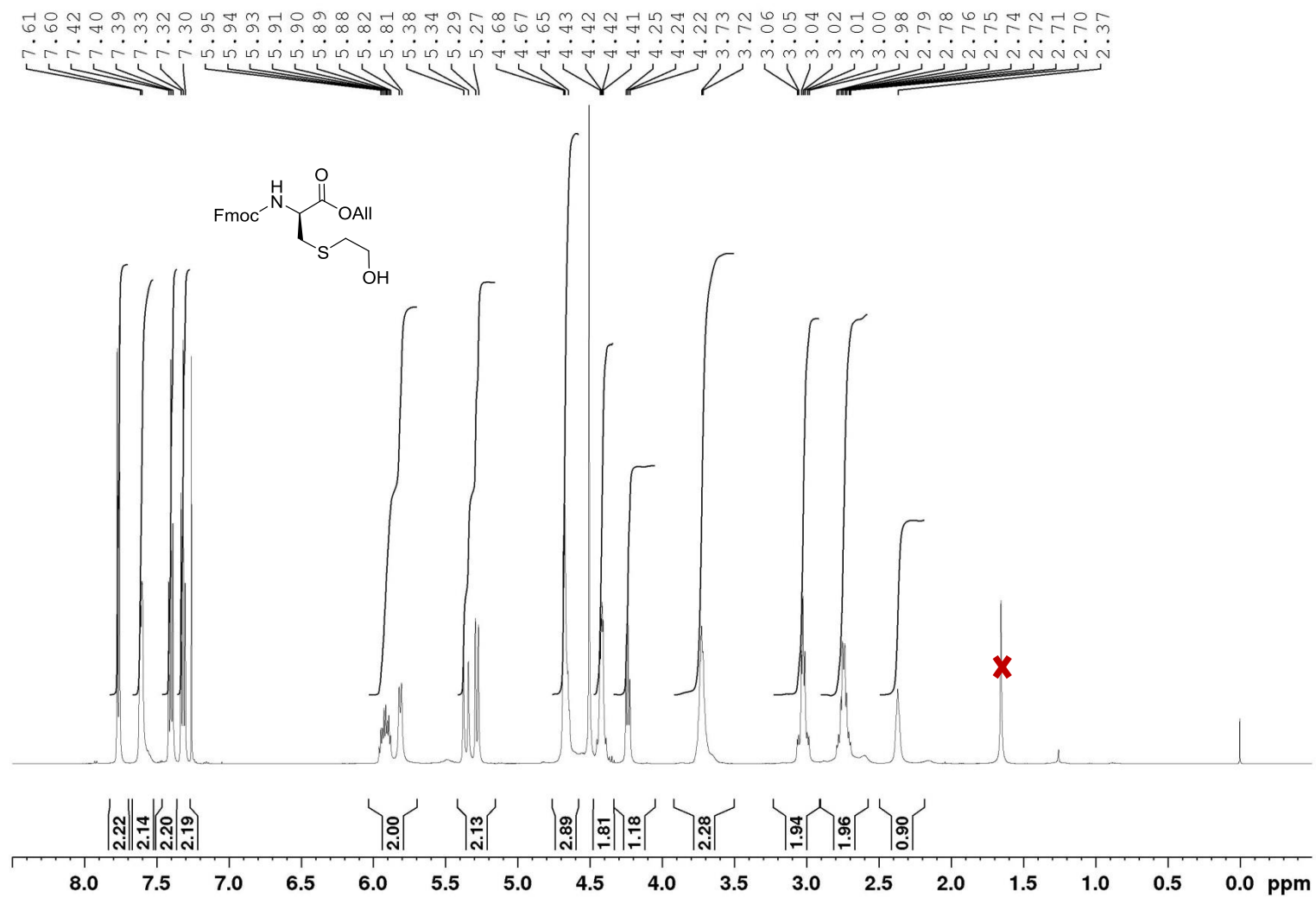




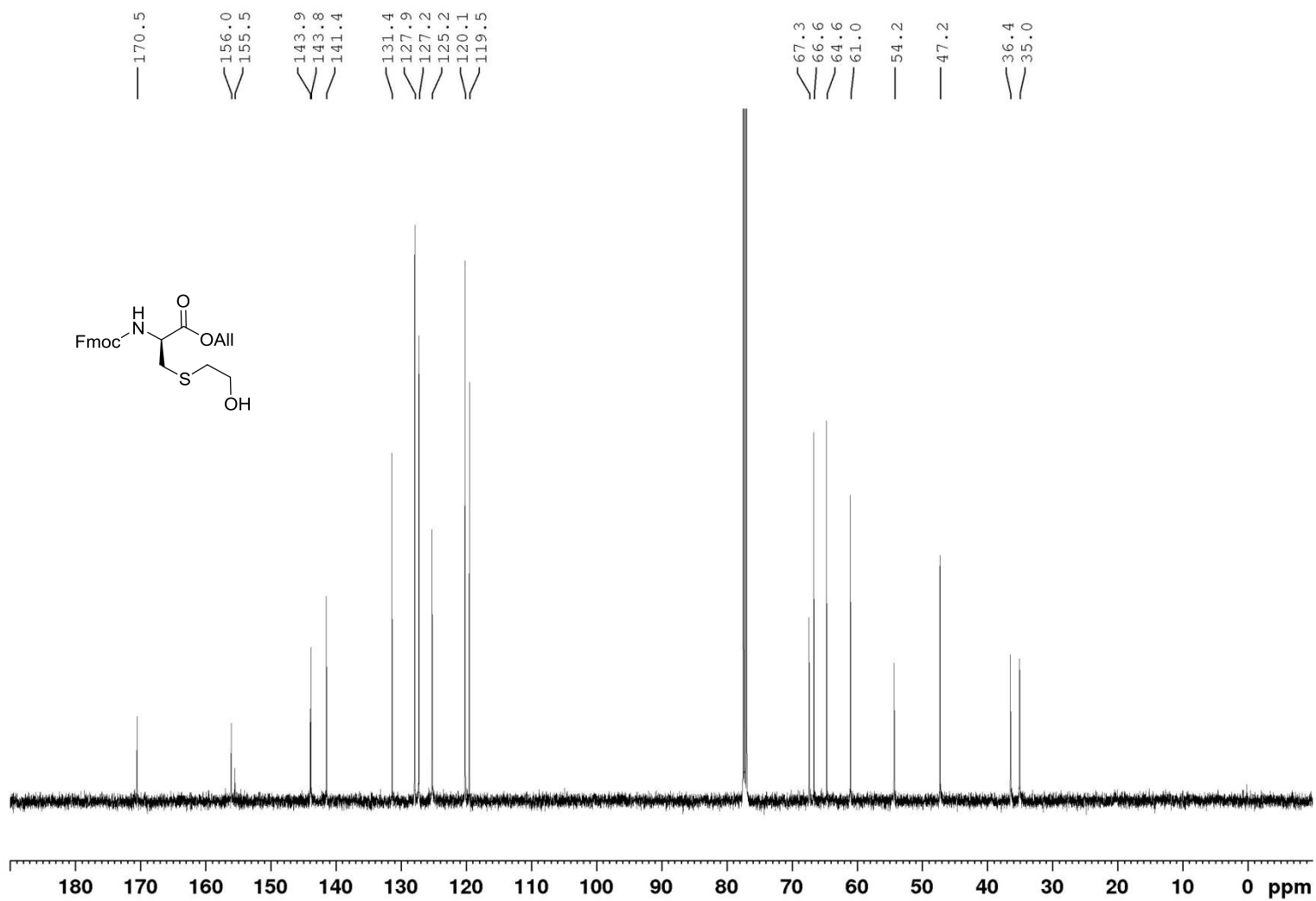
^{13}C NMR, Compound **64**, CDCl_3 , 125 MHz



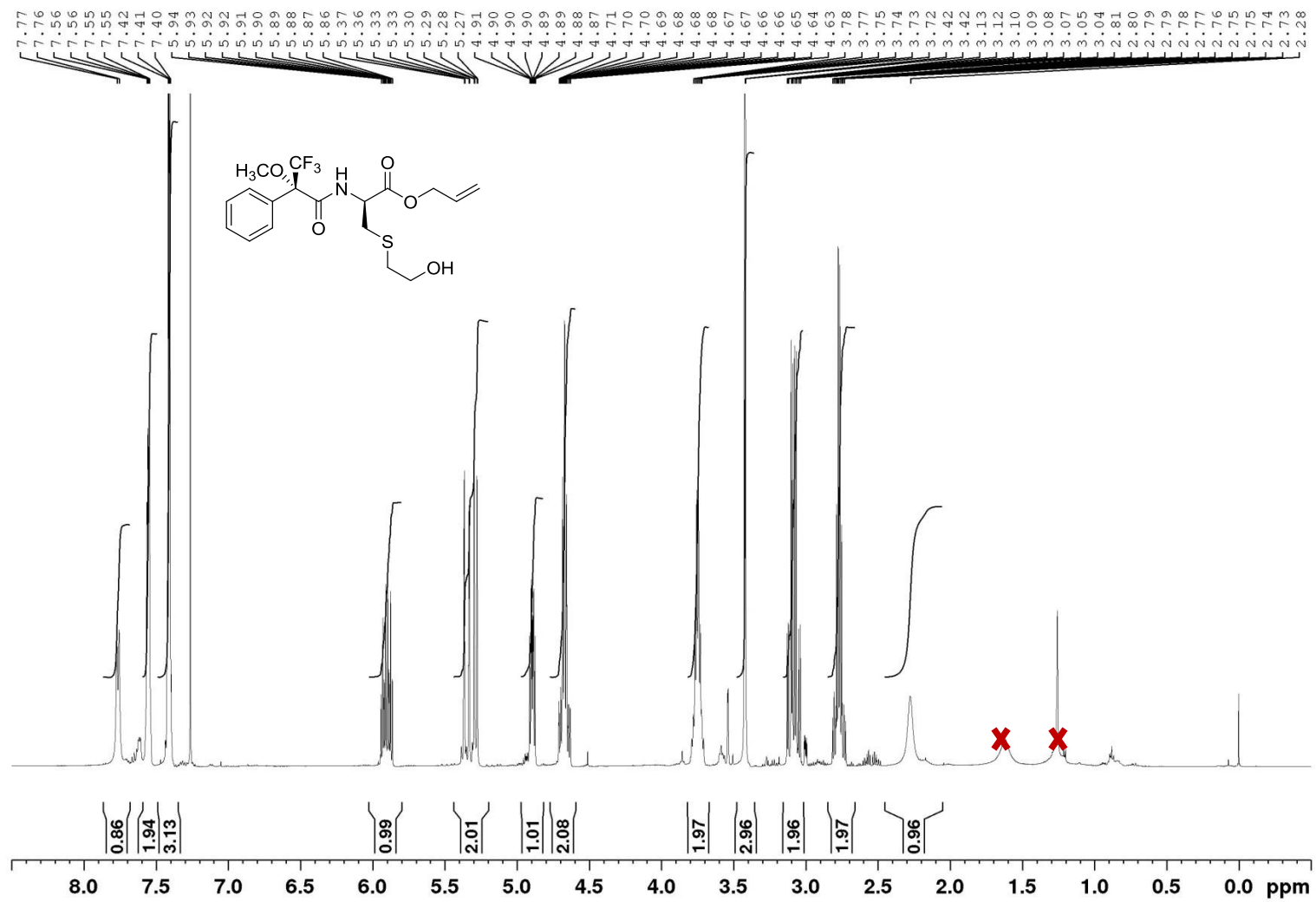
^1H NMR, Compound **75**, CDCl_3 , 500 MHz



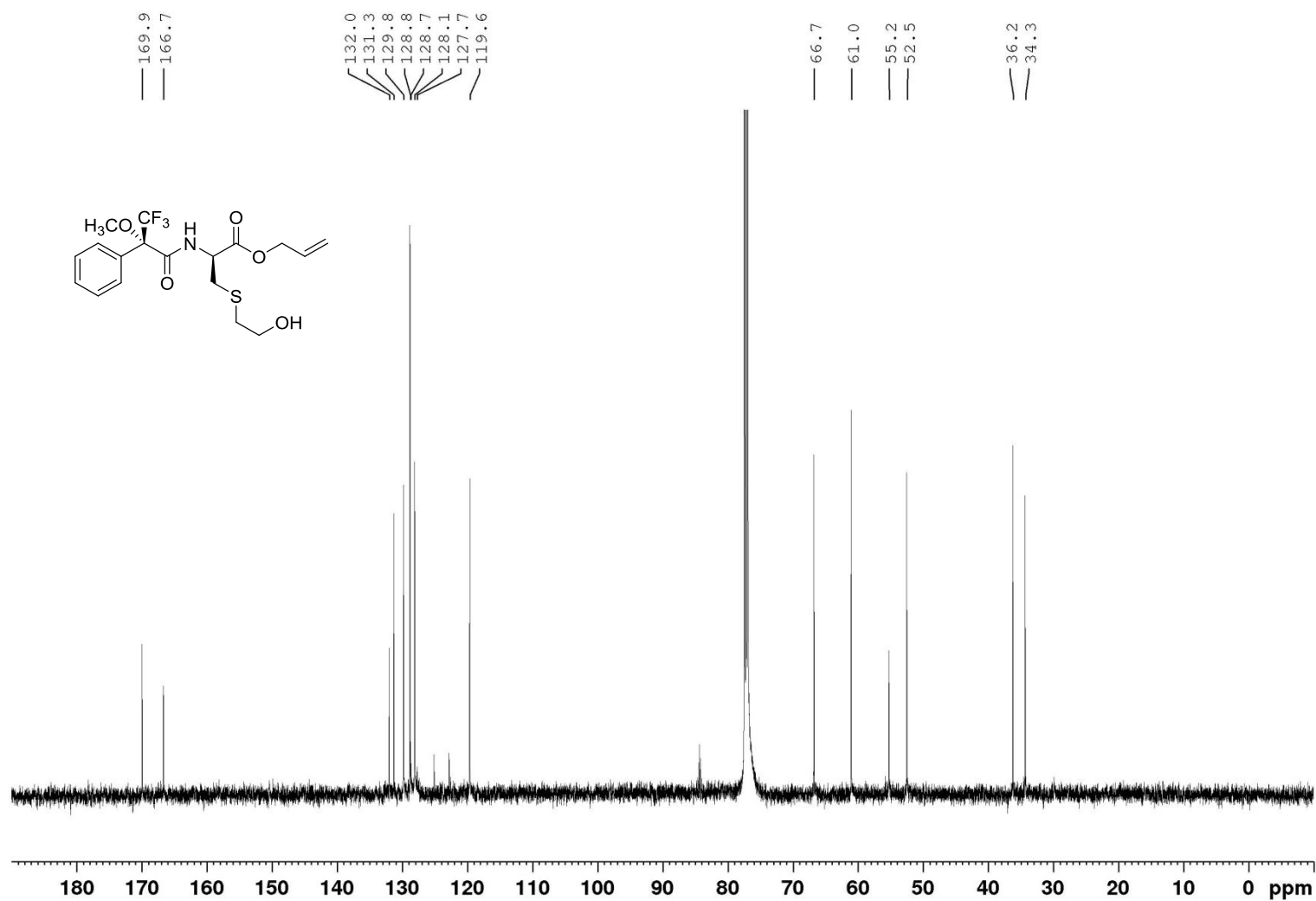
^{13}C NMR, Compound **75**, CDCl_3 , 125 MHz



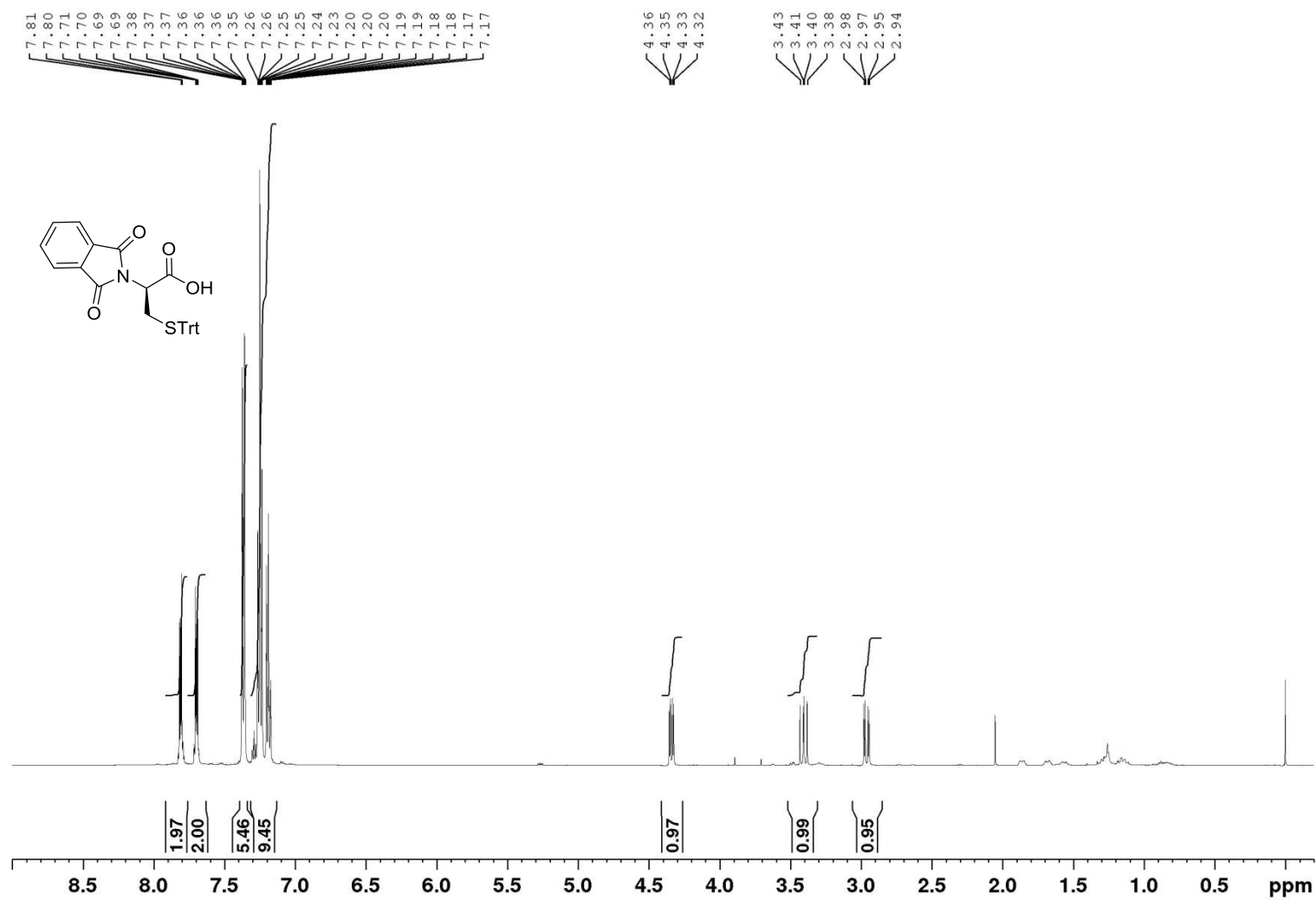
¹H NMR, Compound **76**, CDCl₃, 500 MHz



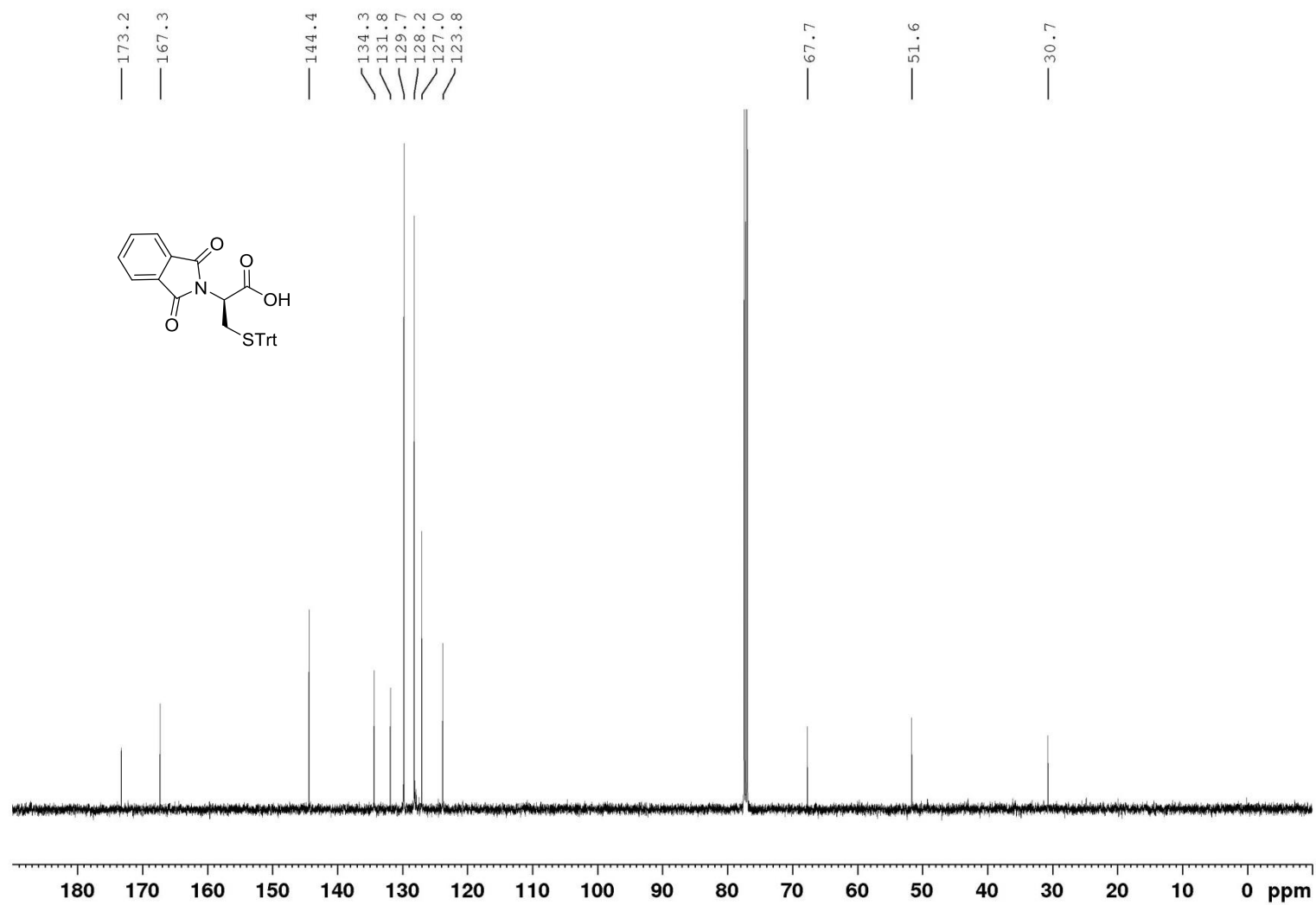
^{13}C NMR, Compound **76**, CDCl_3 , 125 MHz



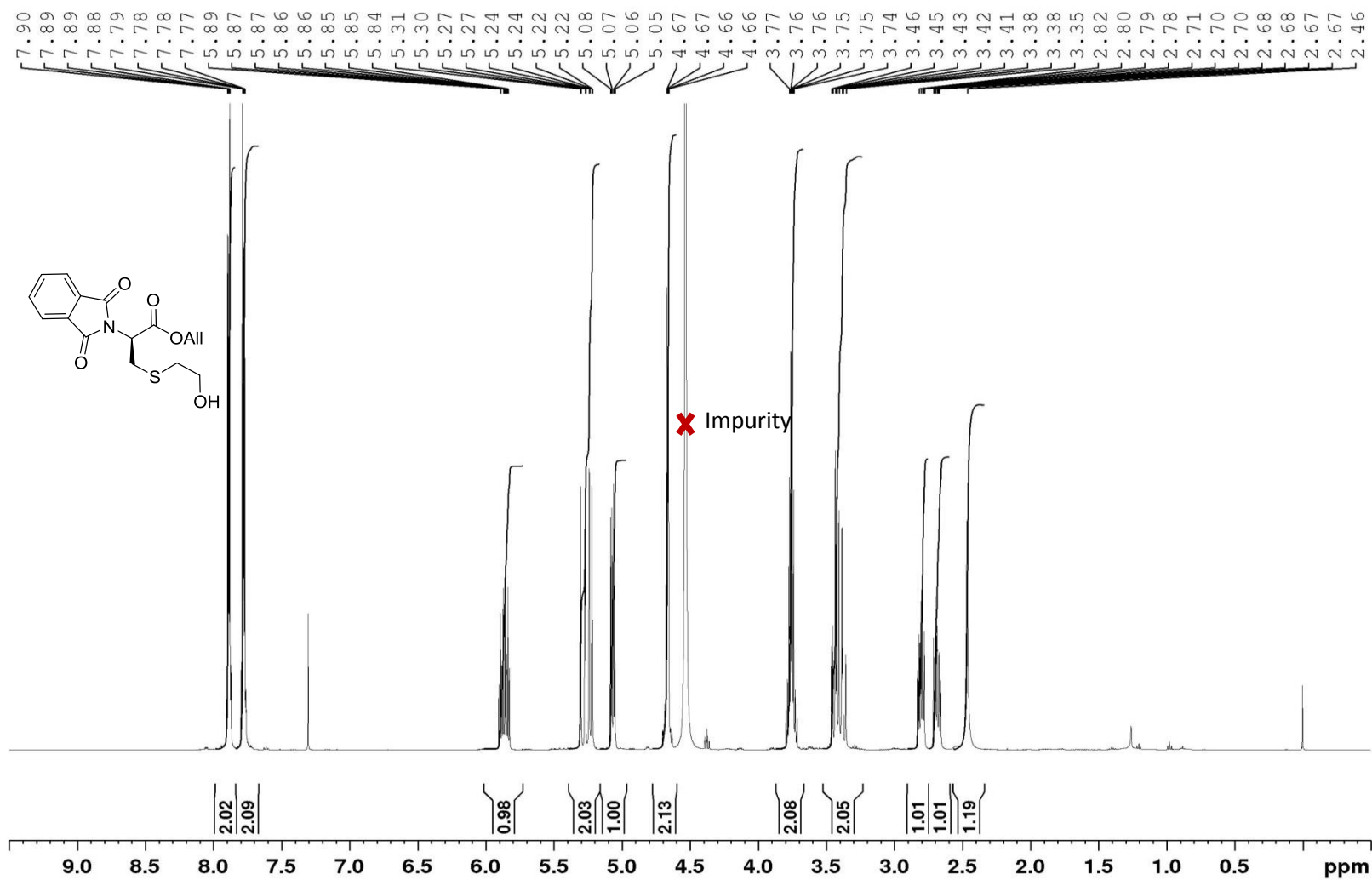
^1H NMR, Compound **82**, CDCl_3 , 500 MHz



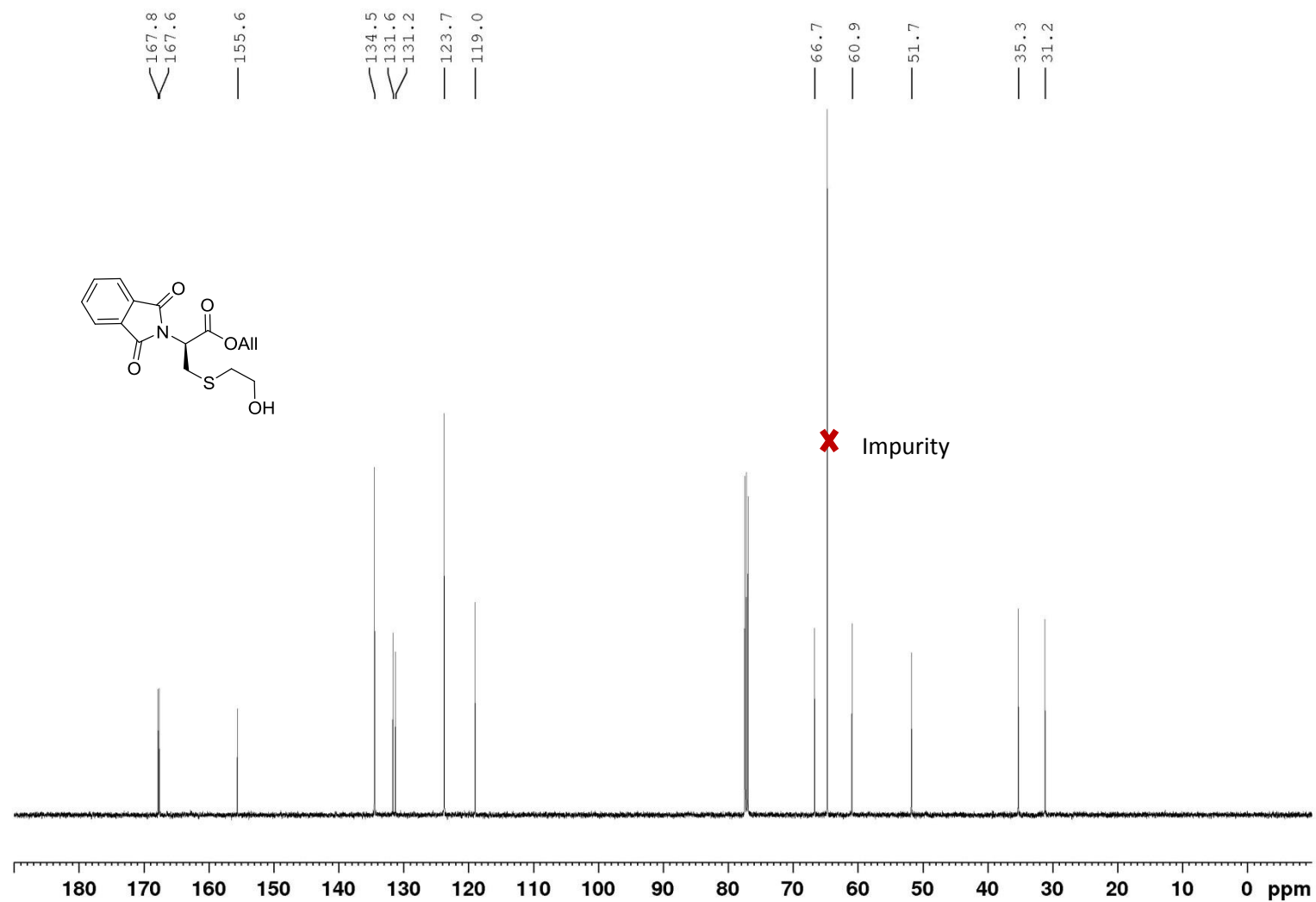
^{13}C NMR, Compound **82**, CDCl_3 , 125 MHz



¹H NMR, Compound (+)-74, CDCl₃, 500 MHz



^{13}C NMR, Compound (+)-**74**, CDCl_3 , 500 MHz



3.11. Chromatograms for Selected Compounds

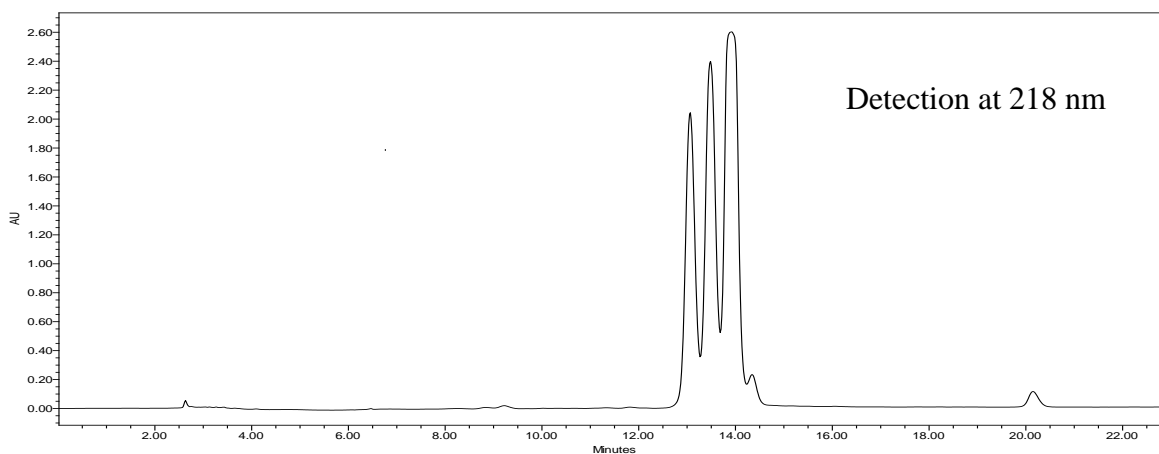
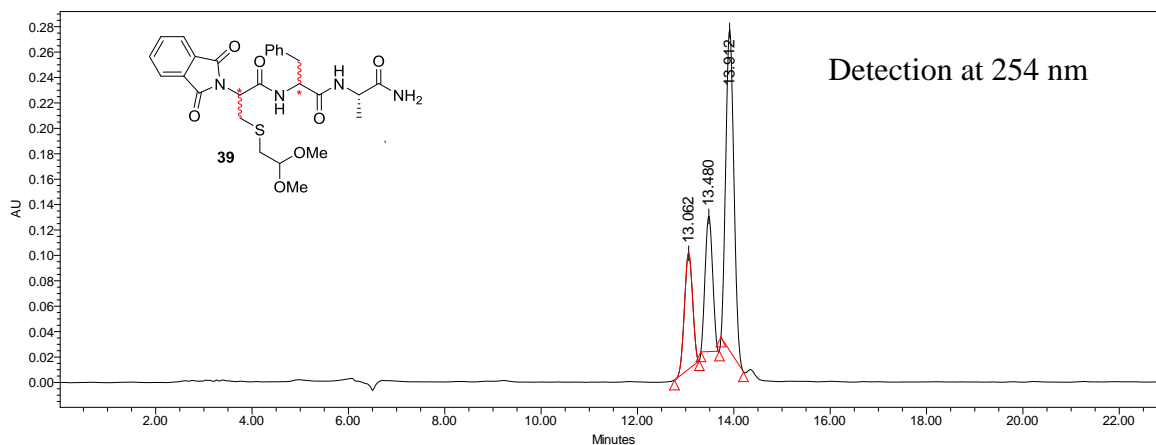
3.11.1. HPLC chromatograms for compounds **39** (jal-1-163)

Normal phase HPLC of 1st generation Tripeptide **39**
Altima® C18 10 μ , 10 x 250 mm column

Method-Gradient

Time (min)	Flow (mL min ⁻¹)	Water (%)	MeCN (%)
0.01	3.00	65.0	35.0
23.00	3.00	30.0	70.0
26.00	3.00	5.0	95.0
31.00	3.00	50.0	50.0
33.00	3.00	50.0	50.0
35.00	3.00	50.0	50.0

	Retention Time	Area	% Area	Height	Int Type
1	13.062	1072371	20.76	91509	bb
2	13.480	1146574	22.20	106666	bb
3	13.912	2946252	57.04	252700	bb

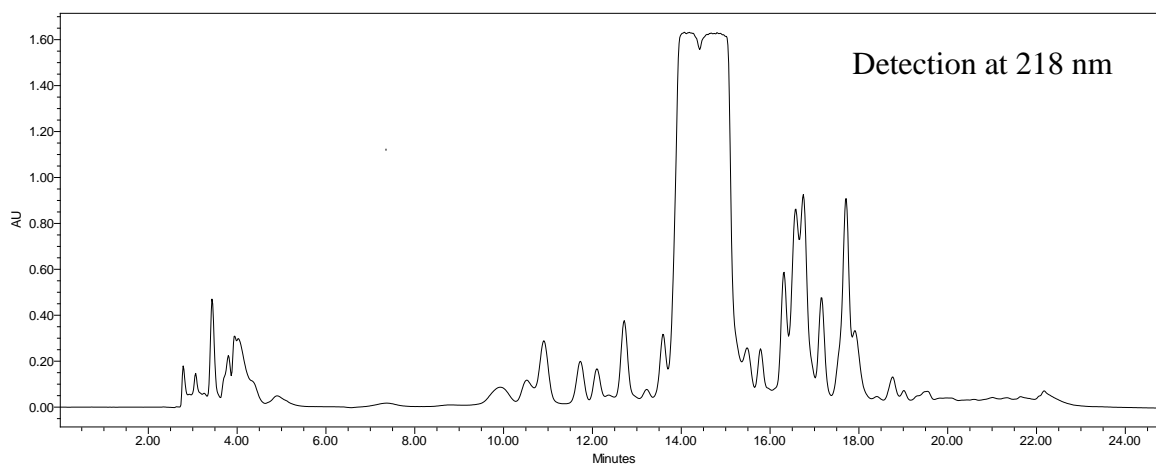
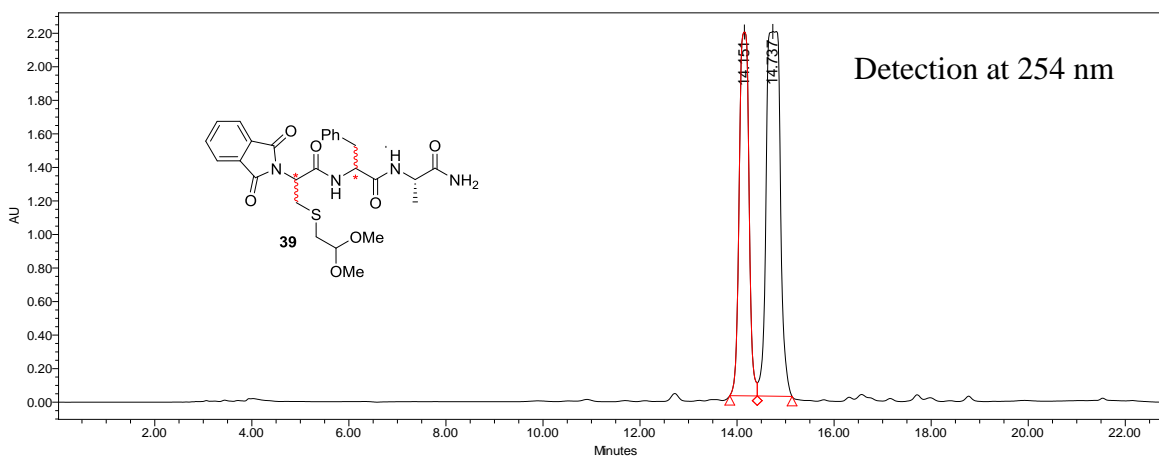


Normal phase HPLC of 2nd generation Tripeptide **39** (jal-2-133)
 Altima® silica 10μ, 10 x 250 mm column

Method-Gradient

Time (min)	Flow (mL min ⁻¹)	H ₂ O (%)	MeCN (%)
0.01	3.00	75.0	25.0
14.00	3.00	35.0	65.0
17.00	3.00	5.0	95.0
21.00	3.00	50.0	50.0
23.00	3.00	50.0	50.0
25.00	3.00	50.0	50.0

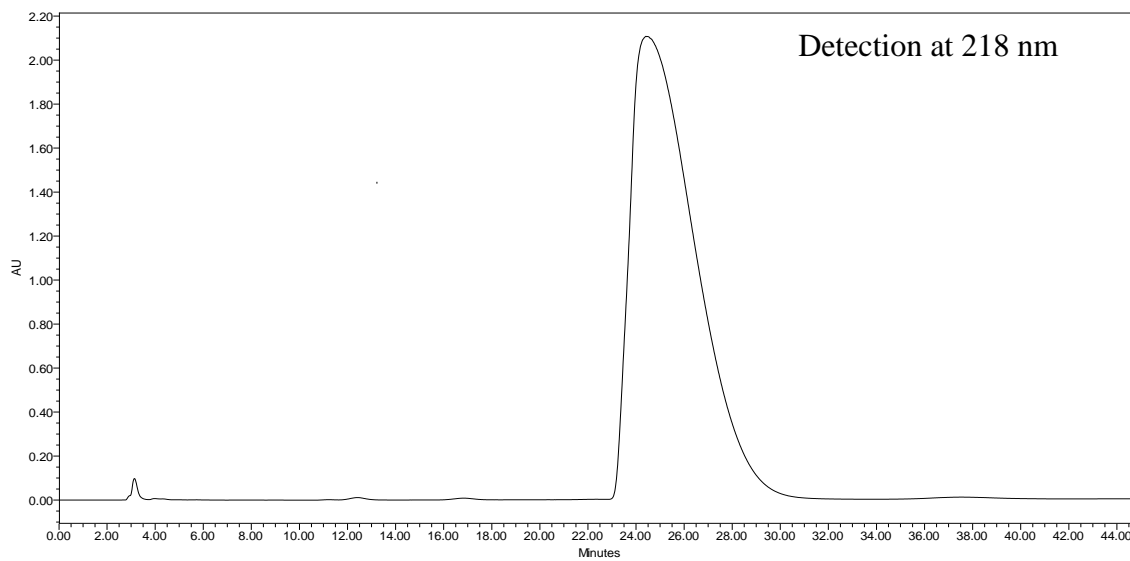
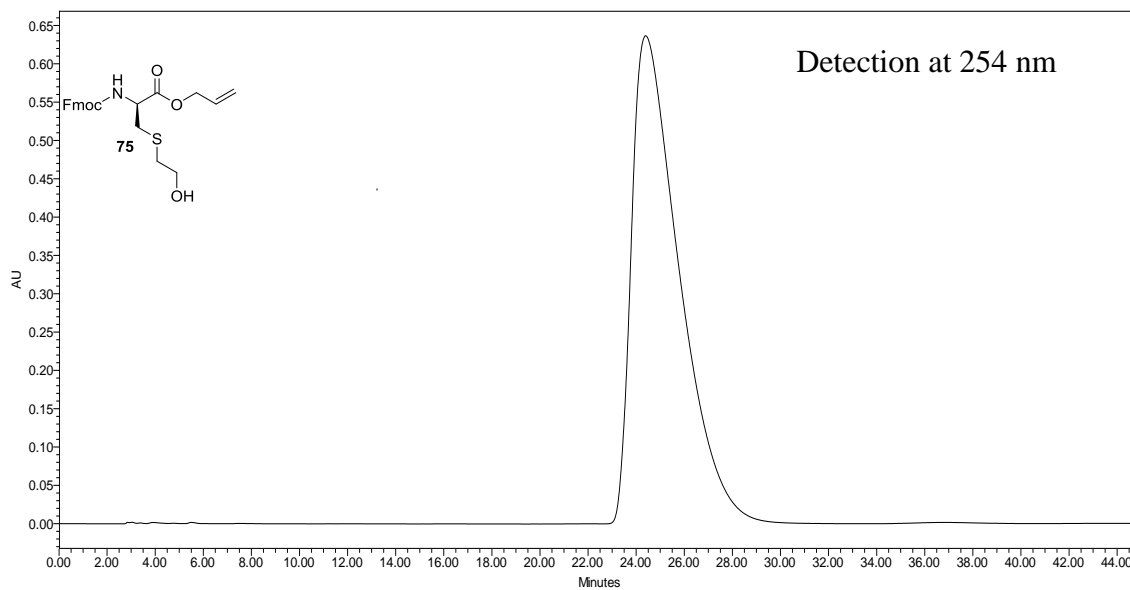
	Retention Time	Area	% Area	Height	Int Type
1	14.151	30250183	40.87	2170291	BV
2	14.737	43766640	59.13	2174022	VB



3.11.3. Chiral HPLC of Fmoc-D-Cys(ethanol)-OAll **75** (jal-7-005)

Chiralcel OD-H column from Daicel; 4.6 x 25 mm

Method-Isocratic 20% isopropanol 80% n-hexane (1 mL min⁻¹)

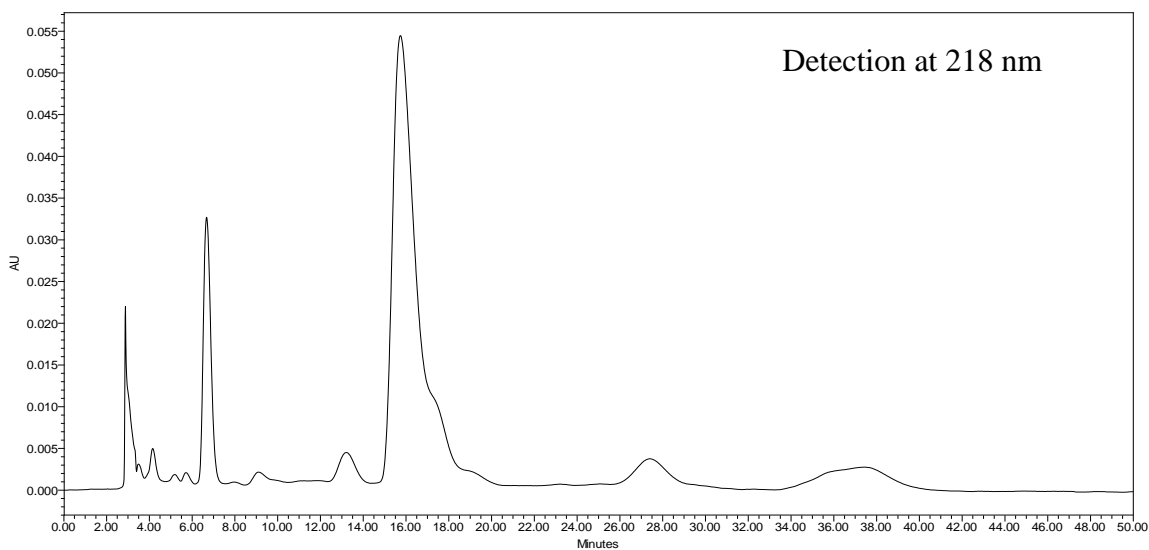
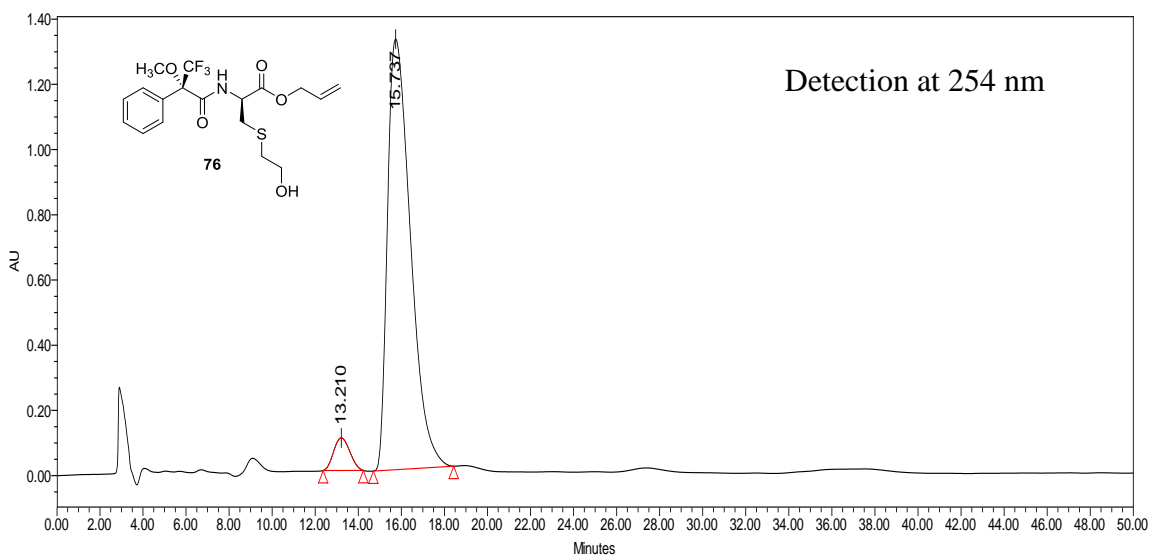


3.11.4. Chiral HPLC of Mosher's-Cys(ethanol)-OAlI **76** (jal-7-012)

Chiralcel OD-H column from Daicel; 4.6 x 25 mm

Method-Isocratic 10% isopropanol 90% n-hexane (1 mL min⁻¹)

	Retention Time	Area	% Area	Height	Int Type	Peak Type
1	13.210	5229150	5.07	100061	bb	Unknown
2	15.737	97970744	94.93	1320891	bb	Unknown

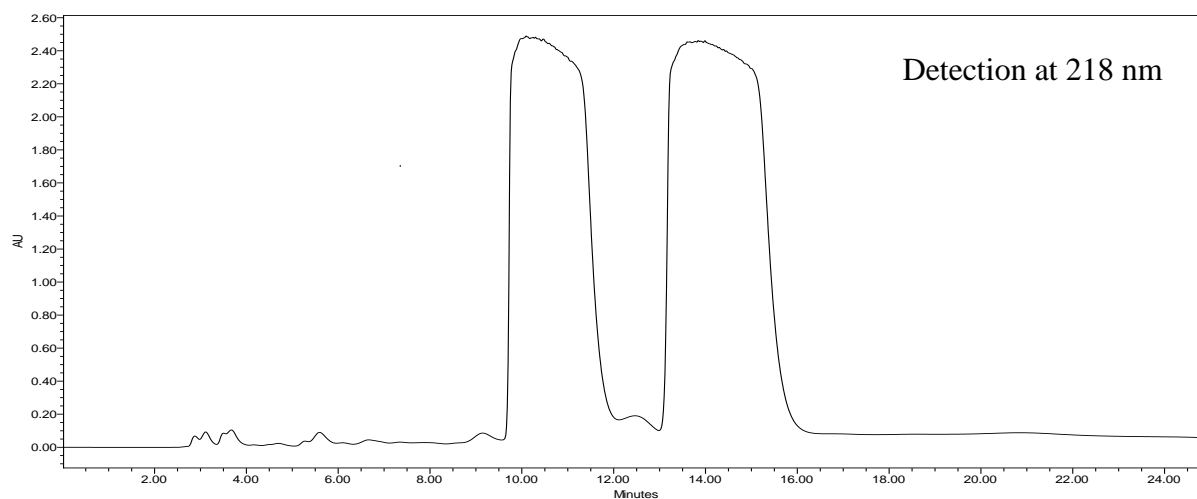
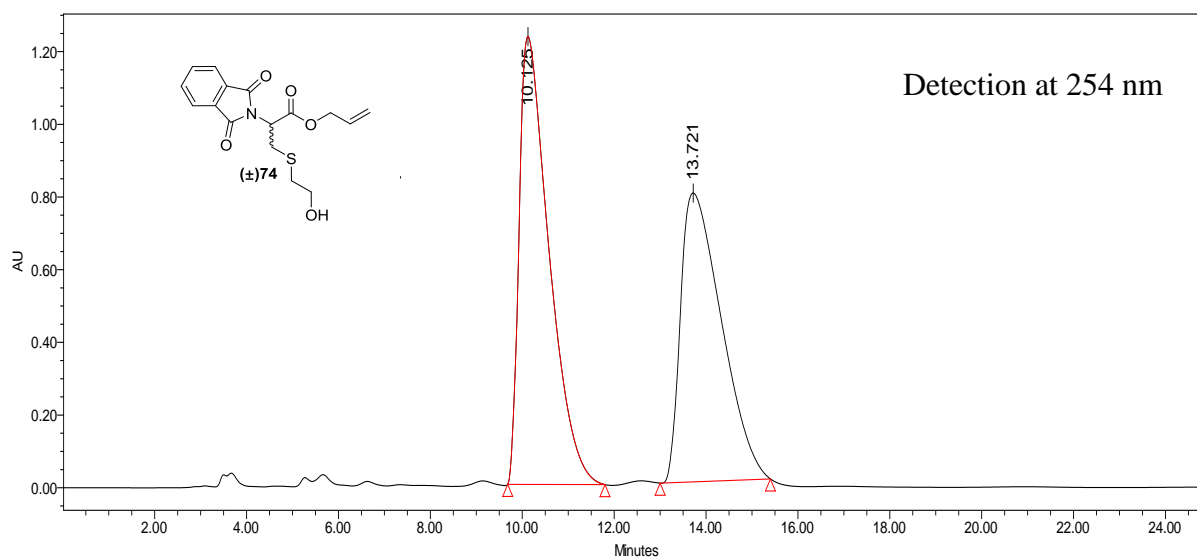


3.11.5. Chiral HPLC of Pht-Cys(ethanol)-OAll (\pm)**74** (jal-6-194)

Chiralcel OD-H column from Daicel; 4.6 x 25 mm

Method-Isocratic 20% isopropanol 80% n-hexane (1 mL min⁻¹)

	Retention Time	Area	% Area	Height	Int Type	Peak Type
1	10.125	55594596	53.15	1232491	Bb	Unknown
2	13.721	49009114	46.85	794789	bb	Unknown

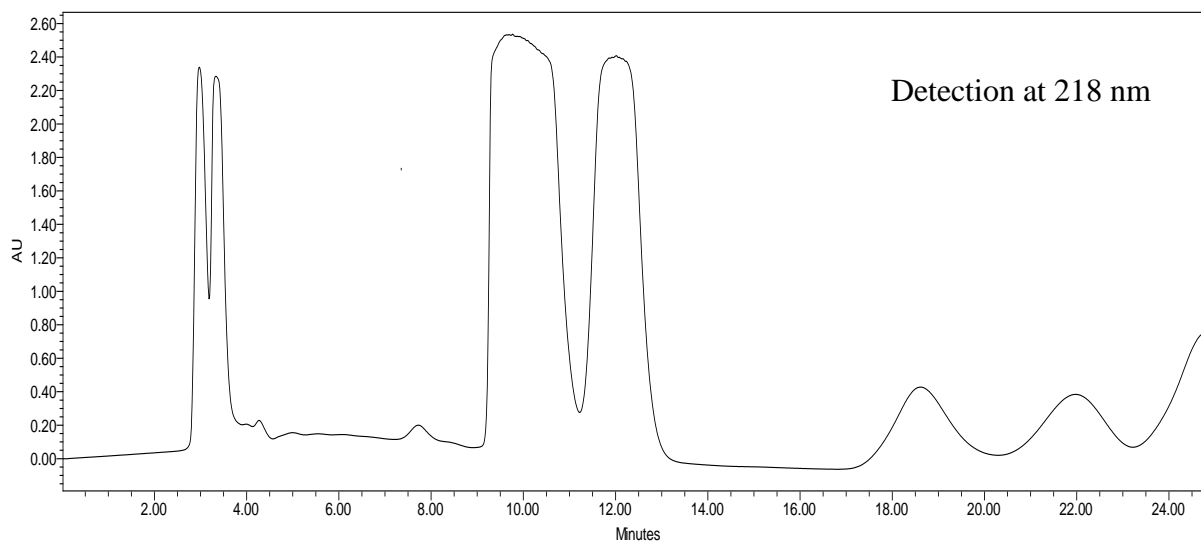
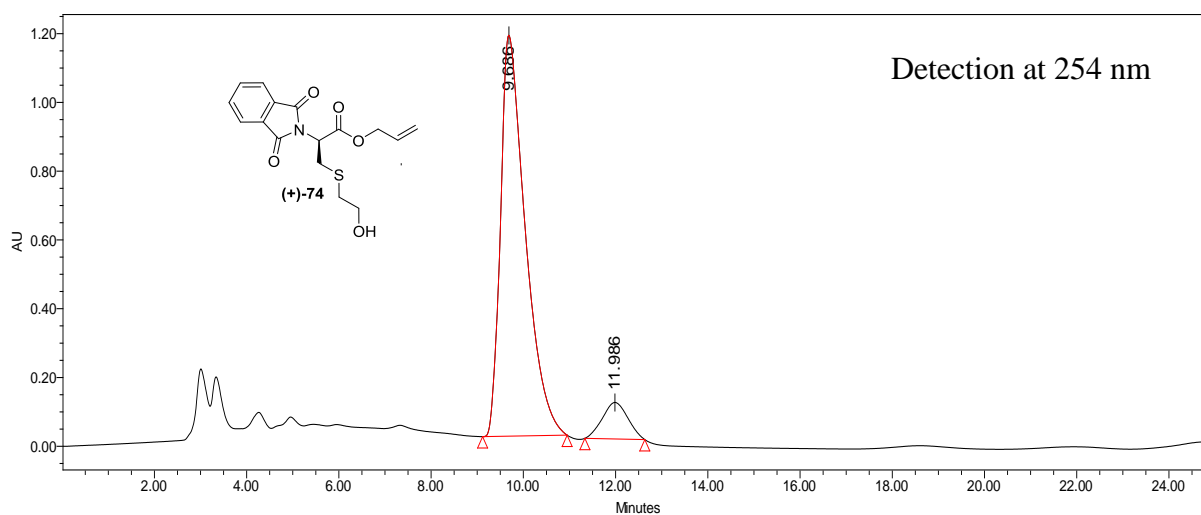


3.11.6. Chiral HPLC of Pht-D-Cys(ethanol)-OAll (+)-74 (jal-7-055)

Chiralcel OD-H column from Daicel; 4.6 x 25 mm

Method-Isocratic 20% isopropanol 80% n-hexane (1 mL min⁻¹)

	Retention Time	Area	% Area	Height	Int Type	Peak Type
1	9.686	43476249	91.43	1165981	bb	Unknown
2	11.986	4074011	8.57	106167	bb	Unknown



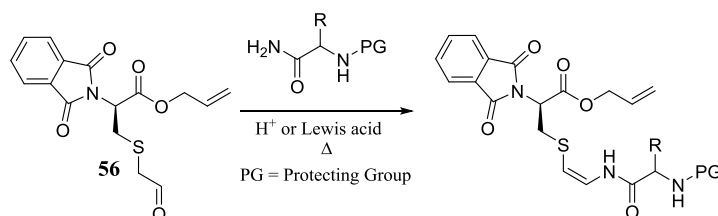
3.12. Notes

1. Arbour, C.A.; Kondasinghe, T.D.; Saraha, H.Y.; Vorlicek, T.L.; Stockdill, J.L.; "Epimerization-Free Access to C-Terminal Cysteine Peptide Acids, Carboxamides, Secondary Amides, and Esters *Via* Complimentary Strategies," *Chem. Sci.*, **2018**, 9, 350-355.
2. Lelievre, D.; Terrier, V.P.; Delmas, A.F.; Aucagne, V.; "Native Chemical Ligation Strategy to Overcome Side Reactions During Fmoc-Based Synthesis of C-Terminal Cysteine-Containing Peptides," *Org. Lett.*, **2016**, 18, 920-923.
3. Han, Y.; Albericio, F.; Barany, G. "Occurrence and Minimization of Cysteine Racemization During Stepwise Solid-Phase Peptide Synthesis," *J. Org. Chem.*, **1997**, 62, 4307-4312.
4. Siedler, F.; Weyher, E.; Moroder, L. "Cysteine Racemization in Peptide Synthesis: a New and Easy Detection Method," *J. Pept. Sci.*, **1996**, 2, 271-275.
5. Kovacs, J.; Mayers, G.L.; Johnson, R.H.; Ghatak, U.R. "Racemization Studies in Peptide Chemistry. Reinvestigation of the β -Elimination-Readdition Mechanism of N-Benzyloxycarbonyl-S-benzylcysteine Derivatives," *Chem. Commun.*, **1968**, 1066-1067.
6. Zhu, X; Schmidt, R.R., "Efficient Synthesis of Differently Protected Lanthionines via β -Bromoalanine Derviatives," *Eur. J. Org. Chem.*, **2003**, 4069-4072.
7. Kusumi, T.; Ohtani, I.I., "Determination of the Absolute Congfiguration of Biologically Active Compounds by the Modified Mosher's Method," *Biology-Chemistry Interface*, **1999**, 103-137.
8. Dale, J.A.; Dull, D.L.; Mosher, H.S., " α -Methoxy- α -trifluoromethylphenylacetic Acid, a Versatile Reagent for the Determination of Enantiomeric Composition of Alcohols and Amines," *J. Org. Chem.*, **1969**, 34, 2543-2549.
9. Casimir, J.R.; Guichard, G.; Briand, J.P., "Methyl 2-((Succinimidooxy)carbonyl)benzoate (MSB): A New, Efficient Reagent for N-Phthaloylation of Amino Acid and Peptide Derivatives," *J. Org. Chem.*, **2002**, 67,3764-3768.

Chapter 4. Peptidyl Thioenamide Synthesis and Macrocyclization

4.1. Imidazolidinone: a Thioenamide Interrupted

Optimization of thioenamide formation using acetamide, featured in Chapter 2, paved the way for this transformation in the context of a peptide framework. This extrapolation required careful consideration of protection strategy (i.e. PG) on the amine group of the amide coupling partner (Scheme 4.1).



Scheme 4.1. Reaction of aldehyde **56** with an α -amino amide

The protecting group would need to weather the Lewis acid and prolonged heating required to produce the desired product. Additionally, we sought a group that could be easily removed, to liberate the free amine, and proceed to coupling with another amino acid. Given the lack of chemistry that has been performed in the presence of aminovinyl-cysteine, the stability of its thioenamide functionality towards reaction conditions in general was a complete unknown.

We learned an early lesson from α -amino amide couplings with Fmoc-protected alaninamide **63** (Scheme 4.2). At this time we were still using protic acids to achieve thioenamide formation. Our original plan was to use alaninamide in place of a cysteinamide to produce a model system of the microbisporicins (Fig. 4.1). Exploring Fmoc protection for the amine made sense, as this group is ubiquitous in peptide chemistry and can often be easily removed. To our surprise, when we attempted to form thioenamide **65** from acetal **28** and alaninamide **63**, we did not observe any desired product at all. Instead, we isolated imidazolidinone **64** in 67% yield (Scheme 4.2).

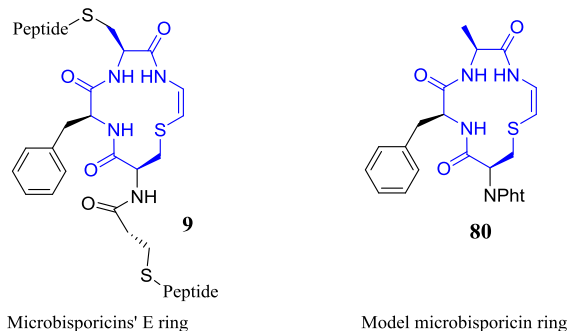
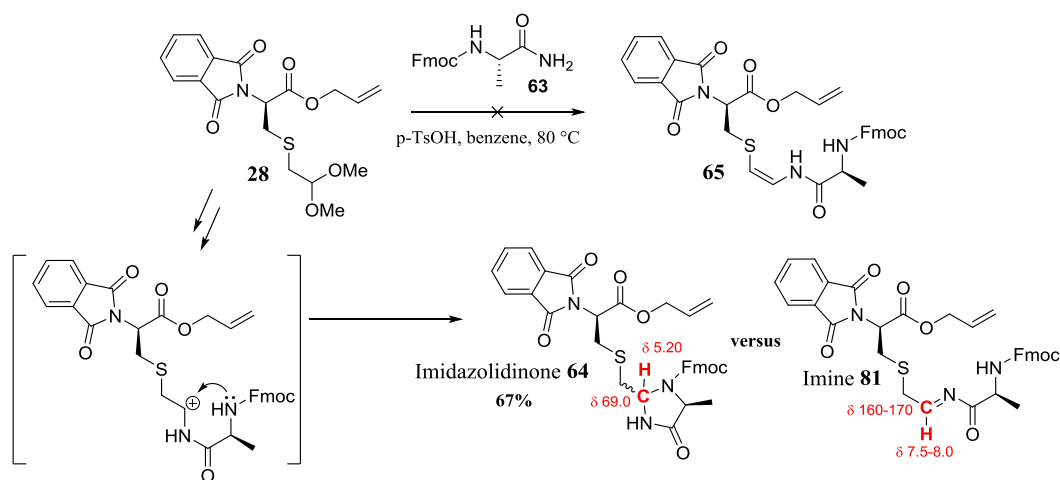


Figure 4.1. Microbisporicin E ring and proposed model system

This side product results from attack of the Fmoc-carbamate nitrogen on a transient carbocation that forms before elimination takes place (See Section 3.2).

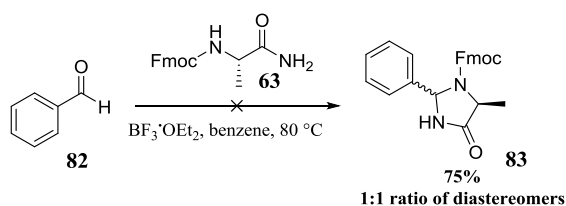


Scheme 4.2. Abridged mechanism of formation of imidazolidinone **64** and comparison with potential imine **81**

The structure of imidazolidinone **64** eluded us for a while, as the NMR was difficult to interpret and the molecular ion observed by HRMS is consistent with not only desired thioenamide **65** but also imine **81**. The key to identification of this product was the comparison of the carbon and proton chemical shifts expected for an imidazolidinone and an imine. In the case of an *N*-acyl imine, the sp^2 CH (colored red in **81** in scheme 4.2) would be expected to give rise to a signal at 7.5-8.0 ppm in the proton NMR, correlated to a ^{13}C signal at 190-170 ppm.¹

In contrast, our compound displayed a proton signal 5.20 ppm correlated to a ^{13}C NMR signal at 69.0 ppm via HSQC, pointing strongly towards imidazolidinone **64**.

This result was further confirmed by analogous reaction between benzaldehyde (**82**) and Fmoc-alaninamide **63** (Scheme 4.3) in the presence of boron trifluoride diethyl etherate. The resulting imidazolidinone **83** was obtained in 75% yield, and could be much more easily characterized than cysteine derivative **64**. The reaction also showed that the transformation takes place with both protic and Lewis acids, as expected.

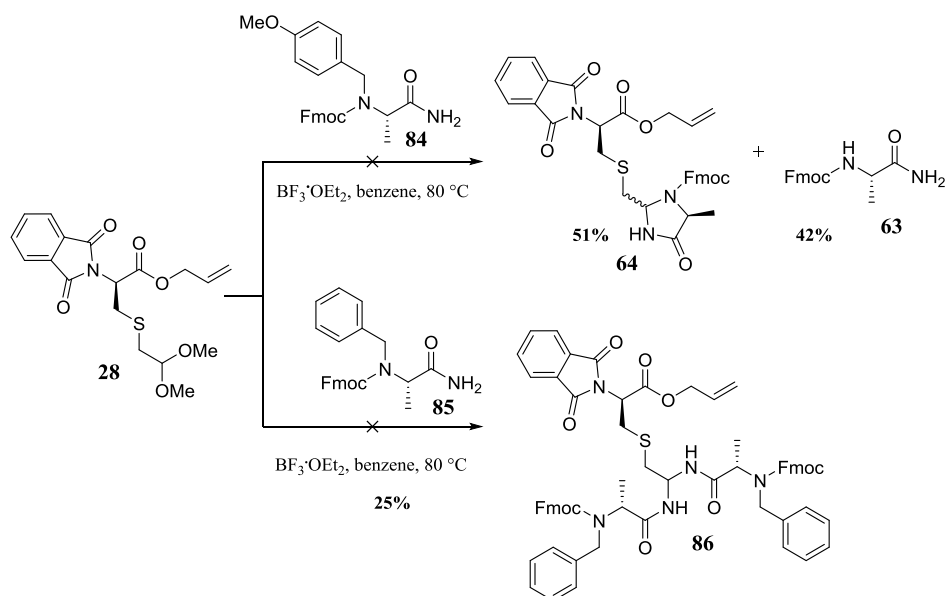


Scheme 4.3. Imidazolidinone formation with benzaldehyde

The fact that the rate of attack of a poorly nucleophilic, carbamate nitrogen is fast enough to intercept thioenamide formation, showed us that nucleophilicity at this site is intolerable. Thus, any amino amide coupling partner must be doubly protected at the amine nitrogen.

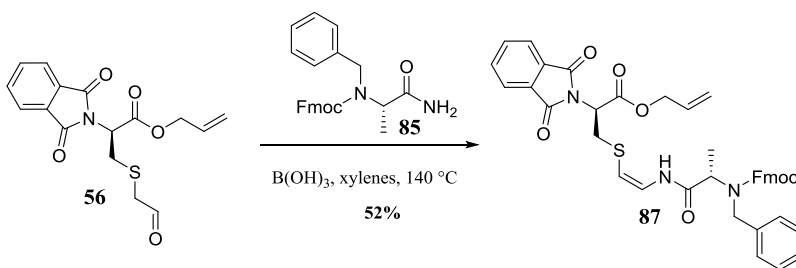
4.2. Double Amine Protection – Benzyl Groups

We began our investigation into doubly protected amines by modifying alaninamide. The first strategy we used was appendage of the *para*-methoxybenzyl group, viz. **84** (Scheme 4.4), hoping to leverage the mild acidic or oxidative conditions with which it can be removed. To our disappointment, the Lewis acidic conditions used to form thioenamide quickly removed the *para*-methoxybenzyl group and the reaction proceeded to yield imidazolidinone **64** yet again. The next group surveyed was the less acid labile benzyl group in alaninamide **85**. As expected, the benzyl group was not removed by the acidic conditions. Nevertheless, no thioenamide was generated by the reaction. Instead, *bis*-amide **86** was isolated in 25% yield.



Scheme 4.4. Condensation of acetal **28** with backbone benzyl protected alaninamides

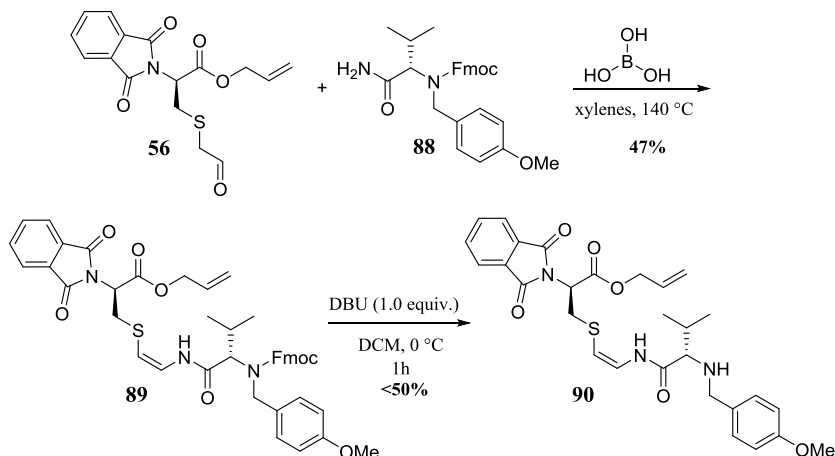
At about this stage in our studies, based on optimization of the reaction with acetamide (See Chapter 2), we switched to boric acid and increased the temperature of the reaction to minimize formation of *bis*-amide **86**. The reaction was still sluggish in toluene (b.p. 110°C); we switched to xylenes (b.p. 140°C) to good effect (Scheme 4.5). With these changes, we synthesized our first “dipeptide” thioenamide **87** in 52% yield. No *E*-isomer could be detected in the crude product mixture via HPLC.



Scheme 4.5. Formation of thioenamide **87**

At this point we switched from alaninamide to valinamide, to begin our synthesis of the C-terminal ring of cypemycin (See Chapter 1, Fig. 1.10). Removal of benzyl protecting groups is typically achieved by reduction of carbon-heteroatom bonds via reductive hydrogenolysis.

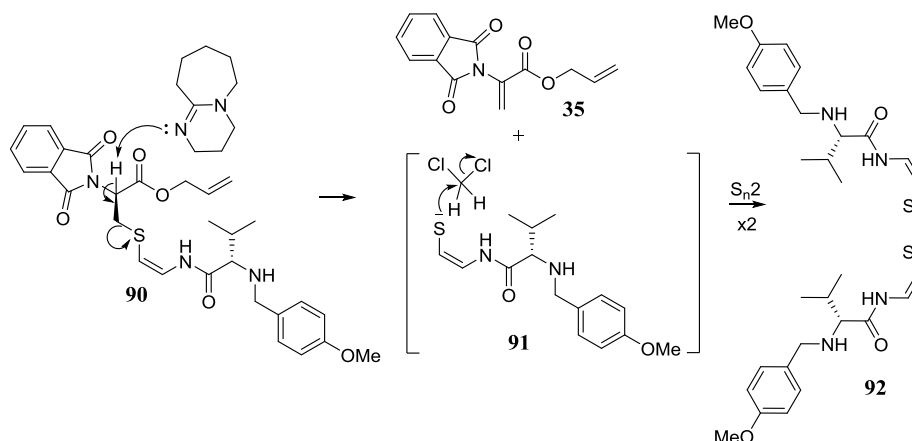
These conditions held the potential to reduce our thioenamide, and hence the benzyl group was not ideal. We found that the *para*-methoxybenzyl group was stable to boric acid, so we reverted to this protecting group that had not held up to $\text{BF}_3 \cdot \text{OEt}_2$. With this strategy we synthesized valine thioenamide **89** and began attempts to deprotect the α -amine to afford secondary amine **90** (Scheme 4.6).



Scheme 4.6. Formation of and removal of fmoc from thioenamide **89**

Curiously, standard conditions for Fmoc removal (piperidine or diethylamine) did not liberate the secondary amine. Removal was possible with a stronger base (DBU), but the reaction required careful monitoring and low temperature. Even with these considerations, the yield was never more than 50%. The poor yield was, in part, due to abstraction of the AviCys α proton (Scheme 4.7). This issue was deduced through characterization “dimer” **92** that arises from elimination to form a reactive enethiolate anion analogous to that in the biosynthesis of AviCys (See Chapter 1, Scheme 1.1). Mechanistically, methylene bridged “dimer” **92** arises from two attacks of enethiolate **91** on dichloromethane, employed as the solvent for the reaction (Scheme 4.7). The yield of dimer **92** was as high as 38%, though this could be reduced by quenching the reaction with aqueous HCl before concentration. Nonetheless, this elimination

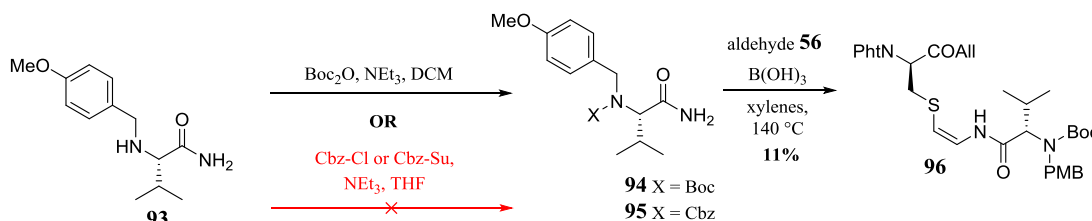
pathway opened up too much potential for epimerization of our AviCys C α stereocenter to continue the pursuit of base labile protecting groups.



Scheme 4. 7. Mechanism for formation of "dimer" **92**

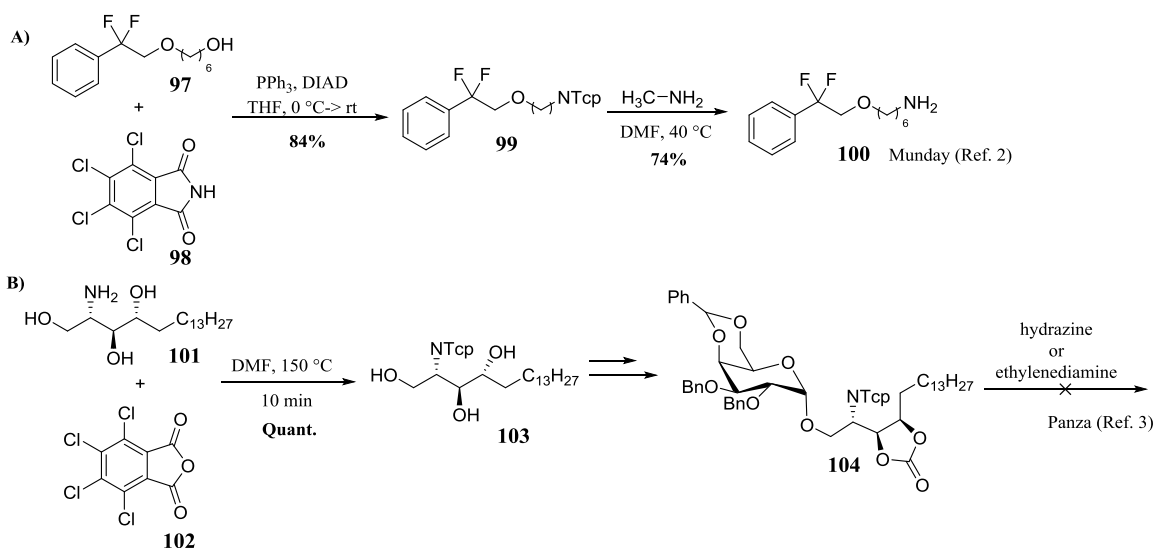
4.3. Tetrachlorophthalimide (Tcpi)

We needed to move away from Fmoc chemistry, yet wanted to stick with well-established carbamate protecting groups that could be removed under acidic or neutral conditions. In this vein, we attempted to generate both the Boc (**94**) and Cbz (**95**) variants of *para*-methoxybenzyl (PMB) valinamide **88** (Scheme 4.8). To our surprise, the Cbz group could not be installed on PMB amine **93** and, less surprisingly, PMB could not be installed on a Cbz carbamate. We were, however, able to install a Boc carbamate as the second protecting group and generate thioenamide **96**, but only in low yield. Efforts to increase the yield of **96** were unsuccessful.



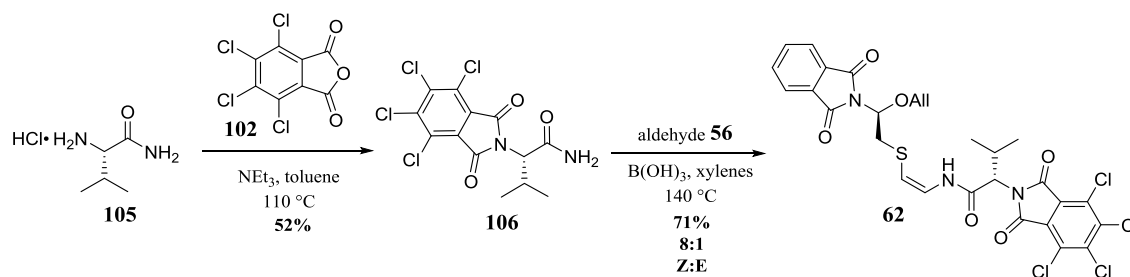
Scheme 4.8. Boc and Cbz in combination with PMB for α -amine double protection

The poor results from *bis*-protection of our valinamide pressed us to think about divalent protection that could be removed in a single step. We turned our attention to tetrachlorophthalimido (Tcp) protection. While we could not find reports of its use in complex peptide chemistry, it has been used recently in medicinal² and glycoside³ chemistry (Scheme 4.9). Munday *et al.* installed the Tcp group using Mitsunobu conditions and removed it with methyl amine in good yields for both transformations (Scheme 4.9A). Panza *et al.*, in contrast, used tetrachlorophthalic anhydride to install the group. However, they were unable to efficiently remove the group without degradation of their material (Scheme 4.9B).



Scheme 4.9. Recent examples of Tcp utilization

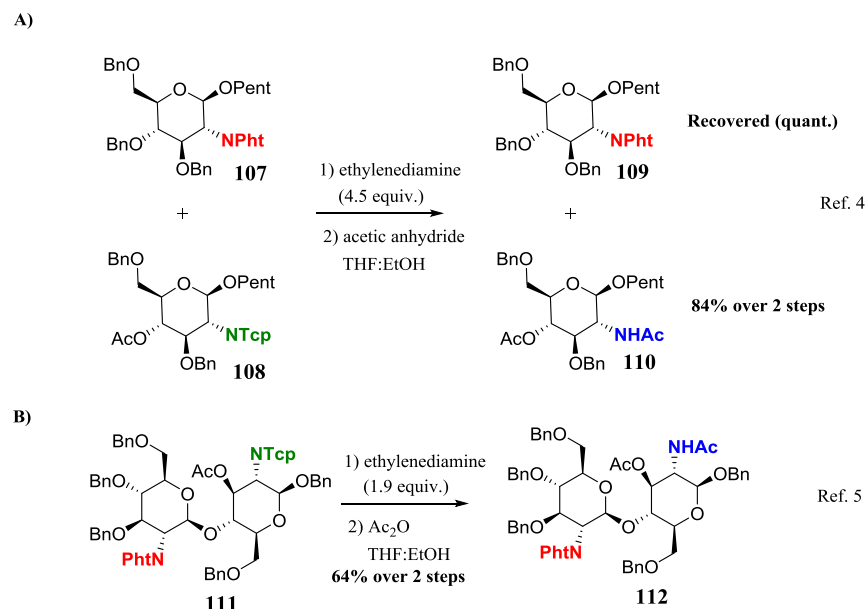
We readily synthesized tetrachlorophthalimido-protected valinamide **106** from commercially available tetrachlorophthalic anhydride (**102**) (Scheme 4.10). Due to the non-acidic nature of the valinamide α -proton, we were able to safely use the basic conditions that caused the epimerization issue featured in Chapter 3. We were very pleased to find that Tcp-valinamide **106** was our most efficient coupling partner yet, yielding thioenamide **62** in 71% yield, while maintaining the favorable 8:1 *Z:E* ratio.



Scheme 4.10. Synthesis of Tcp-valinamide **106** and thioenamide **107**

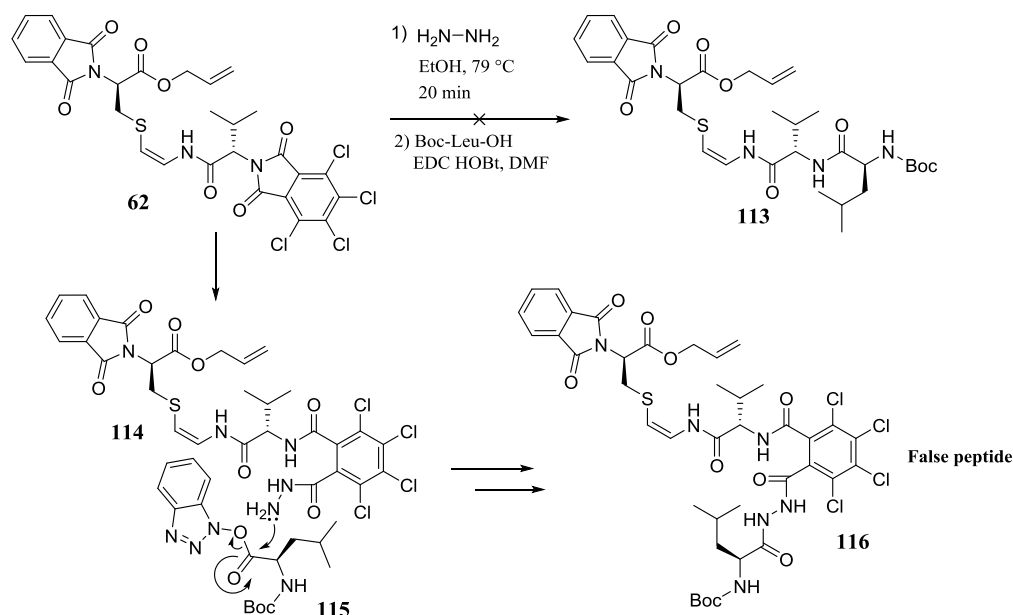
Two reports from Fraser-Reid and coworkers gave us hope that the tetrachlorophthalimido (Tcp) group could be selectively removed in the presence of our unsubstituted phthalimide (Pht).^{4,5} They used ethylenediamine in excess to remove the Tcp group, and then immediately acetylated with acetic anhydride in both cases (Scheme 4.11). While both reactions demonstrate that the Tcp can be removed chemoselectively, only one example discriminates between the two protecting groups within the same molecule. In the case of intramolecular selectivity (Scheme 4.11B), Fraser-Reid had to reduce the equivalents of ethylenediamine from 4.5 to just 1.9, presumably due to partial removal of the Pht group. These two examples, from the same group, were the only literature precedent available for chemoselective removal of the Tcp protecting group in the presence of the Pht group.

For our desired transformation, excess ethylenediamine at room temperature in ethanol was ineffective. Bringing the reaction to reflux could force a reaction with our substrate, but the crude ^1H NMR and TLC quickly became complicated and the risk of epimerization with such a basic reagent at high temperature was untenable. Another common reagent used for the removal of phthalimido protecting groups is hydrazine, which is less basic than ethylenediamine by nearly two orders of magnitude (pKa of conjugate acids: ethylenediamine = 9.98, hydrazine = 8.10). We found that hydrazine gave rise to a cleaner reaction profile, even under reflux.



Scheme 4.11. Fraser-Reid's precedents for selective removal of TcP in presence of Pht

Using hydrazine in similar excess (1.9 equivalents) at elevated temperature, we observed a rapid reaction, with conversion to a single major product in high yield. We were never able to isolate free amine at this point, however, mass spectrometry of the crude product showed the free amine product as the major ion (m/z 432). Following Fraser-Reid's precedent, we proceeded to acylate the free amine *in situ* with Boc-Leu-OH to give what appeared to be a nearly quantitative yield of desired product **113** (Scheme 4.12). The ^1H NMR of the isolated product was quite complicated and difficult to interpret, but evidence of all three amino acids (Cys, Val, Leu) was apparent, along with an intact thioenamide. Nevertheless, the desired mass was never observed. This was a warning sign that something had gone awry in the sequence of reactions. Detailed NMR analysis using 2D methods (COSY, HSQC, HMBC, etc.) was required to solve this issue.

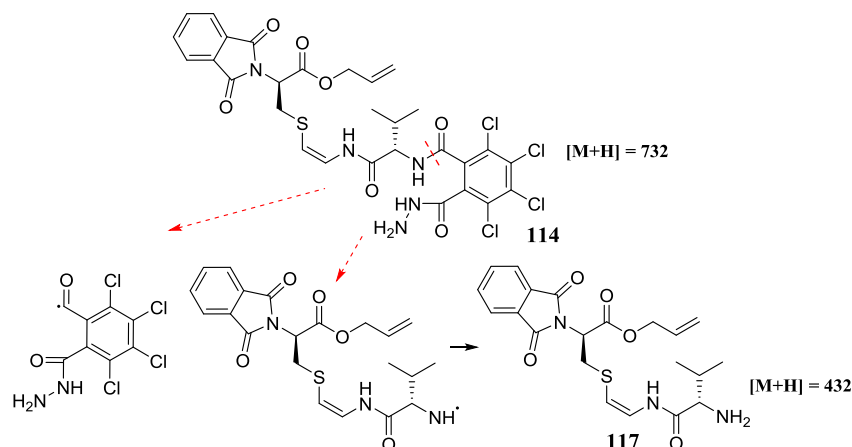


Scheme 4.12. Stalled Tcp removal and the synthesis of "false" peptide **116**

Ultimately the data for the compound could be explained by an “interrupted Tcp removal” (Scheme 4.12). The product of our reaction was not the desired leucine amide **113**, but the diacyl hydrazide **116**. This resulted from premature coupling of leucine to a partially removed Tcp. The resulting side product would show only a single proton difference from our desired product via ^1H NMR, and this lone hydrazide proton exchanges, at least partially, with deuterium in the deuterated methanol that was used for analysis. Carbon-13 NMR and correlation information from HSQC and HMBC were the only methods that could fully elucidate the structure of this strange product.

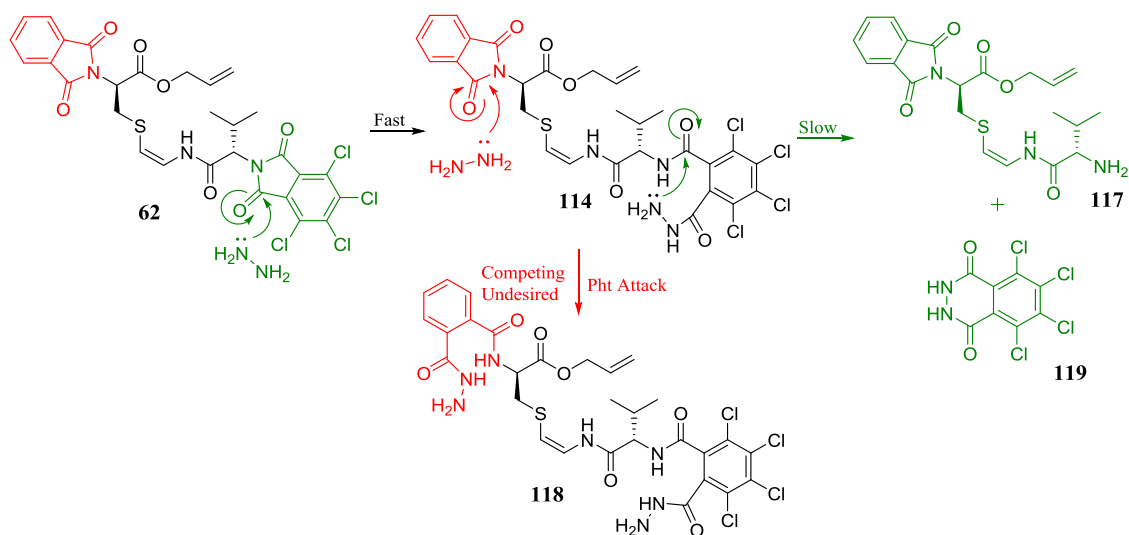
The desired free amine, for which we thought we had observed the molecular ion via mass spectrometry could also be explained by a long-lived hydrazide intermediate (Scheme 4.12). While the ring-opened Tcp **114** could be observed in the mass data (m/z signal centered at 732), it was always a small signal. The fact that the major ion was free amine points to a facile fragmentation that takes place during ionization. This could result in a radical species that abstracts a proton to generate amine **117** within the instrument. With such strong evidence for

partial removal of the Tcp group taking place, the next task was to alter the reaction conditions to generate genuine free amine **117**.



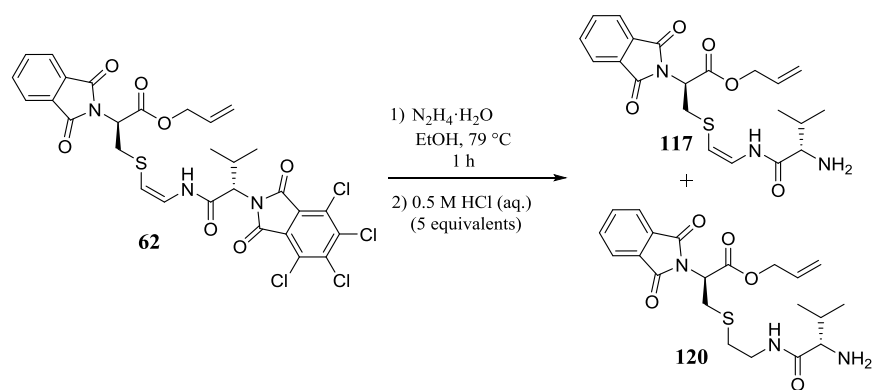
Scheme 4.13. Explanation for a base peak in mass spectrometry corresponding to desired amine **117**

Our experience with “false peptide” **116** gave us insight into the relative rates of the two steps required for complete Tcp removal. The initial attack of hydrazine is very fast, and chemoselective for the Tcp over the Pht (Scheme 4.14). The other required step, an intramolecular attack to form a 6-membered hydrazide ring, is much slower. The natural assumption was that using a single equivalent of hydrazine could achieve this transformation, given enough time and heat. Although it is unclear why, we found that in order to proceed past hydrazide **114** an excess of hydrazine was required. When hydrazine was used in great excess (10% v/v in ethanol), the unsubstituted phthalimido (Pht) was be fully cleaved as well. Even when just 1.8 equivalents of hydrazine were used, partial removal of the Pht group was observed. Using isolated hydrazide **114**, we investigated the crucial second step of the process. Unfortunately, the isolated yield of hydrazide **114** was always low and all attempts to form free amine **117** from it were low yielding as well.



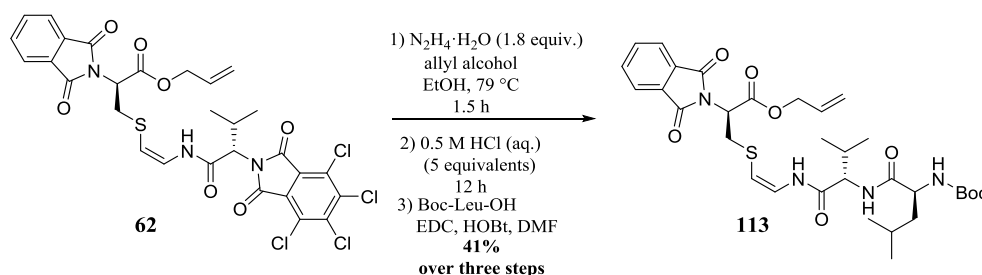
Scheme 4.14. Relative rates of Tcp and Pht attack

The key to generating free amine **117** was, following the initial formation of **114**, to eliminate the nucleophilicity of hydrazine before it could attack the Pht. Several examples in recent literature utilize acidification in order to trap the resulting amine as a cation.⁶⁻⁸ With acidification of the reaction, as soon after the first attack as possible, we would protonate any excess hydrazine still present and prevent further attack. Our early attempts with acidification used 2.5 equivalents of hydrazine in ethanol at reflux. After an hour we added aqueous hydrochloric acid and were able to isolate free amine **117**. However, only very low yields were achieved via this method and often the product was mixed with **120** resulting from reduction of the thioenamide. This mixture was inferred from a complicated ¹H NMR, low integration value for the protons of the thioenamide functional group, and the observed mass value for a reduced product.



Scheme 4.15. Isolation of free amine **117** mixed with reduced product **120**

Hydrazine forms diimide ($\text{HN}=\text{NH}$) over time, and this impurity has previously been noted to cause problematic reductions during Pht removal.⁹ Reduction by diimide has been avoided by introducing an excess of a sacrificial alkene. Indeed, including 2 equivalents of allyl alcohol in our reaction mixture prevented the occurrence of reduced product **120**. We carefully monitored the initial hydrazine attack via ^1H NMR, watching for the disappearance of a signal at 4.49 ppm corresponding to the valine α -proton in **62**, to determine both the best time to quench the reaction with acid and the minimum amount of hydrazine required to consume the starting material. With these insights we settled on the conditions shown in Scheme 4.16, using 1.8 equivalents of hydrazine and a reaction time of 1.5h, then cooling the reaction and acidifying with dilute, aqueous hydrochloric acid. This was followed by a work-up using aqueous sodium bicarbonate to neutralize the HCl and direct coupling with leucine to generate peptide **113** in 41% over the three steps, putting us a big step closer to our macrocyclization. However, the conditions for Tcp removal and peptide coupling led to partial erosion of the stereochemistry. Peptide **113** shows a 3:1 ratio of diastereomeric species, despite entering the reaction with only 8-15% of the undesired diastereomer.



Scheme 4.16. Successful Tcp removal and coupling of Boc-Leu-OH

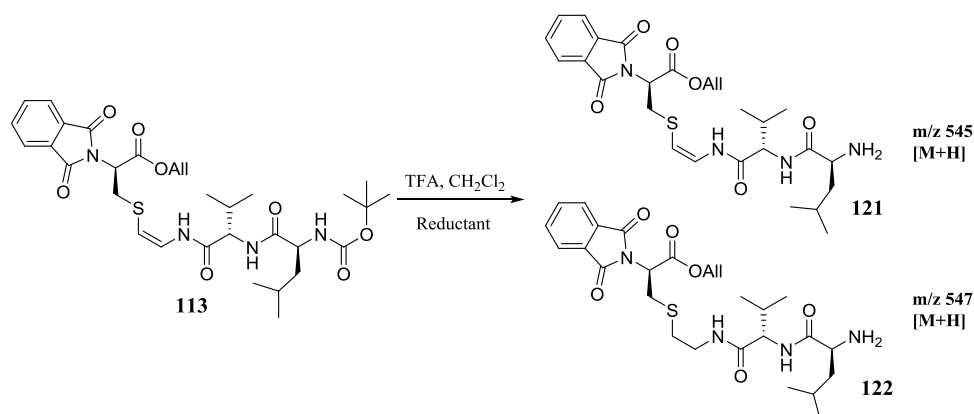
4.4. Acid and Amine Deprotection

The next step *en route* to macrocyclization was to remove the protecting groups at each terminus: the allyl ester and the Boc carbamate, revealing the acid and amine respectively. We investigated each of these reactions separately, in an effort to determine the optimal order of events.

4.4.1. Boc Removal

We began with removal of the Boc protection, using trifluoroacetic acid (TFA) and triethylsilane (TES) as a cation scavenger (Scheme 4.17). While the transformation readily took place, we again isolated a reduced variant of our desired product. This side product could only be isolated via RP-HPLC, showed no thioenamide protons, and electrospray mass spectrometry displayed an $[M+2]$ ion relative to desired free amine **121**. Triethylsilane is known to reduce double bonds, so this was the likely culprit at this step. Switching the cation scavenger to thioanisole) prevented this side reaction (Table 4.1). While no yield was recorded at this point, the crude HPLC trace and ^1H NMR clearly showed an improvement over triethylsilane.

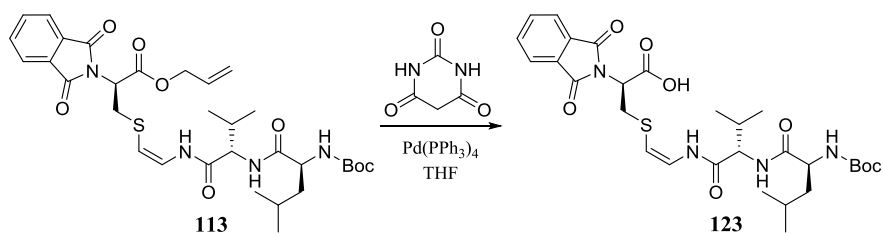
Table 4.1. Boc Removal



Entry	Reductant	Result
1	TES	Mix of 121 & 122
2	thioanisole	121 only

4.4.2. Allyl Ester Removal

We probed removal of the allyl ester from fully protected peptide **113**. Conventional conditions for allyl ester removal are catalytic palladium (0) with an allyl scavenger, often morpholine or barbituric acid. We observed the desired transformation, under traditional conditions. However, the RP-HPLC trace showed two major products and recovery of desired free acid from the instrument was very low.



Scheme 4.17. Allyl removal with barbituric acid

The major side product had a strikingly similar structure to desired acid **123** according to NMR, though the mass was m/z 16 amu higher than the desired free acid. This led us to conclude that our compound had been oxidized, with by far the most likely position being the sulfur atom of our thioenamide (Figure 4.2).

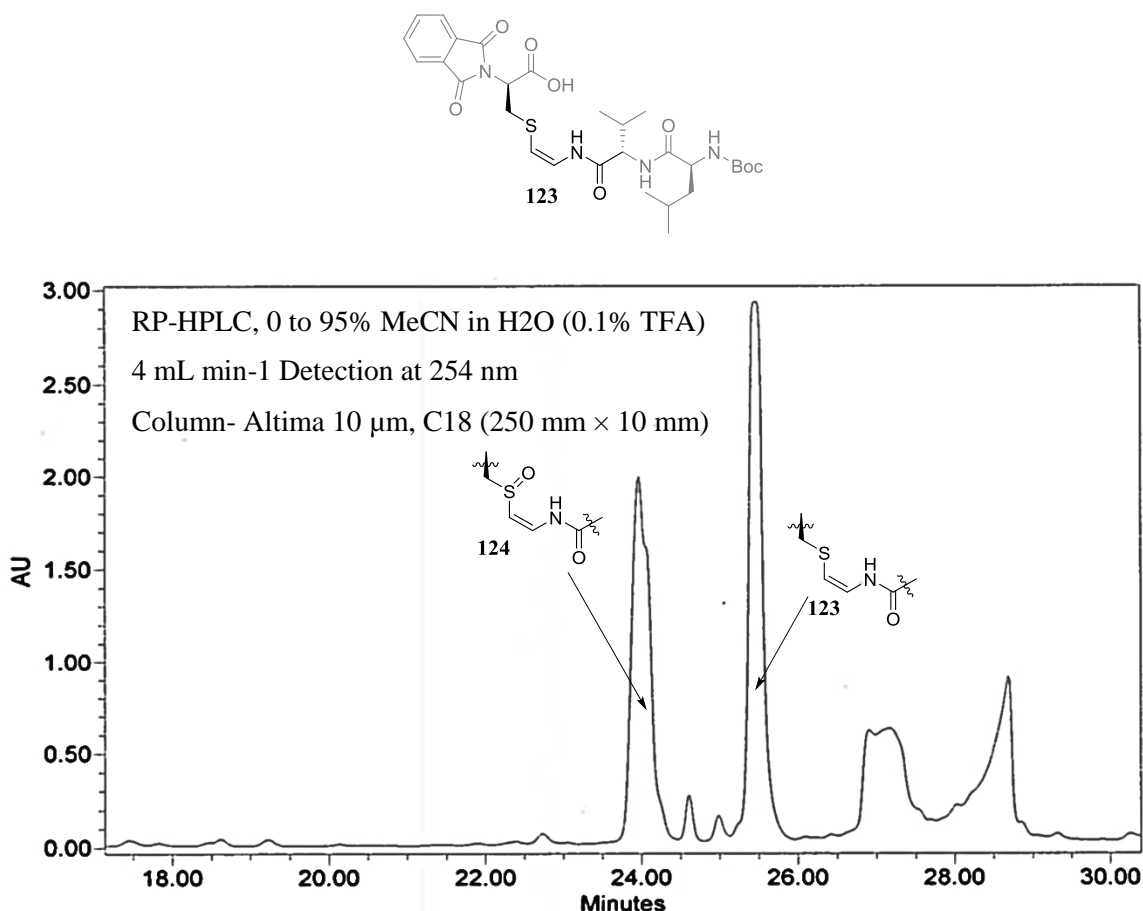
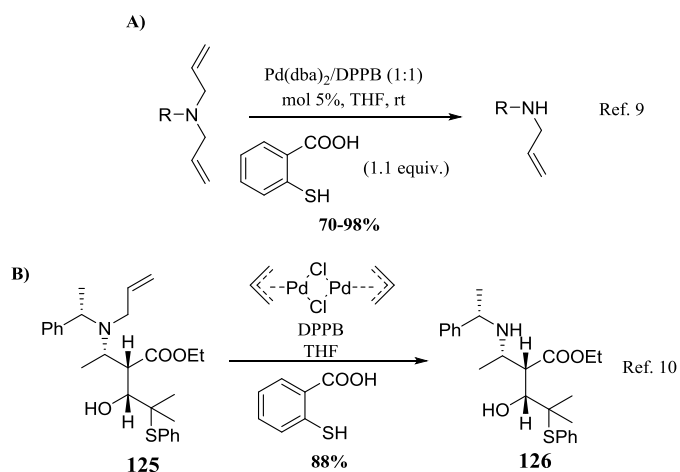


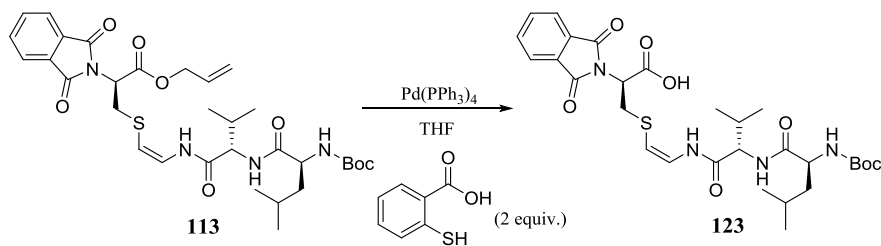
Figure 4.2. Separation of **123** and oxidized by product **124**

This oxidation product accounted for roughly 50% of the material, so it was imperative that we shut down this reaction pathway. Inspired by the sacrificial olefin used in our Tcp removal, we sought a reagent that could be oxidized preferentially over our desired compound. There were reports of thiosalicylic acid being used as an allyl scavenger during this type of transformation with allyl amines (Scheme 4.18).^{10,11}



Scheme 4.18. Deallylations using thiosalicylic acid

We were hopeful that thiosalicylic acid could serve us as both an allyl scavenger and a sacrificial reductant when used in excess. Indeed, when this reagent was substituted for barbituric acid, we observed only trace amounts of oxidized thioenamide (Scheme 4.19).



Scheme 4.19. Allyl removal with thiosalicylic acid

4.5. Free Amino Acid Tripeptide

With both deprotection reactions optimized, for compatibility with the thioenamide functional group, it was now time to determine the most effective order of events to generate free amino acid peptide **127**. Either way, RP-HPLC was required for chromatographic purification, and the recovery was very low.

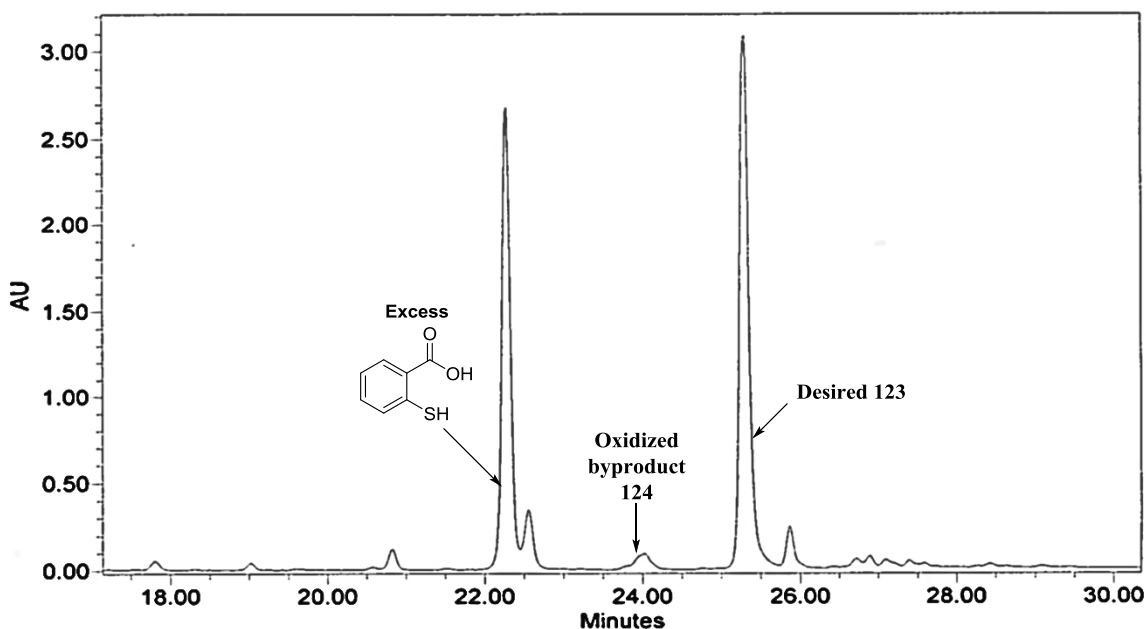
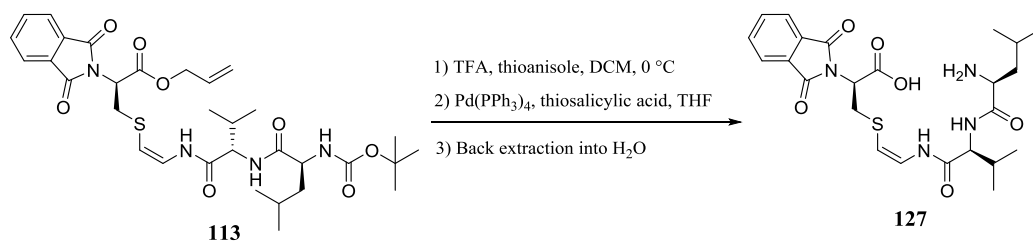


Figure 4.3. RP-HPLC chromatogram showing decrease in oxidized thioenamide

During an aqueous work-up, prior to RP-HPLC, we found that amino acid peptide **127** was almost completely retained in the aqueous layer. We back-extracted peptide **127** into the aqueous layer, making use of the compound's high water solubility. Freezedrying this extract gave remarkably clean peptide **127**, with some remaining thiosalicylic acid. With this semi-purification, we were able to remove both the Boc and allyl protecting groups and acquire peptide **127** in acceptable purity (Scheme 4.20).



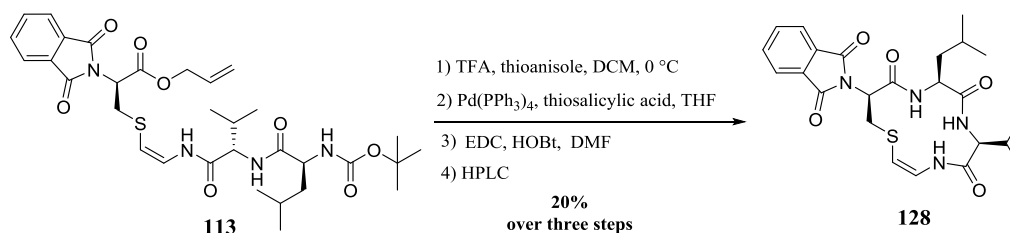
Scheme 4.20. Optimized liberation of free amino acid peptide **127**

4.6. Macrocycle

4.6.1. Macrolactamization

With linear peptide **127** in-hand, we were a single, intramolecular amide bond formation away from a phthalimido-capped cypemycin C-terminal ring. Although we had previously attempted macrocyclizations on the small amount of **127** isolated from RP-HPLC, no desired macrocycle had ever been observed. An increase in the amount of material from our optimized synthesis and purification of **127** breathed new life into this effort.

As expected, starting material concentration played a crucial role. When the reaction was run at a relatively high concentration (0.012 M in DMF), no desired macrocycle was observed. If more dilute conditions were used (0.002 M in DMF), then desired product was generated (Scheme 4.21).



Scheme 4.21. Synthesis of macrocycle **128**

Purification of macrocycle **128** was difficult via flash chromatography due to impurities that elute very closely. A high purity sample was obtained by RP-HPLC (Figure 4.4) in 20% yield of over three steps, with a single chromatographic purification.

4.6.2. Characterization

Full structural characterization was possible at this stage, with the use of mass spectrometry, ¹H NMR, COSY, and HSQC. All amino acids were accounted for, and we observed the correct mass. Figure 4.5 shows the full ¹H NMR with all peaks labeled.

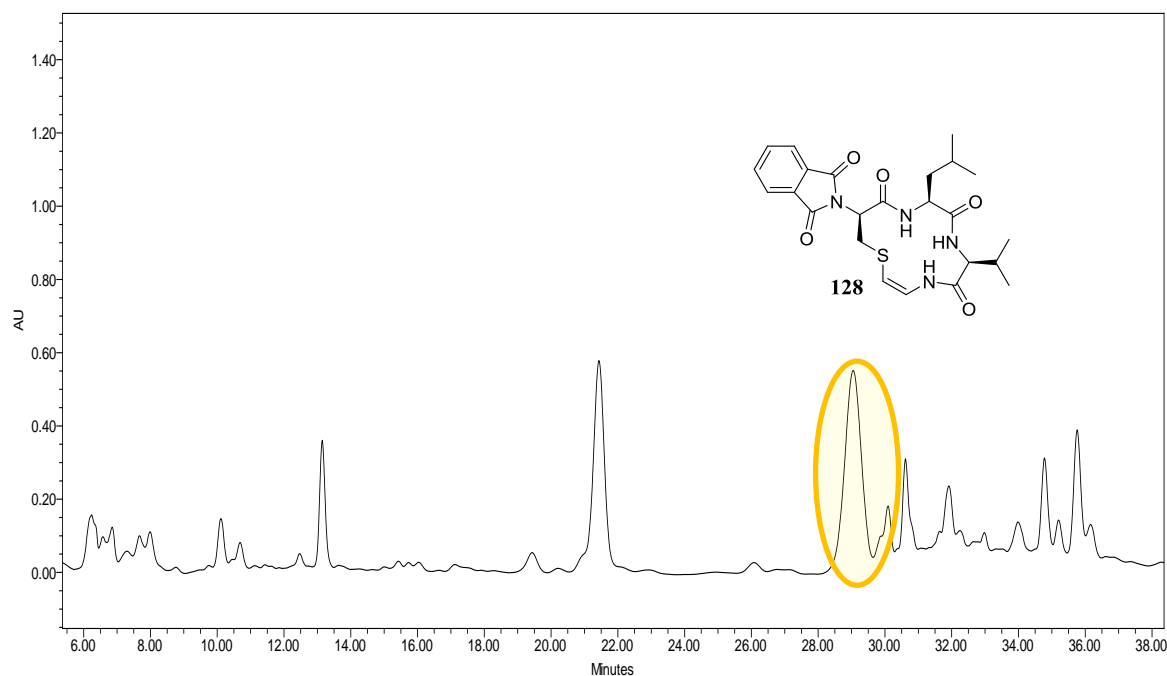


Figure 4.4. RP-HPLC chromatogram of crude macrocyclization product mixture

The coupling constants for the native cypemycin AviCys moiety were not reported,¹² so our synthetic material has afforded this data for the first time. We can plainly observe the coupling constants for the olefin and amide; 7.0 Hz and 10.8 Hz respectively. Additionally, our macrocyclization hints at a propensity for the peptide with the *D*-cysteine configuration in **127** to cyclize more readily than the undesired diastereomer with the *L*-cysteine. Though we entered into the cyclization with roughly 25% of the undesired Cys(Avi) stereoisomer in linear **127**, we have only observed a single diastereomer of **128**.

This is, to date, the first synthesis of a 13-membered AviCys-containing macrocycle. Hence, it is also the first synthesis of an *N*-capped cypemycin *C*-terminal ring. These facts afford us the opportunity to break ground on the characterization of such cyclic systems.

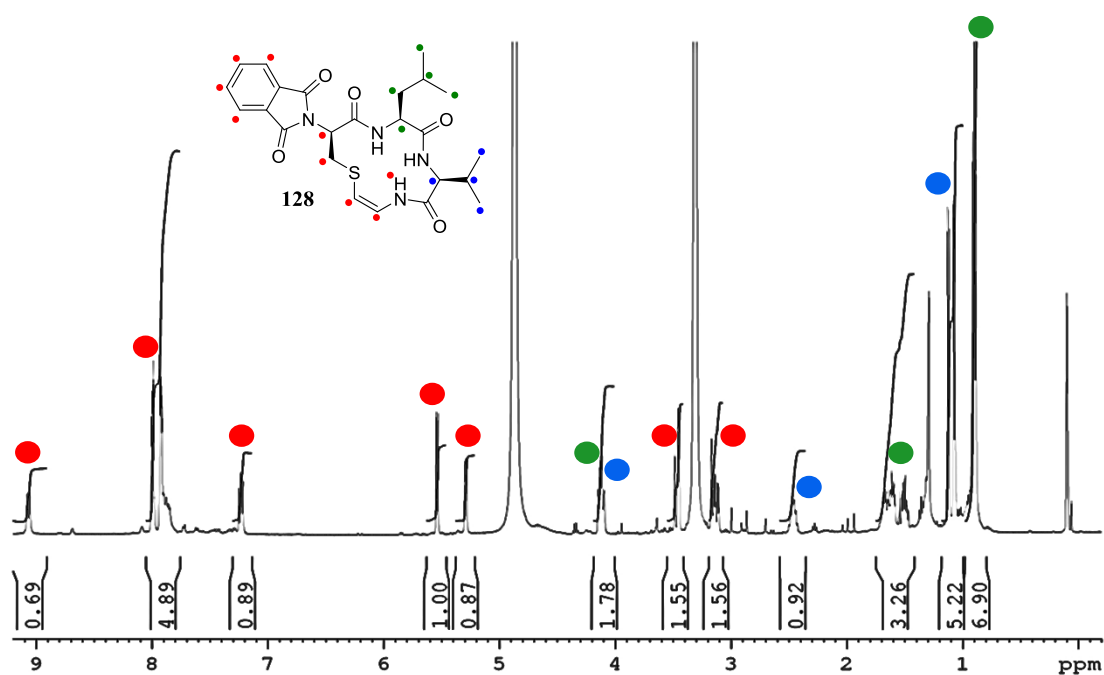


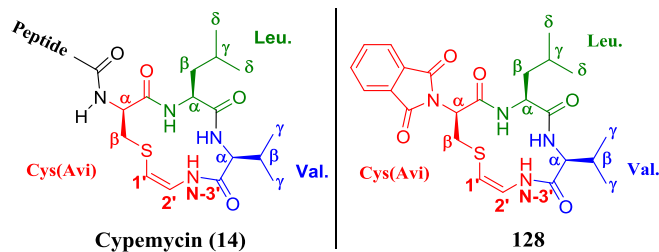
Figure 4.5. ¹H NMR spectrum of macrocycle **128** [See Table 4.2 for full assignments]

We compared the data for macrocycle **128** with reported values for the C-terminal ring of isolated cypemycin (Table 4.2). Our values for the leucine moiety match up nicely, though moderate differences exist in both the Cys(Avi) and valine residues. This difference can likely be explained by solvent effects and the electronic changes the phthalimido protection introduces, as well as the impact of the peptide tail in the native peptide.

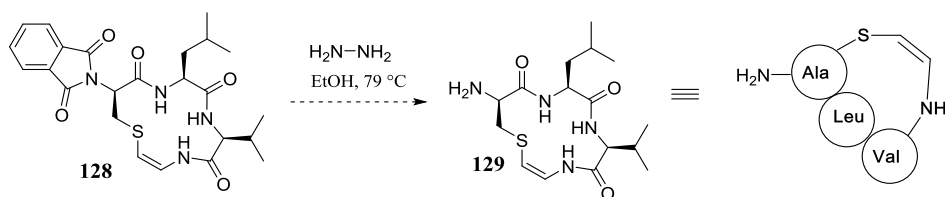
4.7. Future Work

Work on the detailed characterization of macrocycle **128** will continue. Specifically, we will use variable temperature NMR and NOESY to determine the preferred conformation. Variable temperature experiments will elucidate the hydrogen bonding of the amide protons when run in DMSO-d₆ or 10% D₂O in water. This information, along with NOESY correlation peaks, will help us to paint a full picture of the conformation in solution. We will also study the removal of the Pht group to liberate free amine **129** (Scheme 4.22).

Table 4.2. Comparison of macrocycle **128** NMR (CD₃OD, 500 MHz, 25 °C) with cypemycin
Ref. 12 (DMSO-d₆, 400 MHz, 30 °C)



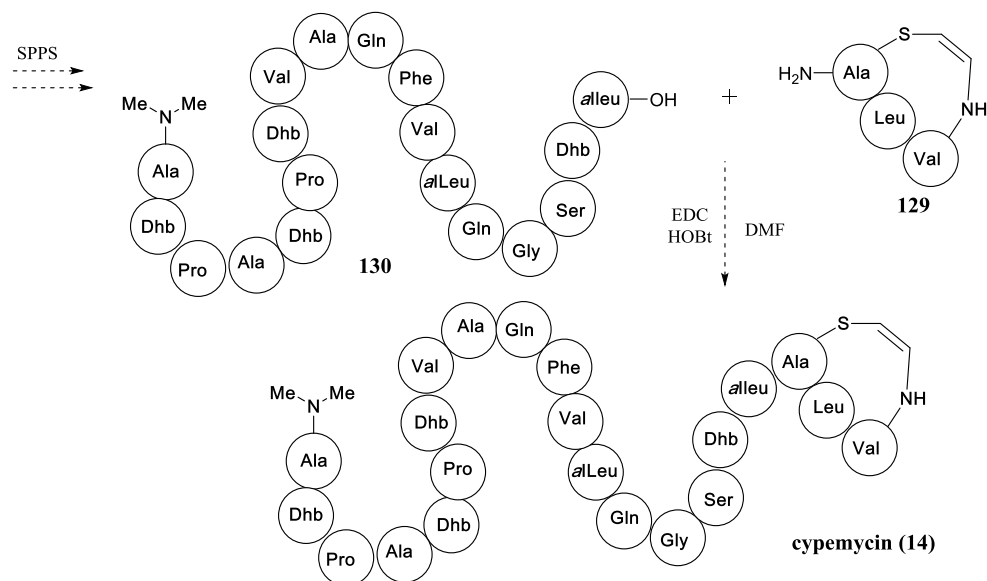
		Proton (ppm)		Carbon (ppm)	
		Ref. 12	128	Ref. 12	128
Cys(Avi)	CON-H	7.65	N/A	169.42	Unknown
	α	4.64	5.29	52.05	55.16
	β	3.08, 2.85	3.47, 3.12	37.04	37.15
	1'	5.47	5.54	99.84	101.27
	2'	7.11	7.23	132.09	134.42
	N-3'	8.7	9.07	N/A	N/A
Leu	CON-H	7.46	Unknown	172.38	Unknown
	α	3.93	4.13	54.9	57.1
	β	1.63, 1.48	1.63, 1.51	39.38	40.61
	γ	1.63	1.67	24.2	25.7
	δ	0.93	0.91	22.27	22.82
		0.84	0.89	21.69	21.61
Val	CON-H	7.71	Unknown	169.01	Unknown
	α	3.92	4.11	59.57	63.05
	β	2.05	2.45	28.51	30.31
	γ	0.78	1.12	18.9	19.82
		0.89	1.07	19.47	19.51



Scheme 4.22. Removal of Pht

The above experiments will be followed by the total synthesis of cypemycin (Scheme 4.23). Solid phase peptide synthesis (SPPS) will be used to generate 18-mer peptide **130**. This

will then be coupled to free amine macrocycle **129**, completing the first total synthesis of cypemycin. This would represent the first total synthesis of any AviCys-containing peptide to date.



Scheme 4.23. Total synthesis of cypemycin

4.8. Experimental Procedures

4.8.1. General Methods As is 2.7.1

4.8.2. Formation of thioenamide **87** (Scheme 4.5)

Dipeptide thioenamide (±)-87. Boric acid (37 mg, 0.60 mmol, 5.0 equiv.) and Fmoc(Bn)-Ala-NH₂ (**85**) (48 mg, 0.120 mmol, 1.0 equiv.) were added to a solution of (±)-**56** (40 mg, 0.120 mmol, 1.0 equiv.) in xylenes (40 mL). This mixture was brought to reflux for 24 h. Additional Fmoc(Bn)-Ala-NH₂ (**85**) (48 mg, 1.0 equiv.) was added and the reaction was continued at reflux for an additional 16 h. The mixture was concentrated and the crude residue was subjected to flash chromatography, eluting with 5:1 hexanes-EtOAc to isolate **Z-87** (45 mg, 52%) as a yellow solid and a mixture of diastereomers at cysteine Cα. *R_f* 0.27 (2:1 hexanes-EtOAc). ¹H NMR (400 MHz, CDCl₃) δ 1.30 (br s, 3H), 3.33-3.53 (m, 2H), 4.17 (dd, *J* = 12.3, 6.0 Hz, 1H), 4.30 (d,

$J = 6.0$ Hz, 0.5H), 4.34 (d, $J = 6.0$ Hz, 0.5H), 4.40-4.73 (m, 4H), 4.64 (d, $J = 5.7$ Hz, 2H), 4.99 (dd, $J = 10.6, 4.2$ Hz, 1H), 5.17-5.25 (m, 2H), 5.29 (br s, 2H), 5.78-5.89 (m, 1H), 6.83 (app. t, $J = 8.1$ Hz, 0.5H), 6.93 (app. t, $J = 8.0$ Hz, 0.5H), 7.05-7.54 (m, 10H), 7.67-7.73 (m, 4H), 7.82 (d, $J = 2.9$ Hz, 1H), 7.89 (d, $J = 3.0$ Hz, 1H), 8.29 (br s, 1H); ^{13}C NMR (125 MHz, CDCl_3) δ 14.5, 29.8, 33.5, 47.3, 52.4, 55.9, 66.9, 68.1, 101.0, 119.2, 120.1, 123.8, 125.0, 125.1, 127.2, 127.8 (2C), 128.6, 128.8, 131.3, 131.4, 131.7, 131.8, 131.9, 134.3, 134.4, 134.5 (2C), 137.9, 138.1, 141.4, 143.7, 143.8 (2C), 143.9, 167.5, 167.6, 167.7. HRMS (ESI) calcd for $\text{C}_{41}\text{H}_{38}\text{N}_3\text{O}_7\text{S}$ ($\text{M}+\text{H}$) $^+$: calcd 716.2425; obsd 716.2420.

4.8.3. Synthesis of thioenamide (\pm)-**89** (Scheme 4.6)

Dipeptide thioenamide (\pm)-89**.** Boric acid (19 mg, 0.32 mmol, 5.0 equiv.) and Fmoc(Bn)-Ala-NH₂ (**88**) (29 mg, 0.06 mmol, 1.0 equiv.) were added to a solution of (\pm)-**56** (21 mg, 0.06 mmol, 1.0 equiv.) in xylenes (21 mL). This mixture was brought to reflux for 24 h. Additional Fmoc(PMB)-Ala-NH₂ (**88**) (29 mg, 1.0 equiv.) was added and the reaction was continued at reflux for an additional 16 h. The mixture was concentrated and the crude residue was subjected to flash chromatography, eluting with 5:1 hexanes-EtOAc to isolate **Z-89** (23 mg, 47%) as a yellow solid and a mixture of diastereomers at cysteine C α . R_f 0.60 (1:1 hexanes-EtOAc). ^1H NMR (500 MHz, CDCl_3) δ 0.53 (d, $J = 4.9$ Hz, 1.5H), 0.59 (d, $J = 4.4$ Hz, 1.5H), 0.87 (d, $J = 5.8$ Hz, 1.5H), 0.91 (d, $J = 4.7$ Hz, 1.5H), 2.46 (br s, 1H), 3.19 (d, $J = 14.5$ Hz, 0.25H), 3.19 (d, $J = 14.6$ Hz, 0.25H), 3.22-3.65 (m, 2.5H), 3.76 (s, 3H), 4.02 (d, $J = 15.3$ Hz, 0.5H), 4.11 (d, $J = 15.3$ Hz, 0.5H), 4.15-4.24 (m, 1H), 4.26 (d, $J = 15.3$ Hz, 0.5H), 4.32 (d, $J = 15.3$ Hz, 0.5H), 4.57 (d, $J = 4.7$ Hz, 1H), 4.60-4.74 (m, 3H), 4.95-5.07 (m, 1H), 5.16-5.32 (m, 3H), 5.80-5.91 (m, 1H), 6.70 (d, $J = 6.4$ Hz, 2H), 6.86 (d, $J = 6.4$ Hz, 1H), 6.79-6.97 (m, 1H), 7.23-7.32 (m, 2H), 7.34-7.41 (m, 1H), 7.44-7.57 (m, 1H), 7.60-7.95 (m, 7H), 8.74 (br s, 0.5H), 8.95 (br s, 0.5H); ^{13}C NMR

(125 MHz, CDCl₃) δ 19.3, 20.1, 27.0, 29.8, 30.6, 33.3, 33.5, 40.6, 47.5, 50.8, 52.2, 52.4, 53.6, 55.3, 66.8, 66.9, 67.5, 101.1, 101.4, 113.8 (2C), 119.2 (2C), 120.1 (2C), 123.8 (2C), 123.9, 124.9 (2C), 127.3, 127.8, 128.1, 128.3, 129.5, 129.6, 131.2, 131.3, 131.8, 134.3, 134.4, 134.5, 141.5, 141.6, 143.9, 144.0, 158.9, 159.0, 167.5 (2C), 167.6 HRMS (ESI) calcd for C₄₄H₄₄N₃O₈S (M+H)⁺: calcd 774.2844; obsd 774.2843.

4.8.4. Synthesis of methylene-bridged “dimer” **92** (Scheme 4.7)

Methylene-bridged dimer 92. DBU (3.8 μ L, 3.8 mg, 0.025 mmol, 1.5 equiv.) was added to a solution of thioenamide **90** (13 mg, 0.0168 mmol, 1.0 equiv.) in DCM (5 mL) at 0 °C. After 4 h, piperidine (8.3 μ L, 7.2 mg, 0.084 mmol, 5.0 equiv.) was added dropwise and the solution was immediately concentrated. The residue was subjected to flash chromatography, eluting with 5:1→3:1 hexanes-EtOAc to isolate **92** (4 mg, 40%) as a colorless solid. *R_f* 0.38 (2:1 hexanes-EtOAc). ¹H NMR (500 MHz, CDCl₃) δ 0.87 (d, *J* = 7.0 Hz, 6H), 0.96 (d, *J* = 7.0 Hz, 6H), 2.14 (sept, *J* = 4.4 Hz, 2H), 3.06 (d, *J* = 4.4 Hz, 2H), 3.59 (d, *J* = 12.7 Hz, 2H), 3.73 (d, *J* = 12.7 Hz, 2H), 3.80 (s, 6H), 3.83 (s, 2H), 5.45 (d, *J* = 7.5 Hz, 2H), 6.87 (d, *J* = 8.6 Hz, 4H), 7.15 (dd, *J* = 11.7, 7.5 Hz, 2H), 7.28 (d, *J* = 8.6 Hz, 4H), 9.62 (d, *J* = 11.7 Hz, 2H); ¹³C NMR (125 MHz, CDCl₃) δ 17.9, 19.7, 31.6, 40.3, 53.4, 55.4, 67.8, 100.9, 114.1, 127.6, 129.7, 131.4, 159.1, 171.6. HRMS (ESI) calcd for C₃₁H₄₅N₄O₄S₂ (M+H)⁺: calcd 601.2877; obsd 601.2877.

4.8.5. Synthesis of “false peptide” **116** from stalled Tcp removal (Scheme 4.12)

“False Peptide” 116. Hydrazine (1.1 μ L, 1.1 mg, 0.024 mmol, 1.1 equiv.) was added to a solution of thioenamide (\pm)-**62** (15 mg, 0.0214 mmol, 1.0 equiv.) in DMF (500 μ L). In a separate vessel, EDC (3.3 mg, 0.0214 mmol, 1.0 equiv.) and HOBt (3.3 mg, 0.214 mmol, 1.0 equiv.) were added sequentially to a solution of Boc-L-Leu-OH (5.4 mg, 0.0214 mmol, 1.0 equiv.) in DMF (400 μ L). After 30 min, the thioenamide solution was added dropwise to the

activated acid and allowed to stir under N₂ for 16 h. The mixture was diluted with EtOAc (100 mL) and washed with 5% aq. citric acid (100 mL). The aqueous layer was extracted a second time with EtOAc (75 mL) and the organic layers were combined, washed with brine (50 mL), filtered through MgSO₄, concentrated, and the residue purified by flash chromatography eluting with 0.5->2% methanol in DCM to isolate “false peptide” **116** as a yellow oil (9 mg, 46%). *R_f* 0.26 (5% methanol in DCM). ¹H NMR* (500 MHz, CDCl₃) δ 0.82-1.05 (m, 12H, obscured by impurity), 1.27-1.40 (m, 1H, obscured by impurity), 1.44 (s, 9H), 1.53-1.67 (m, 2H, obscured by impurity), 2.00-2.25 (m, 1H), 3.42-3.61 (m, 2H), 4.05-4.26 (m, 1H), 4.49 (d, *J* = 6.3 Hz, 0.3H), 4.52 (d, *J* = 6.3 Hz, 0.3H), 4.57 (br s, 0.3H), 4.66 (d, *J* = 5.5 Hz, 2H), 5.03-5.17 (m, 1H), 5.19 (d, *J* = 10.5 Hz, 1H), 5.28 (dt, *J* = 17.2, 1.5 Hz, 1H), 5.38 (d, *J* = 7.8 Hz, 0.5H), 5.40 (d, *J* = 7.8 Hz, 0.5H), 5.84-5.94 (m, 1H), 6.78-7.00 (m, 1H), 7.82-7.94 (m, 4H); ¹³C NMR (125 MHz, CDCl₃) δ 18.6, 19.9, 22.0, 23.4, 25.6, 25.8, 28.7, 28.8, 30.1, 30.8, 31.6, 40.2, 42.3, 53.1, 67.6, 80.6, 118.9, 124.5, 124.7, 124.8, 132.9, 135.7, 135.9, 169.0, 169.3.

**Contains multiple diastereomers and impurities*

4.8.6. Tcp removal and synthesis of thioenamide embedded peptide 113

Tripeptide 113. Allyl alcohol (3.1 μL, 2.7 mg, 0.046 mmol, 2.0 equiv.) and hydrazine (2.1 mg, 2.0 μL, 0.041 mmol, 1.8 equiv.) were added to a solution of (+) **62** (16 mg, 0.023 mmol, 1.0 equiv.) in ethanol (3.0 mL). The solution was brought to reflux and stirred for 1.5 h. Aqueous HCl (0.5 M, 229 μL, 5.0 equiv.) was added and the solution was allowed to cool to rt and stir for 16 h. The mixture was diluted with EtOAc (100 mL) and washed with 5% aq. NaHCO₃ (aq.) (100 mL). The aqueous layer was extracted a second time with EtOAc (75 mL) and the organic layers were combined, washed with brine (50 mL), filtered through MgSO₄ and concentrated.

A separate vessel, EDC (3.6 mg, 0.023 mmol, 1.0 equiv.) and HOBt (3.5 mg, 0.023 mmol, 1.0 equiv.) were added to a solution of Boc-Leu-OH (5.7 mg, 0.023 mmol, 1.0 equiv.) in DMF (700 μ L) and stirred for 30 min. The crude concentrate from the Tc_p removal was dissolved in DMF (500 μ L) and added dropwise to the activated Boc-Leu-OH solution and left to stir under N₂ for 16 h. The mixture was diluted with EtOAc (100 mL) and washed with H₂O (100 mL). The aqueous layer was extracted a second time with EtOAc (75 mL) and the organic layers were combined, washed with brine (50 mL), filtered through MgSO₄, concentrated, and the residue purified by flash chromatography eluting with 5:1->4:1 hexanes-EtOAc to isolate tripeptide **113** as a yellow oil (6 mg, 41%). *R*_f 0.46 (1:1 hexanes-EtOAc). ¹H NMR* (500 MHz, CDCl₃) δ 0.86 (d, *J* = 5.8 Hz, 3H), 0.88 (d, *J* = 6.1 Hz, 3H), 0.94 (d, *J* = 6.8 Hz, 3H), 0.98 (d, *J* = 6.9 Hz, 3H), 1.45 (s, 9H), 1.46-1.53 (m, 1H), 1.55-1.84 (m, 2H), 2.18-2.37 (m, 1H), 3.43 (d, *J* = 7.3 Hz, 1H), 3.46 (dd, *J* = 13.5, 10.6 Hz, 1H), 4.04-4.21 (m, 1H), 4.54 (dd, *J* = 8.6, 5.2 Hz, 1H), 4.64-4.68 (m, 2H), 4.84-4.94 (m, 1H), 4.96 (app. t, *J* = 7.4 Hz, 1H), 5.23 (ddd, *J* = 10.4, 2.3, 1.1 Hz, 1H), 5.25-5.32 (m, 2H), 5.81-5.91 (m, 1H), 6.88 (d, *J* = 7.2 Hz, 1H), 7.10 (dd, *J* = 11.0, 7.4 Hz, 1H), 7.71-7.98 (m, 4H), 8.24 (d, *J* = 10.7 Hz, 1H); ¹³C NMR* (125 MHz, CDCl₃) δ 17.5, 19.4, 22.2, 23.0, 24.8, 28.4, 31.1, 34.4, 40.7, 52.8, 53.3, 58.3, 67.0, 101.5, 119.3, 124.1, 129.4, 131.3, 131.7, 134.6, 134.7, 155.9, 167.5, 167.9, 168.9, 173.0. HRMS (ESI) calcd for C₃₂H₄₄N₄O₈S (M+H)⁺: calcd 645.2953; obsd 645.2963.

**Mixture of diastereomers in a 3:1 ratio, data provided for the major, desired D-cysteine diastereomer*

4.8.7. Boc removal, allyl removal, and macrocyclization to form **128** (Scheme 4.21)

Macrocycle 128. Thioanisole (3.7 μ L, 3.9 mg, 0.031 mmol, 2.0 equiv.) and TFA (1.2 mL, 50% v/v) were added to a solution of tripeptide **113** (10 mg, 0.016 mmol, 1.0 equiv.) in DCM (8 mL)

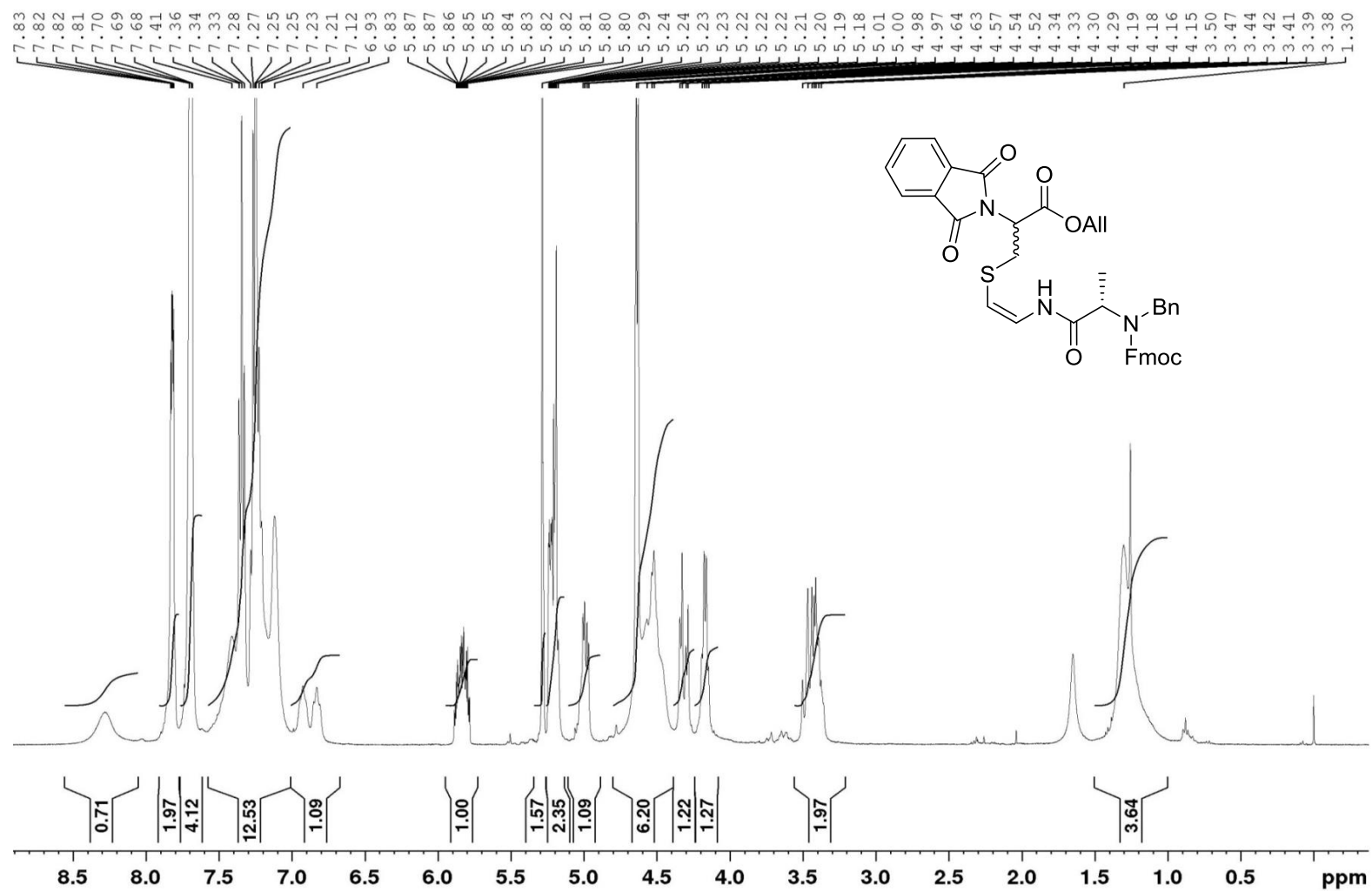
at 0 °C. This solution was stirred under N₂ for 1 h. The mixture was diluted with EtOAc (75 mL) and washed with saturated aq. NaHCO₃ (50 mL). The aqueous layer was extracted a second time with EtOAc (50 mL) and the organic layers were combined, washed with brine (50 mL), filtered through MgSO₄, concentrated.

The residue as dissolved in THF (3 mL) and, to this solution, was added thiosalicylic acid (4.8 mg, 0.031 mmol, 2.0 equiv.) and Pd(PPh₃)₄ (1.8 mg, 0.0016 mmol, 0.1 equiv.). The mixture was stirred under N₂ for 15 min, concentrated and the residue dissolved in H₂O (25 mL) and washed with CHCl₃ (25 mL). The aqueous extract was lyophilized to give crude amino acid tripeptide **127**.

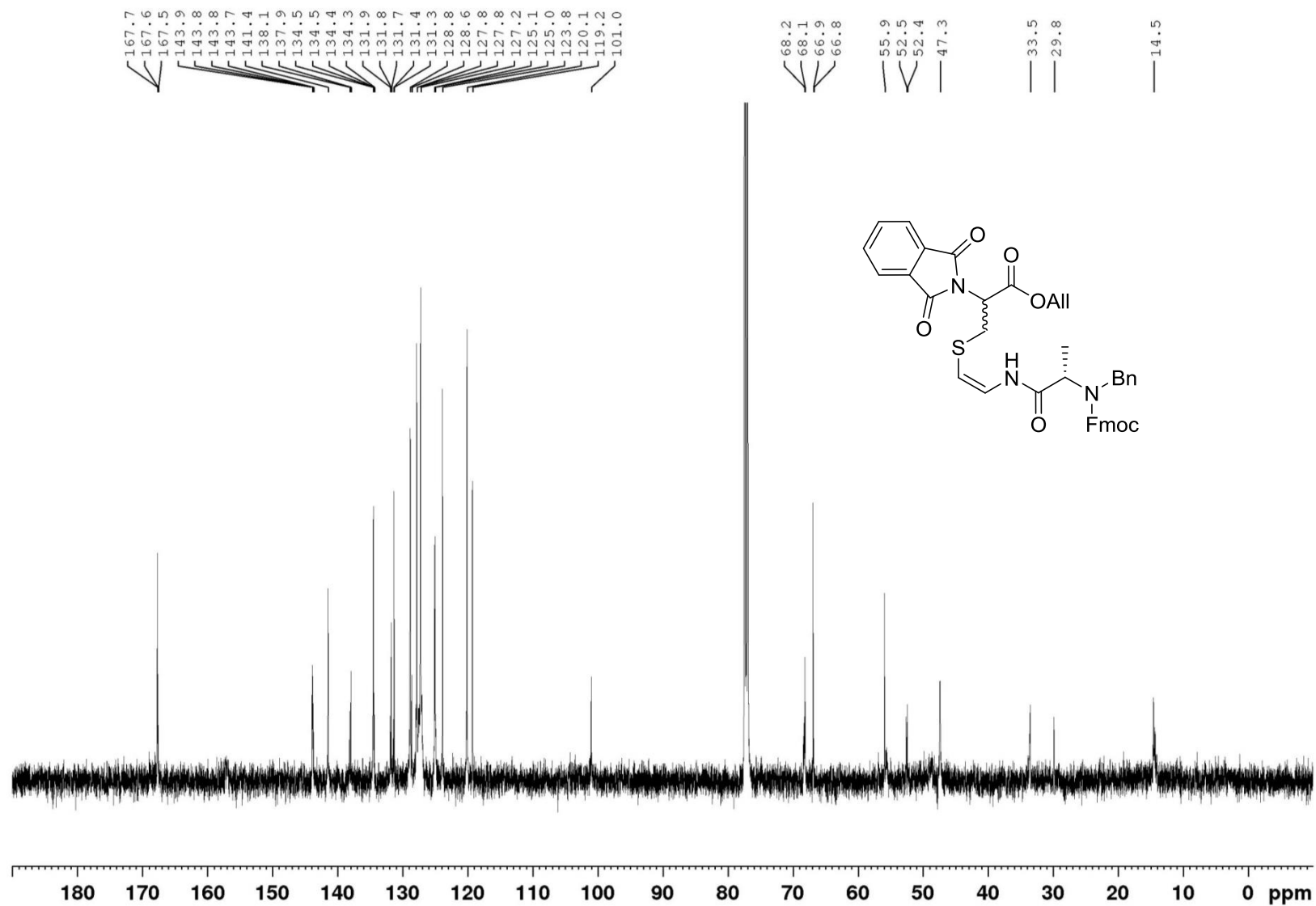
Crude tripeptide **127** was dissolved in DMF (7.8 mL). To this solution was added EDC (2.5 mg, 0.016 mmol, 1.0 equiv.) and HOBt (2.4 mg, 0.016 mmol, 1.0 equiv.). The reaction was stirred under N₂ for 16 h. Water (200 mL) was added to the mixture and the solution was lyophilized. The crude product was isolated by RP-HPLC (see conditions on p. 169) to give macrocycle **128** (1.5 mg, 20%) ¹H NMR (500 MHz, CD₃OD) δ 0.89 (d, *J* = 6.9 Hz, 3H), 0.91 (d, *J* = 6.8 Hz, 3H), 1.07 (d, *J* = 6.7 Hz, 3H), 1.12 (d, *J* = 6.6 Hz, 3H), 1.46-1.73 (m, 3H), 2.40-2.52 (m, 1H), 3.12 (dd, *J* = 14.6, 5.9 Hz, 1H), 3.43-3.50 (m, 1H), 4.07-4.17 (m, 2H), 5.29 (d, *J* = 5.2 Hz, 1H), 5.54 (d, *J* = 7.0 Hz, 1H), 7.23 (dd, *J* = 10.8, 7.1 Hz, 1H), 7.80-7.95 (m, 1H), 7.92 (dd, *J* = 5.4, 3.1 Hz, 2H), 8.00 (dd, *J* = 5.4, 3.1 Hz, 2H), 9.07 (d, *J* = 10.8 Hz, 1H); ¹³C NMR data was inferred from inverse detection in the HSQC experiment (125 MHz, CD₃OD) δ 19.5, 19.8, 21.6, 22.8, 25.7, 30.3, 37.0, 40.6, 55.1, 57.1, 63.0, 101.3, 124.5 (2C), 134.4, 135.9. HRMS (ESI) calcd for C₂₄H₃₁N₄O₅S (M+H)⁺: calcd 487.2010; obsd 487.1998.

4.9. NMR Spectra

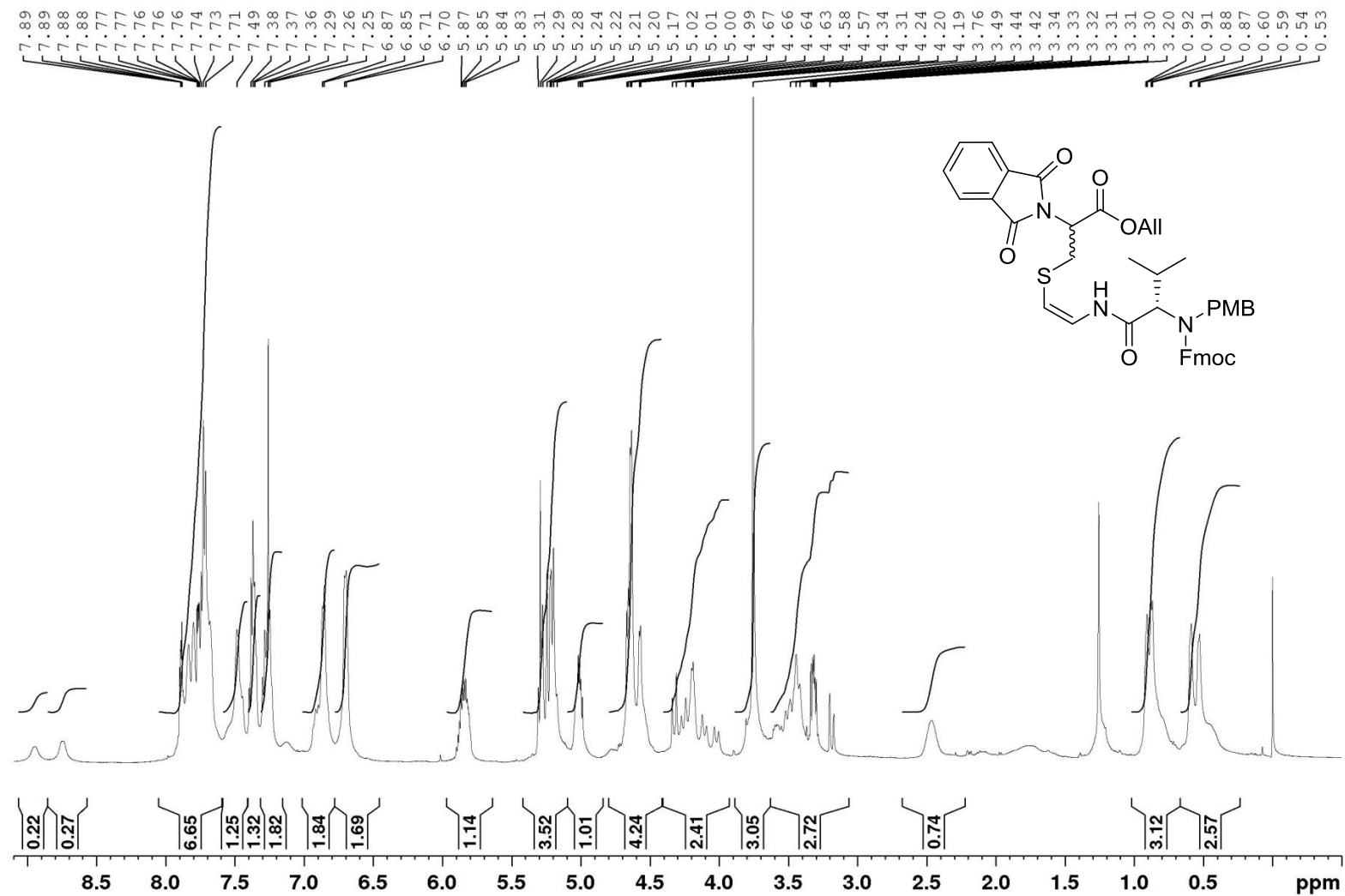
^1H NMR Compound **87**, CDCl_3 , 400 MHz



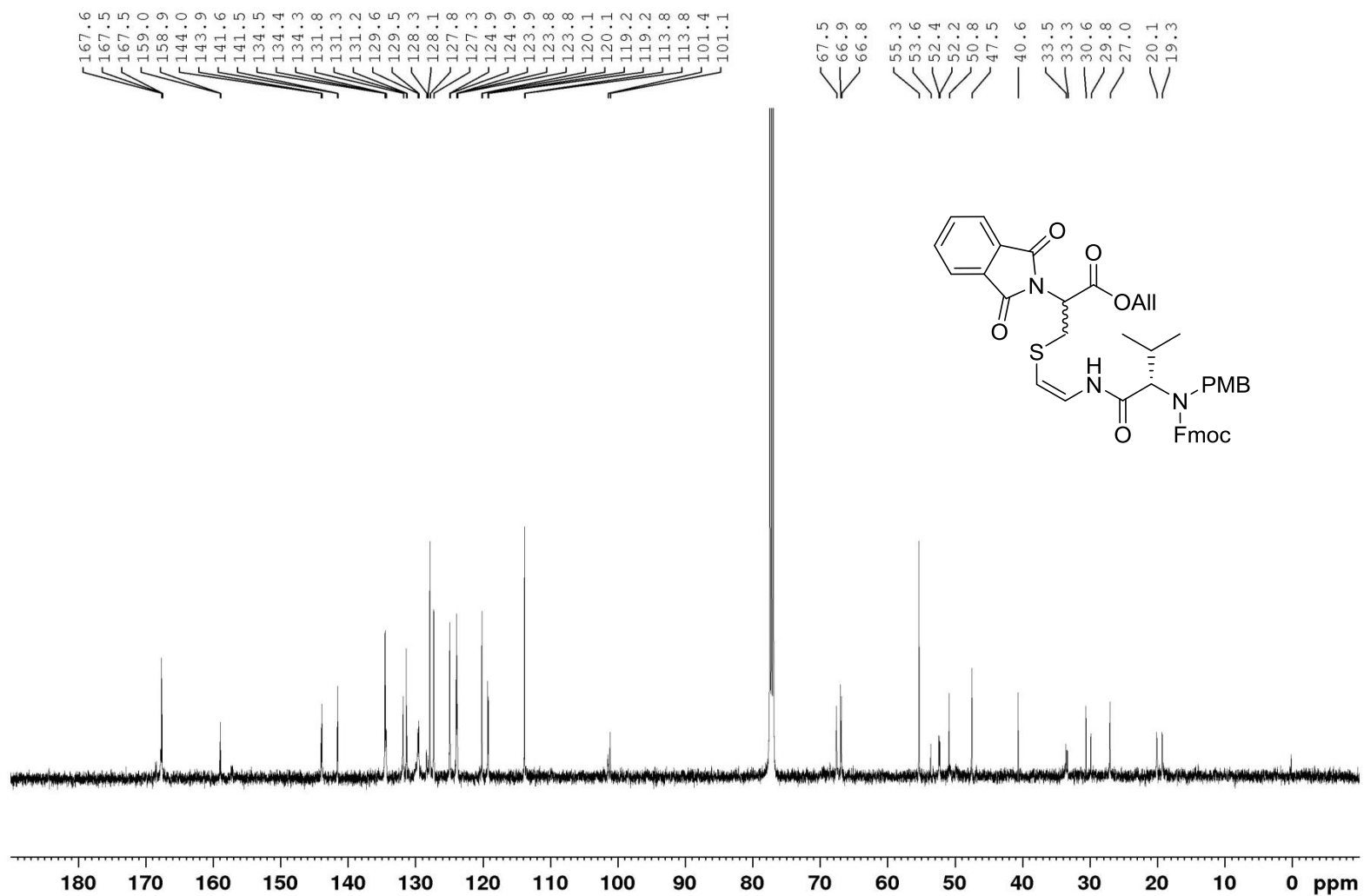
^{13}C NMR Compound **87**, CDCl_3 , 125 MHz



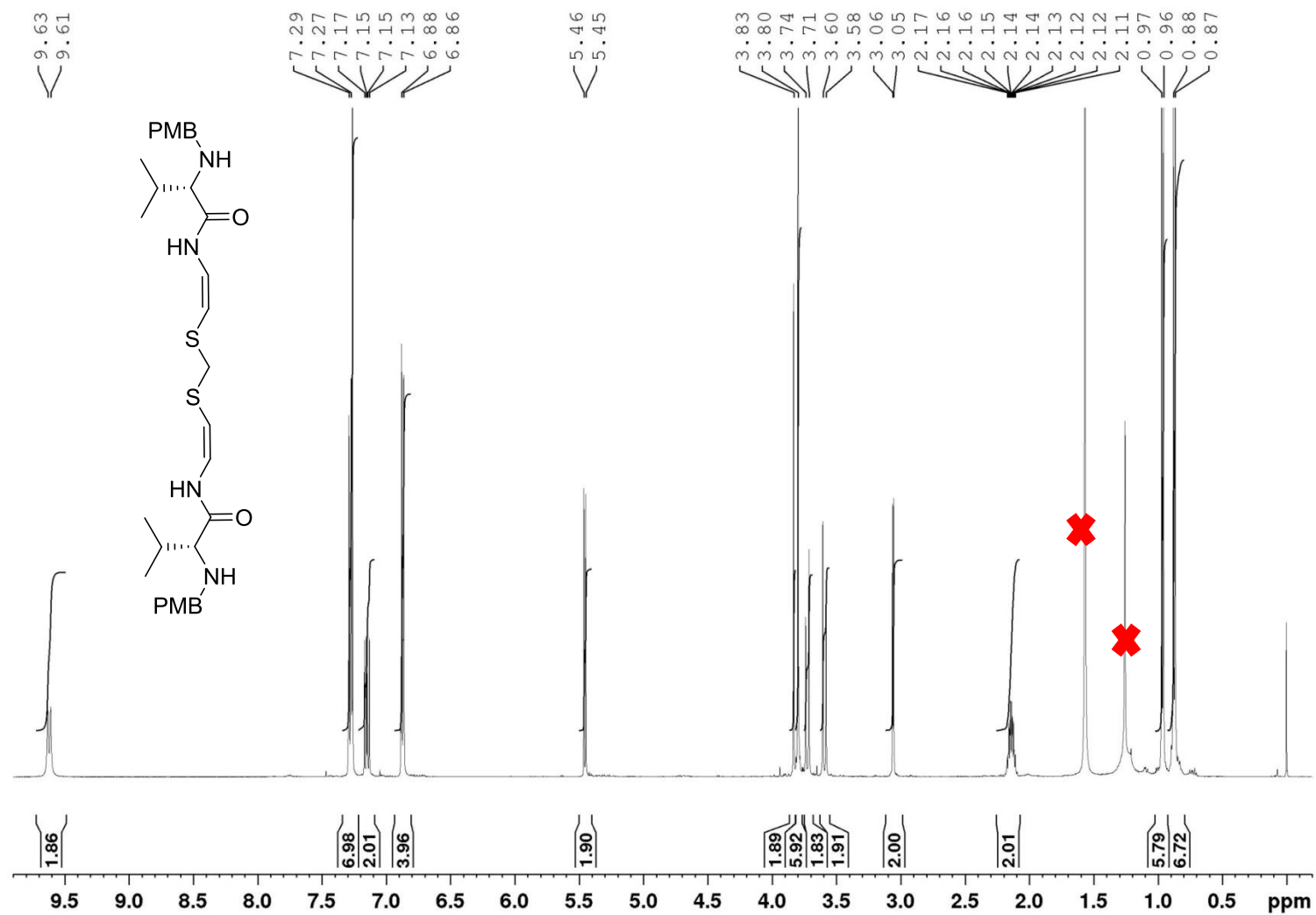
^1H NMR, Compound **89**, CDCl_3 , 500 MHz



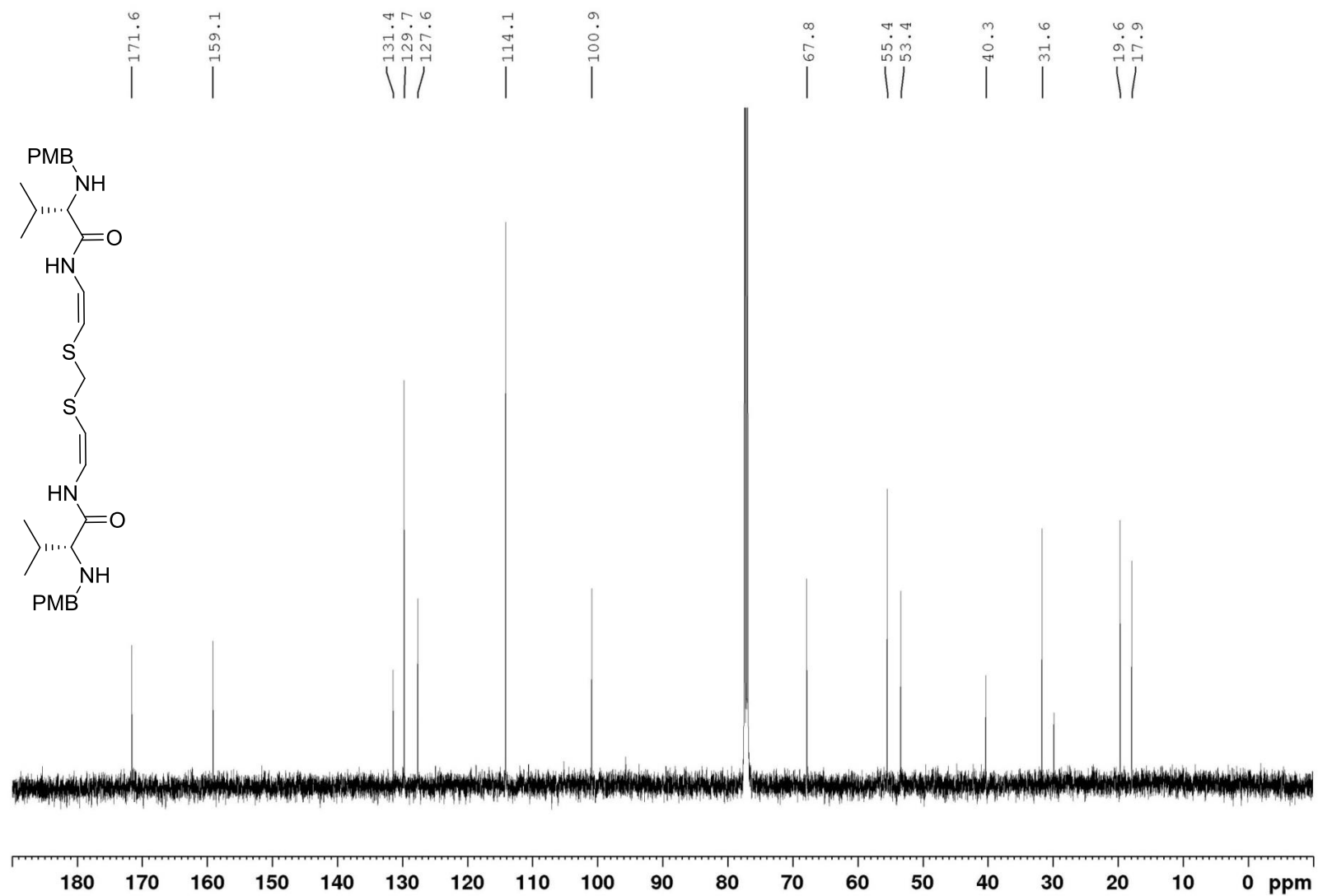
^{13}C NMR, Compound **89**, CDCl_3 , 125 MHz



^1H NMR, Compound **92**, CDCl_3 , 500 MHz

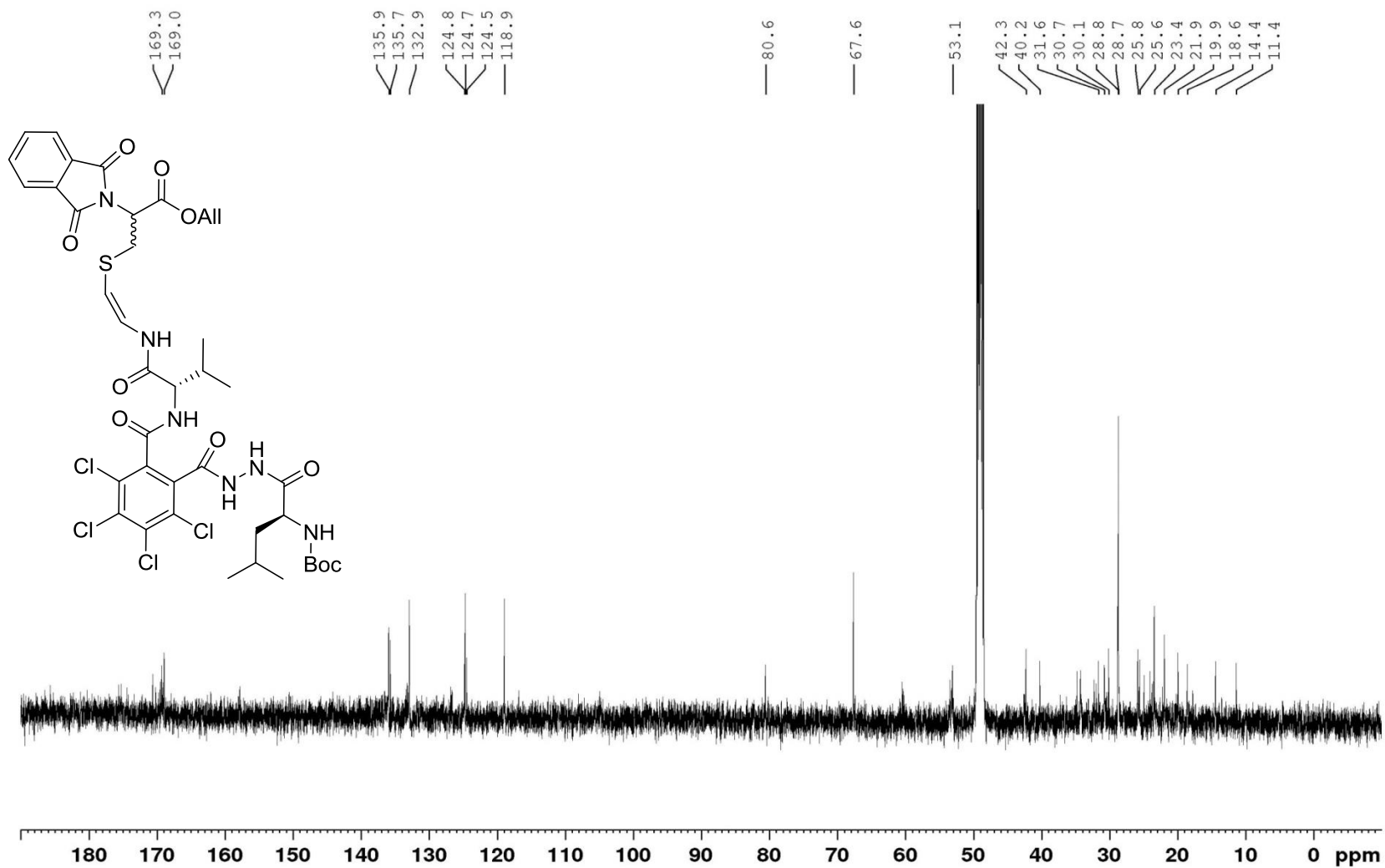


^{13}C NMR, Compound **92**, CDCl_3 , 125 MHz

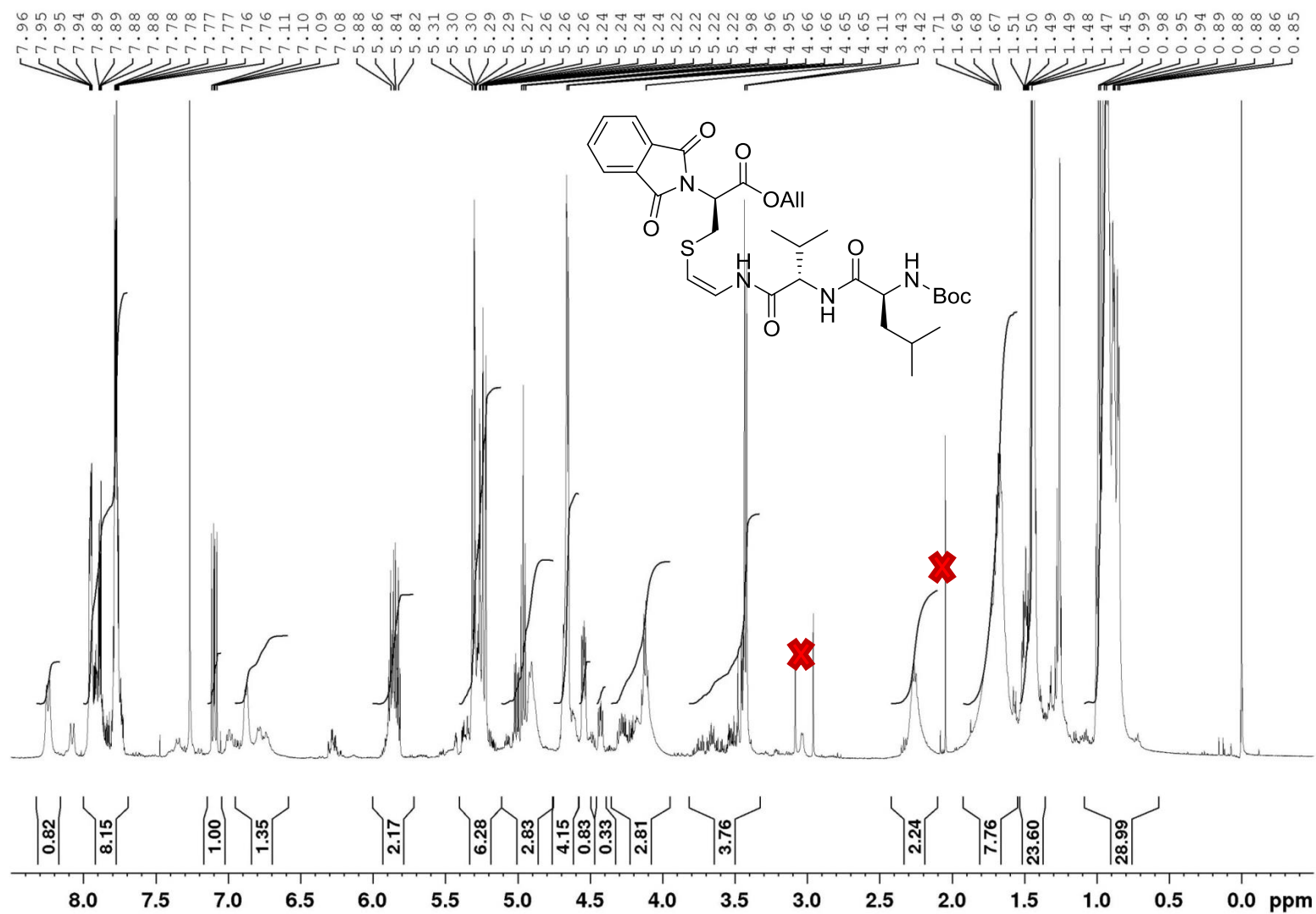


[illegible]

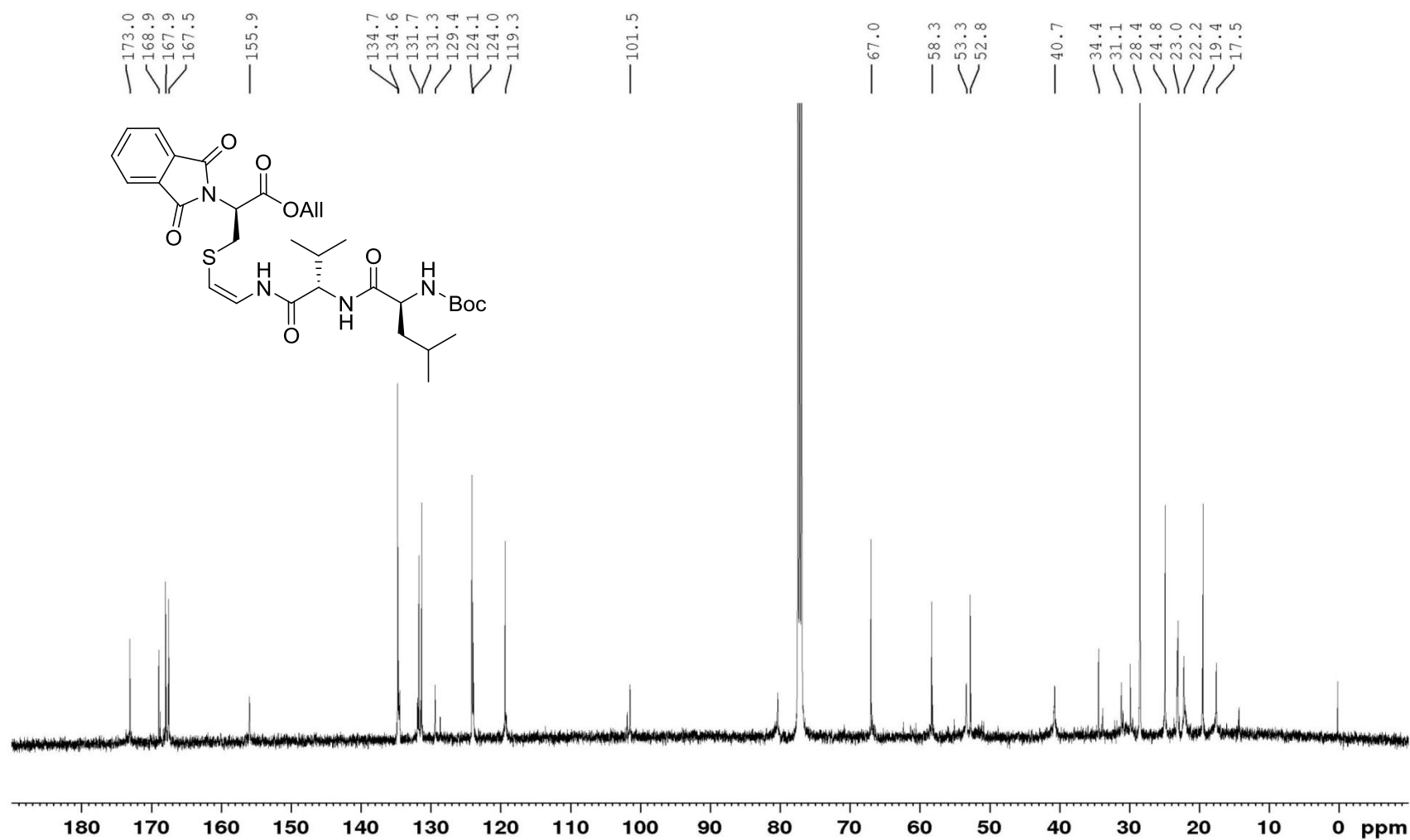
^{13}C NMR, Compound **116**, CD_3OD , 125 MHz



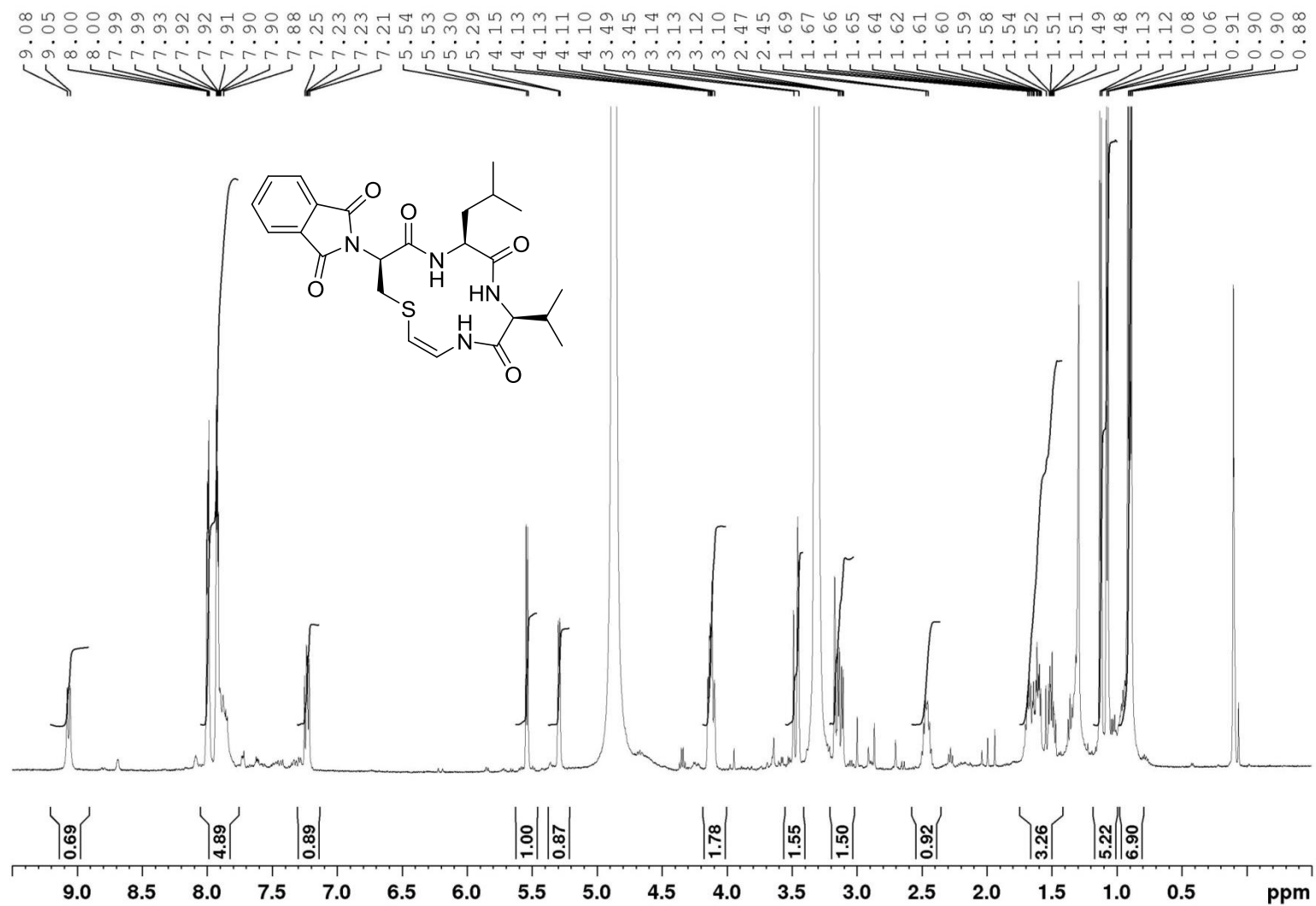
^1H NMR, Compound **113** (3:1 mixture of diastereomers), CDCl_3 , 500 MHz



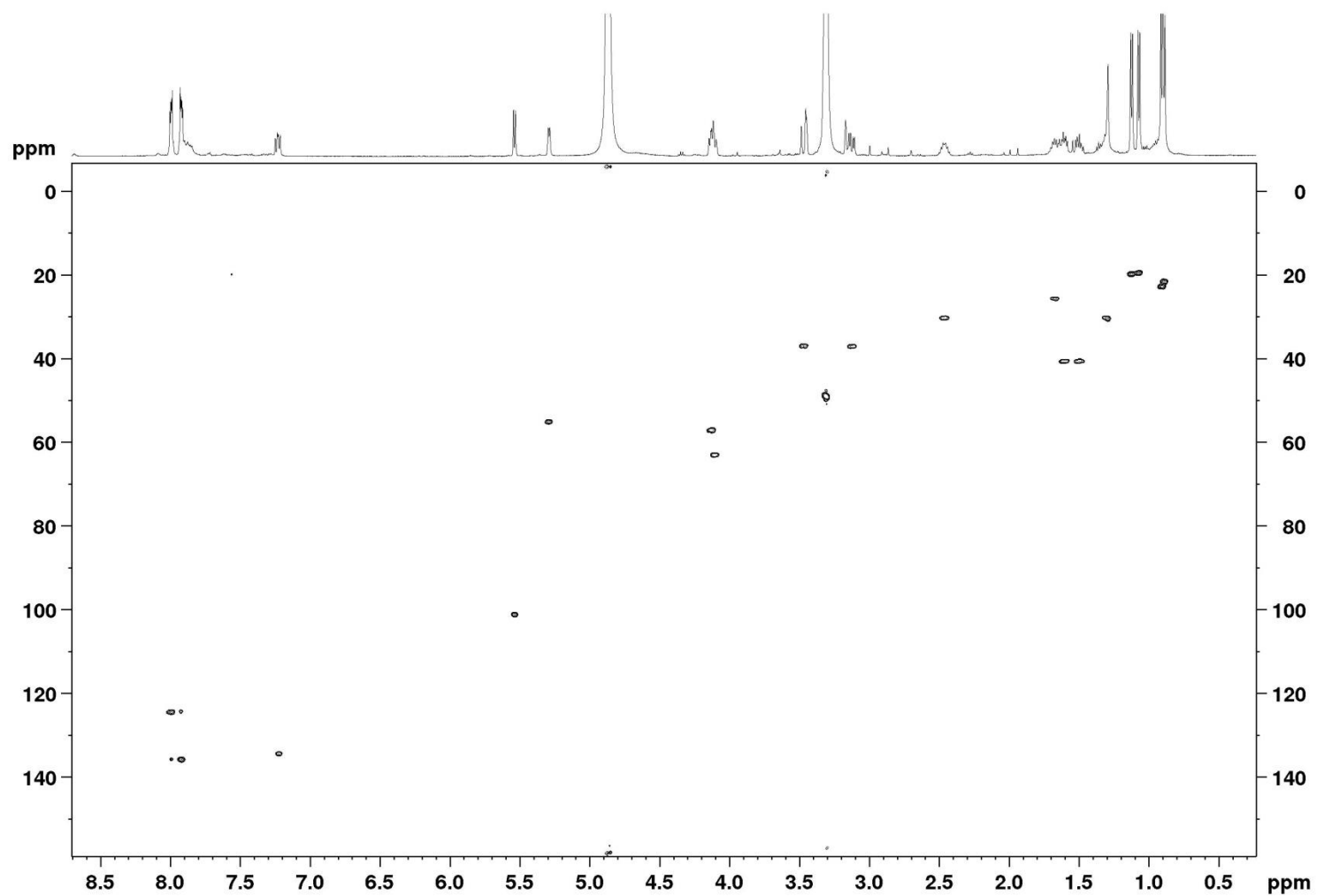
^{13}C NMR, Compound **113** (3:1 mixture of diastereomers), CDCl_3 , 125 MHz



^1H NMR, Compound **128**, CD_3OD , 500 MHz



HSQC NMR, Compound **128**, CD₃OD, 500 MHz



4.10. HPLC Chromatograms of Selected Compounds

4.10.1. Compounds **123** & **124** (jal-6-109)

Reverse phase HPLC following deallylation of

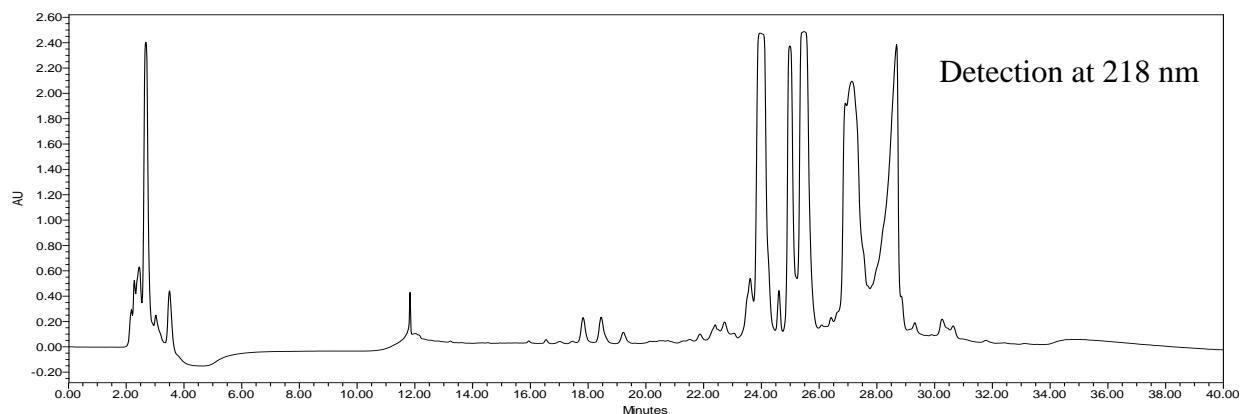
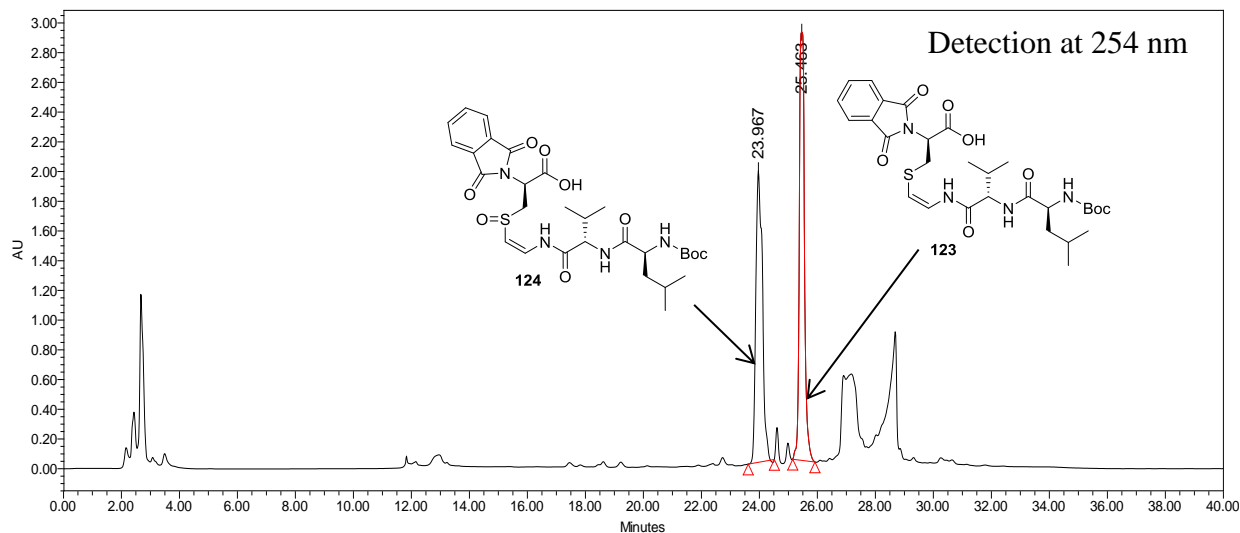
113 with barbituric acid as allyl scavenger

Altima® C18 10μ, 10 x 250 mm column

Method-Gradient

Time (min)	Flow (mL min ⁻¹)	H ₂ O %	MeCN %
0.01	4.00	100.0	0.0
5.00	4.00	100.0	0.0
8.00	4.00	85.0	15.0
12.00	4.00	65.0	35.0
20.00	4.00	40.0	60.0
25.00	4.00	5.0	95.0
30.00	4.00	5.0	95.0
35.00	4.00	50.0	50.0
40.00	4.00	90.0	10.0

	Retention Time	Area	% Area	Height	Int Type	Peak Type
1	23.967	30978120	46.33	1960167	bb	Unknown
2	25.463	35885509	53.67	2891870	bb	Unknown



4.10.2. Reverse phase HPLC Chromatograms of

Compounds **123** & **124** (jal-6-123)

Reverse phase HPLC following deallylation of **113**

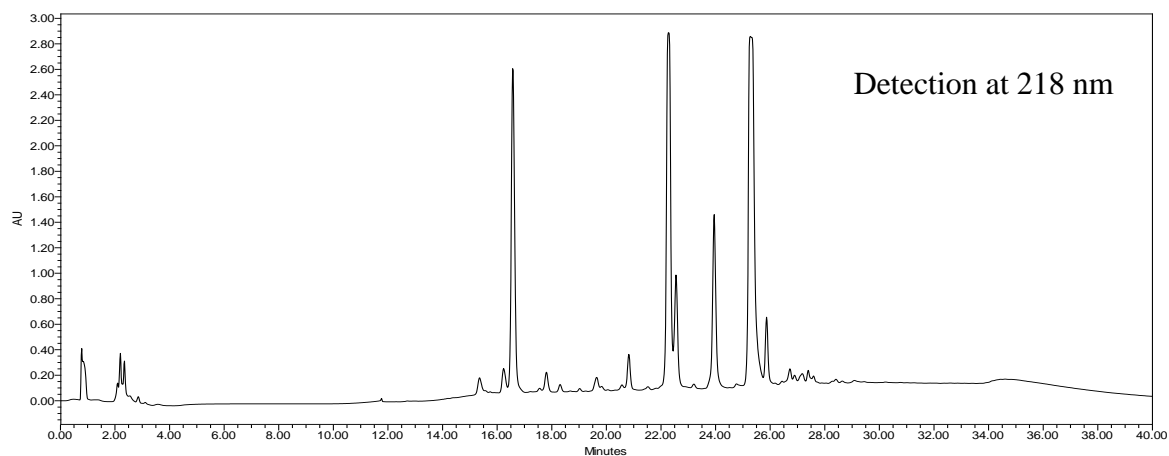
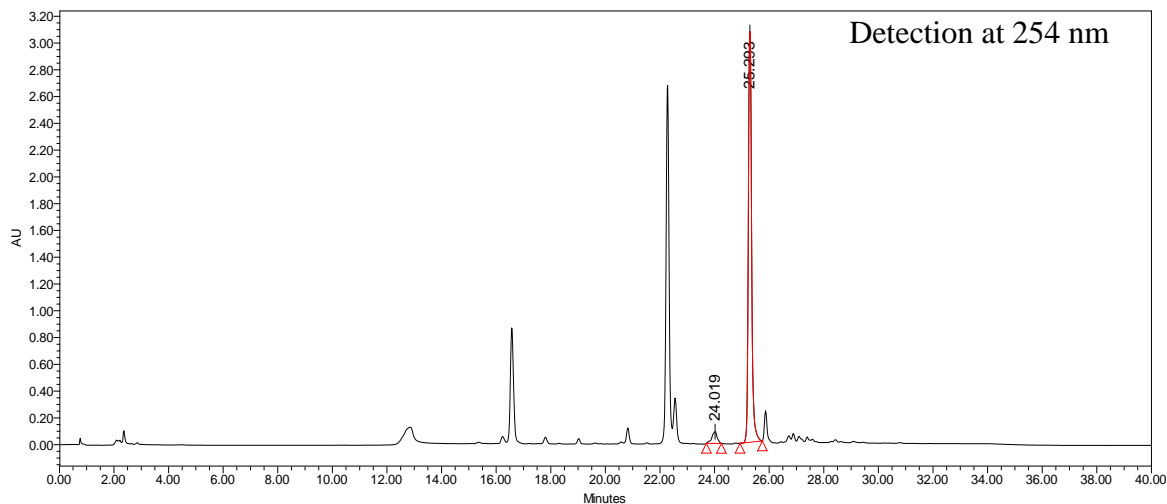
with thiosalicylic acid as allyl scavenger

Altima® C18 10 μ , 10 x 250 mm column

Method-Gradient

Time (min)	Flow (mL min ⁻¹)	H ₂ O %	MeCN %
0.01	4.00	100.0	0.0
5.00	4.00	100.0	0.0
8.00	4.00	85.0	15.0
12.00	4.00	65.0	35.0
20.00	4.00	40.0	60.0
25.00	4.00	5.0	95.0
30.00	4.00	5.0	95.0
35.00	4.00	50.0	50.0
40.00	4.00	90.0	10.0

	Retention Time	Area	% Area	Height	Int Type	Peak Type
1	24.019	1188344	4.43	87943	bb	Unknown
2	25.293	25661725	95.57	3102395	bb	Unknown

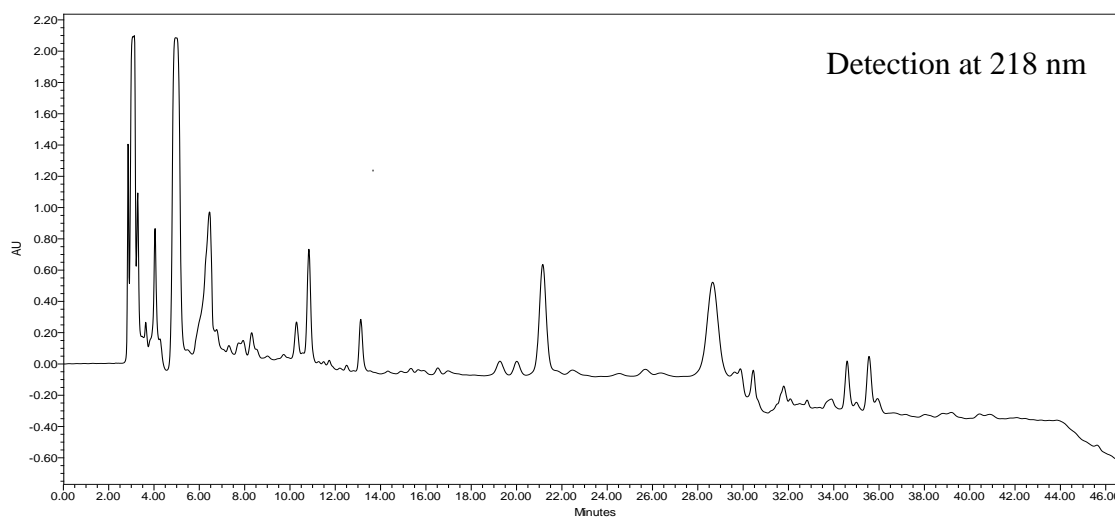
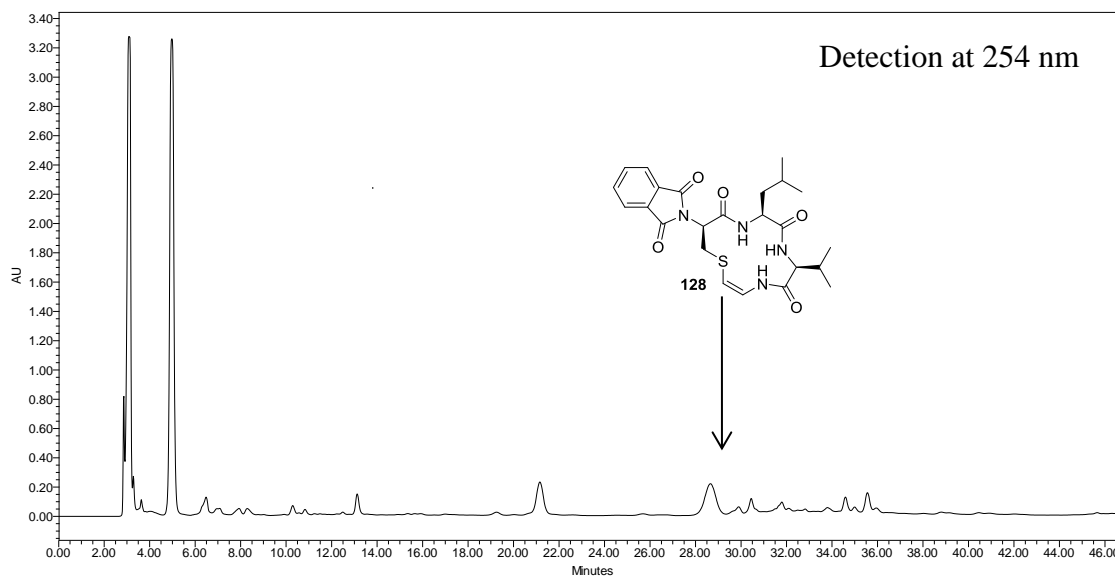


4.10.3. Reverse phase HPLC of Compound 128 (jal-7-143)

Altima® C18 10 μ , 10 x 250 mm column

Method-Gradient

Time (min)	Flow (mL min ⁻¹)	H ₂ O %	MeCN %
0.01	3.00	60.0	40.0
5.00	3.00	60.0	40.0
8.00	3.00	50.0	50.0
25.00	3.00	50.0	50.0
27.00	3.00	25.0	75.0
40.00	3.00	25.0	75.0
42.00	3.00	5.0	95.0
47.00	3.00	5.0	95.0



4.11. Notes

1. Chem 605 - Structure Determination Using Spectroscopic Methods. Proton Chemical Shifts. <https://www.chem.wisc.edu/areas/reich/nmr/h-data/hdata.htm> (accessed August 20th, 2019).
2. Munday, R.H.; Goodman, L.; Noonan, G.M., "An Alternative Synthesis of the Lipophilic Tail Portion of Abediterol Using Linear-Selective Hydroformylation," *Tetrahedron Lett.*, **2019**, 60, 606-609.
3. Panza, L.; Compostella, F.; Imperio, D., "A Versatile Synthesis of α GalCer and its Analogues Exploiting a Cyclic Carbonate as Phytosphingosine 3,4-Diol Protecting Group," *Carbohydr. Res.*, **2019**, 472, 50-57.
4. Debenham, J.S.; Madsen, R.; Roberts, C.; Fraser-Reid, B., "Two New Orthogonal Amine-Protecting Groups that can be Cleaved Under Mild or Neutral Conditions," *J. Am. Chem. Soc.*, **1995**, 117, 3302-3303.
5. Debenham, J.S.; Fraser-Reid, B., "Tetrachlorophthaloyl as a Versatile Amine Protecting Group," *J. Org. Chem.*, **1996**, 61, 432-433.
6. Tafelska-Kaczmarek, A.; Krzeminski, M.P.; Cwiklinska, M., "Asymmetric Synthesis of Benzofuryl β -Amino Alcohols by the Transfer Hydrogenation of α -Functionalized Ketones," *Tetrahedron*, **2017**, 73, 3883-3897.
7. Battah, S.; Hider, R.C.; MacRobert, A.J.; Dobbin, P.S.; Zhou, T., "Hydroxypyridinone and 5-Aminolaevulinic Acid Conjugates for Photodynamic Therapy," *J. Med. Chem.*, **2017**, 60, 3498-3510.
8. De Simone, A.; Russo, D.; Ruda, G.F.; Micoli, A.; Ferraro, M.; Di Martino, R.M.C.; Ottonello, G.; Summa, M.; Armirotti, A.; Bandiera, T.; Cavalli, A.; Bottegoni, G., "Design, Synthesis, Structure-Activity Relationship Studies, and Three-Dimensional Quantitative Structure-Activity Relationship (3D-QSAR) Modeling of a Series of O-Biphenyl Carbamates as Dual Modulators of Dopamine D3 Receptor and Fatty Acid Amide Hydrolase," *J. Med. Chem.*, **2017**, 60, 2287-2304.
9. Maryanoff, B.E.; Greco, M.N.; Zhang, H.C.; Andrade-Gordon, P.; Kaufman, J.A.; Nicolaou, K.C.; Liu, A.; Brungs, P.H., "Macrocyclic Peptide Inhibitors of Serine Proteases. Convergent Total Synthesis of Cyclotheonamides A and B via Late-Stage Primary Amine Intermediate. Study of Thrombin Inhibition under Diverse Conditions," *J. Am. Chem. Soc.*, **1995**, 117, 1225-1239.
10. Lemaire-Audoire, S.; Savignac, M.; Genet, J.P.; Bernard, J.M., "Selective Deprotection of Allyl Amines Using Palladium," *Tetrahedron Lett.*, **1995**, 36, 1267-1270.
11. Baldwin, I.C.; Briner, P.; Eastgate, M.D.; Fox, D.J.; Warren, S., "Synthesis of Enantiomerically Pure 2,2,3,4,5-Pentasubstituted Pyrrolidines by Phenylsulfanyl Migration," *Org. Lett.*, **2002**, 4, 4381-4384.

12. Minami, Y.; Yoshida, K.; Azuma, R.; Urakawa, A.; Kawauchi, T.; Otani, T., "Structure of Cypemycin, a New Peptide Antibiotic," *Tetrahedron Lett.*, **1994**, 35, 80001-80004.

List of References

- Abraham, E.P.; Chain, E., "An Enzyme from Bacteria Able to Destroy Penicillin," *Nature*, **1940**, 146, 837.
- Arbour, C.A.; Kondasinghe, T.D.; Saraha, H.Y.; Vorlicek, T.L.; Stockdill, J.L.; "Epimerization-Free Access to C-Terminal Cysteine Peptide Acids, Carboxamides, Secondary Amides, and Esters *Via* Complimentary Strategies," *Chem. Sci.*, **2018**, 9, 350-355.
- Baldwin, I.C.; Briner, P.; Eastgate, M.D.; Fox, D.J.; Warren, S., "Synthesis of Enantiomerically Pure 2,2,3,4,5-Pentasubstituted Pyrrolidines by Phenylsulfanyl Migration," *Org. Lett.*, **2002**, 4, 4381-4384.
- Banerjee, B.; Litvinov, D.; Kang, J.; Bettale, J.; Castle, S. "Stereoselective Additions of Thiyl Radicals to Terminal Ynamides" *Org. Lett.*, **2010**, 12, 2650-2652.
- Battah, S.; Hider, R.C.; MacRobert, A.J.; Dobbin, P.S.; Zhou, T., "Hydroxypyridinone and 5-Aminolaevulinic Acid Conjugates for Photodynamic Therapy," *J. Med. Chem.*, **2017**, 60, 3498-3510.
- Baxter, A.J.G.; Ponsford, R.J.; Southgate, R. "Synthesis of Olivanic Acid Analogs. Preparation of 7-Oxo-1-azabicyclo-[3.2.0]hept-2-ene-2-carboxylates Containing the 3-(2-Acetamido-ethenylthio) Side Chain," *J.C.S., Chem. Commun.*, **1980**, 429-431.
- Bentley, R., "Mycophenolic Acid: A One Hundred Year Odyssey from Antibiotic to Immunosuppressant," *Chem. Rev.*, **2000**, 100, 3801-3825.
- Berger, J.M.; Gamblin, S.J.; Harrison, S.C.; Wang, J.C, "Structure and Mechanism of DNA Topoisomerase II," *Nature*, **1996**, 379, 225-232.
- Brötz, H.; Josten, M.; Wiedemann, I.; Schneider, U.; Götz, F.; Bierbaum, G.; Sahl, H.G., "Role of Lipid-Bound Peptidoglycan Precursors in the Formation of Pores by Nisin, Epidermin and Other Lantibiotics," *Mol. Microbiol.*, **1998**, 30, 317-327.
- Carrilo, A. K.; VanNieuwenhze, M.S. "Synthesis of the AviMeCys-containing D-ring of Mersacidin," *Org. Lett.*, **2012**, 14, 1034-1037.
- Casimir, J.R.; Guichard, G.; Briand, J.P., "Methyl 2-((Succinimidooxy)carbonyl)benzoate (MSB): A New, Efficient Reagent for *N*-Phthaloylation of Amino Acid and Peptide Derivatives," *J. Org. Chem.*, **2002**, 67, 3764-3768.
- Castiglione, F.; Lazzarini, A.; Carrano, L.; Corti, E.; Ciciliato, I.; Gastaldo, L.; Candiani, P.; Losi, D.; Marinelli, F.; Selva, E.; Parenti, F. "Determining the Structure and Mode of Action of Microbisporicin, a Potent Lantibiotic Active Against Multiresistant Pathogens," *Chem. Biol.*, **2008**, 15, 22-31.
- Chain, E.; Florey, H.W.; Gardner, A.D.; Heatley, N.G.; Jennings, M.A.; Orr-Ewing, J.; Sanders, A.G., "Penicillin as a Chemotherapeutic Agent," *Lancet*, **1940**, II, 226-228.

Chatterjee, S.; Chatterjee, S.; Lad, S.J.; Shashikant, J.; Phansalker, M. S.; Rupp, R. H.; Ganguli, B. N.; Fehllhaber, H. W.; Kogler, H., "Mersacidin, a New Antibiotic from *Bacillus*: Fermentation, Isolation, Purification, and Chemical Characterization," *J. Antibiot.*, **1992**, 45, 832-838.

Chem 605 - Structure Determination Using Spectroscopic Methods. Proton Chemical Shifts. <https://www.chem.wisc.edu/areas/reich/nmr/h-data/hdata.htm> (accessed August 20th, 2019).

Chen, C-C., Chen, L-Y., Lin, R-Y., Chu, C-Y., Dai, S.A. "A Non-acyl Azide Route to Isoquinolin-1(2*H*)-one Derivatives Via β -Styryl Carbamates," *Heterocycles*, **2009**, 78, 2979-2992.

Chukwudi, C.U., "rRNA Binding Sites and the Molecular Mechanism of Action of the Tetracyclines," *Antimicrob. Agents Chemother.*, **2016**, 60, 4433-4441.

Cotter, P. D.; Hill, C.; Ross, R. P. "Bacterial Lantibiotics: Strategies to Improve Therapeutic Potential," *Curr. Protein Pept. Sci.*, **2005**, 6, 61-75.

Cruz, J.C.S.; Iorio, M.; Monciardini, P.; Simone, M.; Brunati, C.; Gaspari, E.; Maffioli, S.I.; Wellington, E.; Sosio, M.; Donadio, S. "Brominated Variant of the Lantibiotic NAI-107 with Enhanced Antibacterial Potency," *J. Nat. Prod.*, **2015**, 78, 2642-2647.

Dale, J.A.; Dull, D.L.; Mosher, H.S., " α -Methoxy- α -trifluoromethylphenylacetic Acid, a Versatile Reagent for the Determination of Enantiomeric Composition of Alcohols and Amines," *J. Org. Chem.*, **1969**, 34, 2543-2549.

De Simone, A.; Russo, D.; Ruda, G.F.; Micoli, A.; Ferraro, M.; Di Martino, R.M.C.; Ottonello, G.; Summa, M.; Armirotti, A.; Bandiera, T.; Cavalli, A.; Bottegoni, G., "Design, Synthesis, Structure-Activity Relationship Studies, and Three-Dimensional Quantitative Structure-Activity Relationship (3D-QSAR) Modeling of a Series of O-Biphenyl Carbamates as Dual Modulators of Dopamine D3 Receptor and Fatty Acid Amide Hydrolase," *J. Med. Chem.*, **2017**, 60, 2287-2304.

Debenham, J.S.; Fraser-Reid, B., "Tetrachlorophthaloyl as a Versatile Amine Protecting Group," *J. Org. Chem.*, **1996**, 61, 432-433.

Debenham, J.S.; Madsen, R.; Roberts, C.; Fraser-Reid, B., "Two New Orthogonal Amine-Protecting Groups that can be Cleaved Under Mild or Neutral Conditions," *J. Am. Chem. Soc.*, **1995**, 117, 3302-3303.

Delves-Broughton, J.; Blackburn, P.; Evans, R. J.; Hugenholtz, J., "Applications of the Bacteriocin, Nisin," *Antonie van Leeuwenhoek*, **1996**, 69, 193-202.

Ding, W.; Yuan, N.; Mandalapu, D.; Mo, T.; Dong, S.; Zhang, Q., "Cypemycin Decarboxylase CypD is not Responsible for Aminovinyl-cysteine (AviCys) Ring Formation," *Org. Lett.*, **2018**, 20, 7670-7673.

Drugs.com website for vancomycin hydrochloride:
<https://web.archive.org/web/20150906002445/http://www.drugs.com/monograph/vancocin.html> (accessed July 2nd, 2019).

eMed Expert. Interesting Facts about Antibiotics.
<https://www.emedexpert.com/tips/antibiotics-facts.shtml> (accessed January 14th, 2019).

Estevez, J.C.; Villaverde, M.C.; Estevez, R.J.; Castedo, L. "A New Synthesis of Styrylamides," *Synth. Commun.*, **1993**, 23, 1081-1085.

Fleming, A. "The Antibacterial Action of Cultures of a *Penicillium*, with Special Reference to their Use in the Isolation of *B. influenzae*," *Brit. J. Exp. Pathol.*, **1929**, 10, 226-236.

Franke, W.; Kraft, R. "Cyclization with Acetoacetaldehyde Bisacetal," *Ber.*, **1953**, 86, 797-800.

Garcia-Reynaga, P.; Carrillo, A.; VanNieuwenhze, M. "Decarbonylative Approach to the Synthesis of Enamides from Amino Acids: Stereoselective Synthesis of the (Z)-Amino-D-Cysteine Unit of Mersacidin," *Org. Lett.*, **2012**, 14, 1030-1033.

Ghuysen, J.M., "Molecular Structures of Penicillin-Binding Proteins and beta-Lactamases," *Trends Microbiol.*, **1994**, 10, 372-380.

Han, Y.; Albericio, F.; Barany, G. "Occurrence and Minimization of Cysteine Racemization During Stepwise Solid-Phase Peptide Synthesis," *J. Org. Chem.*, **1997**, 62, 4307-4312.

Harada, S.; Tsubotani, S.; Asai, M.; Okonogi, K.; Kondo, M. "Synthesis and Biological Activities of the (Z) Isomers of Carbapenem Antibiotics," *J. Med. Chem.* **1983**, 26, 271-275.

Harichandran, G., Amalraj, S.D., Shanmugam, P. "Boric Acid Catalyzed Efficient Synthesis of Symmetrical *N, N'*-(Alkylidene) Bis[amide] Derivatives," *J. Iran Chem. Soc.*, **2011**, 298-305.

Hayakawa, Y.; Sasaki, K.; Nagai, K.; Shin-ya, K.; Furihata, K. "Structure of Thioviridamide, a Novel Apoptosis Inducer From *Streptomyces olivoviridis*," *J. Antibiot.*, **2006**, 59, 6-10.

Health Research Funding. 11 Scary Statistics on Antibiotic Resistance.
<https://healthresearchfunding.org/11-scary-statistics-on-antibiotic-resistance/> (accessed January 26th, 2019).

Hiasa, H.; Yousef, D.O.; Mariani, K.J., "DNA Strand Cleavage is Required for Replication Fork Arrest by a Frozen Topoisomerase-Quinolone-DNA Ternary Complex," *J. Biol. Chem.*, **1996**, 271, 26424-26429.

Hooper, D. C., "Emerging Mechanisms of Fluoroquinolone Resistance," *Emerg. Infect. Dis.*, **2001**, 7, 337-341.

- Kellner, R.; Jung, G.; Horner, T.; Zaehner, H.; Schnell, N.; Entian, K. D.; Goetz, F. "Gallidermin: a New Lanthionine-Containing Polypeptide Antibiotic," *Eur. J. Biochem.*, **1988**, 177, 53-59.
- Kitchin, J. E.; Pomeranz, M. K.; Pak, G.; Washenik, K.; Shupack, J. L., "Rediscovering Mycophenolic Acid: A Review of its Mechanism, Side Effects, and Potential Uses," *J. Am. Acad. Dermatol.*, **1997**, 37, 445-449.
- Knott-Hunziker, V.; Waley, S.G.; Orlek, B.S.; Sammes P.G., "Penicillinase Active Sites: Labeling of Serine-44 in beta-Lactamase I by 6-beta-Bromopenicillanic Acid," *FEBS Lett.*, **1979**, 99, 59-61.
- Komiyama, K.; Otoguro, K.; Segawa, T.; Shiomi, K.; Yang, H.; Takahashi, Y.; Hayashi, M.; Otani, T.; Omura, S. "A New Antibiotic, Cypemycin - Taxonomy, Fermentation, Isolation and Biological Characteristics," *J. Antibiot.*, **1993**, 46, 1666-1671.
- Kovacs, J.; Mayers, G.L.; Johnson, R.H.; Ghatak, U.R. "Racemization Studies in Peptide Chemistry. Reinvestigation of the β -Elimination-Readdition Mechanism of N-Benzylloxycarbonyl-S-benzylcysteine Derivatives," *Chem. Commun.*, **1968**, 1066-1067.
- Kurita, J.; Sakai, H.; Yamada, S.; Tsuchiya T. "Novel Thermal Rearrangements of Tetrahydroazirinocyclobutabenzofuran Derivatives," *J. C. S., Chem. Commun.*, **1987**, 285-286.
- Kusumi, T.; Ohtani, I.I., "Determination of the Absolute Configuration of Biologically Active Compounds by the Modified Mosher's Method," *Biology-Chemistry Interface*, **1999**, 103-137.
- Lazzarini, A.; Gastaldo, L.; Candiani, G.; Ciciliato, I.; Losi, D.; Marinelli, F.; Selva, E.; Parenti, F. "Antibiotic 107891, its Factors A1 and A2, Pharmaceutically Acceptable Salts and Compositions, and Use Thereof," International Publication Number WO 20050233952 A1 20051020, International Publication Date 17 February **2005**.
- Lelievre, D., Terrier, V.P., Delmas, A.F., Aucagne, V.; "Native Chemical Ligation Strategy to Overcome Side Reactions During Fmoc-Based Synthesis of C-Terminal Cysteine-Containing Peptides," *Org. Lett.*, **2016**, 18, 920-923.
- Lemaire-Audoire, S.; Savignac, M.; Genet, J.P.; Bernard, J.M., "Selective Deprotection of Allyl Amines Using Palladium," *Tetrahedron Lett.*, **1995**, 36, 1267-1270.
- Levy, S.B., "Active Efflux Mechanism for Antimicrobial Resistance," *Antimicrob. Agents Chemother.*, **1992**, 36, 695-703.
- Li, Y.; Carter, D.E.; Mash, E.A. "Synthesis and Structure of the Glutathione Conjugate of Chloroacetaldehyde," *Synth. Commun.*, **2002**, 32, 1579-1583.

- Liu, L.; Chan, S.; Mo, T.; Ding, W.; Yu, S.; Zhang, Q.; Yuan, S., "Movements of the Substrate-Binding Clamp of Cypemycin Decarboxylase CypD," *J. Chem. Inf. Model*, **2019**, 59, 2924-2929.
- Lutz, J.A.; Subasinghe Don, V.; Kumar, R.; Taylor, C.M. "Influence of Sulfur on Acid-Mediated Enamide Formation," *Org. Lett.*, **2017**, 19, 5146-5149.
- Maffioli, S.I.; Iorio, M.; Sosio, M.; Monciardini, P.; Gaspari, E.; Donadio, S. "Characterization of the Congeners in the Lantibiotic NAI-107 Complex," *J. Nat. Prod.*, **2014**, 77, 79-84.
- Maryanoff, B.E.; Greco, M.N.; Zhang, H.C.; Andrade-Gordon, P.; Kaufman, J.A.; Nicolaou, K.C.; Liu, A.; Brungs, P.H., "Macrocyclic Peptide Inhibitors of Serine Proteases. Convergent Total Synthesis of Cyclotheonamides A and B via Late-Stage Primary Amine Intermediate. Study of Thrombin Inhibition under Diverse Conditions," *J. Am. Chem. Soc.*, **1995**, 117, 1225-1239.
- Minami, Y.; Yoshida, K.; Azuma, R.; Urakawa, A.; Kawauchi, T.; Otani, T., "Structure of Cypemycin, a New Peptide Antibiotic," *Tetrahedron Lett.*, **1994**, 35, 80001-80004.
- Mo, T.; Liu, W.; Ji, W.; Zhao, J.; Chen, T.; Ding, W.; Yu, S.; Zhang, Q., "Biosynthetic Insights into Linaridin Natural Products from Genome Mining and Precursor Peptide Mutagenesis," *ACS Chem. Biol.*, **2017**, 12, 1484-1488.
- Munday, R.H.; Goodman, L.; Noonan, G.M., "An Alternative Synthesis of the Lipophilic Tail Portion of Abediterol Using Linear-Selective Hydroformylation," *Tetrahedron Lett.*, **2019**, 60, 606-609.
- Munita, J. M.; Arias, C.A., "Mechanisms of Antibiotic Resistance," *Microbiol. Spectr.*, **2016**, 4, 1-24.
- Nakamura, Y.; Ishii, K.; Ono, E.; Ishihara, M.; Kohda, T.; Yokogawa, Y.; Shibai, H. "A Novel Naturally Occurring Carbapenem Antibiotic, AB-110-D, Produced by *Kitasatosporia papulosa* novo Sp." *J. Antibiot.*, **1988**, 41, 707-711.
- Nguyen-Distèche, M.; Leyh-Bouille, M.; Ghuysen J.M., "Isolation of the Membrane-Bound 26,000-Mr Penicillin-Binding Protein of *Streptomyces* Strain K15 in the Form of a Penicillin-Sensitive D-alanyl-D-alanine-Cleaving Transpeptidase," *Biochem. J.*, **1982**, 207, 109-115.
- Nicolaou, K.C.; Rigol, S., "A Brief History of Antibiotics and Select Advances in Their Synthesis," *J. Antibiot.*, **2018**, 71, 153-184.
- Panza, L.; Compostella, F.; Imperio, D., "A Versatile Synthesis of α GalCer and its Analogues Exploiting a Cyclic Carbonate as Phytosphingosine 3,4-Diol Protecting Group," *Carbohydr. Res.*, **2019**, 472, 50-57.
- Park, J.T.; Uehara, T., "How Bacteria Consume Their Own Exoskeletons (Turnover and Recycling of Cell Wall Peptidoglycan)," *Microbiol. Mol. Biol. Rev.*, **2008**, 72, 211-227.

- Rasmussen, D.H., "The Treatment of Syphilis," *Surv. Ophthalmol.*, **1969**, 14, 184-197.
- Reed, A.E.; Weinstock, R. B.; Weinhold, F. "Natural Population Analysis," *J. Chem. Phys.* **1985**, 83, 735-746
- Regueira, T.B.; Kildegaard, K.R.; Hansen, B.G.; Mortensen, U.H.; Hertweck, C.; Nielsen, J., "Molecular Basis for Mycophenolic Acid Biosynthesis in *Penicillium brevicompactum*," *App. Env. Microbiol.*, **2011**, 77, 3035-3043.
- Repka, L.M.; Chekan, J.R.; Nair, S. K.; van der Donk, W. A., "Mechanistic Understanding of Lanthipeptide Biosynthetic Enzymes," *Chem. Rev.*, **2017**, 117, 5457-5520.
- Schneider, A.E., Manolikakes, G. "Bi(OTf)₃-Catalyzed Multicomponent α -Amidoalkylation Reactions," *J. Org. Chem.*, **2015**, 80, 6193-6212.
- Science History Institute. Alexander Fleming. <https://www.sciencehistory.org/historical-profile/alexander-fleming> (accessed January 10th, 2019).
- Siedler, F.; Weyher, E.; Moroder, L. "Cysteine Racemization in Peptide Synthesis: a New and Easy Detection Method," *J. Pept. Sci.*, **1996**, 2, 271-275.
- Sit, C.S.; Yoganathan, S.; Vederas, J.C., "Biosynthesis of Aminovinyl-Cysteine-Containing Peptides and Its Application in the Production of Potential Drug Candidates," *Acc. Chem. Res.* **2011**, 44, 261-268.
- Tafelska-Kaczmarek, A.; Krzeminski, M.P.; Cwiklinska, M., "Asymmetric Synthesis of Benzofuryl β -Amino Alcohols by the Transfer Hydrogenation of α -Functionalized Ketones," *Tetrahedron*, **2017**, 73, 3883-3897.
- Trent, M.S.; Ribeiro, A. A.; Lin, S.; Cotter, R.J.; Raetz, C.R.H., "An Inner Membrane Enzyme in *Salmonella* and *Escherichia coli* that Transfers 4-Amino-4-deoxy-L-arabinose to Lipid A. Induction in Polymixin-Resistant Mutants and Role of a Novel Lipid-Linked Donor," *J. Biol. Chem.*, **2001**, 276, 43122-43131.
- Velkov, T.; Roberts, K.D.; Nation, R.L.; Philip, E.; Li, J., "Pharmacology of Polymixins: New Insights into an 'Old' Class of Antibiotics," *Future Microbiol.*, **2013**, 8, 711-724.
- Williams, K.J., "The Introduction of 'Chemotherapy' Using Arsphenamine—The First Magic Bullet," *J. Royal Soc. Med.*, **2009**, 102, 343-348.
- Willmott, C.J.; Maxwell, A., "A Single Point Mutation in the DNA Gyrase A Protein Greatly Reduces Binding of Fluoroquinolones to the Gyrase-DNA Complex," *Antimicrob. Agents Chemother.*, **1993**, 37, 126-127.
- Wolfe, S.; Tel, L.M.; Liang, J.H.; Csizmadia, I.G. "Stereochemical Consequences of Adjacent Electron Pairs. Theoretical Study of Rotation-Inversion in Ethylene Dicarbanion," *J. Am. Chem Soc.*, **1972**, 4, 1361-1364.

Wu, J. C. "Mycophenolate Mofetil: Molecular Mechanisms of Action," *Perspect. Drug Discov. Des.*, **1994**, 2, 185–204.

Zhou, H.; Fang, J.; Tian, Y.; Lu, X.Y., "Mechanisms of Nisin Resistance in Gram-Positive Bacteria," *Ann. of Microbiol*, **2014**, 64, 413-420.

Zhu, X; Schmidt, R.R., "Efficient Synthesis of Differently Protected Lanthionines via β -Bromoalanine Derivatives," *Eur. J. Org. Chem.*, **2003**, 4069-4072.

Vita

Joshua Allen Lutz, first of his name, was born in Shreveport, Louisiana. He travelled to Baton Rouge to pursue a degree in psychology in the hopes of better understanding the world. Upon completion of his degree he was left unsatisfied, so turned to the central science for clarity. He grew to love organic chemistry while studying in his hometown, and this set him on a path to his doctorate at Louisiana State University. Upon completion of his degree, he will use his knowledge of psychology and skill in organic synthesis to tackle difficult problems at the interface of the two.